Spring 5-18-2018

Long Term Bathymetry Changes in the Lower Mississippi River due to Variability in Hydrograph and Variable Diversion Schemes

Nina J. Reins
University of New Orleans, ninareins@cox.net

Long Term Bathymetry Changes in the Lower Mississippi River due to Variability in Hydrograph and Variable Diversion Schemes

A Dissertation

Submitted to the Graduate Faculty of the
University of New Orleans
in partial fulfillment of the
requirements for the degree of

Doctor of Philosophy
in
Engineering and Applied Science

By

Nina Janita Reins, P.E., PMP

B.S. [Bau-Ing. (FH)] University of Applied Sciences
Oldenburg/Ostfriesland/Wilhelmshaven, 2001

M.S. Tulane University, 2005

May 2018

DEDICATION

I want to dedicate this achievement to my husband Peter Winkler, whose continued support has kept me going. He believed in me when I didn't, which has helped me to stay on this long journey of a lifetime. This journey started when we were dating, included dropping final papers off at UNO on my way to the wedding, and the birth of our two wonderful children, Max Adam Winkler and Hannah Marie Winkler.

Thank you for all the love you have given me and your continued support!

ACKNOWLEDGEMENTS

The biggest acknowledgement and thank you goes to Dr. John Alex McCorquodale for guiding me through this journey over the years. Your advisory has helped me not only through my coursework, but more importantly, through the dissertation phase, even if it included dropping one research and starting a new. Your continued support and patience have taught me so much and without you, there is no doubt, I would have given up. Therefore, this publication would not be possible without you. Thank you!

In addition, I would like to extend my gratitude to Dr. Ioannis Georgiou, who has been an inspiration and mentor throughout my time at UNO and beyond. Thank you!

I also want to thank my parents, Jenni and Friedrich Reins, for teaching me to work hard and to be strong, even if life is not always a smooth path. Your love has made me who I am today, and allowed me to believe in myself and endure.

I would also like to thank my sister, Sonja Rickhoff, and my sisters-in-law Beth Winkler, Alice Wiesner, Regan Winkler and Tracy Winkler, who have been there for me unconditionally through these years supporting me and my long journey.

In addition, I would like to thank my beloved friends, who have encouraged me and shared the pains of working towards achieving the Ph.D.: Dr. Sarah Mack, Dr. Greta Zornes, Dr. Sarah Lindsey and Dr. Tonja Koob – you have been an inspiration and your Ph.D.-stories have given me the strength to endure.

I would further like to thank Dr. Joao Pereira, Dr. Ahmed Gaweesh and Sean Kenny for their consultations and support throughout the various steps of my research.

My final thank you goes to all my friends in this world, all of them have given their support throughout the years, and their love and guidance, regardless of how little or big, has had an important impact in making this achievement a reality. Thank you for all your love!

TABLE OF CONTENTS

LIST OF FIGURES

LIST OF TABLES

LIST OF ACRONYMS

CPRA	Coastal Protection and Restoration Authority
D/S	Downstream
ERDC	Engineer Research and Development Center
ESLR	Eustatic Sea Level Rise
HOP	Head of Passes
LDNR	Louisiana Department of Natural Resources
LSR	Local Subsidence Rate
MRC	Mississippi River Commission
MR&T	Mississippi River and Tributaries
NRC	National Research Council
RM	River Mile
RSLR	Relative Sea Level Rise
SLR	Sea Level Rise
TWIG	The Water Institute of the Gulf
UNO	University of New Orleans
U/S	Upstream
USACE	United States Army Corps of Engineers
USGS	United States Geological Survey
WPAH	West Pointe à la Hache

ABSTRACT

This research is part of an ongoing effort to improve predictions for bathymetric and morphological changes in the Lower Mississippi River. The utilized model is a subset of a previously calibrated Delft3D model. This shorter model has reduced computational time, and can be deployed for analysis focused on the area between Belle Chasse and HOP, which is the domain of the model. Simulation runs conducted under this study vary from 12 years to 48 years, utilizing a developed 12-year variable hydrograph.

The comparison of variable annual hydrograph and repeated representative annual (uniform) hydrograph input data on bathymetric changes indicated that the absolute bathymetric equilibrium is dependent on year to year variability. The utilization of a uniform hydrograph increases the predicted deposition within the river domain. When evaluating diversion sand capture, utilizing a uniform hydrograph can be considered a conservative approach, while utilizing a variable hydrograph will result in more accurate sand load volumes captured by the diversion. In general, sediment capture showed only minor interdependencies amongst multiple diversions, as long as the total diversion flow is less than 140,000cfs.

This study shows that morphological changes are dependent on the number and location of multiple diversions. The largest interdependencies occur for the most downstream diversions, which increase with the total diverted flow. A true equilibrium was not achieved within 48 years, with or without sea level rise. It was observed, that the system with diversions responds to sea level rise by an increase in deposition, which increases with total diverted flow.

Keywords: Lower Mississippi River, diversions, river morphology, annual hydrograph variability, 3-D River Modeling, bathymetric equilibrium

1.0 CHAPTER 1: INTRODUCTION

1.1 BACKGROUND

The Mississippi River has been vital to North America's livelihood and commerce since the founding of New Orleans 300 years ago. While providing abundant benefits and resources it also remains a powerful natural force. The progress from permanent settlements to loss of property followed by the installation of private embankment and finally to a methodic regional levee construction has logical merit. Following the devastating flood from 1927, the previously established Mississippi River Commission (MRC) was charged with prosecuting the comprehensive Mississippi River and Tributaries (MR&T) project, which was authorized through the Flood Control Act of 1928. The four major elements of the MR&T project are: (1) Levees for containing flood flows; (2) Floodways for the passage of excess flows past critical reaches of the Mississippi River; (3) Channel improvement and stabilization to provide an efficient and reliable navigation channel, increase the flood-carrying capacity of the river, and protect the levee system; and (4) Tributary basin improvements for major drainage basins to include dams and reservoirs, pumping plants, auxiliary channels and pumping stations (MRT 2017). This levee system has been maintained and has permanently altered the natural dynamics of the Mississippi River.

As outlines in the 2017 Master Plan, Louisiana's coast lost more than 1,800 square miles of land between 1932 and 2010. From 2004 to 2008 alone, more than 300 square miles of marshland were lost to Hurricanes Katrina, Rita, Gustav and Ike. The culprits to this land loss include the effects of climate change, seal level rise, subsidence, hurricanes, storm surges, flooding, disconnecting the Mississippi River from coastal marshes, and human impacts. (CPRA 2017)

The above excerpt highlights a wide array of factors causing land loss but the established MR&T levee system, which disconnects the Mississippi River from the coastal marshes, is one of the noteworthy elements. In order to identify potential

solutions to the Mississippi River Management, while still offering the required protection and navigation is a multi-facetted challenge.

This research is a continuation of an ongoing effort to improve predictions for bathymetric and morphological changes in the Lower Mississippi River as well as the associated analysis and prediction on impacts from planned diversions.

Previous research conducted included a wide array of hydrodynamic models, from 1-dimensional to 3-dimensional, and each application has brought new insight to the complex and difficult to predict system of the Lower Mississippi River and the impact of potential future diversions. The 'Previous Research Section' (Chapter 2.2) describes some of the modeling efforts and the progression to the Delft 3D Model utilized in this research, referred to as the "shortmodel" (Figure 1.1.1)

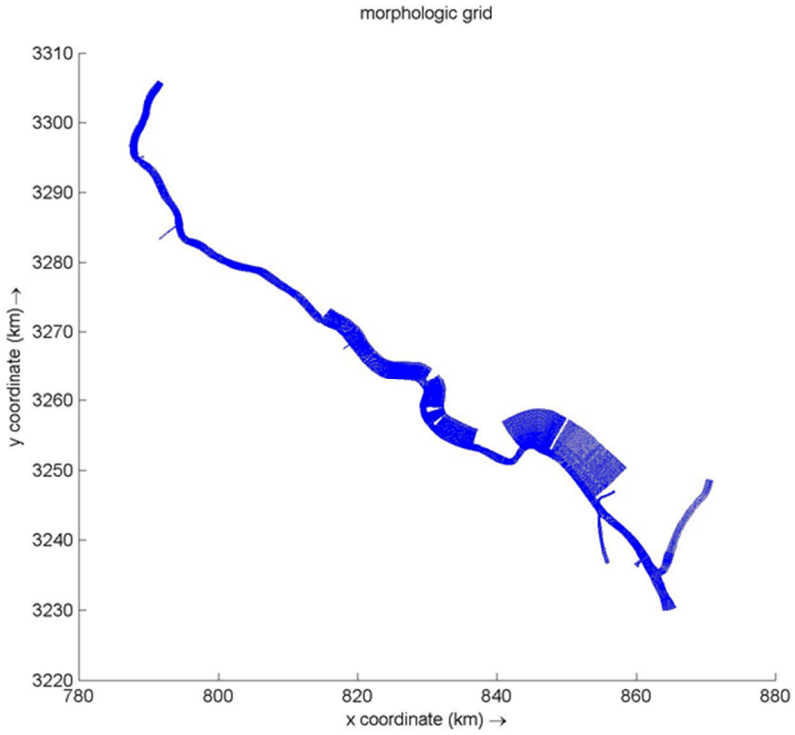

Figure 1.1.1: The Model Domain for 'Shortmodel'

1.2 STATEMENT OF THE PROBLEM

The Coastal Protection and Restoration Authority (CPRA) has issued to date the 2007, 2012 and 2017 Comprehensive Master Plan for a Sustainable Coast (CPRA 2007, 2012, 2017), and all plans include a variety of diversions below Belle Chasse on the Lower Mississippi River. The concept of diversions to transport sediments from the Mississippi River back into the adjacent Barataria and Breton Basins as a supplemental method to restoration dredging has been introduced a long time ago and has been captured in the Coast 2050 Report (LDNR 1998) and the Louisiana Coastal Area (LCA) Ecosystem Restoration Study (USACE 2004).

The CPRA is currently in the design and/or permitting phase for the Mid-Barataria Diversion and the Mid-Breton Diversion. Any permitting of a diversion on the Lower Mississippi River will require an assessment of cumulative impacts as well as impacts from individual diversion flows. Therefore, this research helps to identify interdependencies between various flows and a variety of diversion cases with a focus on the morphologic changes within the Mississippi River itself. In addition, this research will aim to improve the Delft 3D model developed under the MRHDM Study, by performing analysis on parameters like the input hydrograph, Eddy Viscosity/Diffusivity, Relative Sea-Level (RSL) Rise and sediment flux in the Mississippi River.

1.3 OBJECTIVE

The objective of this research is to establish a numerical model for the Lower Mississippi River that improves on computational time in comparison to an existing model, while still remaining comparable to the developed existing model in the reach where there are proposed diversions, i.e. downstream of Belle Chasse. The improved speed will allow a variety of hypothesis and research questions to be answered, which will benefit future modeling with both, the previously developed model and the shortened Lower Mississippi River Model presented in this research.

1.3.1 HYPOTHESIS

The following three (3) hypotheses were established for the analysis conducted under this dissertation research:

- **H1:** The equilibrium bathymetry is independent of the annual variability of the hydrograph, provided the flow duration curve is the same.
- **H2:** The average annual sediment captured by the diversions is independent of the annual variability of the hydrographs, provided the flow duration curve is comparable.
- **H3:** If the total flow diverted through multiple diversions is less than a certain total critical diversion discharge, each diversion will function as an independent structure in terms of local deposition and sediment captured.

1.4 GENERAL METHODOLOGY AND RESEARCH PLAN

Delft3D (Deltares 2011) is an integrated modeling framework with a multi-disciplinary approach that can carry out 2-D and 3-D computations for coastal, river, lake and estuarine areas. It can perform simulations of flows, sediment transports, waves, water quality, morphological developments and ecology. Delft3D is composed of several modules which are grouped on a mutual interface being capable to interact with one another. The hydrodynamic simulations are run with Delft3D-FLOW, a multi-dimensional program that performs unsteady flow and transport phenomena resulting from tidal and hydrologic/meteorological forcing on a rectilinear or curvilinear grid. The sigma coordinate is used to define the vertical distribution for the three dimensional simulations (Deltares, 2011).

Since Delft 3D was already selected to develop a model for the Lower Mississippi River from Bonnet-Carré Spillway to Head of Passes (see Chapter 2.2 for chronological details), it was the intent of this research to expand on existing knowledge and model developments by improving computational time for analysis of the Mississippi River below Belle Chasse, by shortening the existing model as well as further analyzing the models sensitivity to input changes, like discharge predictions or relative sea level rise adjusted boundary conditions. Any sensitivity findings would informative to both Delft3D

models, the original model developed and validated by McCorquodale et al. (2017) as well as the model developed as part of this research.

In order to evaluate Hypothesis 1 a variable hydrograph, with a similar flow duration curve to the uniform hydrograph utilized by McCorquodale et al. (2017), has to be developed (See Chapter 3.1.3); followed by an evaluation of depositional changes between model results utilizing the uniform and the developed variable hydrograph input. Chapter 4 outlines the complete analysis of Hypothesis 1.

To further investigate the impacts of a variable hydrograph versus a uniform hydrograph, the sediment capture within proposed diversions was analyzed for evaluation of Hypothesis 2. Chapter 5 outlines the complete analysis of Hypothesis 2.

After the differences between the utilization of a uniform and a variable discharge pattern have been determined a sequence of multiple four (4) diversion scenarios and individual diversion cases will be modeled to evaluate Hypothesis 3. The run results will be compared to evaluate the sediment captured by diversions as well as the depositional changes within the Mississippi River due to individual and multiple diversion cases. Chapter 6 outlines the complete analysis of Hypothesis 3.

In order to identify geomorphologic changes it was determined to best evaluate laterally averaged cumulative deposition as an indicator for changes along the river between Belle Chasse and Head of Passes. For sediment capture a cumulative volume analysis will be conducted and totals will be compared for evaluation.

2.0 CHAPTER 2: LITERATURE REVIEW

2.1 GENERAL

The reviewed literature provides the background necessary to understand the array of different models utilized for analysis of morphologic changes and sediment transport in the Lower Mississippi River in recent years as well as the development of the original Delft 3D Model (McCorquodale et al. 2017), and its associated calibration and validation.

2.2 PREVIOUS RESEARCH

The following provides a chronological summary of applicable literature utilized as the basis of this research and for the development of the "shortmodel" developed as part of this research. The key components of each contributing research document are listed and how they relate to the shortmodel and the associated research presented in this dissertation.

2.2.1 Lower Mississippi River Sedimentation Study (1992)

In June 1992 the U.S. Army Corps of Engineers released the final report (HL-92-6) of a numerical model investigation conducted by Ronald R. Copeland and William A. Thomas titled *"Lower Mississippi River Tarbert Landing to East Jetty Sedimentation Study"*. The report covers the development of a one-dimensional numerical model (TABS-1) of the Mississippi River between Tarbert Landing (RM 306) and East Jetty (RM -20). The model intent was to evaluate long-term aggradation and degradation trends and the effect of various flow diversion schemes on dredging in Southwest Pass.

In terms of net change in bed volume in the 300-mile reach the calculated results between hydrographic surveys (12 years) and the numerical model were similar; however the longitudinal distribution of aggradation and degradation was not. The difference was attributed to the variation in prototype bed elevations, which are associated with the rise and fall of annual hydrographs and with dredging. Since the hydrographic surveys were taken over two year periods at various points on the annual hydrographs, data from two surveys at specific cross sections were not homologous.

Due to this inconsistency, it was not possible to use the hydrographic survey data to verify the long-term predictive capabilities of the numerical model. However, based on successful duplication of long-term dredging records and measured sediment transport, it has been concluded that the numerical model is appropriate for evaluations of dredging scenarios; the effects of specified flow diversions on sedimentation downstream; bed response to changes in discharge, sediment concentration, or bed elevation; and the effect of flow constrictions such as dike fields.

The study concluded that the operation of the Bonnet Carré Spillway during a six-week flood of 1,400,000cfs would result in deposition of the river downstream of the spillway and it would take several years for this flood deposit to move into Southwest Pass., where it would influence dredging requirements. Without operation of the diversion the extra material would be delivered to Southwest Pass during the flood, while the extra discharge would be available to transport some of it to the Gulf.

Furthermore it was concluded that diverting 10% of the Mississippi River at River at river mile 6.7 would result in an increase of the total annual dredging and deposition in Southwest Pass between 13 and 22 percent depending on the sand concentration in the diversion. When evaluation the effects of diverting 70% of the Mississippi River upstream of Venice, the net effects would be an overall increase in dredging and deposition in the lower Mississippi River. However, in Southwest Pass, dredging and deposition would be decreased, which indicates deposition between diversion sites and HOP.

The results also indicated that significant differences in dredging and deposition occur depending on the assumed sand concentration in the diversion. Also, the location of the diversion had a less significant effect on dredging and deposition than did closing the outlets.

(Copeland & Thomas 1992)

2.2.2 CPRA Comprehensive Coastal Master Plans

Because of the devastation of hurricanes Katrina and Rita, the Louisiana Legislature, restructured the State's Wetland Conservation and Restoration Authority, to form the Coastal Protection and Restoration Authority (CPRA) through Act 8 of the First Extraordinary Session of 2005.

Established by the Louisiana Legislature, CPRA is the single state entity with authority to set priorities and focus development and implementation efforts to achieve comprehensive coastal protection for Louisiana. CPRA couples hurricane protection with the protection, conservation, restoration and enhancement of coastal wetlands, barrier shorelines and reefs.

In 2007 the Coastal Protection and Restoration Authority (CPRA) published the first *"Louisiana's Comprehensive Master Plan for a Sustainable Coast"* in Baton Rouge, which was the first mandated adaptive Master Plan, which has to be updated every five (5) years. Subsequent publications in 2012 and 2017 followed and the 2017 version is the current vision of the State on project implementation and impact predictions.

The State Master Plan states that the major causes of the land loss include the effects of climate change, sea level rise, subsidence, hurricanes, storm surges, disconnection of the Mississippi River from coastal marshes, and human impacts (CPRA 2017). Therefore, the Mississippi River and its sediments play a significant role in the State's vision for coastal restoration, as the source for sediment mining for marsh creation and for controlled diversion of the sediment into marshes for mash sustainability. The State Master Plan highlights that the Atchafalaya River Delta, the Wax Lake Outlet, and areas near Fort St. Philip and West Bay along the Lower Mississippi River provide evidence that coastal landscapes can be created in the face of rising sea levels and subsidence. These locations are therefore examples of the power of nature and the natural processes CPRA seeks to restore through restoration efforts, which is why the Coastal Master Plans includes sediment diversion projects that aim to replicate these land building processes (CPRA 2017).

CPRA further states in the 2017 Master Plan that the Mississippi River-based sources of sediment are renewable approximately every five years. Specifically, the 2017 Master Plan recommends two Atchafalaya River diversions and eight Mississippi River diversions in the first implementation period. The Mid-Barataria Diversion (002.DI.102) was recently awarded federal “fast track” status from the White House, which will streamline the federal permitting process and significantly reduce the time needed to move the project to construction. (CPRA 2017)

CPRA acknowledges in the 2017 Master Plan that assumptions about future Mississippi River flow and sediment loads have to be made and assess how changes could affect our coastal landscape (CPRA 2017). Therefore, it is important to understand the assumptions made for any analysis regarding the Mississippi River or Diversion sediment and/or flow trends. Diversion impacts are complex and given the State’s focus on their implementation in the near future, the importance of evaluation and analysis of cumulative impacts becomes a high priority.

2.2.3 Sediment Transport Modeling Review

In January 2008, Athanasios N. (Thanos) Papanicolaou et al published the article *“Sediment Transport Modeling Review – Current and Future Developments”* in the ASCE Journal of Hydraulic Engineering.

The article highlights the fact that the use of computational models for solving sediment transport and fate problems is relatively recent compared with the use of physical models. The objectives of the article are stated as twofold. First, the article aims to trace the developmental stages of current representative (1D, 2D, and 3D) models and describe their main applications, strengths, and limitations. Second, the article provides insight about future trends and needs with respect to hydrodynamic/sediment transport models.

The article further states, that in many hydraulic engineering applications, one has to resort to 3D Models when 2D models are not suitable for describing certain hydrodynamic/sediment transport processes.

Under the Three-Dimensional Model heading it is explained that most 3D models solve the continuity and Navier-Stokes equations, along with the sediment mass balance equation through the methods of finite difference, finite element, or finite- volume. The Reynolds average Navier-Stokes (RANS) approach has been employed to represent the governing equations. The RANS models can be separated into hydrostatic and non-hydrostatic models. The hydrostatic models, like Delft3D, are not able to accurately predict flow and transport phenomena in regions where there is strong curvature of flow in the vertical plane, but it is accurately predicting effects of curvature in the horizontal plane.

At the time the article was written the following statement was included: “As a result, 3D models should be used to simulate flow in smaller scales where detailed mapping of turbulent microstructure is required. This finding goes hand in hand with the realization that the use of 3D models to simulate basin-scale processes may not be realistic because it currently is a very costly endeavor at the present.”

Since January 2008, when this article was published, the utilization and implementation of Delft3D has become not only possible for a larger domain as the Lower Mississippi River but has also become feasible due to its free distribution and parallelization of codes.

2.2.4 West Bay Sediment Diversion Effects

One of the earliest modeling studies was conducted by Spasojevic and Holly in 1994 called “Three-Dimensional Numerical Simulation of Mobile–Bed Hydrodynamics”. This study used CH3D, a USACE sponsored program, which has similar capabilities to Delft3D. This model was applied at Older River Control Complex and West Bay (Spasojevic & Holly 1994).

The presentation titled: *"West Bay Sediment Diversion Work Plan Task 1 : Data Collection and Analysis"* dated September 2, 2009 by Thad Pratt, USACE, Engineer Research and Development Center (ERDC) highlighted the data collection and analysis performed for the West Bay Sediment Diversion Project. The data analysis presented concluded that ~45% of the total discharge is lost to the multiple cuts from Venice to below Cubit's Gap, with approximately 50% of the suspended sediment leaving the main channel (Pratt 2009).

Also in 2009, Paul Kemp issued a Memorandum to the WFF Science Team titled: *ERDC West Bay Sediment Diversion Effects.*

This memorandum is highlighting the fact that the total suspended sediment concentration at Tarbert has declined by 33% between 1959 and 2005, but that the loss is predominantly within the fine sand (mud) fraction (<0.0625mm). However, the trends for mean annual load and the fine sediment load are not statistically different from zero, which is attributed in his memorandum to a statistically significant increase in mean annual water discharge at Tarbert that offsets the reduction in concentration.

The memorandum further states that suspended sediment transport, particularly for the coarse fraction, is cyclic, without being regular periodic. High and low periods tend to be interposed in multi-year groupings that suggest waves of sand moving out of upstream storage through the station. If storage areas are depleted, then even large floods will not move much sand.

An analysis of annual sediment accumulation or loss by reach between 1992 and 2004 was conducted and concludes that the identified depocenter near West Bay Diversion has shifted upstream and now includes the West Bay Diversion Reach. Kemp further states that this upstream shift was already underway prior to construction of the West Belle Diversion in 2009 based on the data investigated. While it is noted that adjustment to channel stabilization efforts took many years, but that the current channel responses

appear to be dominated by other regional factors, like relative sea level rise, which impacts depositional trends and changes in pass discharges.

In regards to impacts from relative sea level rise Kemp summarizes that an increase in base Gulf elevation of about 0.5 feet per decade should be expected to reduce sand transport through the lowermost Mississippi River downstream of Venice by causing deposition upstream in deeper areas that do not yet require dredging. In addition, it should be expected to observe that the more upstream distributaries increase in discharge at the expense of those located farther downstream.

Overall, the emphasis is that long term regional trends need to be considered when evaluating observed phenomena in addition to local management actions.

2.2.5 HEC-RAS Mississippi River Model

In 2010, Malory Davis published her Masters of Science Thesis *"Numerical Simulation of Unsteady Hydrodynamics in the Lower Mississippi River"* at the University of New Orleans, Louisiana.

In order to better evaluate river dynamics and changes within the Lower Mississippi River System an extensive HEC-RAS 4.0 1-D mobile bed numerical model was developed by Malory Davis (Davis 2010). Her abstract highlights the fact that alterations along the Mississippi River, such as dams and levees, have greatly reduced the amount of freshwater and sediment that reaches the Louisiana coastal area. To aid the analysis of proposed freshwater and sediment diversions the 1-D numerical model was developed, calibrated, validated by Ms. Davis and used to predict the response of the river to certain stimuli, such as proposed diversions, channel closures, channel modifications, and relative sea level rise.

Since HEC-RAS has limitation on sediment evaluations other models were developed utilizing the already calibrated HEC-RAS model configurations, inputs and outputs.

2.2.6 Numerical Modeling of the Lower Mississippi River

In 2011, Joao Pereira published his Ph.D. Dissertation *"Numerical Modeling of River Diversions in the Lower Mississippi River"* at the University of New Orleans, Louisiana.

Dr. Pereira states in his research that numerical modeling of hydrodynamics and sediment transport of the Mississippi River is a useful tool to evaluate restoration projects and to improve our understanding of the resulting River response. Therefore, the emphasis of his study was on the fate of sand in the river and the distributaries.

His research utilized the 3-D unsteady flow mobile bed model ECOMSED to analyze the Lower Mississippi River between Belle Chasse (RM 76) and downstream of Main Pass (RM3) for a weekly time scale as well as the 1-D unsteady flow mobile bed model CHARIMA for monthly time scale evaluations. The model evaluated the introduction of new diversions at different locations with different geometries and outflows. The simulated diversions varied from 1,000cfs to 200,000cfs. The model showed that smaller diversions had little impact on the downstream sand transport but large diversions had the following effects:

1) reduction in slope of the hydraulic grade line downstream of the diversion;
2) reduction in the available energy for transport of sand along the distributary channels;
3) reduced sand transport capacity in the main channel downstream of the diversion
4) increased shoaling downstream of the diversion; and
5) a tendency for erosion and possible head-cutting upstream of the diversion

(Pereira 2011)

Also in 2011, Matthijs Bos published a Final Report on the *Morphological Effects of Sediment Diversions on the Lower Mississippi River* (Bos 2011). Mr. Bos developed a 2-D model in Delft3D to model hydro- and morphodynamic behavior between Point a la Hache and the mouth of the river. Sediment boundary condition was based on the equilibrium option of Delft3D, since sediment data was not available for the chosen upstream boundary.

The conclusions state that having a diversion in a reach requiring dredging negatively influences dredging activities. The closure of West Bay is given as an example, which was calculated to reduce dredging requirements by 10%.

Simulations of new diversions endorse the method of using a control structure for the sediment diversion. As a result of the simulations, it was assumed that a control structure would positively influence dredging activities, since it allows for closure of the diversion during low flow times, which also positively impacts the navigable depth. Diverting sediment during low flow would not have much effect, because of the low sediment transport rates.

The conclusions further state that extracting flow and sediment further upstream has beneficial effects compared to extracting flow and sediment right above HOP. Flow, or river energy, is optimally used to transport sediment in these upstream locations instead of depositing in unwanted locations. Therefore, delta building capability is increased in these upstream diversion locations.

(Bos 2011)

In 2015, Steven Ayres published his research *"A Simulation of the Mississippi River Salt Wedge Estuary Using a Three-Dimensional Cartesian Z Coordinate Model".* The research stated that the maximum absolute distance of saltwater intrusion observed anywhere in the world occurred on the Mississippi River in 1939 and 1940 when saltwater was observed approximately 225 km upstream from the mouth of Southwest Pass. The flow in the Mississippi River is stratified during low flow periods, since the heavier wedge of saline water extends upriver, and a buoyant fresh water plume extends into the Gulf of Mexico, past the Southwest Pass jetties. Currently, the USACE constructs a temporary subaqueous barrier in the river channel during droughts to prevent the wedge from migrating upstream.

Ayres constructed a curvilinear grid representative of the modern Mississippi River delta. Boundary conditions were developed for the drought year of 2012 and the grid was tested in order to evaluate the salinity intrusion and sediment transport capabilities of the Cartesian Z-coordinate Delft3D code. The Z-model proved to have the ability to propagate the saline density current as observed in the prototype. The sigma coordinate option produced very high numerical diffusion, which made it difficult to accurately model stratified flow; this was also observed by Cornelissen in 2004. Cornelissen's research also confirmed that sigma coordinate models accurately implement shear stresses near the bottom and near the free surface and accurately describes typical boundary layer processes with sloping as well as horizontal topography (Cornelissen 2004).

Ayres concludes his research with a statement that a model capable of analyzing all of the major processes affecting fine sediment transport within the Mississippi River salt wedge estuary has been developed under his research with the ability to reproduce the seasonal saline density current and its effect on sedimentation within the turbidity maxima as well as sedimentation characteristics in a fully turbulent shear flow.

(Ayres 2015)

2.2.7 Mississippi River Hydrodynamic and Delta Management (MRHDM) Study

Another long term effort undertaken to further enhance the knowledge as well as the prediction tools for hydrodynamic and morphologic changes in the Mississippi River, it's distributaries and potential future diversions is the Mississippi River Hydrodynamic and Delta Management (MRHDM) Study, which was initiated by the U.S. Army Corps of Engineers (USACE) and the State of Louisiana's Coastal Protection and Restoration Authority (CPRA) Board. The MRHDM Study is the first large-scale, long-term restoration assessment investigated under the LCA Program, as authorized under Section 7003 of the Water Resource Development Act (WRDA) 2007. The study intend is to identify and evaluate a combination of large-scale management and restoration features to address the long-term sustainability of the lower Mississippi River Deltaic Plain, and to balance the interests of ecosystem restoration, flood risk reduction and navigation.

The MRHDM study domain includes the Mississippi River from Vicksburg to HOP. In addition to the lower Mississippi River the study area includes the surrounding deltaic regions. The hydrodynamic study effort focuses on the Mississippi River, see Chapters 2.2.7 & 2.2.8, while the delta management study effort focuses on the adjacent basins. (MRHDM 2017)

Other models were developed as part of the MRHDM Study, which included the AdH-SedLib Multi-D Model developed by Brown et al., Delft3D-2D Version by Meselhe et al. at TWIG, FVCOM Model by Ioannis Georgiou at UNO and the HEC-6T Model by Tony Thomas and BCG. (Richards 2014)

2.2.8 Delft 3D Model Development for the Lower Mississippi River

In 2014, Terán González published Masters of Science Thesis *"3-D Hydrodynamic and Non-Cohesive Sediment Transport Modeling in the Lower Mississippi River"* at the University of New Orleans, Louisiana, which was part of the comprehensive MRHDM Study efforts. The purpose of this research was to develop a 3-D numerical model with sigma coordinates on the Lower Mississippi River to simulate hydrodynamics and non-cohesive sediment transport. Chapter 2.4 - "Delft3D Formulation" of the thesis

documents all applicable equations utilized by the program for this regional Mississippi River Model. Delft3D uses the shallow water wave equations, which are based on the continuity, lateral & longitudinal momentum equations and the hydrostatic assumption for the vertical pressure.

Figure 2.2.7.1 shows the modeling domain and boundaries along the MRHDM model domain.

Figure 2.2.7.1: Boundaries along the MRHDM Model Domain (Terán González 2014)

The study reach extended from Bonnet Carré Spillway (RM 127) to Head of Passes (RM 0). This model River domain is characterized by a complex distributary system that connects the Mississippi River to the Gulf of Mexico. The boundary conditions were: water levels in the Gulf and Head of Passes; and discharges upstream. Several periods of high discharge were simulated to compare water level, discharge, velocity profiles

and sediment transport with measurements and accomplish calibration and validation of the model. A calibrated 3-D model has been developed with the following %RMSE: 5% for stage; 6% for discharge; and 5% for sand load (Terán González 2014).

The downstream end, Head of Passes (RM 0), and outlets (Main Pass, West Bay, Baptiste Collette, Grand Pass + Tiger Pass, Fort St, Philip and Bohemia Spillway) boundary conditions consist on daily stage values obtained from USACE data (USACE:rivergages, 2012) and NOAA data (NOAA:Tides&Currents, 2012). The outlets data corresponds to data at the Gulf of Mexico for the corresponding periods (Terán González 2014).

2.2.9 Regional Delft 3D Model

In 2017, McCorquodale et al. finalized a report titled *"Development of a Regional 3-D Model for the Lower Mississippi River"* for CPRA. Authors included Alex McCorquodale, Sina Amini, Grecia Teran, Tshering Gurung, Sean Kenny and Ahmed Gaweesh from the University of New Orleans as well as Joao Pereira and Ehab Meselhe, from The Water Institute of the Gulf (TWIG).

The objective of the regional MRHDM model (see Figure 2.2.5.1) and its development was to evaluate the hydrodynamic and morphological responses of the River to sediment diversions.

The model has lateral grid sizes of the order of 50 m with 10 parabolically distributed sigma layers with refinement at the bed, which allows for a more accurate representation of the shear stress at the bed.

The lateral resolution of the grid was adjusted from approximately 100 meters to 50 meters. It was found that the secondary flow and the observed recirculation eddy in Dr. Mead Allison's Acoustic Doppler Current Profiler (ADCP) (Meselhe et al 2012) data were reproduced in the model with a 50 meter lateral cell size (McCorquodale et al. 2017). This observation is consistent with the grid conversion study conducted by

Pereira (2011), who found a grid size between 25 and 50 meters was sufficient to produce spatially stationary velocity patterns.

The Van Rijn 1984 sand transport model was used for the non-cohesive sediment transport. The model was calibrated and validated using the high flows in 2008 and 2011. The model calibration was based on using stage boundary conditions at all of the major outflows with distributary rating curves from the West Bay Study/USACE, Dr. Mead Allison/The Water Institute of the Gulf (TWIG) and the Lake Pontchartrain Basin Foundation (LPBF). The model was re-calibrated using the flow measurements that were taken during the January 2016 flood by TWIG and USACE (McCorquodale et al. 2017).

Based on an analysis of morphological factors (MORFAC) conducted as part of the Development of a Regional 3-D Model for the Lower Mississippi River (McCorquodale et al. 2017) it appeared that a MORFAC of 40 would yield the best compromise between turn-around and accuracy of the morphological predictions. The results of the analysis indicated that a factor of 40 would yield deposition results that were consistent with a factor of 1, while significantly improving computational speed. As part of the analysis, the one year TWIG hydrograph was selected and duplicated 5-times for 5-year production runs (McCorquodale et al. 2017). The ‘long model’ was calibrated by McCorquodale et al (2017) for stage, using the USACE gaging stations, for flow and velocity distribution, using data from Dr. Mead Allison and the USACE, and sand transport, using USGS data and local data collected by Dr. Mead Allison and TWIG.

Based on all the development made to date in establishing a functional, calibrated and validated Delft 3D Model as part of the MRHDM Study and academic research, it was possible to further modify the existing MRDHDM Model and shorten it for computational improvements as well as to allow the establishment of a domain focused on morphologic changes below Belle Chasse. The model domain was reduced end the upstream boundary conditions were based on Belle Chasse time series for discharge and sediment input.

The shortmodel was severed from the long model at Belle Chasse extending to Head of Passes (HOP). The roughness and bathymetry were maintained in the new reach (shortmodel). The shortmodel was then validated to ensure that stage, flow distribution and sand transport of the long model were retained. Validation used the USACE River Gages data for stage validation as well as the calibration and validation data for the sand transport and flow distribution from the Regional Model (McCorquodale et al. 2017).

3.0 CHAPTER 3: RESEARCH PLAN

3.1 BACKGROUND

3.1.1 The Different Types of Sediment Load

Bed Load

Non-cohesive bed particles enter motion as soon as the shear stress applied on the bed material exceeds the critical shear stress. Generally, silt and clay particles enter suspension and sand and gravel particles roll and slide in a thin layer near the bed called the bed layer. Bedload, or contact load, refers to the transport of sediment particles that frequently maintain contact with the bed.

Suspended Load

As the hydraulic forces exerted on sediment particles exceed the threshold conditions for impending motion, coarse sediment particles move in contact with the bed surface, as described above. Finer particles are brought into suspension when turbulent velocity fluctuations are sufficiently large to maintain the particles within the mass of fluid without frequent bed contact.

Suspended Load + Bed Load = Total Load of the Stream (see Figure 3.1.1.1)

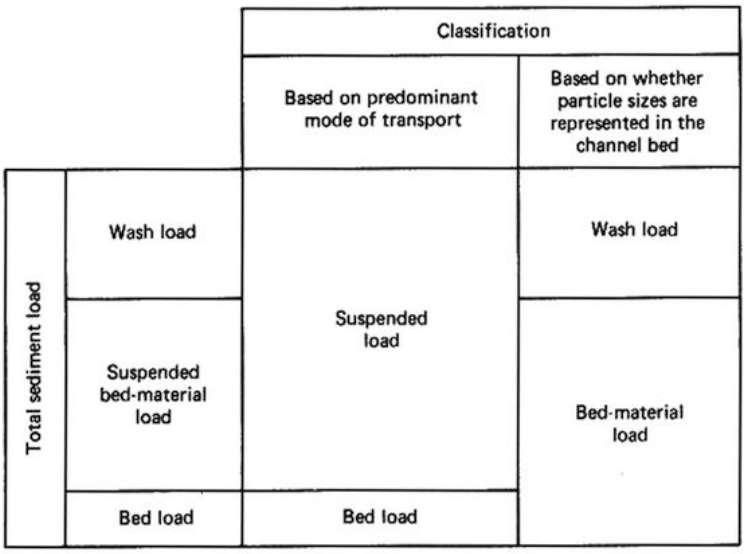

Figure 3.1.1.1: Relationship between the Two Classifications of Sediment Load (http://apo.sdu.edu/cive530_lecture_17b.html)

The sediment properties of the five (5) utilized sediment classes are described in Table 3.1.1.1. The silt and clay classes were included because the regional model study showed that the presence of fines resulted in a significant change (up to 40%) in the modeled sand load (McCorquodale et. al. 2017). In addition, the fines impact the annual erosion and deposition regime.

Table 3.1.1.1: Sediment Properties utilized in Delft3D Model

Sediment Class	Acronym	D_{50} [mm]	S_s	Bulk Density [kg/m^3]	Settling Velocity (fresh water) [m/s]	Bed Shear Stress (deposition) [Pa]	Bed Shear Stress (erosion) [Pa]
Clay	Clay	N/A	2.7	500	2.75E-06	0.1	0.1
Silt	Silt	N/A	2.7	500	7.10E-04	0.1	0.1
Very Fine Sand	VF	0.0917	2.7	1600	VanRijn 1984	Shields	Shields
Fine Sand	F	0.1833	2.7	1600	VanRijn 1984	Shields	Shields
Medium Sand	M	0.3667	2.7	1600	VanRijn 1984	Shields	Shields

The sediment concentration at the Belle Chasse boundary was developed based on the flow record of the applied hydrograph and the dynamic rating curve (see Section 3.1.3).

3.1.2 Trend Analysis of Mississippi River Discharges

In order to accurately predict discharge trends for modeling the future it is important to understand the historic trends, especially in a system that has been altered by levees, dams and flood control structures as the Mississippi River has. Figure 3.1.2.1 indicates the Project Design Flood as well as the various control points and/or flood control locations like the Bonnet Carré Spillway.

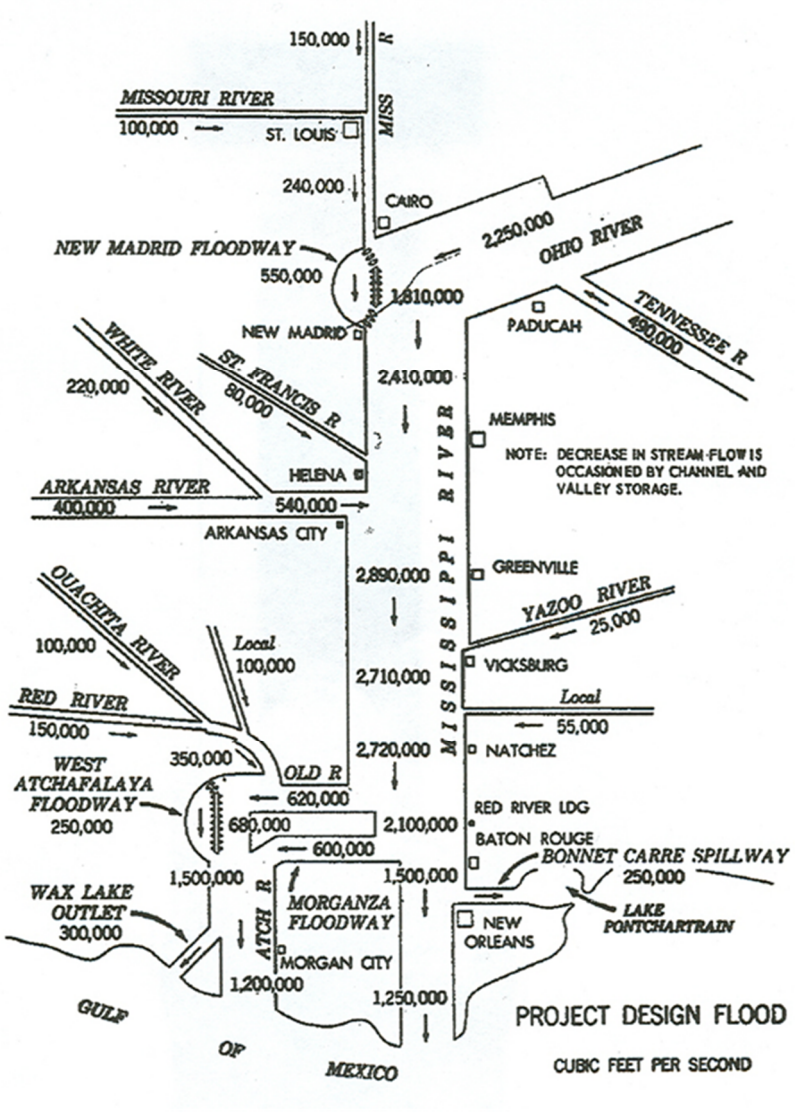

Figure 3.1.2.1: Mississippi River Project Design Flood (Reins 2005)

River gauges along the Mississippi River are monitored by the USACE and discharge data is publicly available at http://rivergages.mvr.usace.army.mil/WaterControl.

The start-up of the Old River Control Structures in 1963 altered the discharge regime of the Lower Mississippi River to a 70%/30% split and prevented unregulated flow from the Mississippi to the Red-Atchafalaya system. A history of the Old River Control Complex (ORCC), and the nearby river gages is documented it the Master's Thesis *"Sediment Investigation in the Vicinity of the Old River Complex: Red River above Old River Outflow Channel"* (Reins 2005). Figure 3.1.2.2 depicts the locations of the river gages

near the ORCC, which includes Tarbert Landing, which was utilized for the trend analysis described in this chapter.

Figure 3.1.2.2: Mississippi River Gage Locations near Old River Control (Reins 2005)

Question 1: Is there a trend of increase in Mississippi River Discharge from 1960 to today?

The discharge data for Tarbert Landing was extracted from the USACE RiverGages website (www.rivergages.com) for analysis. A Mississippi River discharge plot for Tarbert Landing was generated for the time period between 1930 and 2017 (Figure 3.1.2.3) and for the time period between 1960 and 2017 (Figure 3.1.2.4).

The two graphs show that the general increasing trend for the period from 1930 to 2017 is steeper than the increase for the shorter period from 1960 to 2017. However, both periods indicate an increase in the mean flow. One potential explanation could be an increase in participation within the watershed due to climate change.

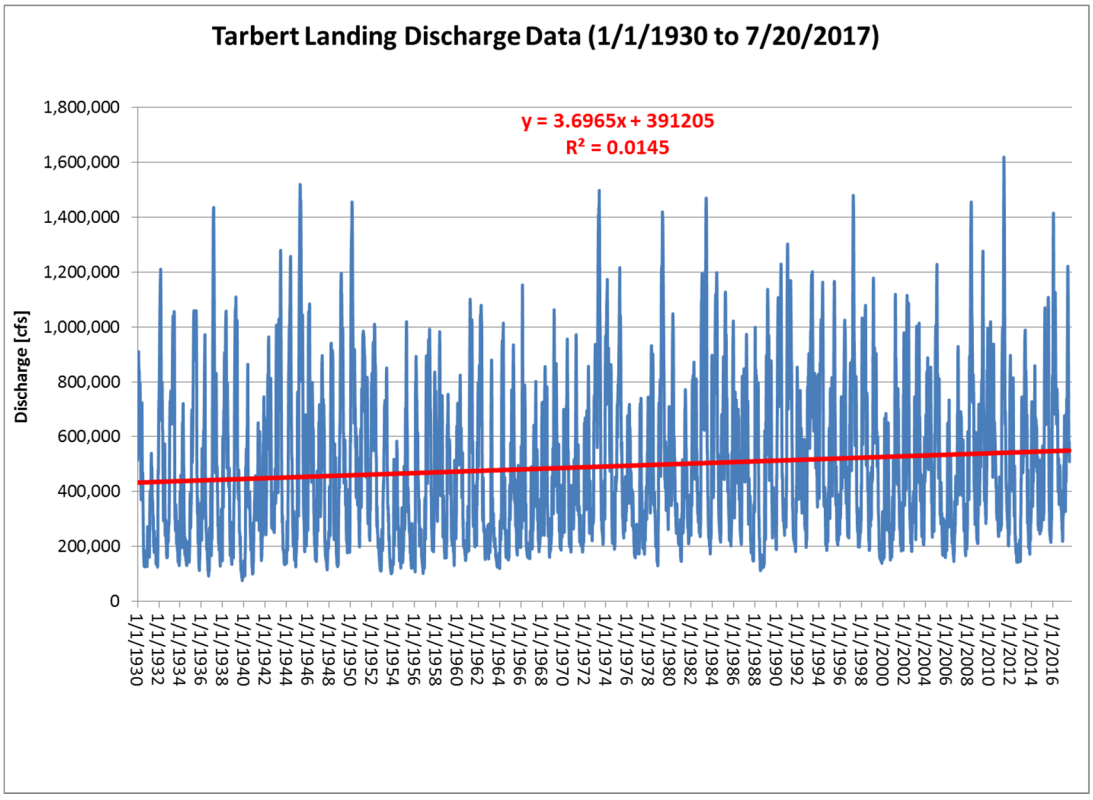

Figure 3.1.2.3: Tarbert Landing Discharge Data (1/1/1930 to 7/20/2017)

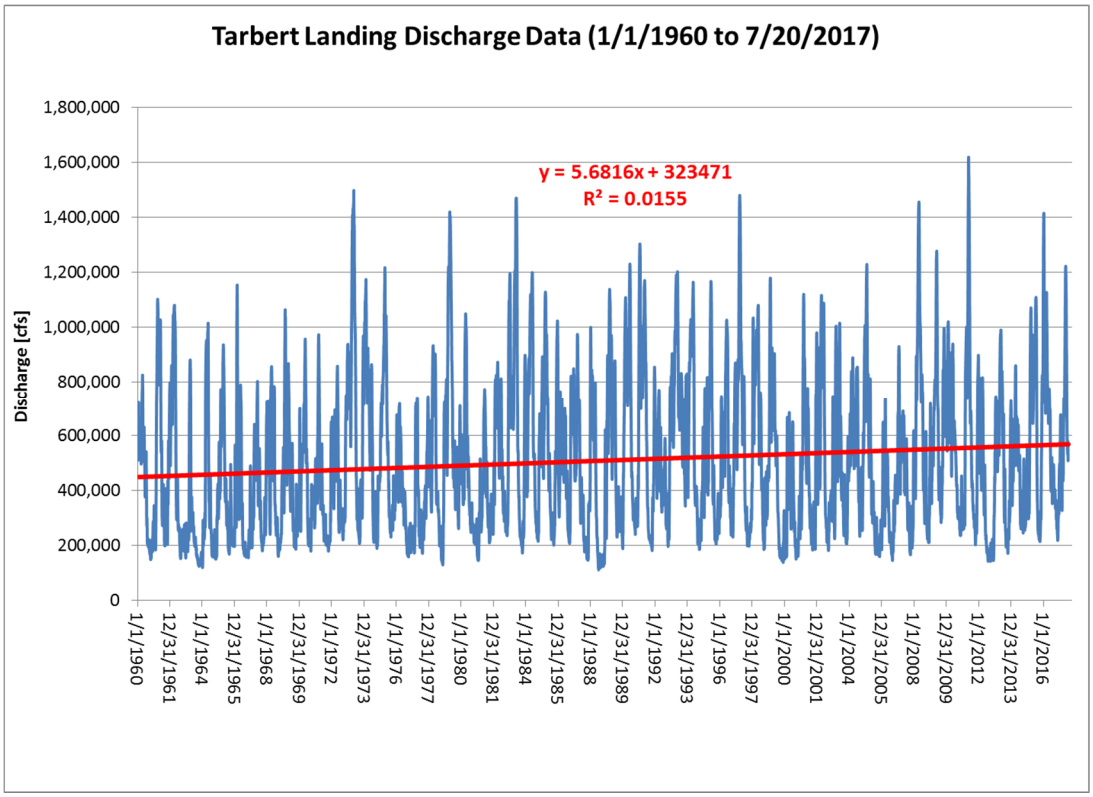

Figure 3.1.2.4: Tarbert Landing Discharge Data (1/1/1960 to 7/20/2017)

To analyze trends in discharge, the exceedance above key discharge values were evaluated for different periods. Key discharge values selected at Tarbert Landing were 600,000cfs, at which flow the anticipated diversions are proposed to be opened (McCorquodale et al. 2017) and 1,000,000cfs, which is a river peak nearing the maximum design flood of 1,250,000cfs. Figures 3.1.2.4 and 3.1.2.6 show the incremental flow above 1,000,000cfs and 600,000cfs at Tarbert Landing respectively for the time period 1/1/1930 to 7/20/2017. Figures 3.1.2.5 and 3.1.2.7 show the incremental flow above 1,000,000cfs and 600,000cfs at Tarbert Landing respectively for the time period 1/1/1960 to 7/20/2017.

For both incremental flows, the later time period results in a steeper incline for the longer period (1930 to 2017) than the more recent period (1960 to 2017). In any case an incline in exceedances can be observed.

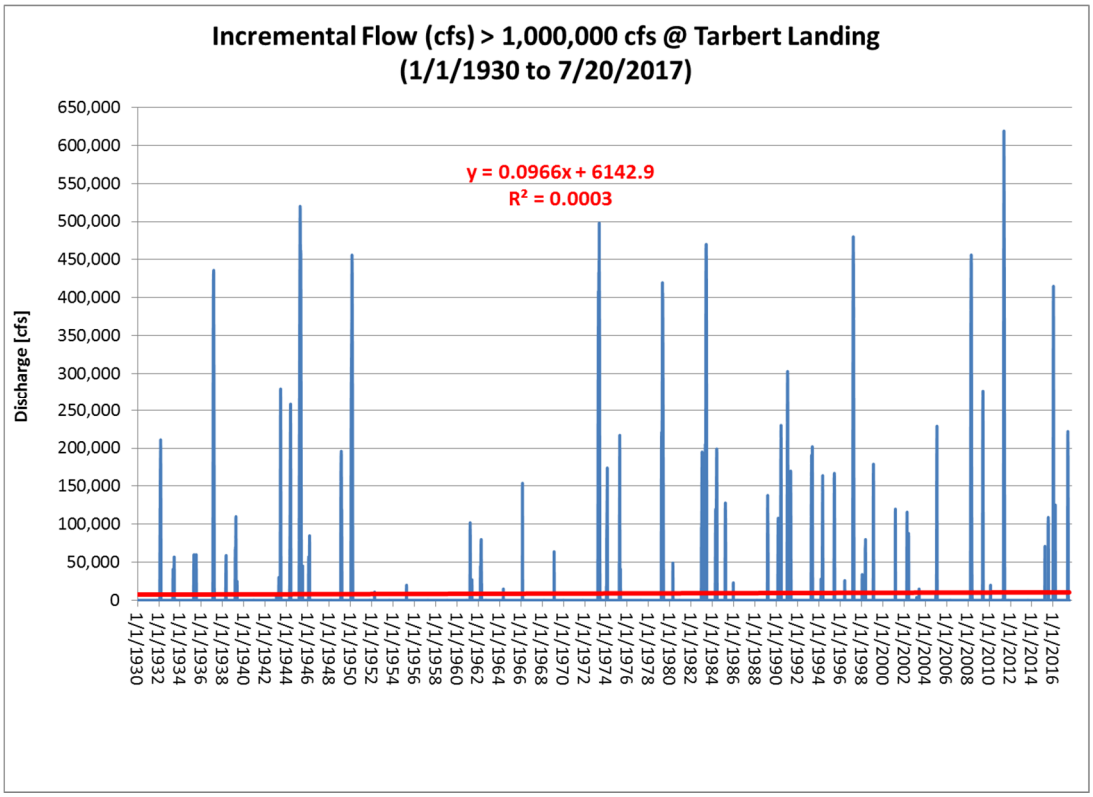

Figure 3.1.2.5: Incremental Flow (cfs) > 600,000 cfs at Tarbert Landing (1930-2017)

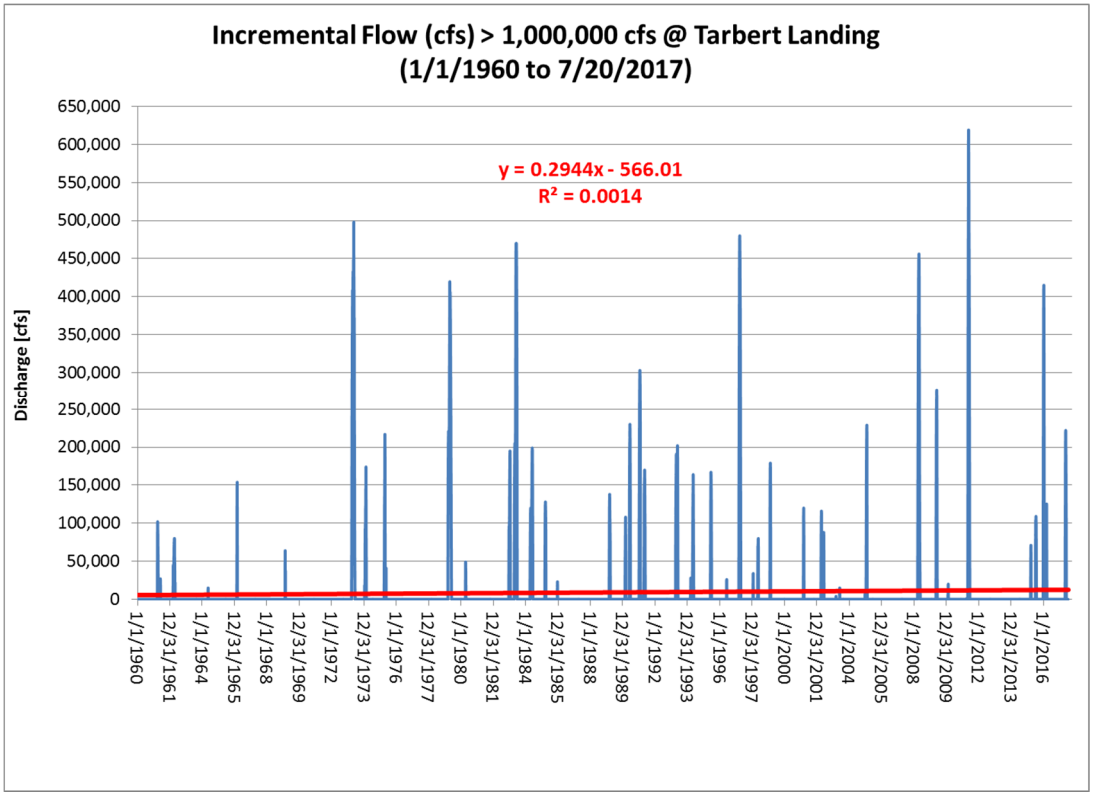

Figure 3.1.2.6: Incremental Flow (cfs) > 600,000 cfs at Tarbert Landing (1960-2017)

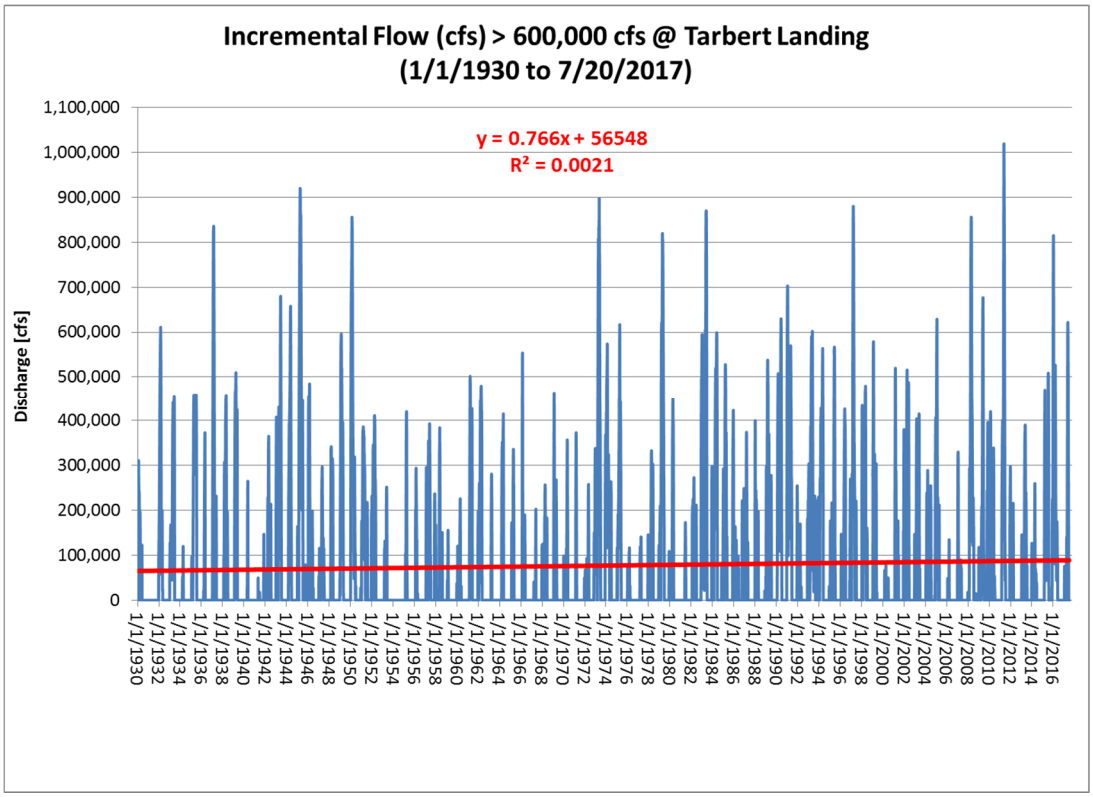

Figure 3.1.2.7: Incremental Flow (cfs) > 1,000,000 cfs at Tarbert Landing (1930-2017)

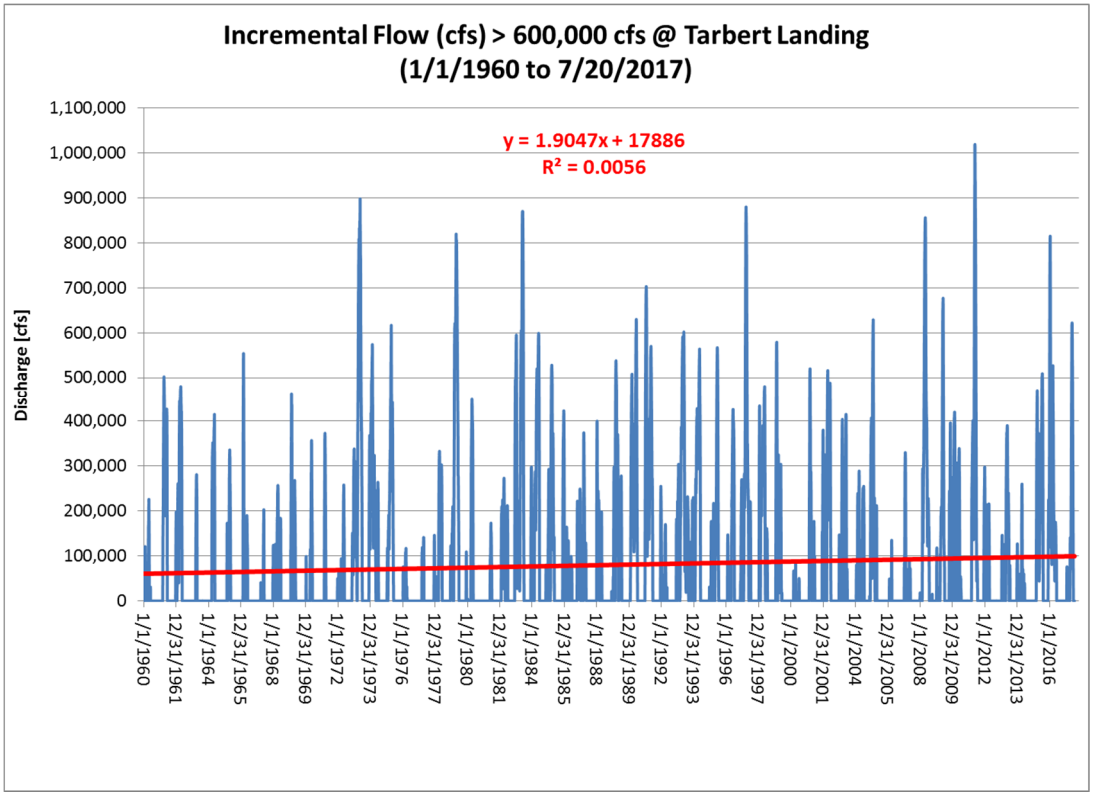

Figure 3.1.2.8: Incremental Flow (cfs) > 1,000,000 cfs at Tarbert Landing (1960-2017)

To further analyze for a discharge trend pattern and historic changes, four time periods were established as listed in Table 3.1.2.1, which lists the days of discharge exceedance for four key discharge values, 600,000cfs, 800,000cfs, 1,000,000cfs and the design flood 1,250,000cfs. Figure 3.1.2.9 depicts the days of discharge exceedances at Tarbert Landing for four (4) 15-year periods and Figure 3.1.2.10 depicts the percentage of discharge exceedance at Tarbert Landing for four (4) 15-year periods. While it can be noted that the first period from 1957 to 1972 had no exceedances greater than 800,000cfs, there is no significant pattern that can be observed in the exceedances evaluation.

Table 3.1.2.1: Days of Exceedance in 15Year Time Periods:

Period	Start Date	End Date	Days of Exceedance			
			> 600,000	> 800,000	> 1,200,000	> 1,250,000
1	7/15/1957	7/14/1972	1147	426	0	0
2	7/15/1972	7/14/1987	1963	992	147	114
3	7/15/1987	7/14/2002	2190	1205	60	42
4	7/15/2001	7/17/2017	1946	882	113	86

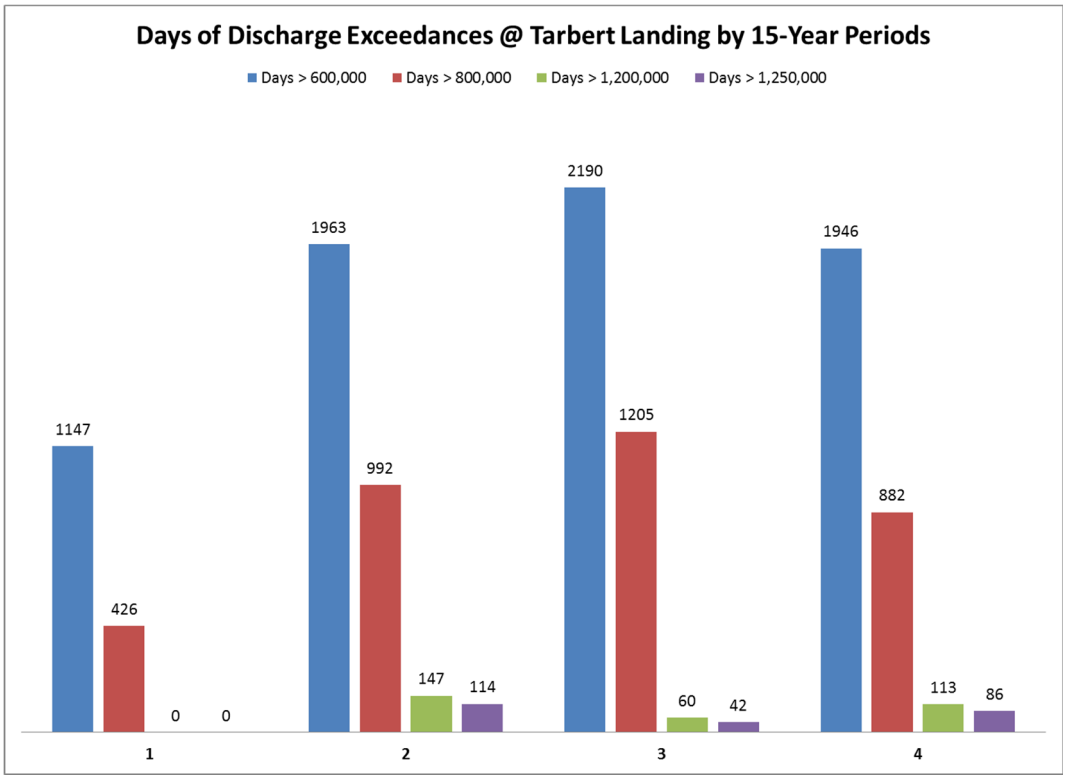

Figure 3.1.2.9: Days of Discharge Exceedances at Tarbert Landing by 15-Year Periods

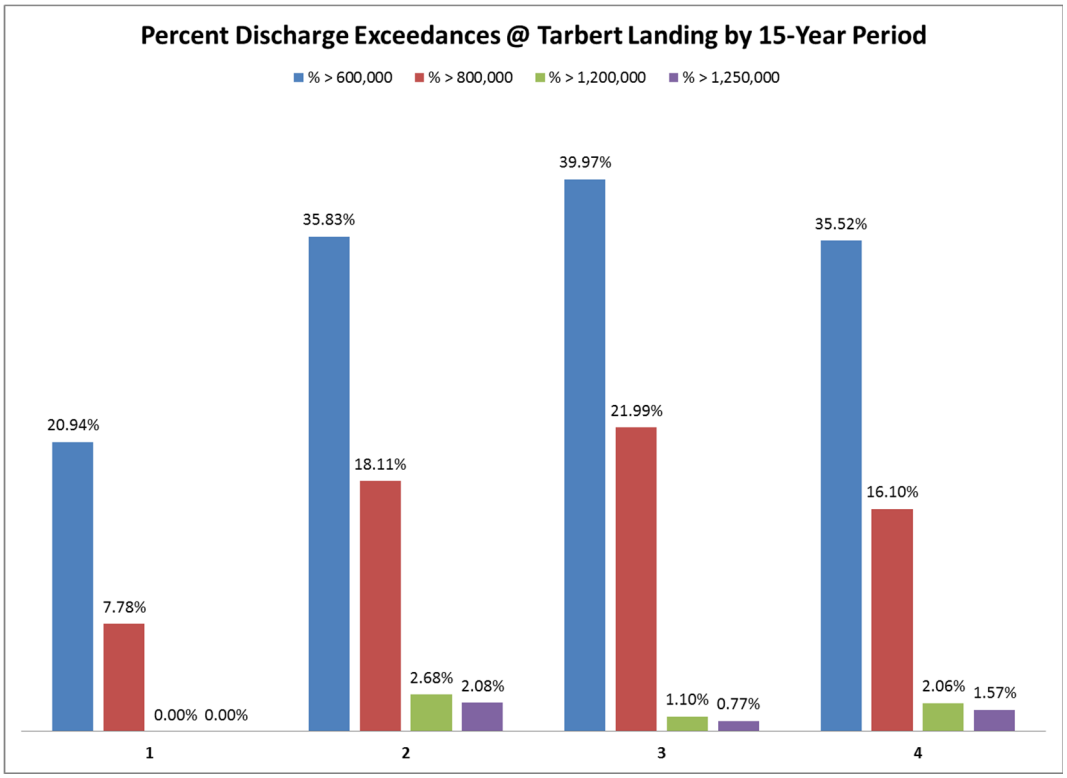

Figure 3.1.2.10: Percent Discharge Exceedances at Tarbert Landing by 15-Year Periods

In summary, there is no apparent significant trend in peak flows since 1957.

Discharge entering the lower Mississippi River in the future can be assumed to follow historic patterns as observed in the past 60 years. Discharge in access of 600,000 and 800,000 cfs, which are triggering numbers for potential diversion openings, do not show an apparent trend or change in duration.

Question 2: Is there a trend of increase in peaks requiring more frequent openings of the Bonnet-Carré Spillway?

Information about the operation of the spillway was gathered from USACE publications, including a brochure published in October 2014 by the New Orleans District titled "Bonnet Carré Spillway" and the USACE website:
http://www.mvnusace.army.mil/Missions/Mississippi-River-Flood-Control/Bonnet-Carre-Spillway-Overview/Spillway-Operation-Information/

The collected data on opening year, days opened, start and end day of opening, maximum bays opened and maximum cfs flow during opening was summarized in Table 3.1.2.2 below. Figures 3.1.2.11 depicts the days opened and maximum bays opened over time and Figure 3.1.2.12 analyzes the number of openings and total days opened for four (4) 20-year periods.

Since prior to 1963 the flow of the Mississippi River and the Atchafalaya River were not operated following the 70% to 30% split, the Mississippi flows were not subject to consistent diversions conditions, which could have resulted in larger flows within the Mississippi River, prompting openings at Bonnet-Carré Spillway. When excluding the first period (see Figure 3.1.2.12), the data could be interpreted as an increase in openings since 1963 or a particular high flow period in the last 20 years.

Table 3.1.2.2: Bonnet-Carré Spillway Operation (1937 to 2017)

Year	Days Openend	Start Day	End Day	Maximum Bays Opened	Maximum cfs
2016	22	01/10/16	01/31/16	210	203,000
2011	43	05/09/11	06/20/11	330	316,000
2008	28	04/11/08	05/08/08	160	160,000
1997	32	03/17/97	04/17/97	298	243,000
1983	35	05/20/83	06/23/83	350	268,000
1979	45	04/17/79	05/31/79	350	191,000
1975	13	04/14/75	04/26/75	225	110,000
1973	75	04/08/73	06/21/73	350	195,000
1950	38	02/10/50	03/19/50	350	223,000
1945	57	03/23/45	05/18/45	250	318,000
1937	48	01/28/37	03/16/37	285	211,000

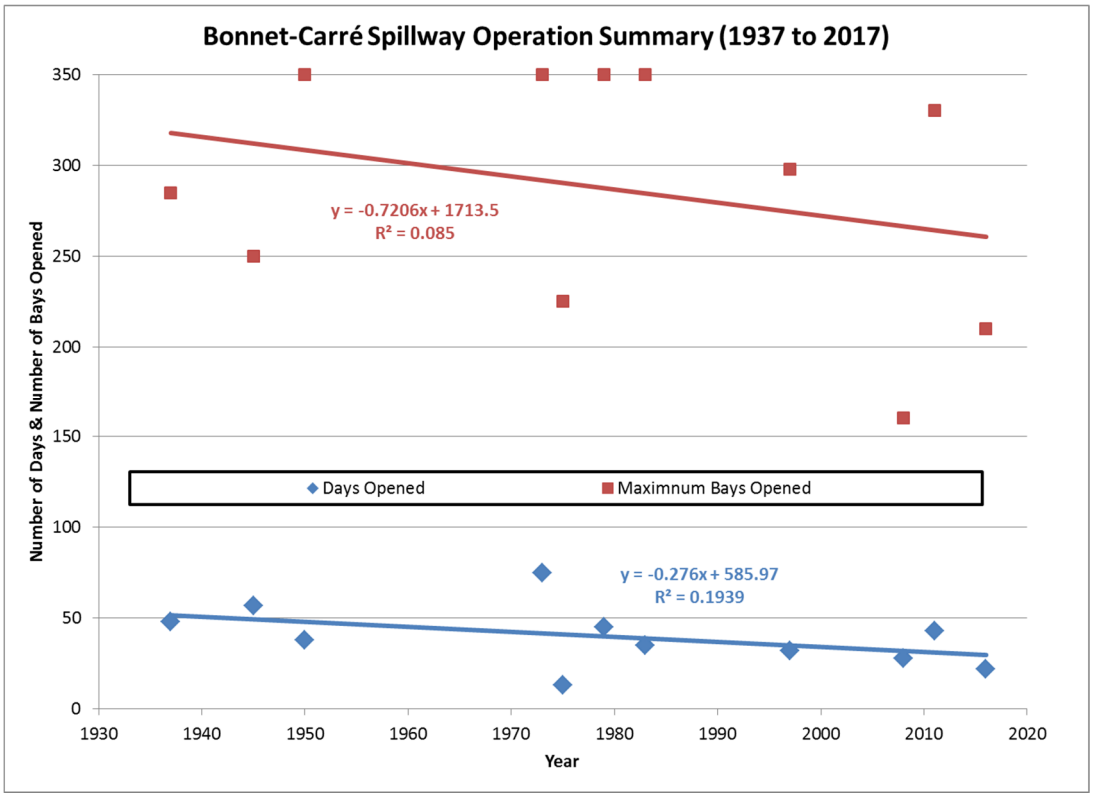

Figure 3.1.2.11: Bonnet-Carré Spillway Operation Summary (1937 to 2017)

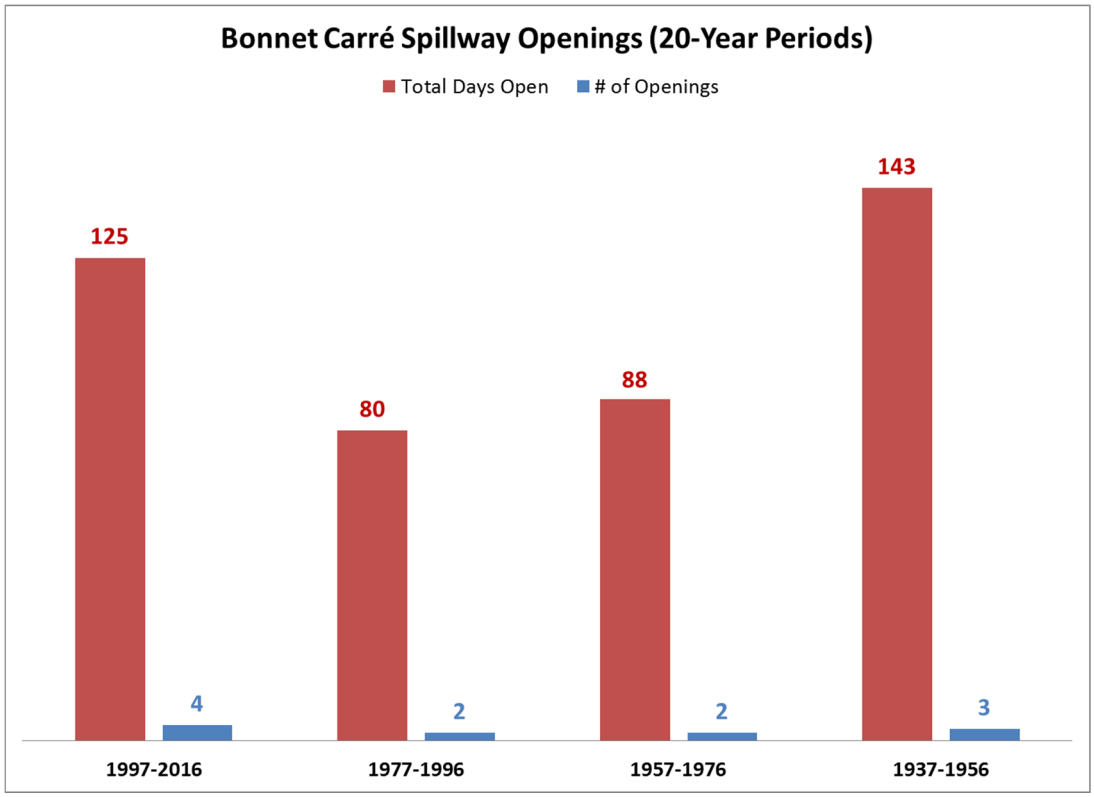

Figure 3.1.2.12: Bonnet-Carré Spillway Openings (20-Year Periods)

3.1.3 Variable Hydrograph Development

A variable annual hydrograph pattern was developed, which has similar flow probabilities to the existing uniform hydrograph, but variability in flow distribution from year to year. The uniform hydrograph currently used by the Water Institute of the Gulf (TWIG) for modeling associated with the MRHDM Study was used as the baseline hydrograph. A previously developed 10-year hydrograph (UNO) was utilized and the 1-year hydrograph from TWIG added at year 1 and 12. Hydrograph connection points were smoothed via interpolation. Then the 12-year variable hydrograph was modified to match flow probabilities of the 12-year uniform hydrograph for flows exceeding 600,000 cfs as well as 800,000 cfs. Figure 3.1.3.1 depicts the hydrographs in comparison.

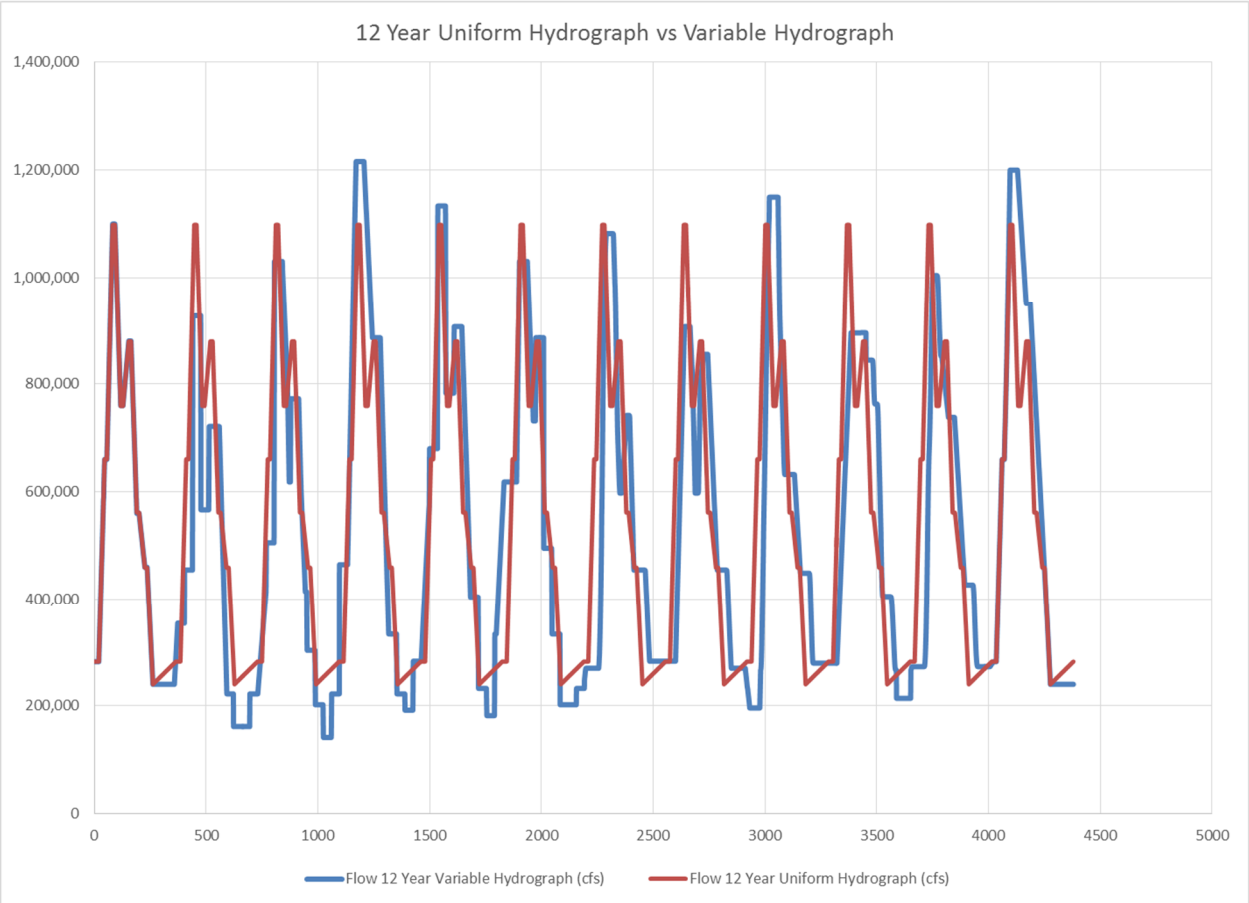

Figure 3.1.3.1: 12-Year Uniform Hydrograph versus Variable Hydrograph

The variable hydrograph compares as follows to the uniform hydrograph for the flow exceedances above 600,000cfs and 800,000cfs (See Table 3.1.3.1):

Table 3.1.3.1: Probability of Flow at Key Flow Rates for 12-year Uniform and Variable Hydrograph

Hydrograph	Probability at 600,000cfs mark	Probability at 800,000cfs mark
Uniform	39.99	23.00
Variable	40.10	23.10

To generate the 12 year input data files for Delft 3D, the flow data was entered in an adjusted time sequence to apply a MORFAC of 40. Therefore, 12 years equal 4,380 days or 6,307,200 minutes and are entered as 157,680 time steps. It is noted that the Delft 3D files are all set up in minutes for all time steps in the time series.

To answer this hypothesis, the first step is to prove that the flow duration curve of the uniform hydrograph is comparable to the flow duration curve of the developed variable hydrograph (see Figure 3.1.3.2). Therefore, the discharge Q at Belle Chasse was ranked from the highest to the lowest. For the 12-year timeline this equals 4,381 discharge values. The probability of each flow is calculated by dividing the rank by the total number of values. Then the probability (x-axis) is plotted versus the discharge (y-axis).

The compatibility will be determined by calculating the Root Mean Square Error (RMSE) and the Bias Error. Given the fact that the variable hydrograph will capture some of the higher and lower discharge values not included in the uniform hydrograph a RMSE of <10% is considered acceptable. For the Bias Error less than 1% is considered an acceptable value.

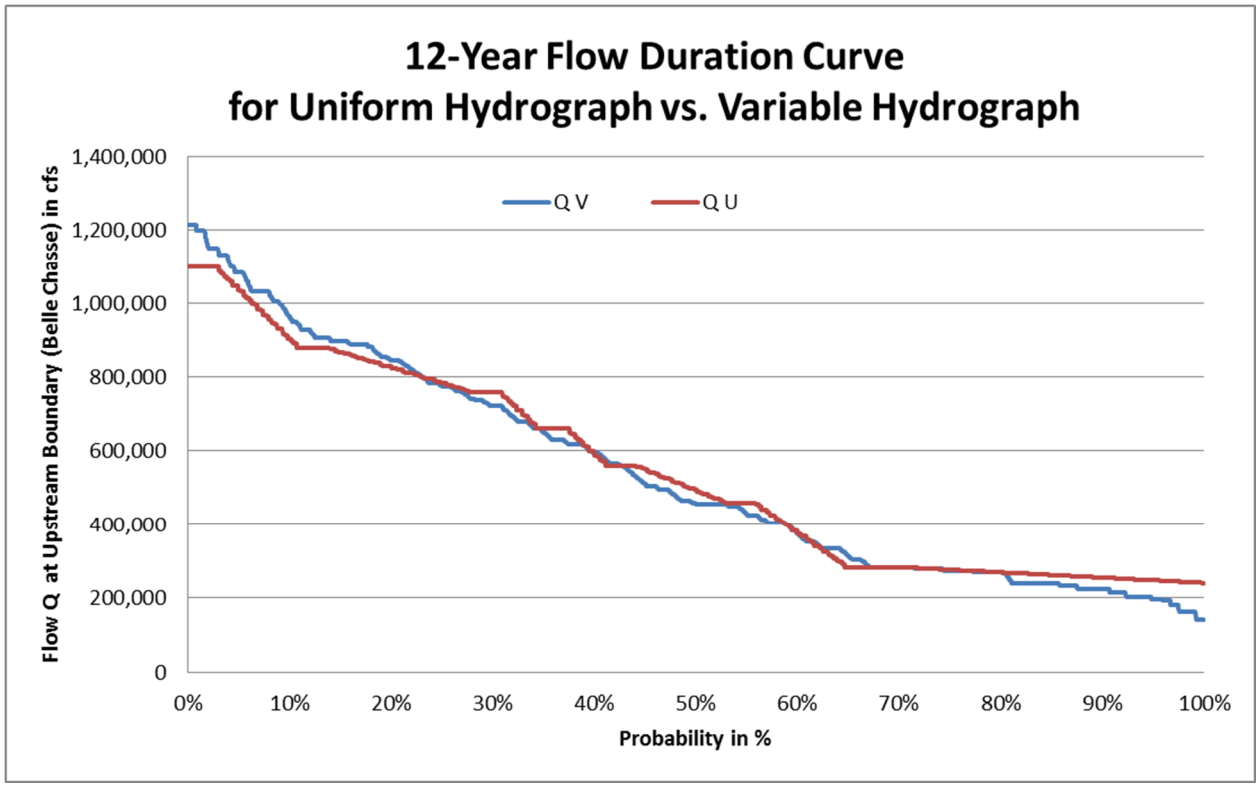

Figure 3.1.3.2: 12-Year Flow Duration Curve Comparison (Uniform vs. Variable)

The RMSE of the duration curve is 6.6%, which is primarily due to the fact that the uniform hydrograph does not capture the peak high and peak low values for flow.

The Bias Error of the duration curve comparison is -0.75% (Uniform = Base Case), which is less than 1 percent, which is considered acceptable.

Once the comparability is proven the average annual sediment captured by a diversion has to be compared for a model run utilizing the uniform hydrograph and a model run utilizing the variable hydrograph. A 48-year model run period was selected for this comparison. The 48-year hydrograph is representative of 4 sequential 12-year hydrographs as developed for comparison.

To fully compare capture, the available sediment in the river has to be compared upstream of the diversion to be evaluated.

The sand rating curve utilized for both, the uniform and variable hydrograph, was a dynamic rating curve given by McCorquodale et al (McCorquodale et al. 2017). The sand concentrations are in mg/L.

$$[3.1] \quad C_{sand} = \begin{Bmatrix} C_{sand\ High} for \frac{dQ}{dt} positive \\ C_{sand\ Low} for \frac{dQ}{dt} negative \end{Bmatrix} \left\{ \frac{3.5}{1+\frac{\langle Q \rangle_{12\ mo}}{\langle Q \rangle_{56\ yr}}} \right\} \left\{ \frac{3.5}{1+\frac{\langle Q \rangle_{3\ mo}}{\langle Q \rangle_{56\ yr}}} \right\}^{\frac{3}{4}}$$

$$[3.2] \quad C_{sand\ high} = 1.7327 * 10^{-4} Q_{cfs} - 5.580 * 10^{-11} Q_{cfs}^2 - 50.$$

$$[3.3] \quad C_{sand\ low} = 15.48667 * 10^{-5} Q_{cfs} - 6.48148 * 10^{-11} Q_{cfs}^2 + 13.$$

In which C_{sand} is the sand concentration, Q is the discharge in cfs. This equation accounts for the rising and falling limb as well as the past history of the discharges in the river.

One significant difference in utilizing the variable versus the uniform hydrograph is the associated sand load boundary condition at Belle Chasse (see Figure 3.1.3.3). The variable hydrograph has approximately 19% less sand input at the upstream boundary (Belle Chasse) over the modeled 48 year time period. The reason for the difference is that the dynamic rating curve accounts for rising and falling limbs and the flow history, which are different between uniform and variably hydrographs, even though the flow duration curves for both hydrographs are essentially the same, as previously determined. The flow history component of the equation 3.1 is the same for a repeating uniform hydrograph, while it varies over a 12-year cycle for the developed 12-year variable hydrograph.

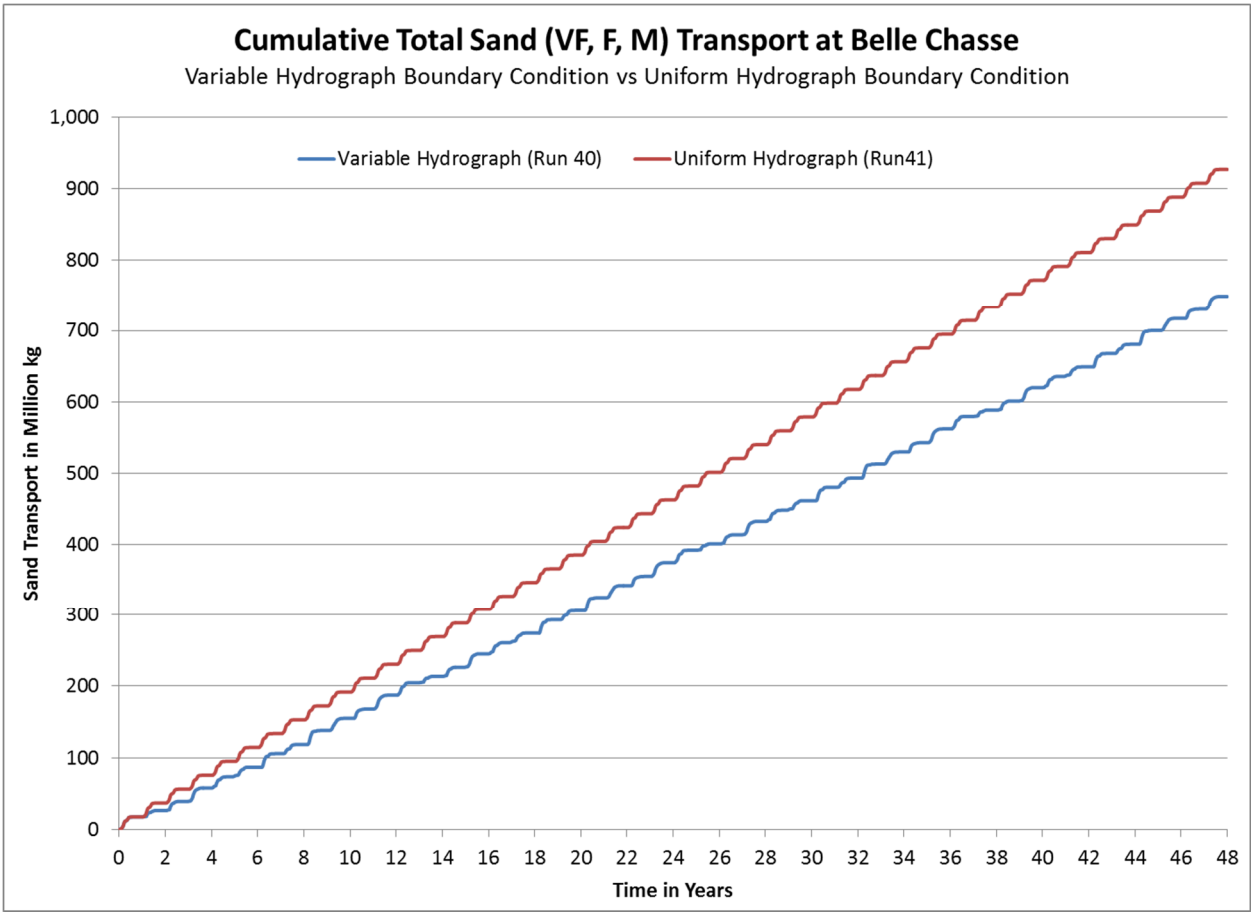

Figure 3.1.3.3: Sand Load Boundary Condition Comparison – Variable vs. Uniform

3.1.4 RESEARCH QUESTIONS

The following four (4) research questions were established to further the analysis conducted under this dissertation research:

- **R1:** Does the river have sufficient energy to divert the targeted discharges for the four (4) main diversion locations?
- **R2:** How does spatially variable Eddy Viscosity change impact the outcomes for cumulative sedimentation/erosion?
- **R3:** How does a system with no diversions respond to sea level rise (NRCIII Curve)? How does the response vary depending on Hydrograph?
- **R4:** How does change in sediment load impact morphologic changes?

4.0 CHAPTER 4: H1- VARIABLE VERSUS UNIFORM HYDROGRAPH IMPACTS ON BATHYMETRY

4.1 HYPOTHESIS

Hypothesis 1:

The equilibrium bathymetry is independent of the annual variability of the hydrograph, provided the flow duration curve is the same.

4.2 METHODOLOGY

The model runs summarized in Table 4.2.1 were set-up to obtain data in support of an evaluation of Hypothesis 1. Both runs cover a 48 year computational run time and utilize the uniform hydrograph as well as a repetition of the 12-year variable hydrograph.

Table 4.2.1: Model Runs for Hypothesis 1:

#	Hydrograph		Years	Diversions
	U	V		
40		X	1-48	None
41	X		1-48	None

Bathymetry changes can be represented by the change in deposition and erosion at a specific location along the river. Delft3D provides the option to extract cumulative erosion/sedimentation from the trim-***.dat file. A visual output highlighted that a difference in deposition at year 48 exists, which grants further evaluation. Figures 4.2.1 – 4.2.5 show the delta between the cumulative erosion/sedimentation results of the variable and the uniform hydrographs at various locations. To develop the images a variable was defined for the cumulative erosion/sedimentation output of Run 40

(Variable Hydrograph) and the output of Run 41 (Uniform Hydrograph), followed by a subtraction of these defined variables. The uniform case was subtracted from the variable case (Run 40-Run41).

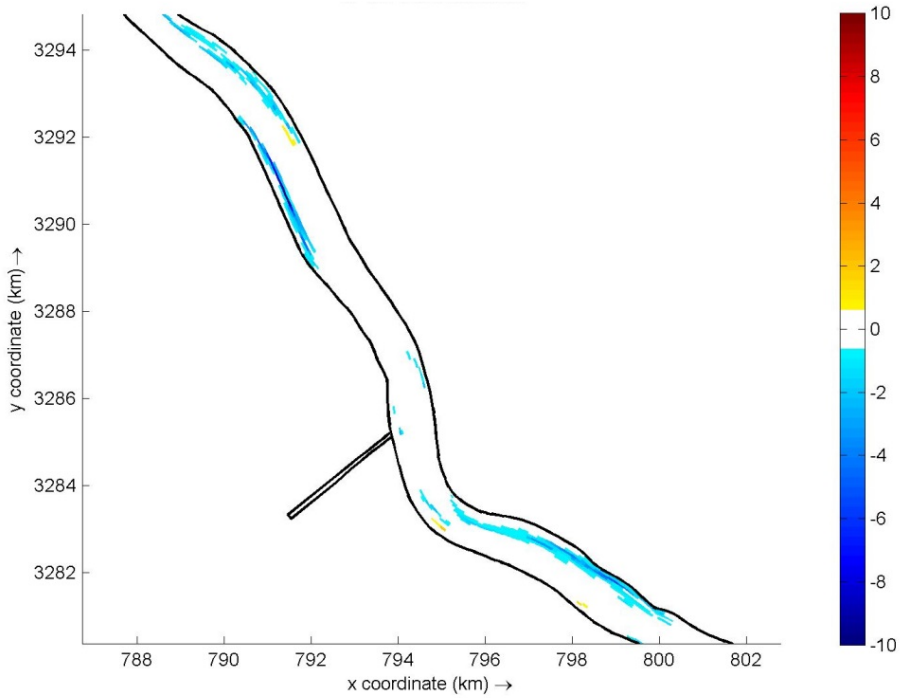

Figure 4.2.1: Delta (Variable – Uniform) in Cumulative Deposition [m] near Mid Barataria at Year 48

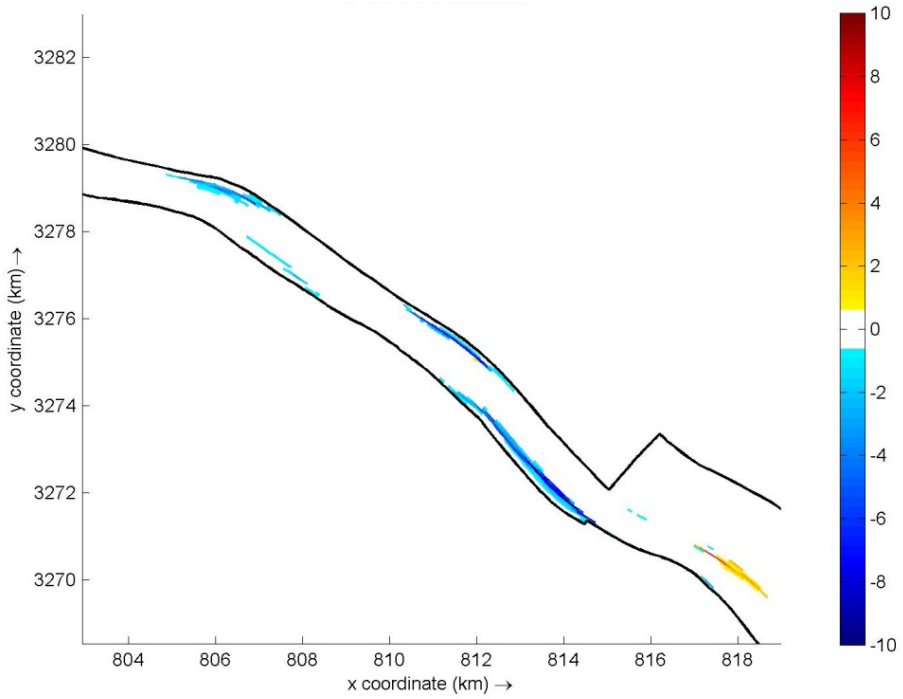

Figure 4.2.2: Delta (Variable – Uniform) in Cumulative Deposition [m] near WPAH at Year 48

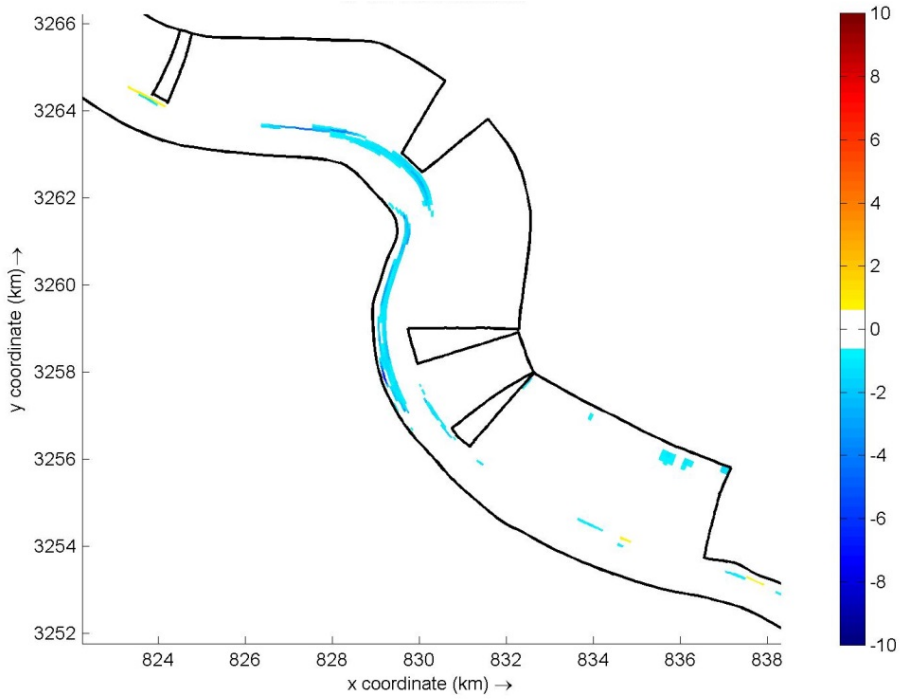

Figure 4.2.3: Delta (Variable – Uniform) in Cumulative Deposition [m] near Bayou Lamoque at Year 48

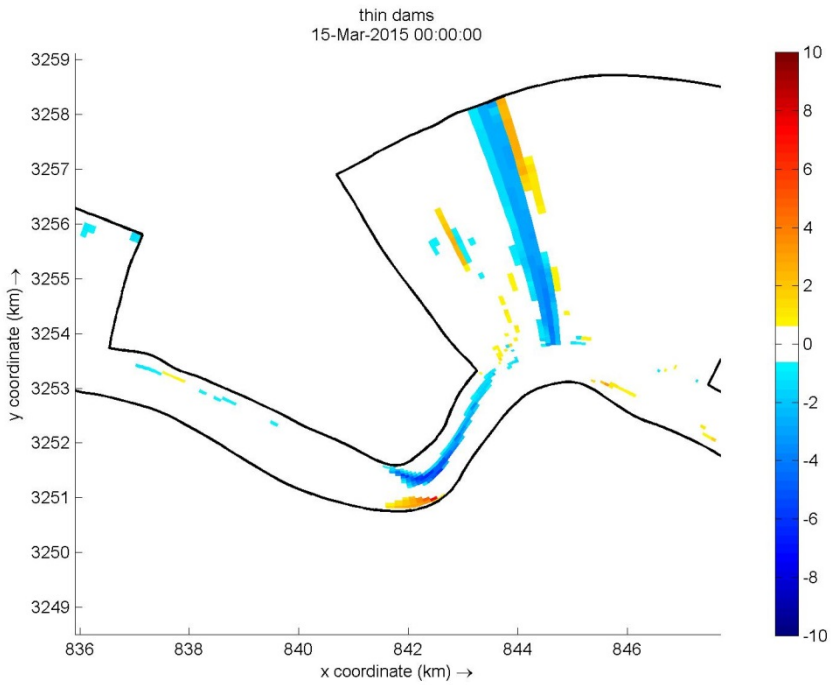

Figure 4.2.4: Delta (Variable – Uniform) in Cumulative Deposition [m] near Upstream Fort St. Phillip at Year 48

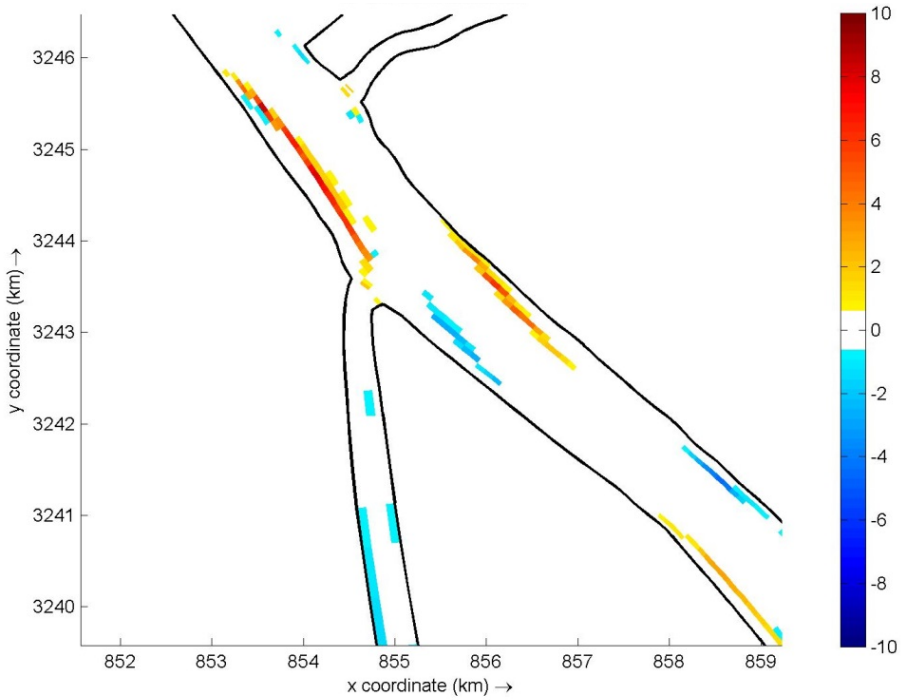

Figure 4.2.5: Delta (Variable – Uniform) in Cumulative Deposition [m] near Venice at Year 48

To further analyze the depositional differences due to the hydrograph selection, the laterally averaged cumulative erosion/sedimentation was extracted along the Mississippi River. The data were extracted for the individual cases to determine the deposition related to each type of hydrograph selected as well as the difference in laterally averaged cumulative erosion/sedimentation, obtained by subtracting the results from the uniform hydrograph run (Run 41) from the variable hydrograph run (Run 40).

When plotting the extracted laterally averaged cumulative erosion/sedimentation it was determined that it would be beneficial to eliminate local variation in the data resulting from the scale of the grid, which varies between 50 to 100 meters.

Four (4) different filters were applied to identify that the 3-Point filter, which applies a weight of 2 to the center and a weight of 1 to the predecessor and successor, and dividing the sum by 4. See Figure 4.2.6 for a comparison of the filters investigated.

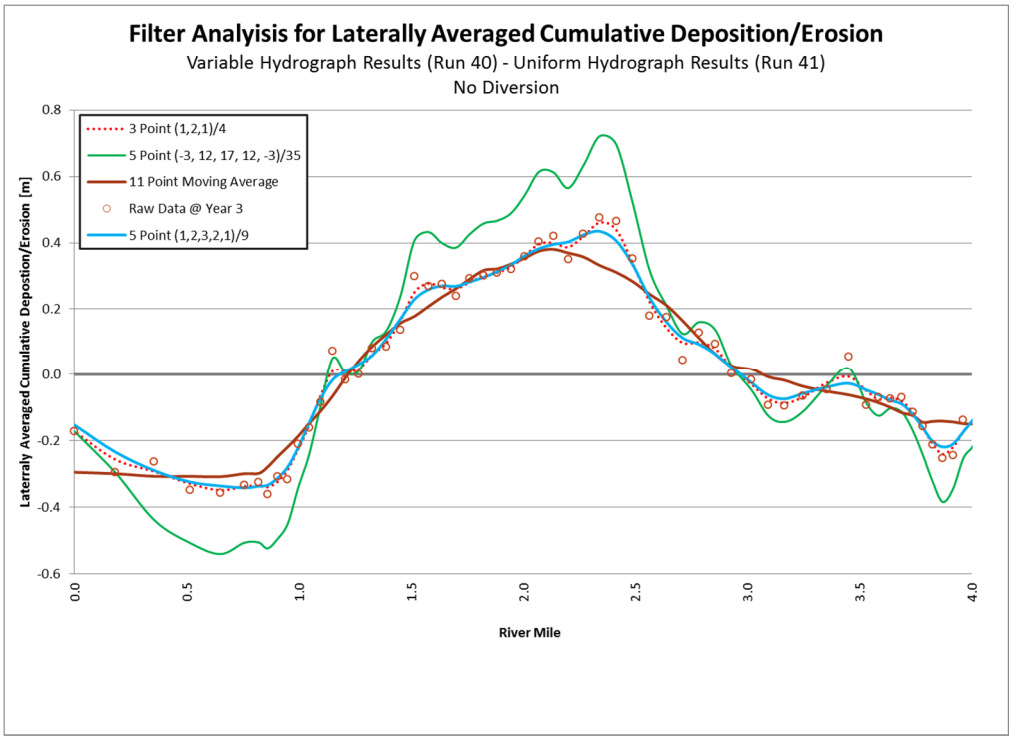

Figure 4.2.6: Filter Analysis for Laterally Averaged Cumulative Deposition/Erosion

4.3 RESULTS

The bathymetric difference Figures 4.2.1 to 4.2.5, for several reaches of the River, show that the long term deposition/erosion is dependent on the nature of variability of the annual hydrographs. The variable annual hydrograph tends to have greater erosion in the upper reach and greater deposition in the lower reaches, especially downstream of Fort St. Phillip.

The laterally averaged cumulative sedimentation/erosion results from the variable hydrograph run (Run 40) and the uniform hydrograph run (Run 41) were plotted along the river domain from Belle Chasse to HOP at year 24 (see Figure 4.3.1) and year 48 (see Figure 4.3.2). For geographic reference the plots contain landmark locations along the domain (see Table 4.3.1).

Table 4.3.1: Reference Points along the River Domain

RIVER MILE	DESCRIPTION
75.5	Belle Chasse (Upstream Boundary)
68.6	Mid-Breton
65.0	White Ditch
60.7	Mid-Barataria
48.9	West Pointe à la Hache (WPALH)
42.8	Lower Breton
34.0	Upstream (U/S) Bohemia Spillway
32.5	Bayou Lamoque
31.0	Downstream (D/S) Bohemia Spillway
29.5	Lower Barataria
24.0	Ostrica
19.8	Start Fort (Ft) Saint (St) Phillip
15.5	7 Cut Weir
11.9	Baptiste Collette
11.2	Venice
9.9	Grand & Tiger Pass
4.0	Main Pass
0.0	Head of Passes (HOP) (Downstream Boundary)

Trendlines were added to the graphs to better identify overall trends in deposition. The variable hydrograph run results are depicted in blue while the uniform hydrograph run results are depicted in red.

At year 24 (Figure 4.3.1), the uniform hydrograph flows result in more deposition than the variable hydrograph flow pattern. The trendline, which depicts the uniform run results, remains at all times above the trendline depicting the variable run results with a higher peak. The uniform hydrograph trendline is approximately 0.2 m higher in deposition at its maximum than the variable hydrograph trendline.

At year 48 (Figure 4.3.2), the uniform hydrograph flows still result in more deposition than the variable hydrograph flow pattern, but instead of a significant increase in deposition, the deposition pattern shifts slightly. As a result, the trendline depicting the uniform run is no longer higher than the variable run results along the entire river domain. At 48 years the deposition downstream of Fort St. Phillip increases for the variable run while the erosion above Fort St. Phillip increases when compared to the uniform run results, which is confirmed in Figure 4.2.5.

The following difference analysis between the laterally averaged cumulative deposition of the variable case and the uniform case was conducted. The Root Mean Square Error (RMSE) was calculated based on the difference between the uniform case values and the variable case values along the domain, and normalized for the maximum value for the variable case. A shown below the RMSE analysis resulted in values less than 1% when related to the maximum value. However, the percentage increased with time.

Root Mean Square Error (RMSE) Analysis:

- 24 Years: 0.0364m Related to Maximum Value: 0.4%
- 48 Years: 0.0592m Related to Maximum Value: 0.6%

Small values with increase over time

Furthermore, a bias error analysis was conducted. The bias was calculated based on the difference between the variable and the uniform case and normalized for the maximum value of the variable case. As shown below, the bias was approximately -0.1m (-1%), decreasing over time. This indicates the variable case is more erosional than the uniform case.

Bias Error Analysis:

- 24 Years: -0.1196m Related to Maximum Value: -1.3%
- 48 Years: -0.0943m Related to Maximum Value: -0.9%

Small values with decrease over time

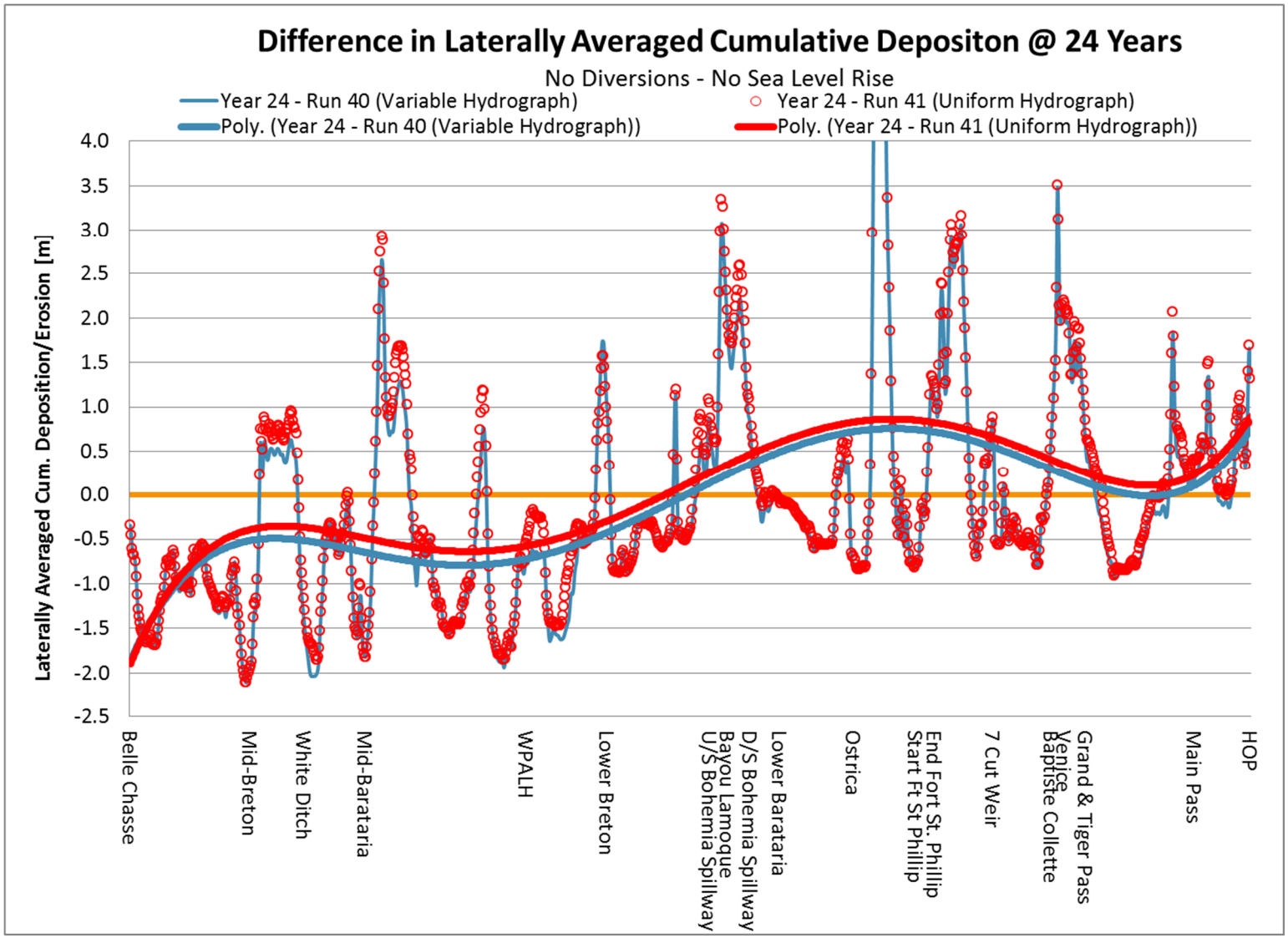

Figure 4.3.1: Difference in Laterally Averaged Cumulative Deposition at 24 Years (Variable vs. Uniform)

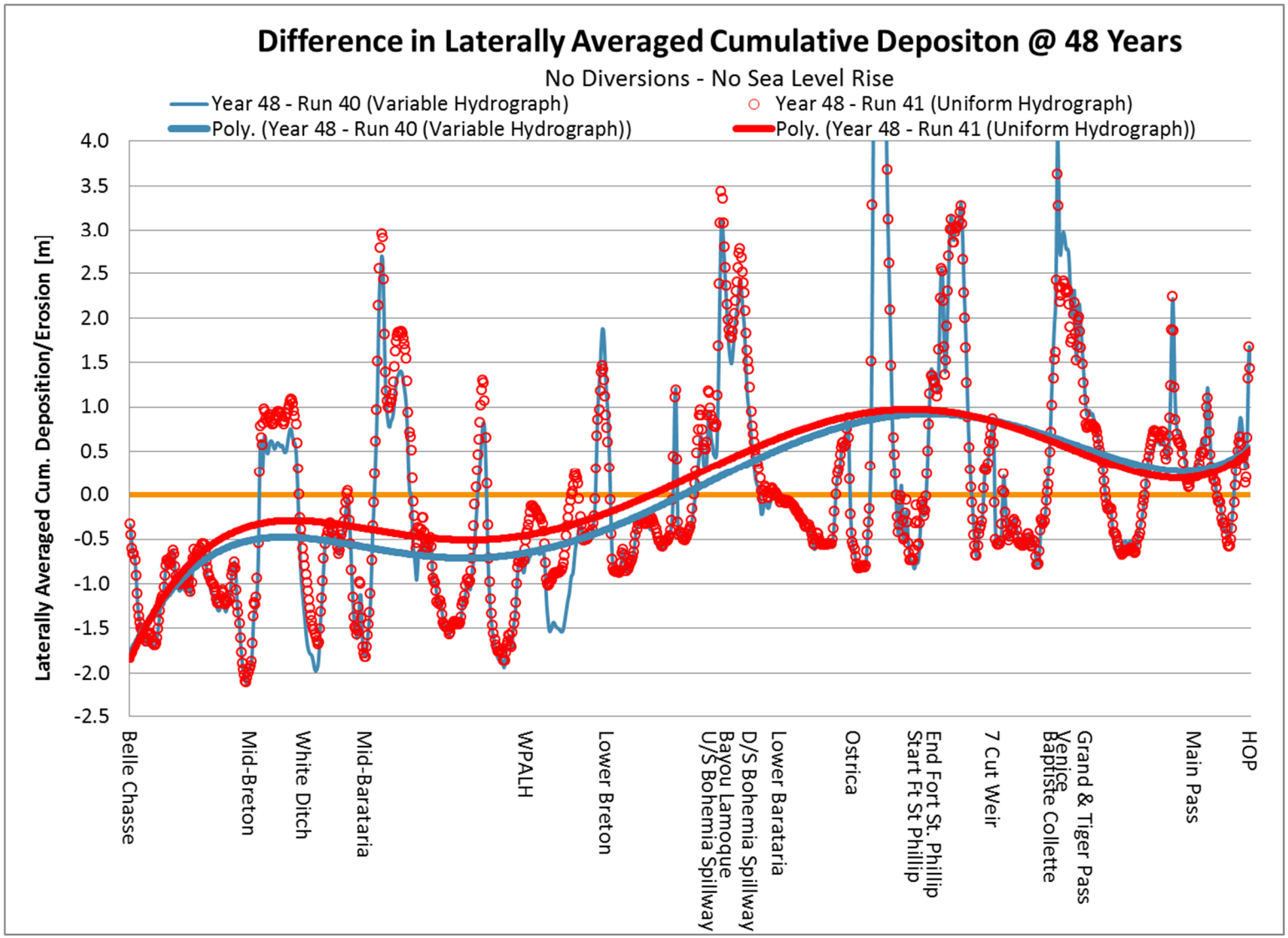

Figure 4.3.2: Difference in Laterally Averaged Cumulative Deposition at 48 Years (Variable vs. Uniform)

4.4 DISCUSSION

Morphological equilibrium is defined as the condition at which the rate of change in deposition approaches zero. Dynamic morphological equilibrium is defined as the condition at which the mean rate of change approaches zero, but the derivative oscillates about the mean.

The model results for Run 40 and 41 depict an initial period of adjustment in both, the mean and the standard deviation of the 3-Year deposition change data (see Figure 4.4.1). From 18 to 42 years the net rate of deposition change for the uniform hydrograph is approaches zero; however, it does not reach zero. The variable hydrograph gave a net rate of change, which oscillated about a mean value with a period that is reflective of the 12 year repetition of the 'variable' annual hydrograph.

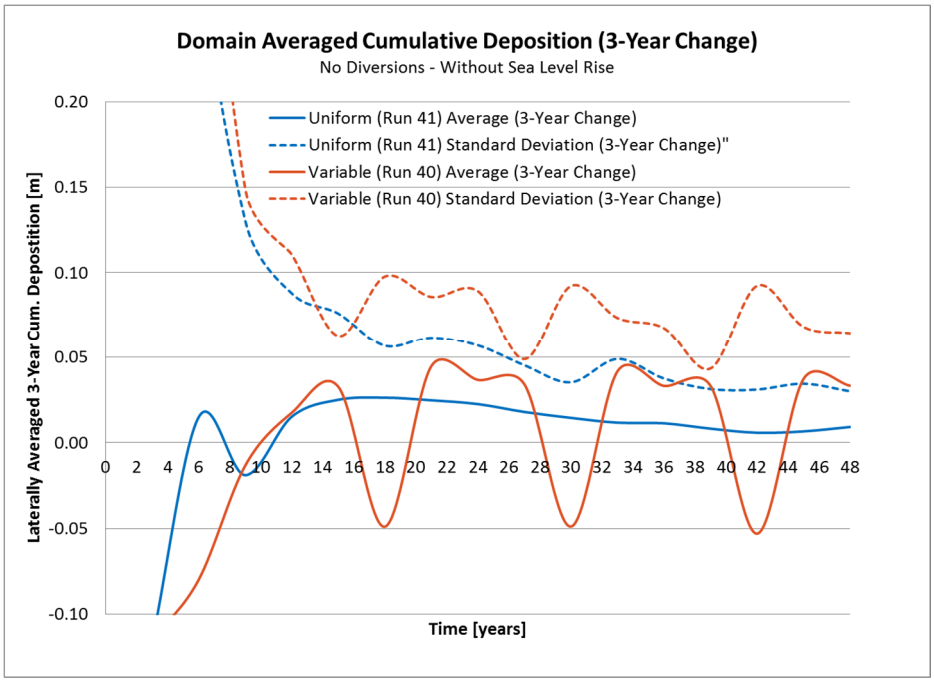

Figure 4.4.1: Domain Averaged Cumulative Deposition (3-Year Change) for Uniform and Variable Hydrograph Results (Run 41 & Run 40)

It is noted that the running average of the oscillating variable hydrograph deposition 3-year change values are slightly lower than the corresponding means of the uniform hydrograph case, which may be related to the fact that the upstream boundary has a

higher sand load for the uniform case versus the variable hydrograph case. The difference in sand load is attributed to the nature of the rating curve and how it treats the rising and falling limbs and the flow history.

To investigate the local equilibrium four (4) representative locations were selected: near Mid-Barataria, near WPAH, upstream of Fort St. Phillip and near Grand & Tiger Pass. These represent respectively depositional, erosional, depositional and depositional reaches. To smooth the results the net deposition was averaged over 80 cells centered on the location. Figure 4.4.2 depicts the plotted local mean deposition for the uniform hydrograph case in 3-year intervals.

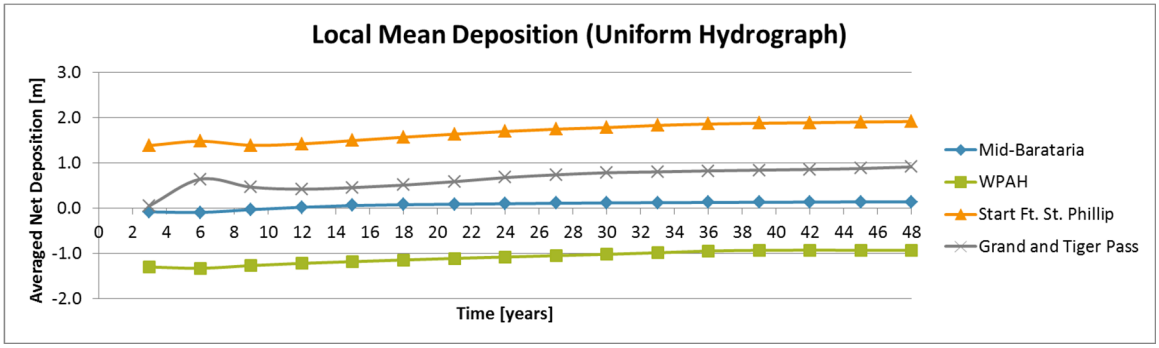

Figure 4.4.2: Local Mean Deposition for Uniform Case (Run 41)

To establish possible equilibrium at the 4 sites, the 3-year differences were computed and plotted as shown in Figure 4.4.3.

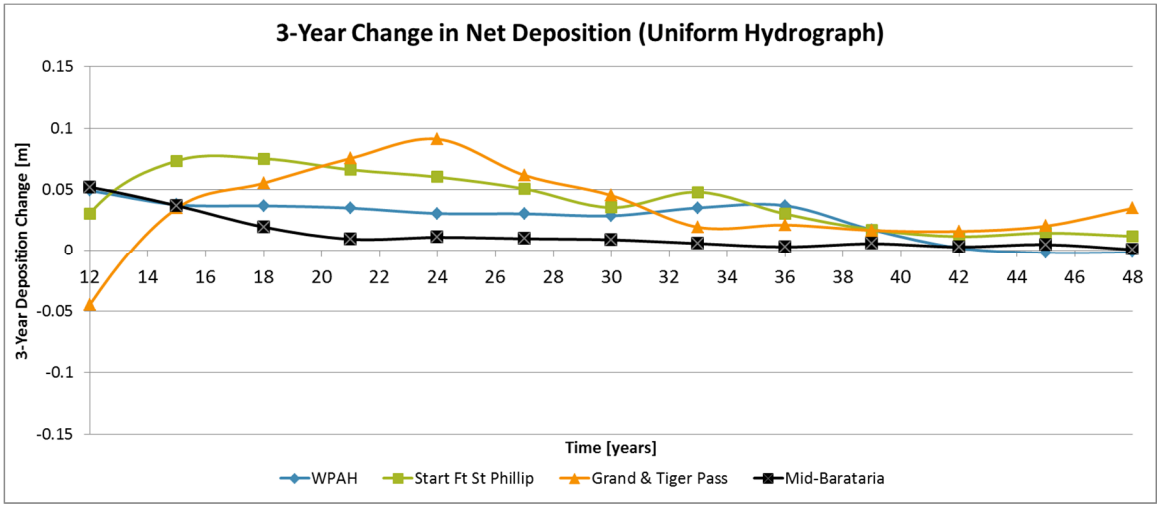

Figure 4.4.3: Three-Year Change in Net Deposition for Uniform Case (Run 41)

Figure 4.4.3 indicates a near equilibrium for the Mid-Barataria and WPAH sites, while the Fort St. Phillip location is approaching equilibrium, but has not achieved a near equilibrium at year 48. Furthermore, downstream of Fort St. Phillip is in a non-equilibrium state, since the 3-year differentials are increasing over time, which is represented by the Grand & Tiger Pass site. In general, the further downstream the site, the longer it takes to reach equilibrium, and in the reach downstream of Fort St. Phillip no equilibrium is indicated since the rate of change of deposition is increasing at the end of the 48 year period.

The corresponding graphs were developed for the variable hydrograph case and are depicted in Figures 4.4.4 and 4.4.5. Similar trends for the local mean deposition, as described for the uniform case, can be observed in the variable hydrograph case.

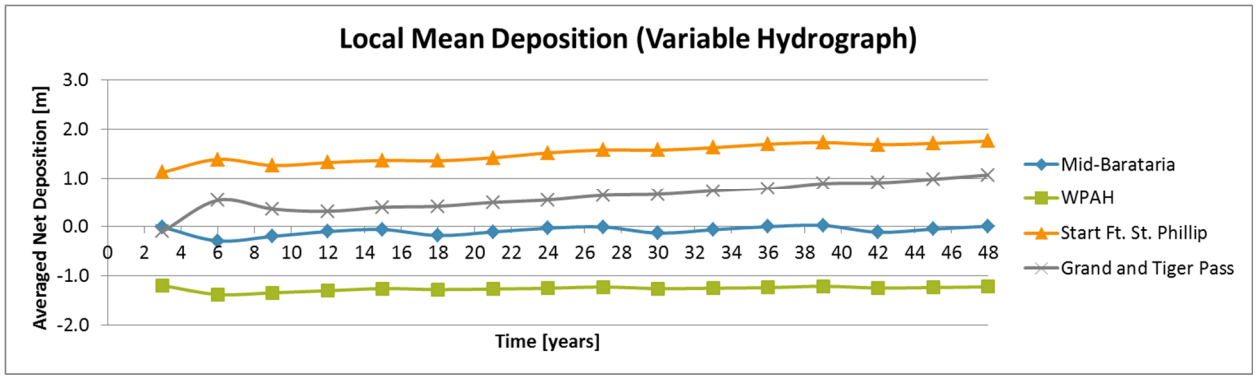

Figure 4.4.4: Local Mean Deposition for Variable Case (Run 40)

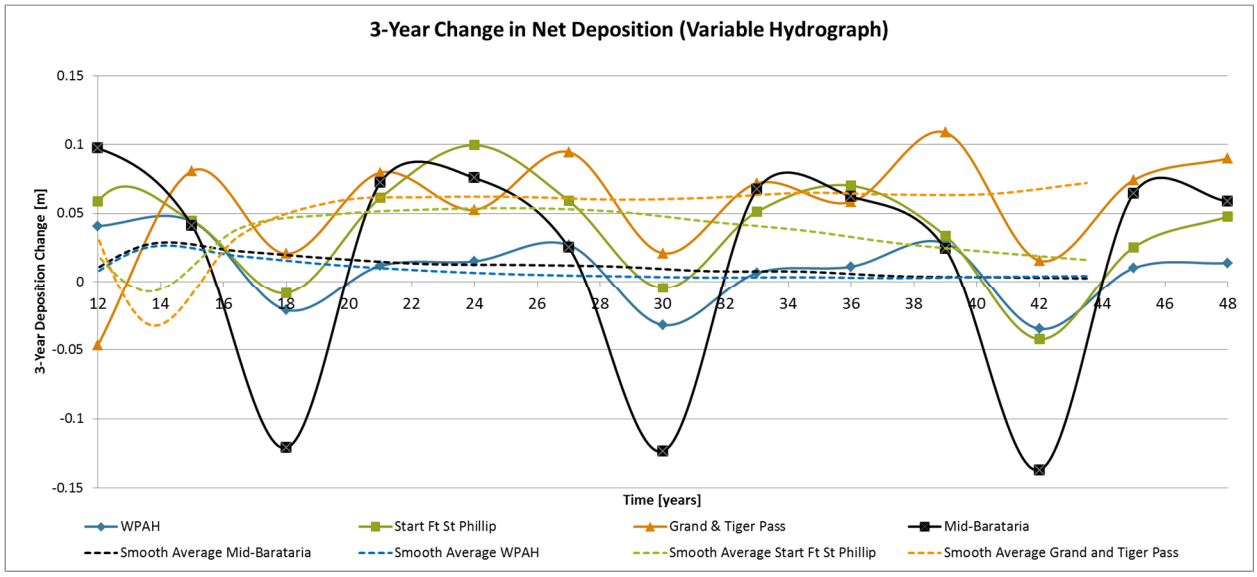

Figure 4.4.5: Three-Year Change in Net Deposition for Variable Case (Run 40)

Since the 3-year change plot for the variable case resulted in oscillating data as shown in Figure 4.4.5, a 12 year average was calculated from four 3-year change data points and referenced as a “smooth average” in the plot.

To better compare the trends between the uniform and variable hydrograph cases Figure 4.4.6 depicts the 3-year changes for the uniform case and the smooth average of the 3-year changes of the variable case. Mid-Barataria is following a very similar pattern towards equilibrium in both cases, while WPAH is also reaching the same equilibrium, but is following an offset pattern. The Start of Fort St. Phillip site is also similar in its pattern and both cases have not reached equilibrium at year 48, but are approaching equilibrium. The Grand & Tiger Pass site is showing in both cases (variable & uniform) an increase in depositional change indicating a non-equilibrium. The variable case is generating higher depositional change values than the uniform case at this site.

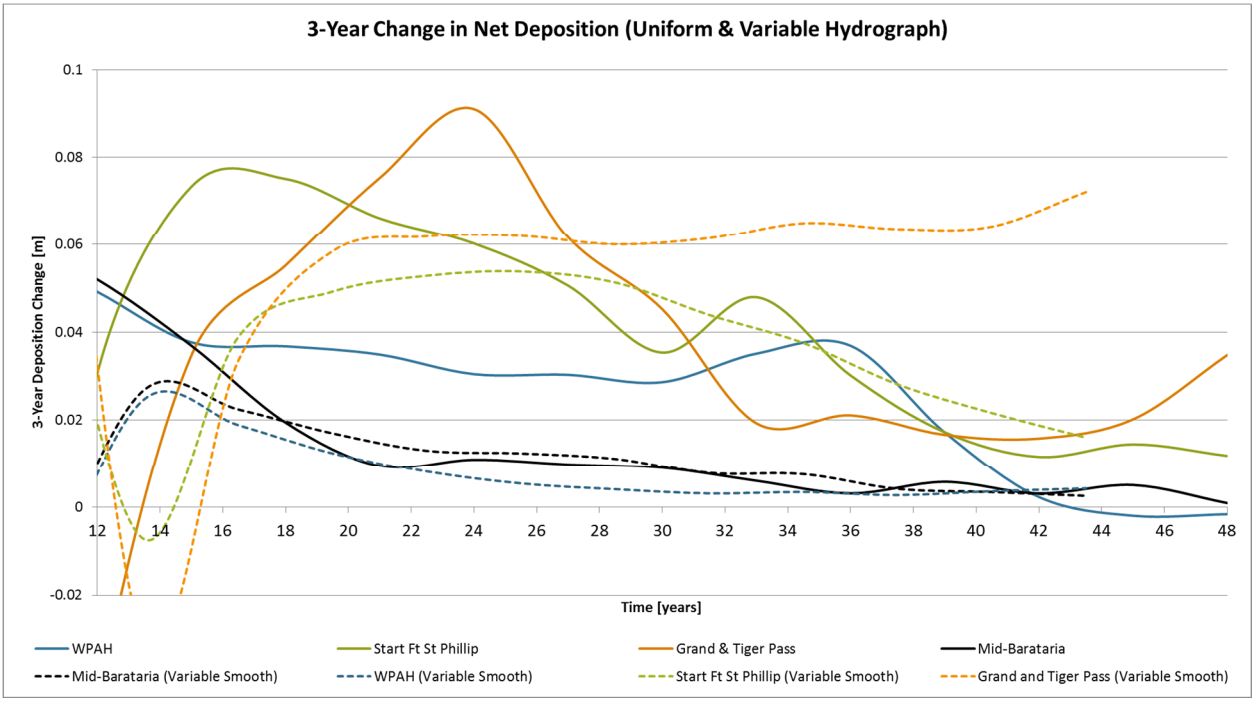

Figure 4.4.6: Three-Year Change in Net Deposition for Variable Case (Run 40) & Uniform Case (Run 41)

To investigate the difference in the responses between the variable and the uniform hydrograph scenarios, the difference in net deposition between the two cases was computed by subtracting the uniform case bathymetry from the variable case bathymetry (see Figure 4.4.7). It can be noted that the differences at 24 years indicate relatively more erosion for the variable case while at 48 years the relative erosion shifts to relative deposition downstream of Fort St. Philip, which is in agreement with the bathymetry difference plots depicted in Figures 4.2.1 to 4.2.5.

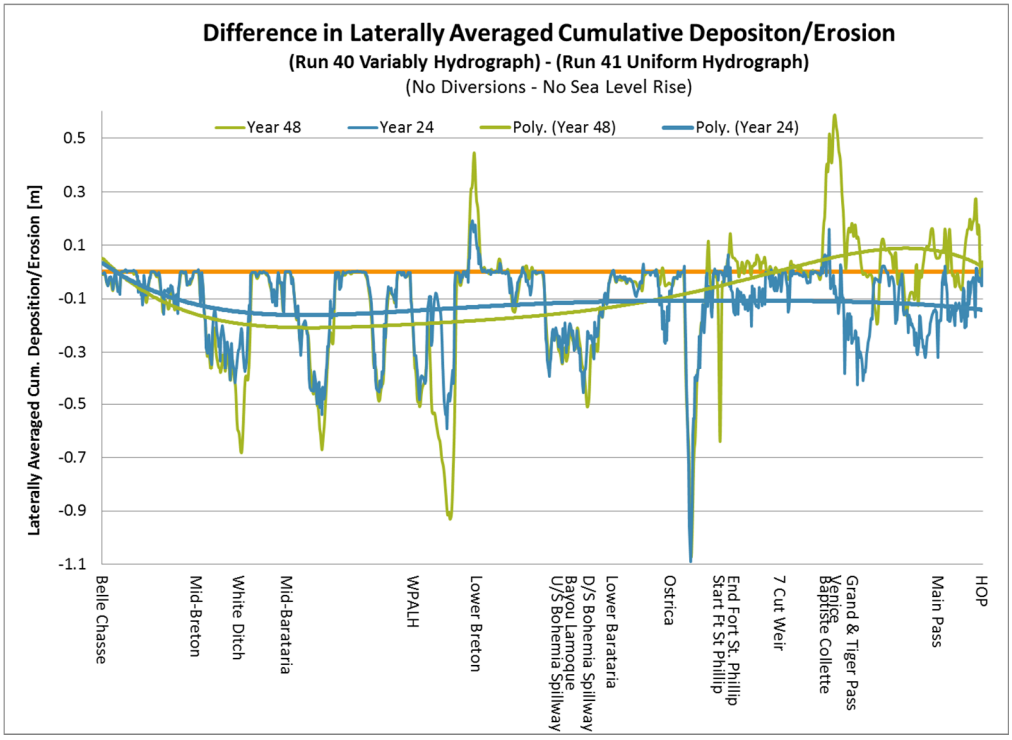

Figure 4.4.7: Difference in Laterally Average Cumulative Deposition/Erosion (Run 40 – Run 41)

Therefore, there appears to be a relative equilibrium upstream of Fort St. Philip, while there is no equilibrium downstream of Fort St. Philip. The 'uniform' and 'variable' hydrographs approach different equilibria in the upper reaches while neither hydrograph options approach an equilibrium downstream of Fort St. Philip. This is consistent with the finding, that neither the variable run nor the uniform run, reach a full equilibrium in net depositional change. The explanation for this non-equilibrium state is the interaction of deposition with the flow distribution through the passes and the subsequent changes

in streampower, which reinforces the change in the downstream bathymetry (see Figure 4.2.5).

An examination of the bathymetric surveys and dredging records of the Mississippi River in the reach downstream of Bonnet-Carré Spillway conducted by Kemp (2009) found no equilibrium and a general increasing trend from erosion to deposition in the four decades previous to 2004. In addition, McCorquodale et al. (2017) analyzed net deposition trends by reach for the time period 1992 to 2004, utilizing Kemp's data and the regional model results (see Figure 4.4.8). The data show a non-equilibrium with increasing deposition from RM 49 to HOP.

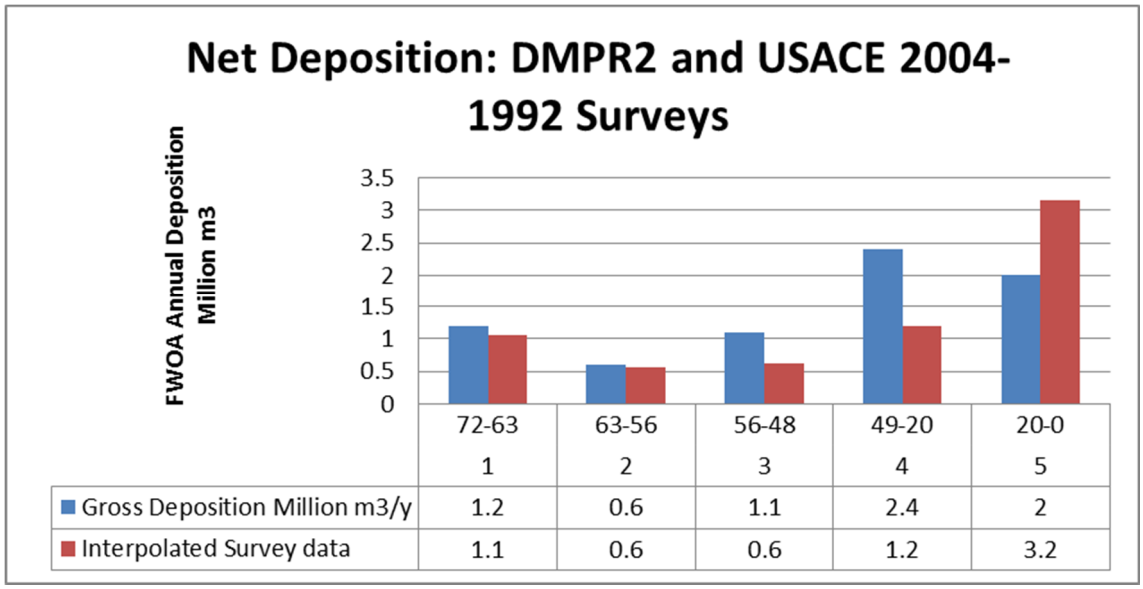

	72-63	63-56	56-48	49-20	20-0
	1	2	3	4	5
Gross Deposition Million m3/y	1.2	0.6	1.1	2.4	2
Interpolated Survey data	1.1	0.6	0.6	1.2	3.2

Figure 4.4.8: Comparison of Delft3D Net Deposition and Interpolated USACE 1992-2004 Survey

Figure 4.4.9 depicts the differences in deposition between the variable (Run 40) and the uniform (Run 41) cases in 6 year increments, including the previously depicted years 24 and 48. Again the differences between the variable and uniform cases diminish in the upper reaches and not in the reach downstream of Fort St. Philip.

To analyze the periodicity impacts of the 12-year hydrograph, Figures 4.4.10 and 4.4.11 were developed. Figure 4.4.10 depicts the 12-Year Changes (i.e. at the end of each 12 year cycle) in Laterally Averaged Cumulative Deposition for the difference between the variable hydrograph run (Run 40) and the uniform hydrograph run (Run 41). Four periods are depicted, year 12 - year 0, year 24 - year 12, year 36 – year 24 and year 48 – year 36. Figure 4.4.11 depicts a comparison of the domain averaged cumulative deposition change over 3-year and the 12-year periods for the difference between the variable hydrograph run (Run 40) and the uniform hydrograph run (Run 41). The 12-year averaging removes the impact of the 12-year periodicity.

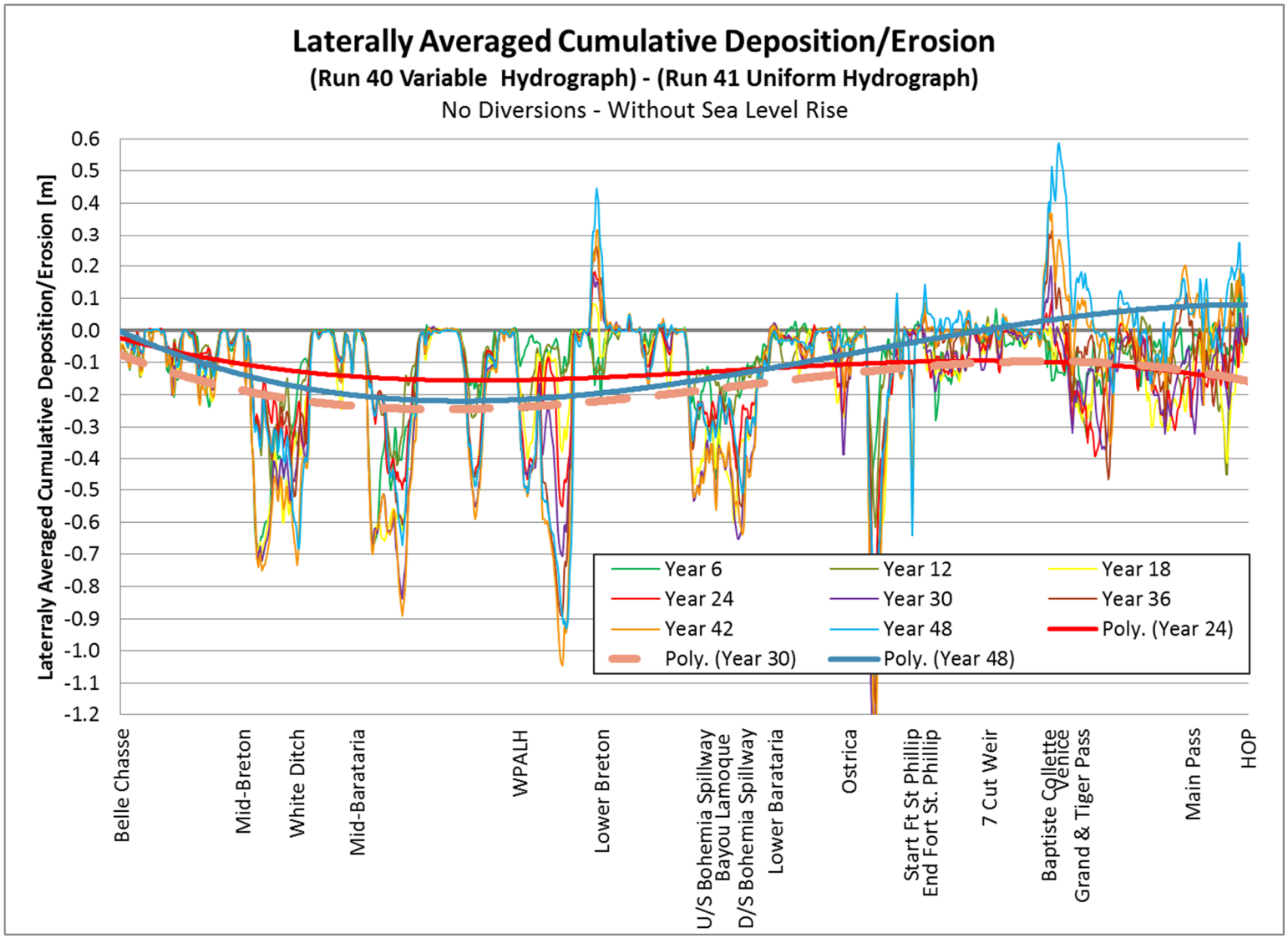

Figure 4.4.9: Delta of Laterally Averaged Cumulative Deposition (Run 40 – Run 41)

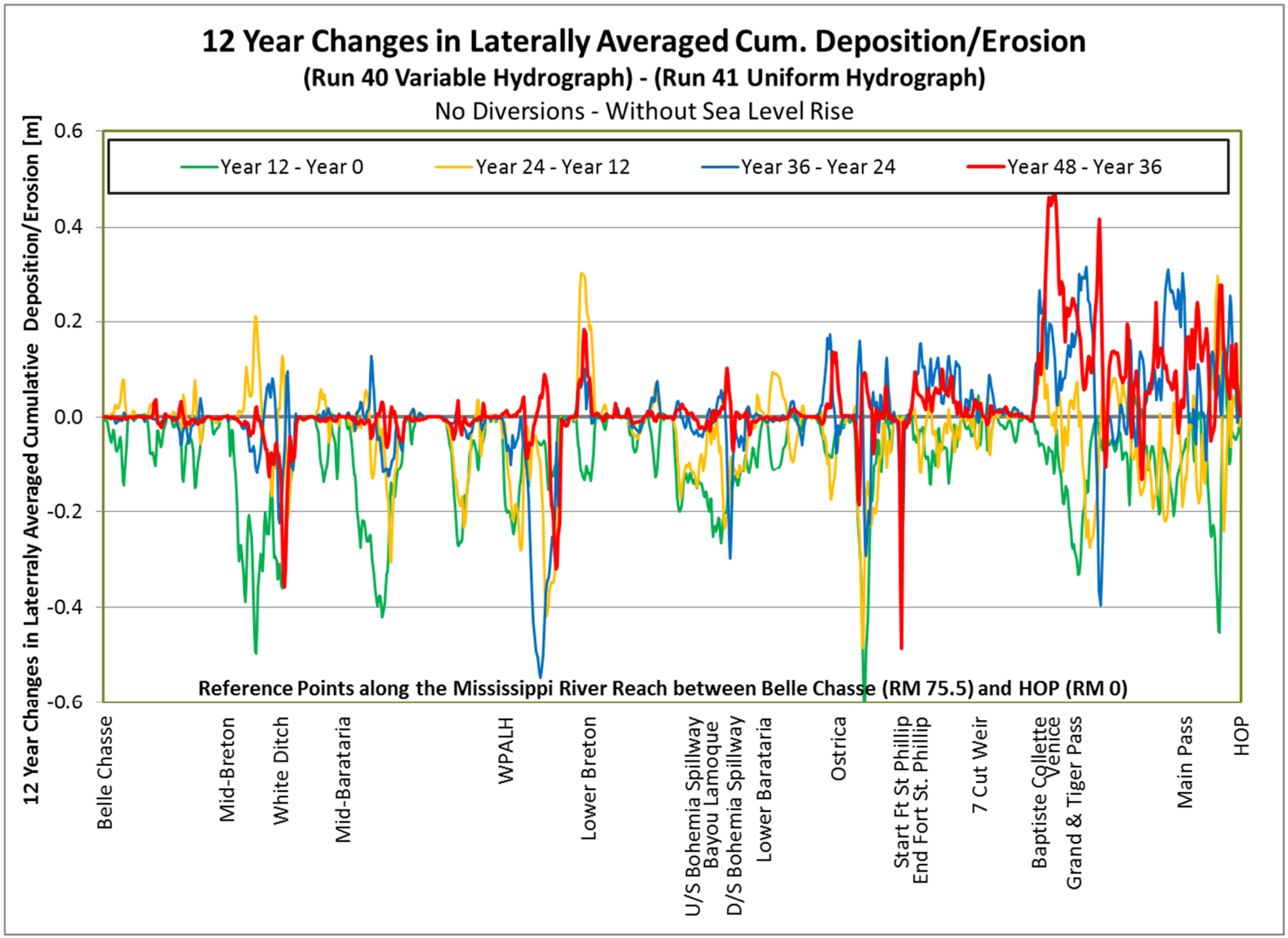

Figure 4.4.10: 12-Year Changes in Laterally Averaged Cumulative Deposition (Run 40 – Run 41)

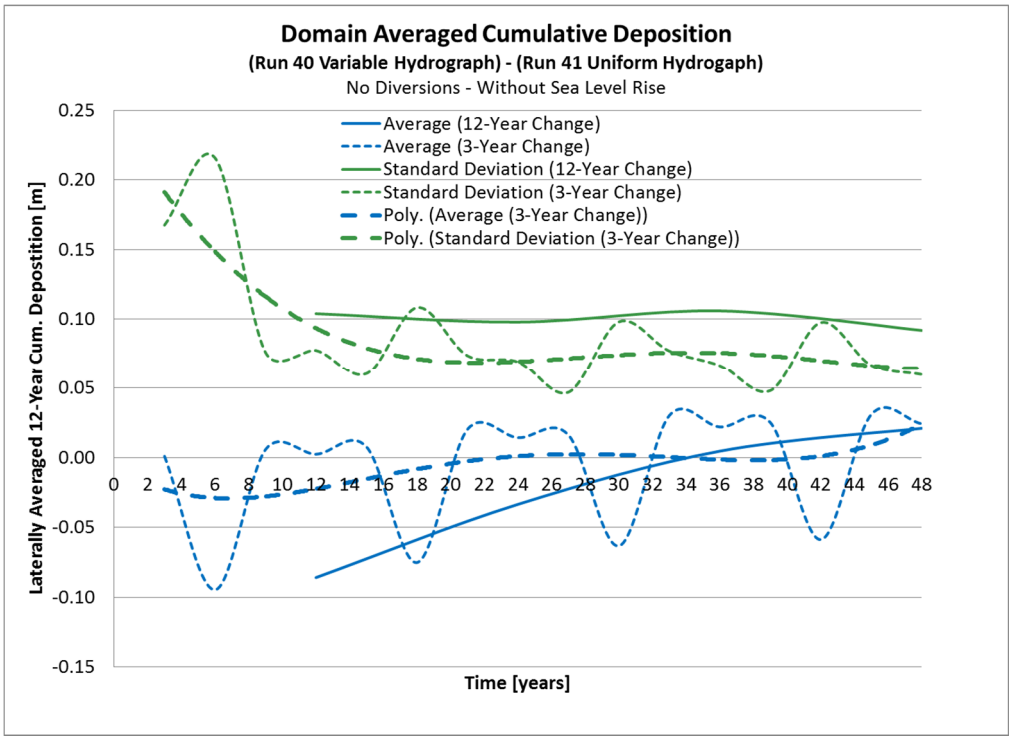

Figure 4.4.11: Domain Averaged Cumulative Deposition (Run 40 – Run 41)

When comparing the 3-Year to the 12-Year change, it can be concluded that the oscillation in the 3-Year change graph show a 12-year period, which corresponds to the established period of the variable hydrograph while the 12-year averaging produced a limiting non-zero value similar to the uniform case. These results indicate that there is no global equilibrium.

4.5 CONCLUSIONS

The derivative of the global and laterally averaged deposition for both, the variable and uniform hydrograph cases, does not achieve l zero by the end of the 48 year simulation. However, the uniform approached a minimum of 0.2 cm per year at year 42 (see Figure 4.4.1), while the variable approaches a similar average of 0.16 cm per year based on averaging of the oscillating values.

The variable hydrograph results are approaching a dynamic equilibrium upstream of Fort. St. Philip, while the uniform hydrograph results are approaching an absolute equilibrium upstream of Fort St. Philip. The implication of this is that the equilibrium in the upstream reach will reflect any periodicity in the hydrograph record.

A near equilibrium is reached upstream of Fort St. Philip, where only minor distributaries influence the river dynamics; however, downstream of Fort St. Philip, where nearly 50% of the river flow is discharged to the distributaries, no equilibrium occurred within the 48 year period of the simulation. Downstream of Fort St. Philip there is an increase in rate of deposition for both, the variable and uniform scenario.

In summary, the equilibrium bathymetry is not independent of the annual variability of the hydrograph, even if the flow duration curve is the same. Therefore, the hypothesis is not accepted for riverine systems with distributaries.

5.0 CHAPTER 5: H2- VARIABLE VERSUS UNIFORM HYDROGRAPH IMPACTS ON DIVERSION SAND CAPTURE

5.1 HYPOTHESIS

Hypothesis 2:

The average annual sediment captured by the diversions is independent of the annual variability of the hydrographs, provided the flow duration curve is comparable.

5.2 METHODOLOGY

The two model runs listed in Table 5.2.1 were set-up to obtain data in support of Hypothesis 2. Both runs cover a 48 year simulation times and utilize the uniform and a repeating 12-year variable hydrograph. The diversion case selected for evaluation is the Mid-Barataria Diversion at 75,000 cfs.

Table 5.2.1: Model Runs for Hypothesis 2:

#	Hydrograph		Years	Diversions	Diversion Info
	U	V			
43	X		1-48	1	Mid-Barataria = 75,000cfs
47		X	1-48	1	Mid-Barataria = 75,000cfs

From both, the uniform and variable cases, the sand loads in the river upstream (U/S) of the diversion and inside the Mid-Barataria Diversion are extracted and compared. The analysis divided the total sand by sand class (very fine = VF, fine = F and medium = M) for further comparison.

5.3 RESULTS

The cumulative total sand transport in the Mid-Barataria Diversion by sand class (VF, F, M) for the 48-year modeled time period is depicted in Figure 5.3.1. The figure includes a comparison between the uniform and variable hydrograph case results.

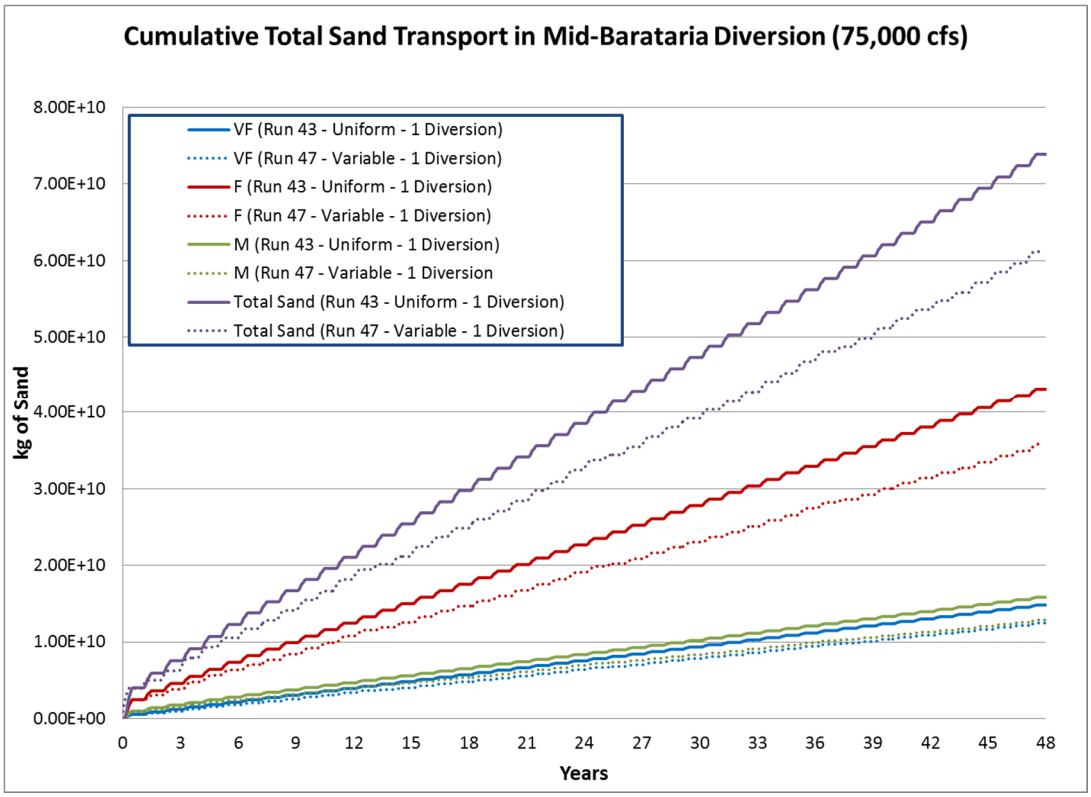

Figure 5.3.1: Cumulative Total Sand Transport in Mid-Barataria Diversion Uniform versus Variable Hydrograph

Figure 5.3.1 shows that the model run utilizing the uniform hydrograph yielded more sand in the diversion than the run utilizing the variable hydrograph, which is the case for very fine, fine, and medium sand fractions as well as the total sand load.

To further analyze the difference in sand distribution between the Mississippi River and the diversions the instantaneous load of the 3 sand fractions (VF, F, M) was extracted for the 48-year period for both cases, uniform (Run 43) and variable (Run 47), at a location just upstream of the proposed Mid-Barataria Diversion and within the Mid-Barataria Diversion. Figure 5.3.2 depicts the percent of total sand load for very fine

(VF), fine (F) and medium (M) sand in the Mississippi River upstream (U/S) of Mid-Barataria and inside the Mid-Barataria Diversion, while Table 5.3.1 captures the percent values. Figure 5.3.2 and Table 5.3.1 provide the percentages for the two hydrograph cases.

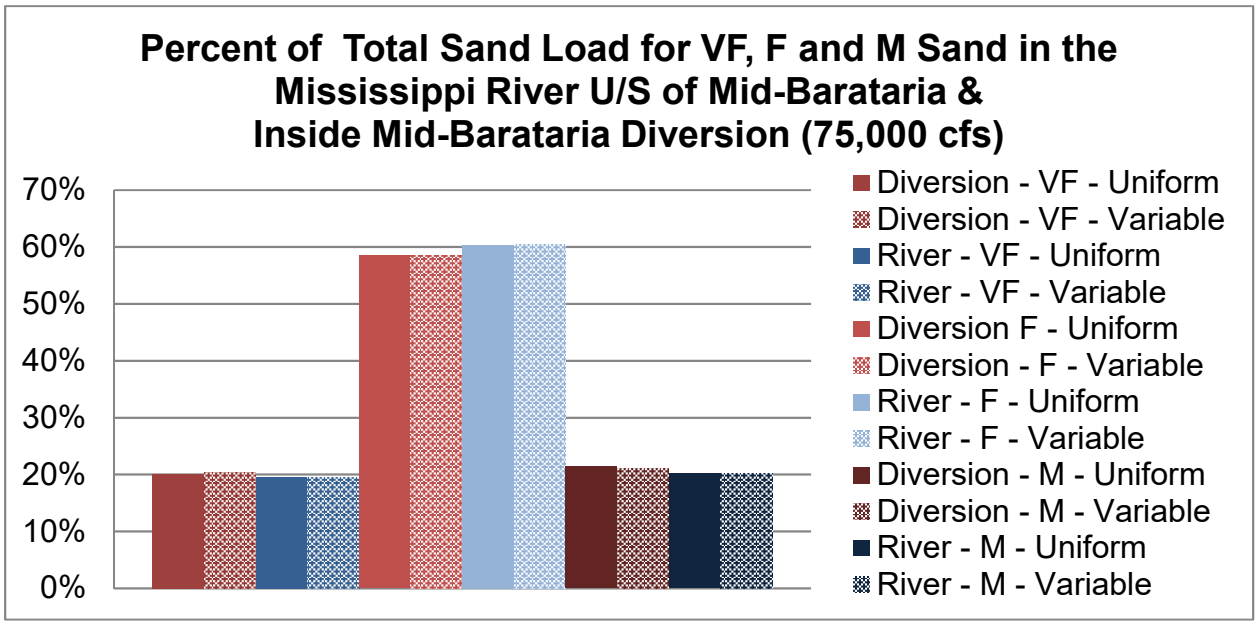

Figure 5.3.2: Percent of Total Sand Load for VF, F and M Sand in the Mississippi River U/S of Mid-Barataria and Inside the Mid-Barataria Diversion Uniform vs. Variable Hydrograph

Table 5.3.1: Percent of VF, F and M Sand in the Mississippi River U/S of Mid-Barataria and Inside the Mid-Barataria Diversion, Uniform vs. Variable Hydrograph

Location	Load	UNIFORM			VARIABLE		
		VF	F	M	VF	F	M
Inside Mid-Barataria Diversion	Total	20.1%	58.5%	21.4%	20.4%	58.6%	21.0%
U/S Mid-Barataria Diversion (River)	Total	19.5%	60.3%	20.1%	19.4%	60.3%	20.2%

5.4 DISCUSSION

The results, which show 16% higher sand capture by the uniform case (see Figure 5.3.1), can be misleading, since it has to be considered that the variable hydrograph has an approximately 19% reduced sand load at the upstream boundary condition (Belle Chasse) when compared to the uniform hydrograph data (see Section 3.1.2 & Figure 3.1.2.3). Therefore, the uniform case has an approximately 19% higher sand availability in the river while only showing 16% higher sand capture when compared to the variable case. The total net sand load difference in the diversion between the variable and uniform scenarios can be calculated to approximately 3%.

To evaluate the sand capture efficiency of the diversion without influencing the data by the difference in sand load in the two different hydrograph systems, the fraction of sand captured from the available Mississippi River sand was calculated for the Mid-Barataria Diversion over time and depicted in Figure 5.4.1. In this study, sand capture efficiency is defined as the fraction of the sand load upstream of the diversion that is captured by the diversion. If all of the sand load in the river upstream of the diversion was captured by the diversion, the efficiency would be 100%. In other studies, the efficiency has been represented by sediment-water ratio, which is the ratio of the sediment concentration in the diversion divided by the sediment concentration in the river.

Figure 5.4.1 shows that in the uniform hydrograph case (green line) the Mid-Barataria Diversion captures a slightly smaller fraction of the available river sand than in the variable case (red line). The variable case has a capture efficiency of approximately 2% more than the uniform case. This slight variance can be explained by the slightly higher river flow peaks occurring over time in the variable hydrograph case, providing more energy to transport sand in suspension and diverting it through a diversion structure.

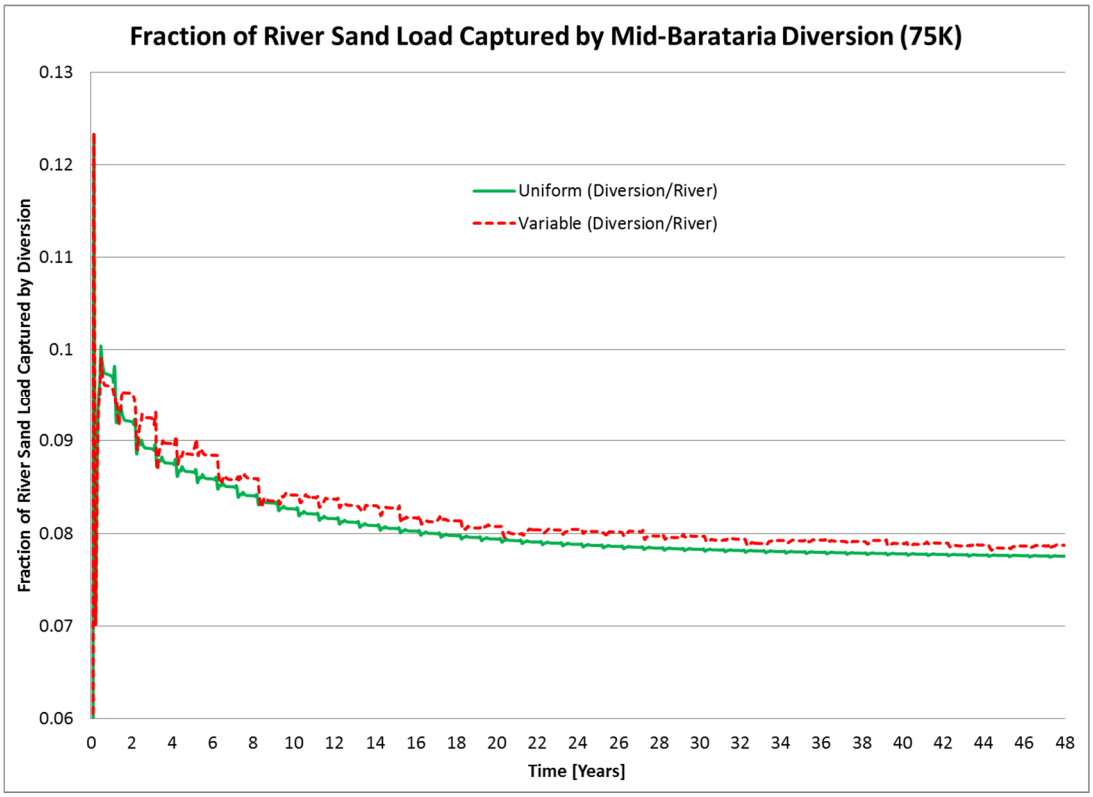

Figure 5.4.1: Fraction of River Sand Captured by the Mid-Barataria Diversion Uniform vs. Variable Hydrograph

5.5 CONCLUSIONS

There is approximately 19% more sand entering the upstream boundary (Belle Chasse) in the uniform scenario, however, there is only 16% more sand captured by the Mid-Barataria Diversion, which is a 3% deficit when compared to the variable case. From Figure 5.4.1 it can be determined that the diversion efficiency of the variable case is approximately 2% higher than in the uniform case, which highlights the deficit in diversion efficiency of the uniform case. Furthermore, the variable scenario resulted in less deposition and therefore more efficient transport to the diversion site, which can account for the remaining 1% difference in net sand capture.

The variable hydrograph resulted in a higher capture efficiency than the uniform case. Therefore, the hypothesis is not accepted since the fraction of sediment captured by the diversion depends on the availability of sand in the system as well as the flow hydrograph pattern.

Utilizing a uniform hydrograph results in a more conservative approach to evaluating diversion efficiency and sand capture, since utilizing a uniform hydrograph is resulting in a smaller fraction of sand diverted from the river into the diversion. Similarly, utilizing a more realistic variable hydrograph pattern will result in more accurate sand load volumes captured by the diversion.

6.0 CHAPTER 6: H3- INTERACTION AMONGST MULTIPLE DIVERSIONS

6.1 HYPOTHESIS

Hypothesis 3:

If the total flow diverted through multiple diversions is less than a certain total critical diversion discharge, each diversion will function as an independent structure in terms of local deposition and sediment captured.

6.2 METHODOLOGY

The model runs listed in Table 6.2.1 were set-up to obtain data in support of Hypothesis 3. All runs cover a 12 year computational run time and utilize the developed 12-year variable hydrograph.

Table 6.2.1: Model Runs for Hypothesis 3:

Diversion	Scenario 1	Scenario 2	Scenario 3	Scenario 4
No Diversions	0 cfs (Run 3)	0 cfs (Run 3)	0 cfs (Run 3)	0 cfs (Run 3)
Mid - Breton	35,000 cfs (Run 12)	25,000 cfs (Run 16)	35,000 cfs (Run 12)	40,000 cfs (Run 25)
Mid-Barataria	75,000 cfs (Run 6)	25,000 cfs (Run 17)	35,000 cfs (Run 21)	40,000 cfs (Run 26)
Lower Barataria	50,000 cfs (Run 13)	25,000 cfs (Run 18)	35,000 cfs (Run 22)	40,000 cfs (Run 27)
Lower Breton	50,000 cfs (Run 14)	25,000 cfs (Run 19)	35,000 cfs (Run 23)	40,000 cfs (Run 28)
Total	**210,000 cfs (Run 15)**	**100,000 cfs (Run 20)**	**140,000 cfs (Run 24)**	**160,000 cfs (Run 29)**

Each scenario listed in Table 6.2.1 has a maximum of 4 diversions (Mid-Breton, Mid-Barataria, Lower Breton, and Lower Barataria) at various flows, generating a total diversion flow of 100,000 cfs (Scenario 2), 140,000 cfs (Scenario 3), 160,000 cfs (Scenario 4) and 210,000 cfs (Scenario 1). Scenario 1 was the original 2012 Master Plan Scenario (CPRA 2012).

The interdependence of diversions is investigated based on the impact on river morphology and the impact on the river sediment capture rate of the diversions.

The intention of this analysis is to compare the cumulative laterally averaged deposition by reach over time to identify and compare the influence zones of the various individual diversions operating alone or in combination with various 4 diversions scenarios as described above. Furthermore, the cumulative transport by a diversion at year 12 operating alone will be compared to the same diversion operating at the same flow but with all four diversions in operation.

Furthermore, one of the practical reasons for considering the interaction of multiple diversions and total diverted flow is to assign a possible error to local models relative to regional models in terms of sediment capture rates by individual diversions. In this study it is assumed that a 1% to 3% error in sediment capture rate would be acceptable when using a project-based, site specific model. This total diversion flow analysis will identify a critical total diversion flow below which individual diversions capture sediment at the same rate when operating individually or in combination with multiple diversion and remain below the 1% and 3% assumed error.

6.3 RESULTS

The river domain was divided into seven (7) reaches as defined in Figure 6.3 and the cumulative deposition within each reach was extracted from the model output. An analysis by reach is necessary to identify changes caused by diversions in upstream or downstream reaches of a diversion.

The laterally average cumulative deposition by reach was plotted over the 12-year time period (Figures 6.3.1a & b to Figures 6.3.7a & b). These figures show the difference between the active diversions and the no-diversion case.

Reach	DESCRIPTION
1	Belle Chasse to Upstream Mid-Breton
2	Upstream Mid-Breton to Upstream Mid-Barataria
3	Upstream Mid- Barataria to Upstream West Pointe à la Hache (WPAH) (at beginning of outflow)
4	Upstream West Pointe à la Hache (WPAH) (at beginning of overflow) to Upstream Lower Barataria
5	Upstream Lower Barataria to Upstream Lower Breton
6	Upstream Lower Breton to Upstream Fort St. Phillip
7	Upstream Fort St. Phillip to Head of Passes

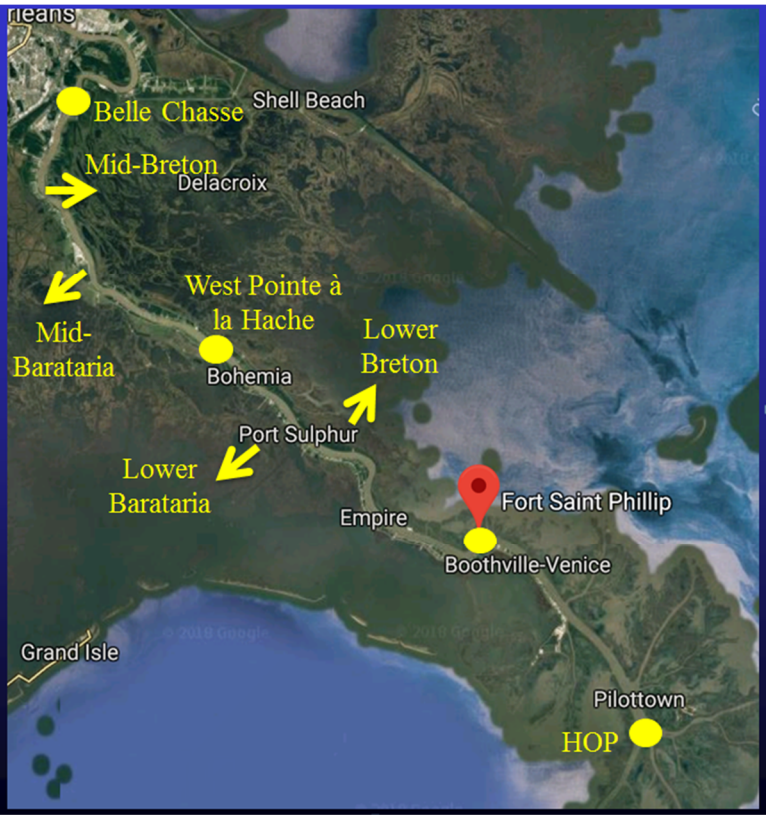

Figure 6.3: River Reaches Analyzed for Hypothesis 3

Reach 1 = Belle Chasse to Upstream Mid-Breton

This reach does not have a notable change in deposition due to any of the individual diversions (Figure 6.3.1a) operating separately at various flows or due to any of the 4 diversion scenarios (Figure 6.3.1b) ranging between 100,000cfs and 210,000cfs.

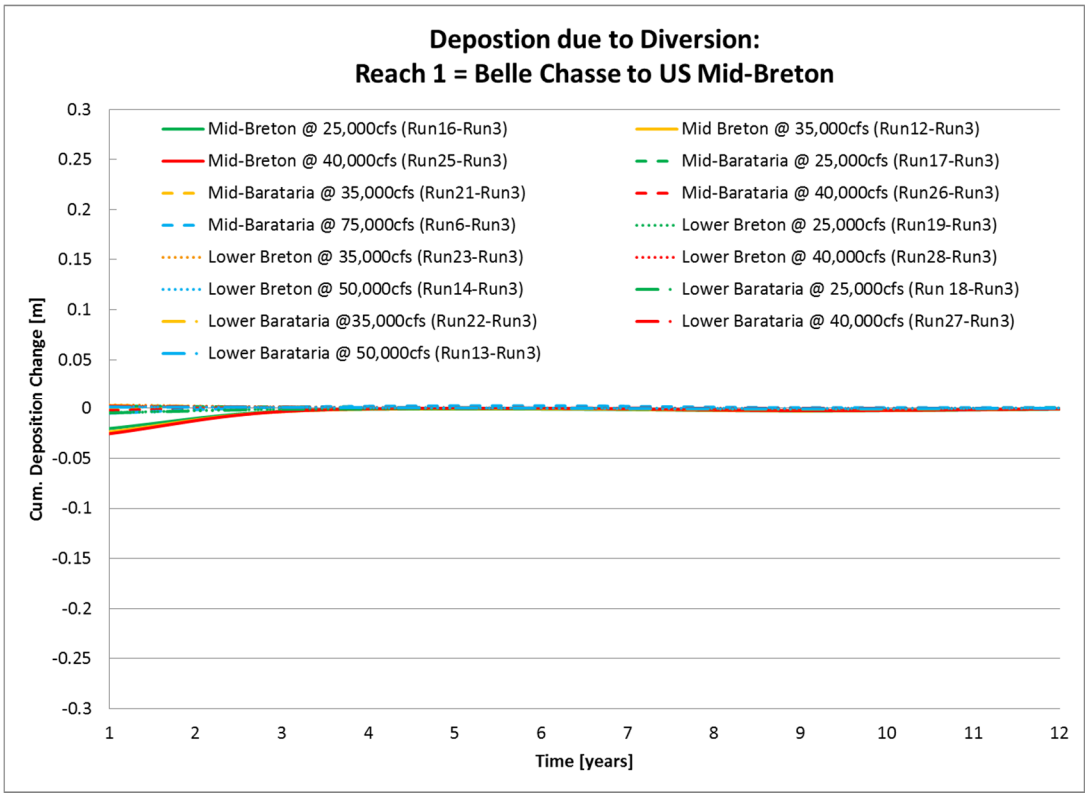

Figure 6.3.1a: Cumulative Deposition Change due to Individual Diversions - Reach 1

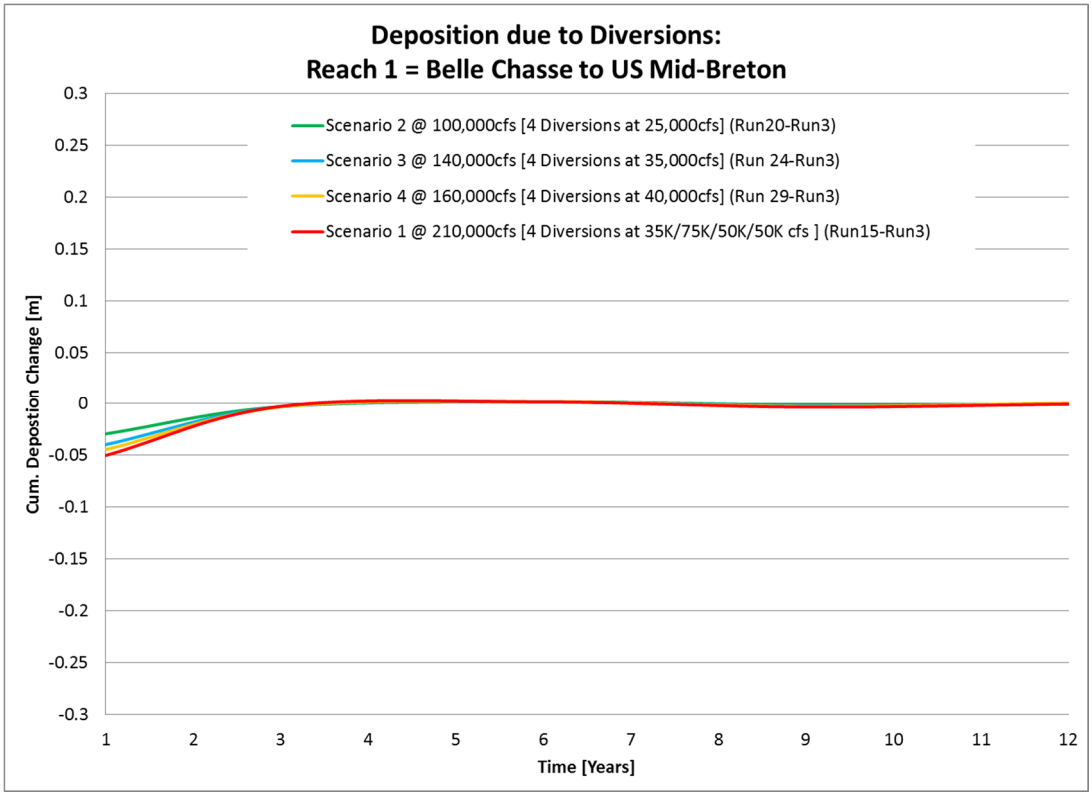

Figure 6.3.1b: Cumulative Deposition Change due to 4 Diversion Scenarios - Reach 1

Reach 2 = Upstream Mid-Breton to Upstream Mid-Barataria

The Lower Breton and Lower Barataria individual diversions (Figure 6.3.2a) have no notable impact on this reach. The Mid-Barataria Diversion at a flow of 75,000cfs, which has a minor erosional impact; the Mid-Breton Diversion has the most influence on this reach, and its erosional impact increases steadily with increase of diversion flow. The laterally averaged erosion due to the Mid-Breton Diversion does not exceed -0.4m in this reach. The reach is dominantly erosional.

The erosional impact due to the various 4 diversion scenarios is dominated by the erosional impact of the individual Mid-Breton diversion. The individual Mid-Breton causes a maximum change in bathymetry of approximately -0.3m/12 years (erosion) while the 4 diversion scenarios result in a maximum (erosion) of -0.35m/12 years (Figure 6.3.2 a & b). However, the individual Mid-Breton Diversion at 35,000 cfs flow exceeds -0.25m erosion at approximately year 10 (Figure 6.3.2 b). while Scenario 3 (4 Diversions, 140,000cfs), which also has a 35,000 cfs Mid-Breton Diversion, reaches the same value after 8 years, and Scenario 1 (4 Diversions, 210,000cfs), which has a larger total diversion flow than Scenario 3, but also a 35,000 cfs Mid-Breton Diversion, reaches this value at approximately 7 years. Therefore, the operation of other diversions has a minor impact to this reach, which is dominated by erosional impacts from the individual Mid-Breton Diversion.

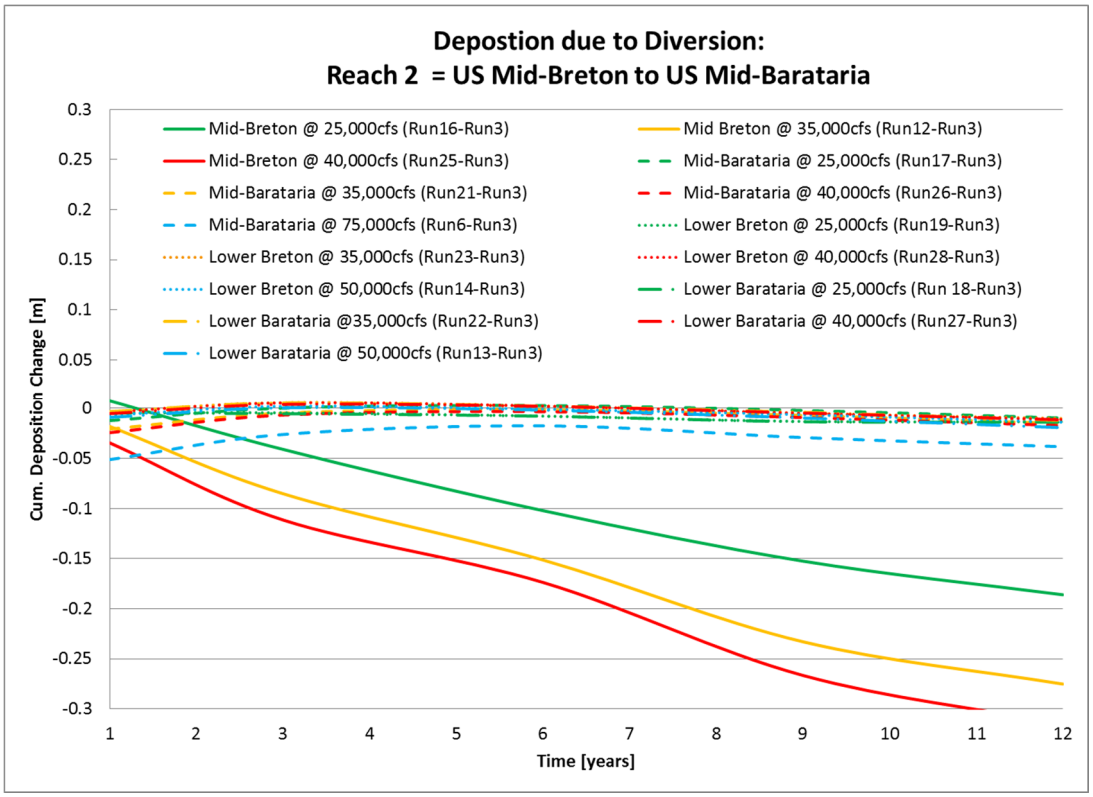

Figure 6.3.2a: Cumulative Deposition Change due to Individual Diversions - Reach 2

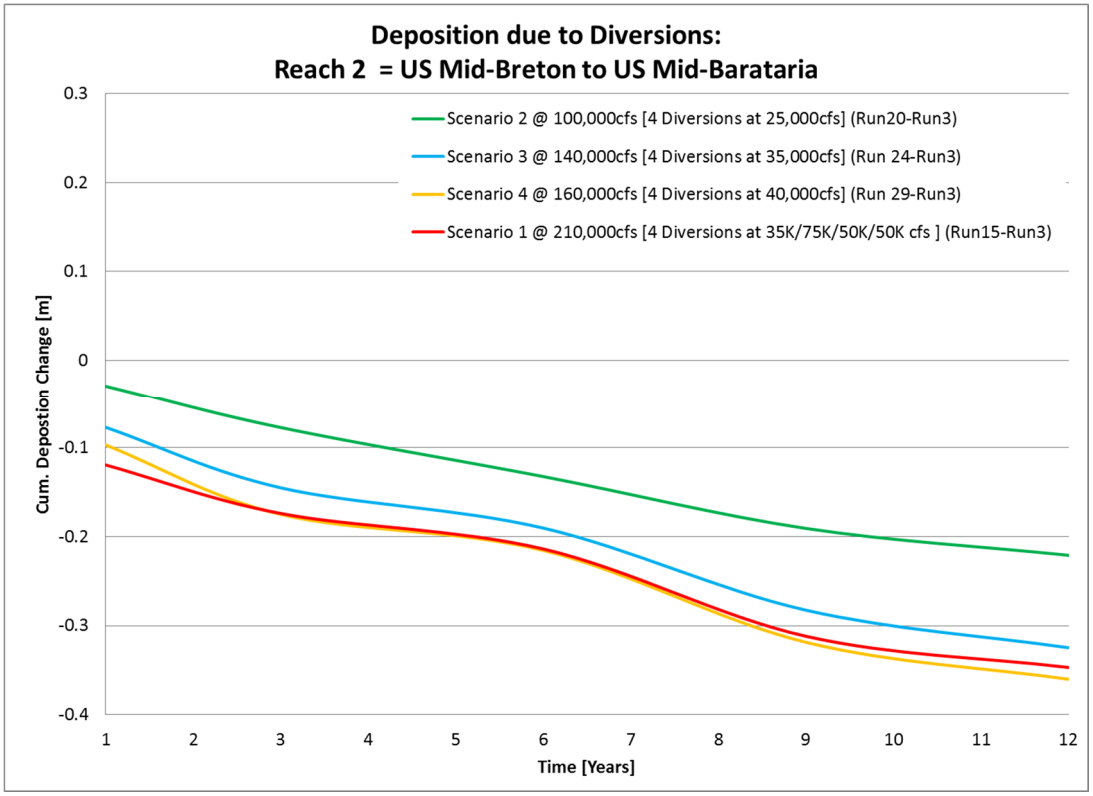

Figure 6.3.2b: Cumulative Deposition Change due to 4 Diversion Scenarios - Reach 2

Reach 3 = Upstream Mid-Barataria to Upstream WPAH (at beginning of outflow)

This reach is mostly depositional. The diversions on the lower part of the domain (Lower Breton and Lower Barataria) have no notable impact on this reach. The largest Mid-Breton Diversion (40,000cfs) results in a depositional peak of 0.1m at approximately year 3 and reaches a steady value of 0.05m by year 9, while the smallest Mid-Breton Diversion (25,000cfs) results in a depositional peak of 0.06m at approximately year 3 and reaches a steady value of 0.025m by year 9. The largest Mid-Barataria Diversion (75,000cfs) results in a depositional peak of 0.19m at approximately year 3 and reaches a value of 0.1m by year 9 with a minor continuous incline, while the smallest Mid-Barataria Diversion (25,000cfs) results in a 0.08m depositional over the first 3 years and reaches a steady value of 0.03m by year 9 (see Figure 6.3.3a)

The laterally averaged deposition due to an individual diversion does not exceed 0.2m in this reach, which is caused by the largest Mid-Barataria Diversion, but when operating 4 Diversions (Figure 6.3.3.b) even Scenario 4, which only has a 40,000cfs Mid-Barataria Diversion, is generating the same depositional maximum but reaches a value of 0.085m by year 9 with a minor continuous decline. Scenario 1, which includes the larges Mid-Barataria Diversion (75,000cfs), exceeds the impacts of the individual diversion of the same size. The peak of Scenario 1 is at 0.26m, approximately 0.07m higher than the individual impact, and reaches a continuous value of 0.13m at year 9, approximately 0.03m higher than the individual impact. Therefore, the depositional trend in this reach is predominantly impacted by the Mid-Barataria Diversion, slightly impacted by the Mid-Breton Diversion and trends are increased when operating all 4 Diversions.

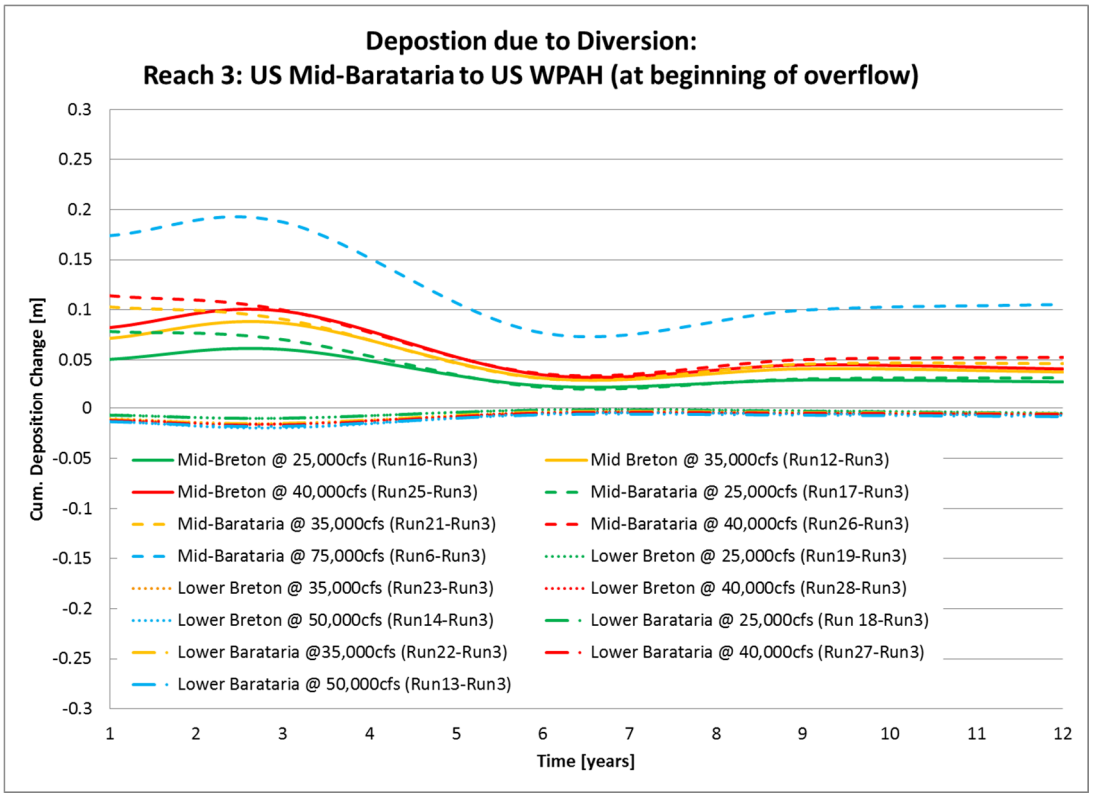

Figure 6.3.3a: Cumulative Deposition Change due to Individual Diversions - Reach 3

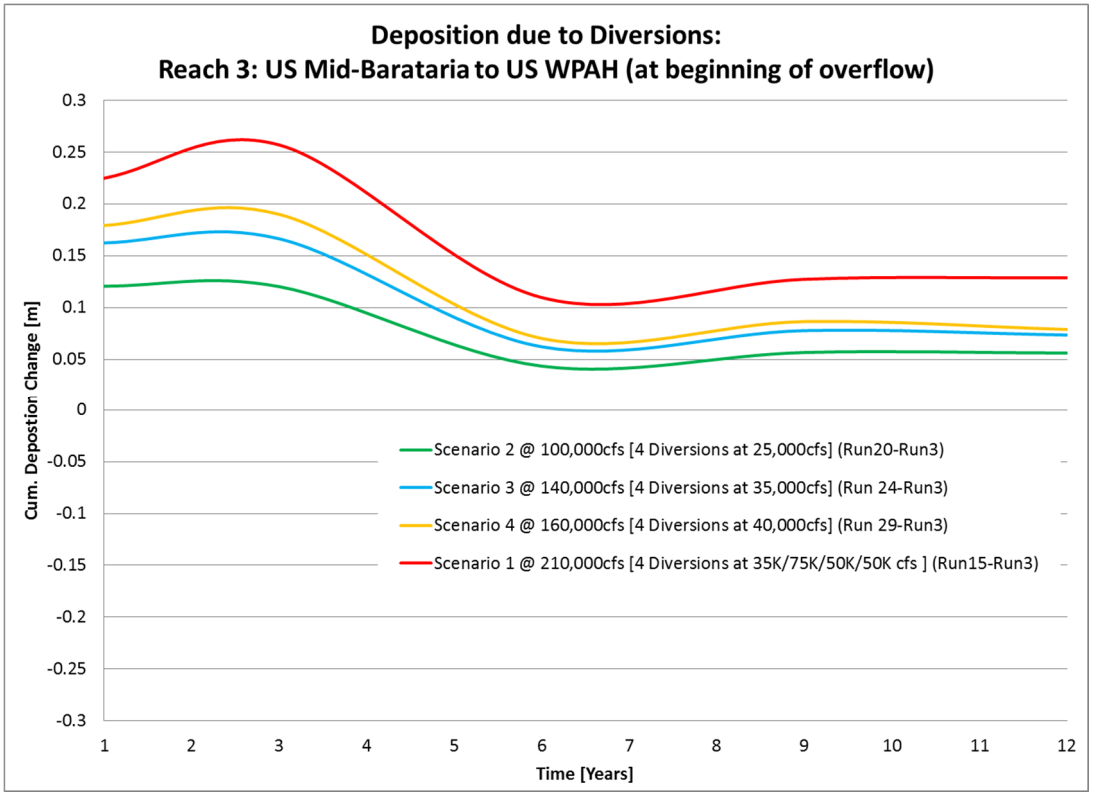

Figure 6.3.3b: Cumulative Deposition Change due to 4 Diversion Scenarios - Reach 3

Reach 4 = Upstream WPAH (at beginning of overflow) to Upstream Lower Barataria

This reach is mostly depositional, with only small erosional tendencies when Lower Breton or Lower Barataria is operated without Mid-Breton or Mid-Barataria. Over time, no individual diversion has a long term depositional or erosional impact exceeding 0.03m or -0.03m (see Figure 6.3.4a). The diversions on the lower part of the domain (Lower Breton and Lower Barataria) have only a minor erosional impact on this reach, with a maximum impact of 0.045m caused by the operation of Lower Breton or Lower Barataria at the maximum evaluated flow of 50,000cfs.

The smallest Mid-Breton Diversion (25,000cfs) has an initial depositional effect of 0.05m over the first 3 years and then oscillates between minimal erosional and depositional periods. The largest Mid-Breton Diversion (40,000cfs) has an initial depositional effect of 0.08m over the first 3 years, but then follows the same pattern as the 25,000cfs case, resulting in very similar long term impact.

The second largest Mid-Barataria Diversion (40,000cfs) differs in its trend from the other Mid-Barataria runs and results in a depositional peak of 0.1m at approximately year 3, followed by a non-steady decline to nearly 0. The smaller Mid-Barataria Diversions (25,000cfs and 35,000cfs) have a lesser peak but result in a deposition of 0.02m at year 12. The largest Mid-Barataria Diversion (75,000cfs) has a depositional peak of 0.2m at approximately year 3, followed by a non-steady decline to nearly 0.03m in deposition.

When operating 4 Diversions (Figure 6.3.4b) all scenarios result in deposition in the reach ranging from a peak at year 3 between 0.1m and 0.25m and reach a depositional value between 0.025m and 0.065m at year 9 with a minor decline over time reaching values between 0.015m and 0.055m at year 12, the end of the computation run. Therefore, the depositional trend in this reach is predominantly impacted by the Mid-Barataria Diversion, slightly impacted by the Mid-Breton Diversion. The depositional trends are increased when operating all 4 Diversions, which causes the reach to be dominantly depositional.

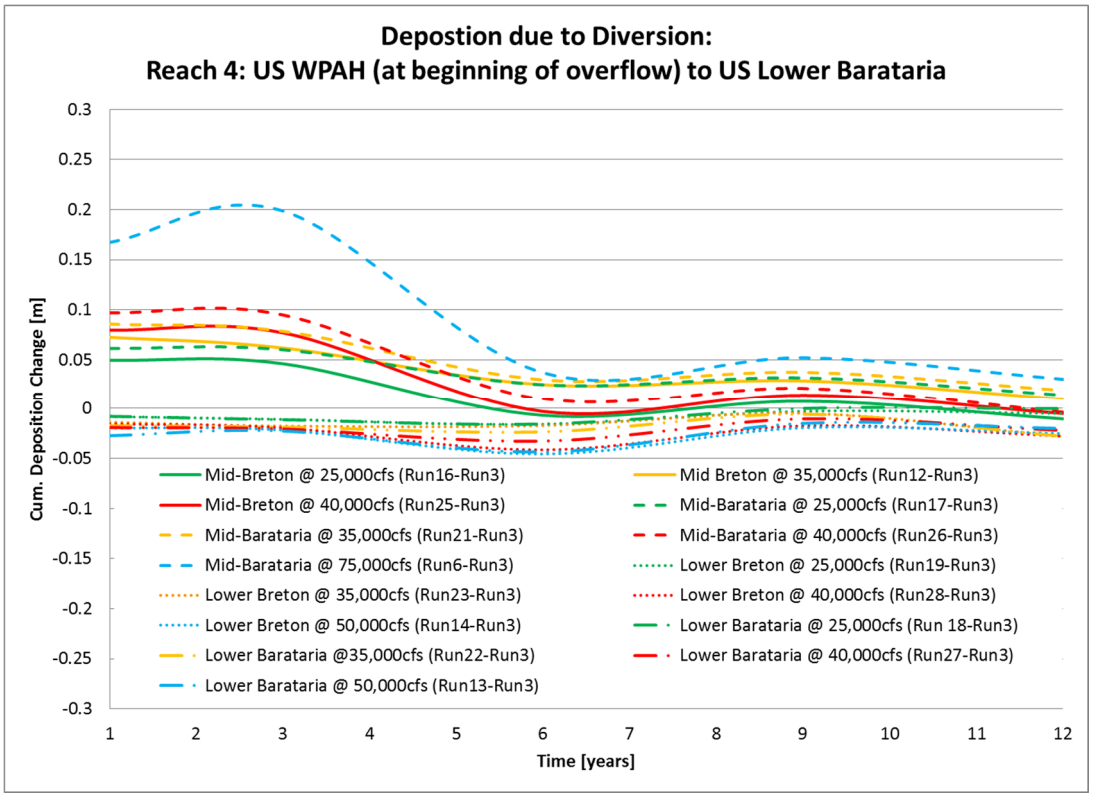

Figure 6.3.4a: Cumulative Deposition Change due to Individual Diversions - Reach 4

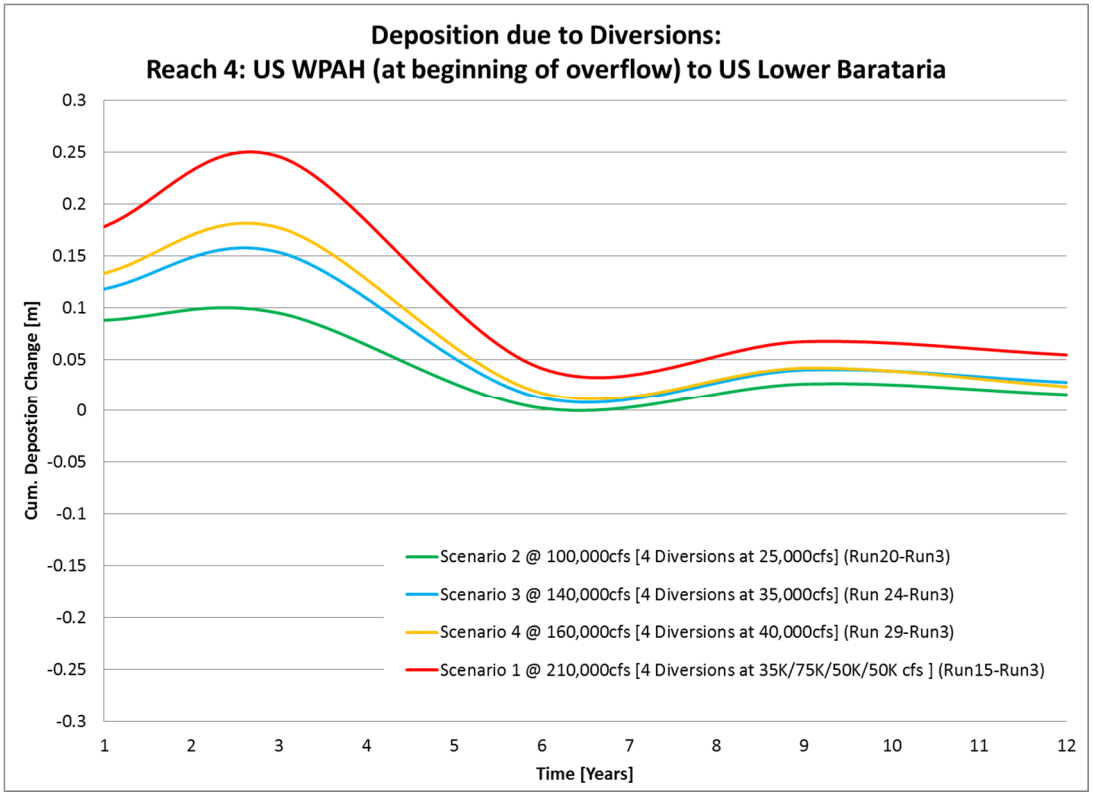

Figure 6.3.4b: Cumulative Deposition Change due to 4 Diversion Scenarios - Reach 4

Reach 5 = Upstream Lower Barataria to Upstream Lower Breton

This reach is slightly depositional, with significant initial depositional impacts due to the Lower Barataria Diversion (see Figure 6.3.5a)

Mid-Barataria is also showing some initial deposition peaking at year 3 while approaching zero at year 9. Mid-Breton is also showing some initial deposition peaking at year 3 (< Mid-Barataria), while also showing a slight depositional equilibrium near zero at year 9. The Lower Breton Diversions causes slight erosional impacts, which decline from an initial value of approximately -0.025m to an equilibrium of approximately -0.01m at year 9.

When operating 4 Diversions (Figure 6.3.5.b) all scenarios result in deposition in the reach ranging from a peak at year 3 between 0.28m and 0.62m and reach a depositional value between 0.01m and 0.03m at year 9 with a minor decline over time reaching values between 0.01m and 0.02m at year 12, the end of the computation run. Therefore, the depositional trend in this reach is only impacting the first 9 years after which the reach reaches quasi-equilibrium near 0.

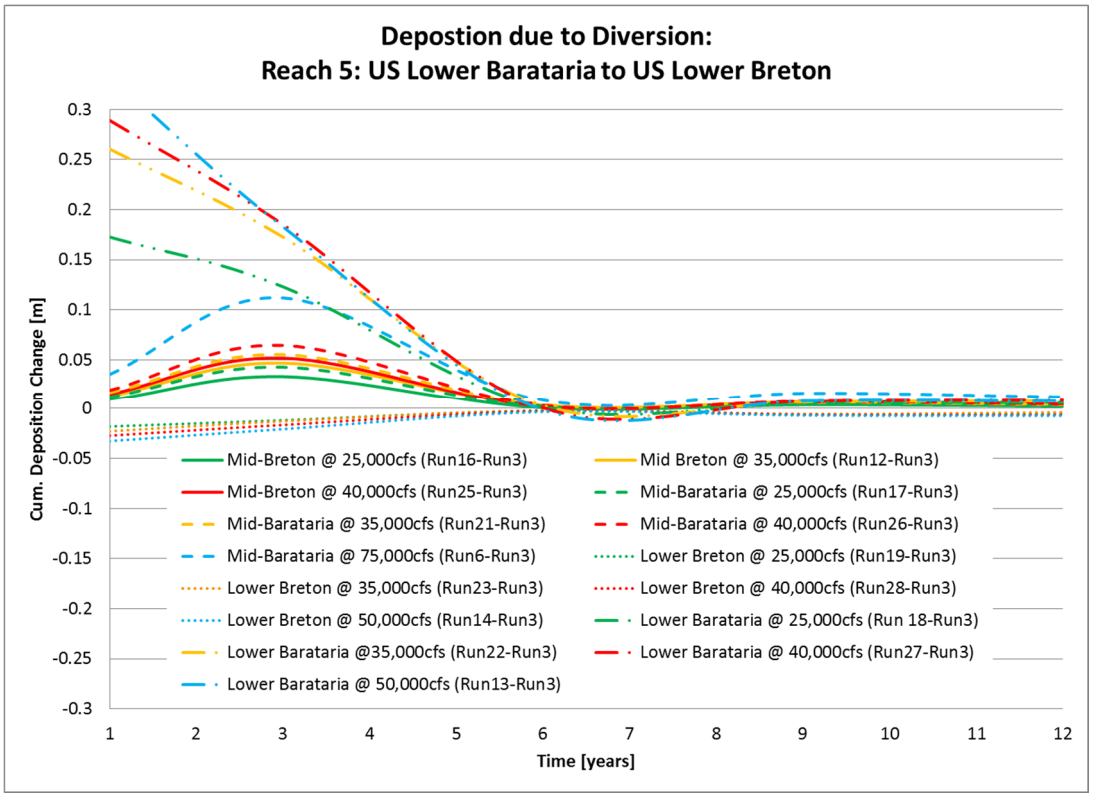

Figure 6.3.5a: Cumulative Deposition Change due to Individual Diversions - Reach 5

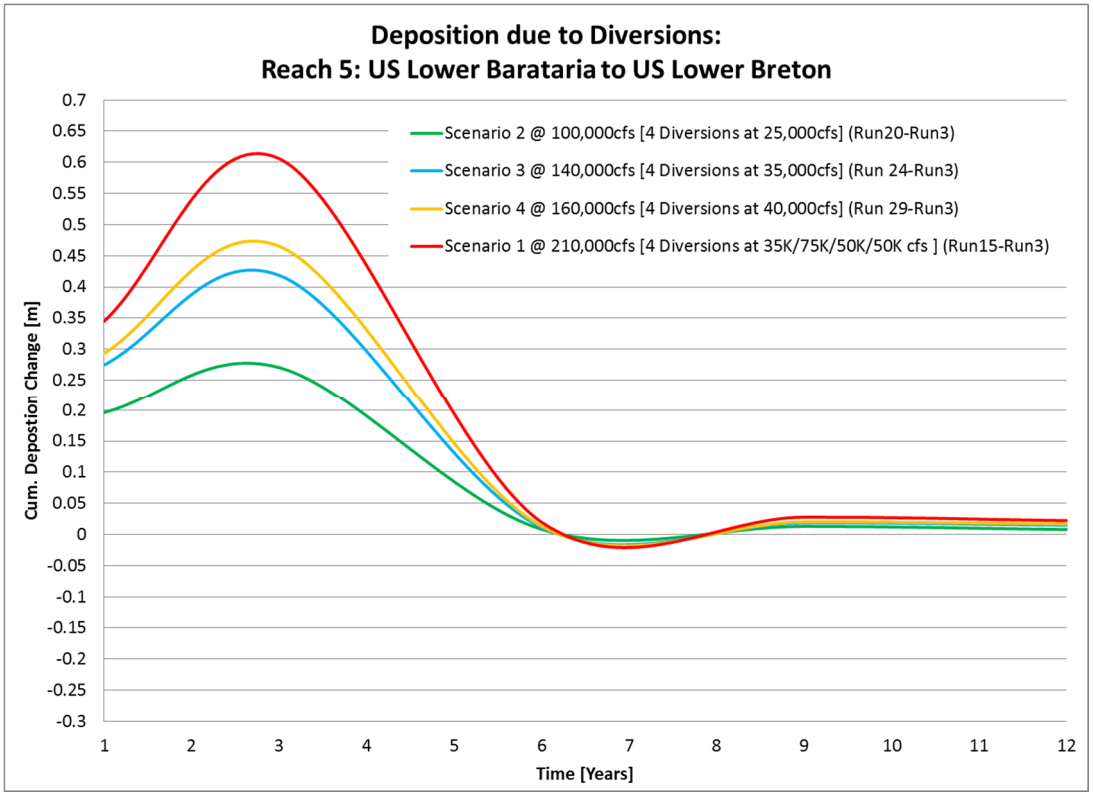

Figure 6.3.5b: Cumulative Deposition Change due to 4 Diversion Scenarios - Reach 5

Reach 6 = Upstream Lower Breton to Upstream Fort St. Phillip

This reach is depositional (see Figure 6.3.6a). The largest Mid-Barataria Diversion (75,000cfs) and the largest Lower Barataria Diversion (50,000cfs) cause the most deposition at year 12, 0.2m and 0.14m respectively. The Lower Barataria deposition value remains steady between year 9 and 12, while the Mid-Barataria Diversion deposition continues to increase between years 9 and 12, from 0.18m to 0.2m. The Mid-Breton and Mid-Barataria Diversions cause erosion in the first 3 years, with the largest Mid-Barataria Diversion (75,000cfs) causing the most significant erosional impact. Lower Barataria and Lower Breton Diversions increase in Deposition in the first 3 years and then slowly decline to values between 0.05m and 0.14m at year 12. The Lower Barataria Diversions cause higher values within the range while the maximum deposition at year 12 for Lower Breton does not exceed 0.1m.

When operating 4 Diversions (Figure 6.3.6.b) all scenarios result in deposition in the reach ranging from a peak at year 3 between 0.45m and 1.02m and reach a depositional value between 0.3m and 0.75m at year 9 with a minor decline over time reaching values between 0.3m and 0.72m at year 12, the end of the computation run. Therefore, all Scenarios follow the same trend, which increases with increase in total diversion flow for all four diversions in operation. The depositional impacts are highly linked to the overall diversion flow, dominated by Mid-Barataria and Lower Barataria.

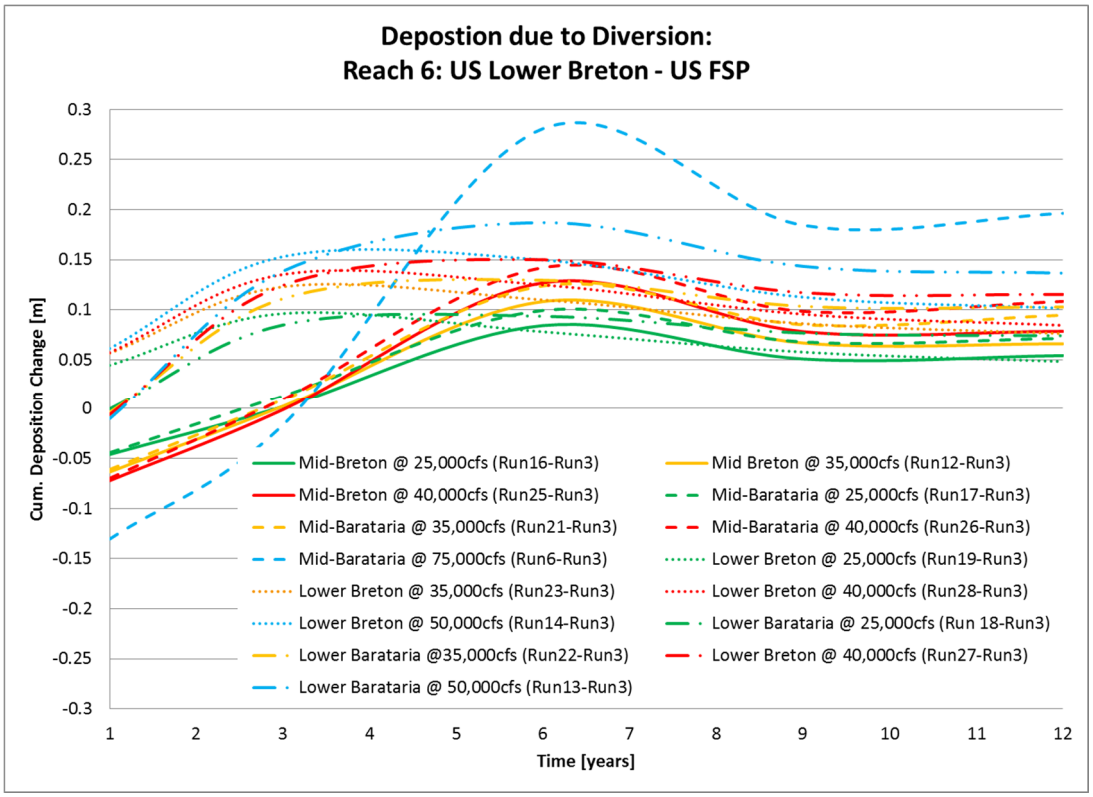

Figure 6.3.6a: Cumulative Deposition Change due to Individual Diversions - Reach 6

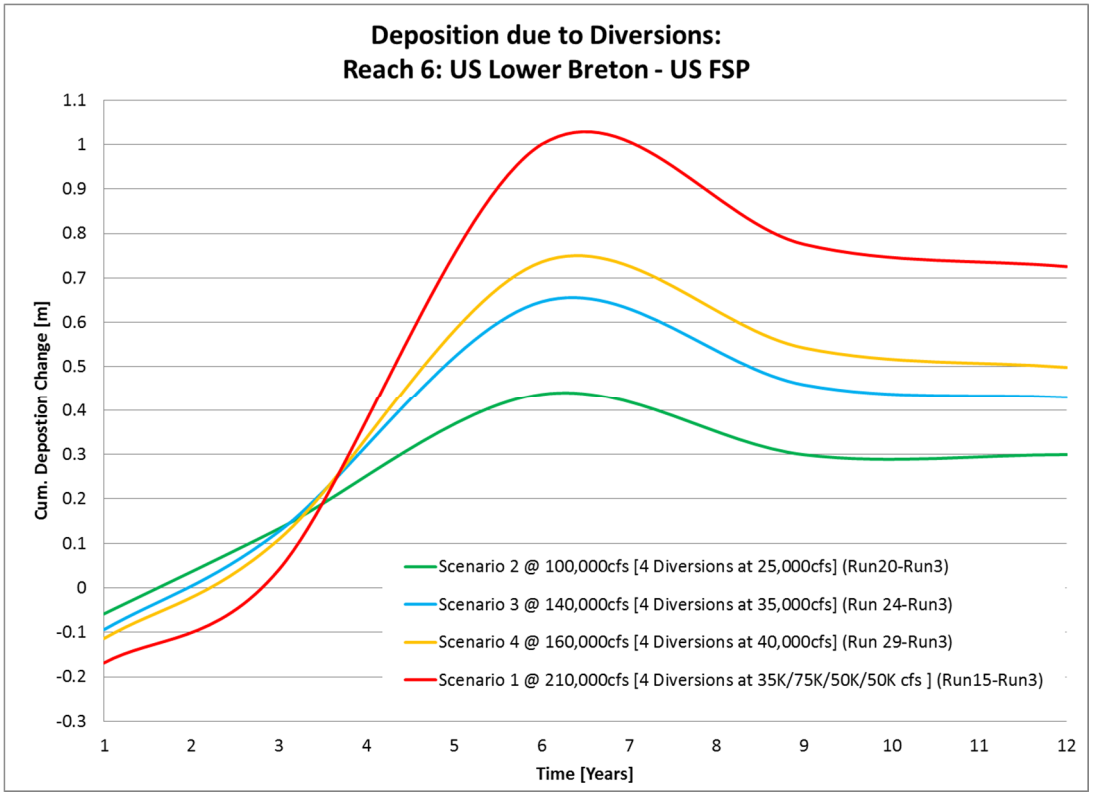

Figure 6.3.6b: Cumulative Deposition Change due to 4 Diversion Scenarios - Reach 6

Reach 7 = Upstream Fort St. Phillip to Head of Passes

This reach is mostly depositional, with only small erosional tendencies in the first 4 years. Over time the maximum deposition caused by individual diversions ranges between 0.07m and 0.2m (see Figure 6.3.7a). Mid-Barataria at 75,000cfs has the largest impact followed by the Lower Barataria Diversion at 50,000cfs and the Lower Breton Diversion at 50,000cfs.

The trend for operating all 4 Diversions (Figure 6.3.7b) follows a similar pattern than the individual impacts, only prolonged, meaning the long term trends are not fully captured in the 12 year analysis. The overall depositional impact of all scenarios at year 12 ranges from 0.36m to 0.78m. The maximum value is reached by the maximum flow scenario (Scenario 1 at 210,000cfs) and is still increasing at year 12. Scenarios 3 (140,000cfs) and 4 (160,000cfs) result in depositional impacts at year 12 of 0.54m and 0.62 respectively, also showing a small increase at year 12. Therefore, the depositional trend in this reach is predominantly impacted by the overall diversion flow with the Mid-Barataria Diversion being the biggest contributor.

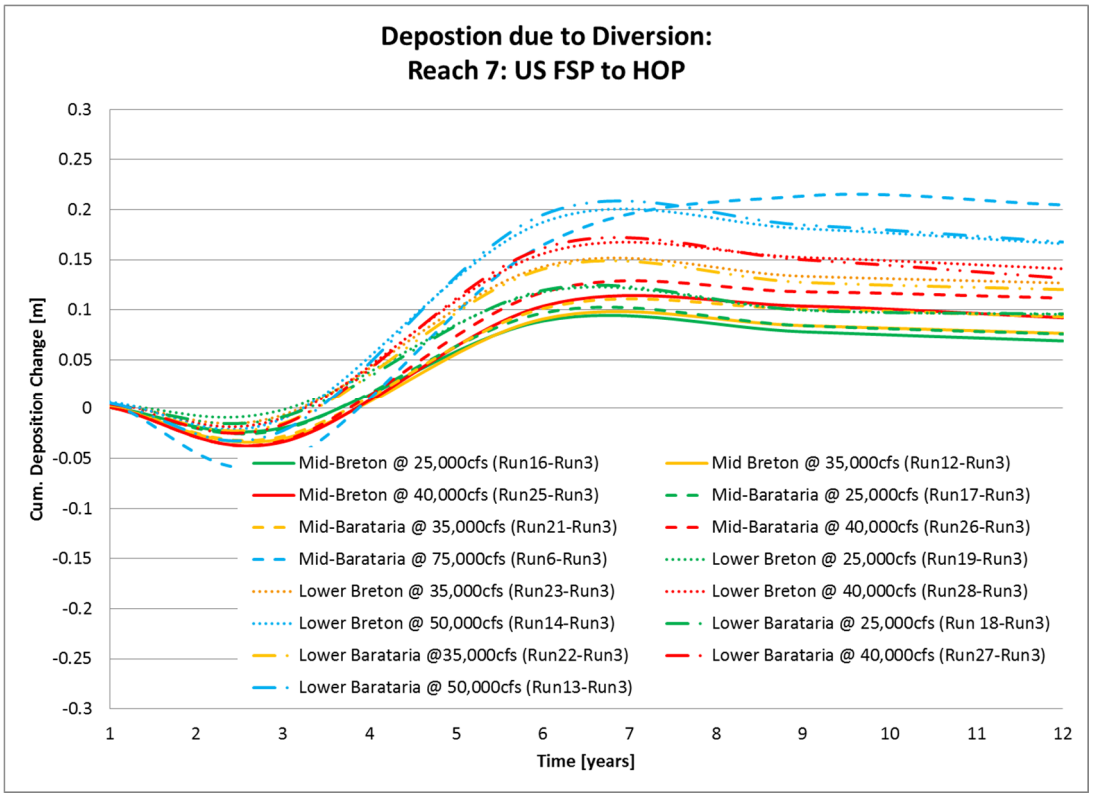

Figure 6.3.7a: Cumulative Deposition Change due to Individual Diversions - Reach 7

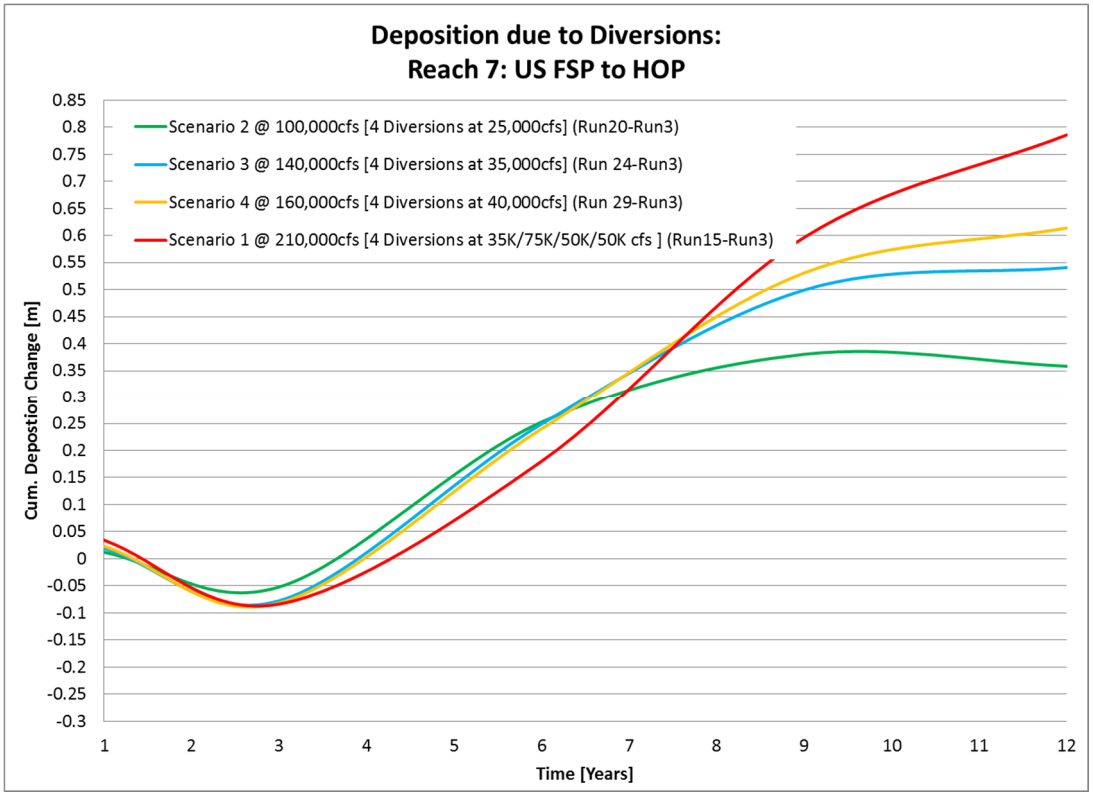

Figure 6.3.7b: Cumulative Deposition Change due to 4 Diversion Scenarios - Reach 7

To analyze the interaction of diversions on the diverted sediment transport, the cumulative total sediment transport was extracted for each case described in Table 6.2.1. The results are summarized in Table 6.3.1 below and visually depicted in Figures 6.3.8 – 6.3.11. Negative transport values in Table 6.3.1 indicated flow to the Breton Sound or left descending bank.

Table 6.3.1: Comparison of Cumulative Total Sediment Transport:

Hypothesis 3: Analysis of Cumulative Total Transport in Diversions						
Diversion	**Open Diverisons**	**Case:**	**Senario 2**	**Scenarion 3**	**Scenario 4**	**Scenario 1**
Mid-Breton		**Diversion Flow [cfs]**	25,000 cfs	35,000 cfs	40,000 cfs	35,000 cfs
	1	**cum total transport @ Year 12 [million cubic meters]**	**-24,087**	**-35,107**	**-40,578**	**-35,107**
		Run	16	12	25	12
	4	**cum total transport @ Year 12 [million cubic meters]**	**-24,176**	**-35,239**	**-40,712**	**-35,366**
		Run	20	24	29	15
	Cum. Transport/Diversion Flow (1 Diversion)		-0.96	-1.00	-1.01	-1.00
	Difference between 4 and 1 Diversion Case		0.37%	0.38%	0.33%	0.74%
Mid-Barataria		**Diversion Flow [cfs]**	25,000 cfs	35,000 cfs	40,000 cfs	75,000 cfs
	1	**cum total transport @ Year 12 [million cubic meters]**	**17,548**	**25,933**	**30,055**	**59,202**
		Run	17	21	26	6
	4	**cum total transport @ Year 12 [million cubic meters]**	**17,609**	**25,837**	**30,125**	**59,558**
		Run	20	24	29	15
	Cum. Transport/Diversion Flow (1 Diversion)		0.70	0.74	0.75	0.79
	Difference between 4 and 1 Diversion Case		0.35%	-0.37%	0.23%	0.60%
Lower Barataria		**Diversion Flow [cfs]**	25,000 cfs	35,000 cfs	40,000 cfs	50,000 cfs
	1	**cum total transport @ Year 12 [million cubic meters]**	**17,545**	**25,880**	**30,885**	**40,527**
		Run	18	22	27	13
	4	**cum total transport @ Year 12 [million cubic meters]**	**17,329**	**25,632**	**31,212**	**39,442**
		Run	20	24	29	15
	Cum. Transport/Diversion Flow (1 Diversion)		0.70	0.74	0.77	0.81
	Difference between 4 and 1 Diversion Case		-1.23%	-0.96%	1.06%	-2.68%
Lower Breton		**Diversion Flow [cfs]**	25,000 cfs	35,000 cfs	40,000 cfs	50,000 cfs
	1	**cum total transport @ Year 12 [million cubic meters]**	**-17,951**	**-26,024**	**-30,461**	**-39,314**
		Run	19	23	28	14
	4	**cum total transport @ Year 12 [million cubic meters]**	**-17,598**	**-25,418**	**-29,505**	**-37,409**
		Run	20	24	29	15
	Cum. Transport/Diversion Flow (1 Diversion)		-0.72	-0.74	-0.76	-0.79
	Difference between 4 and 1 Diversion Case		-1.97%	-2.33%	-3.14%	-4.85%

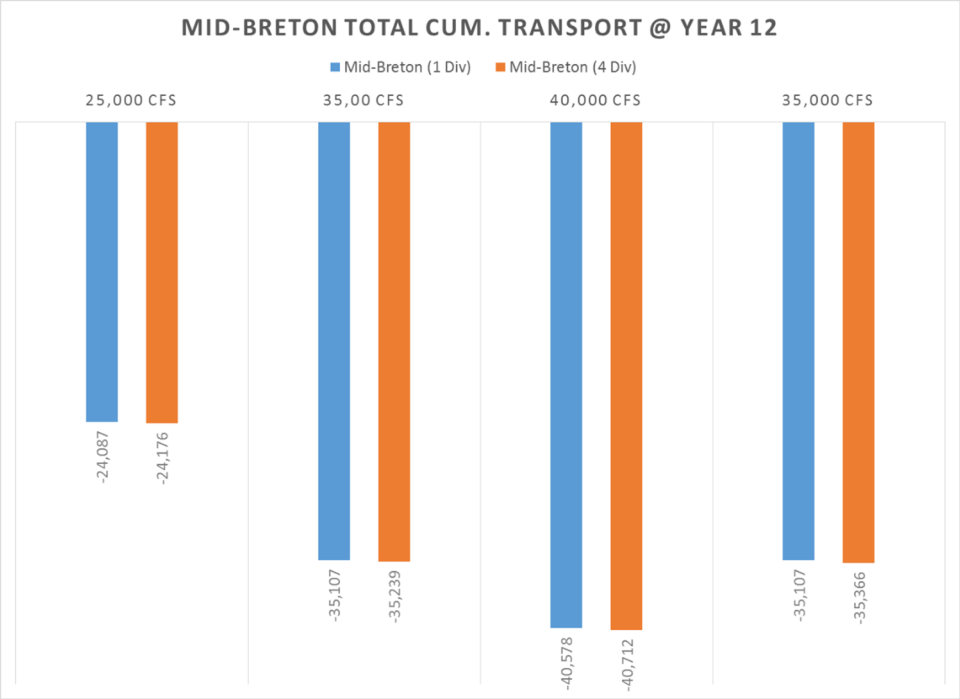

Figure 6.3.8: Comparison of Cumulative. Total Transport through Mid-Breton Diversion for Individual and Multiple Operations

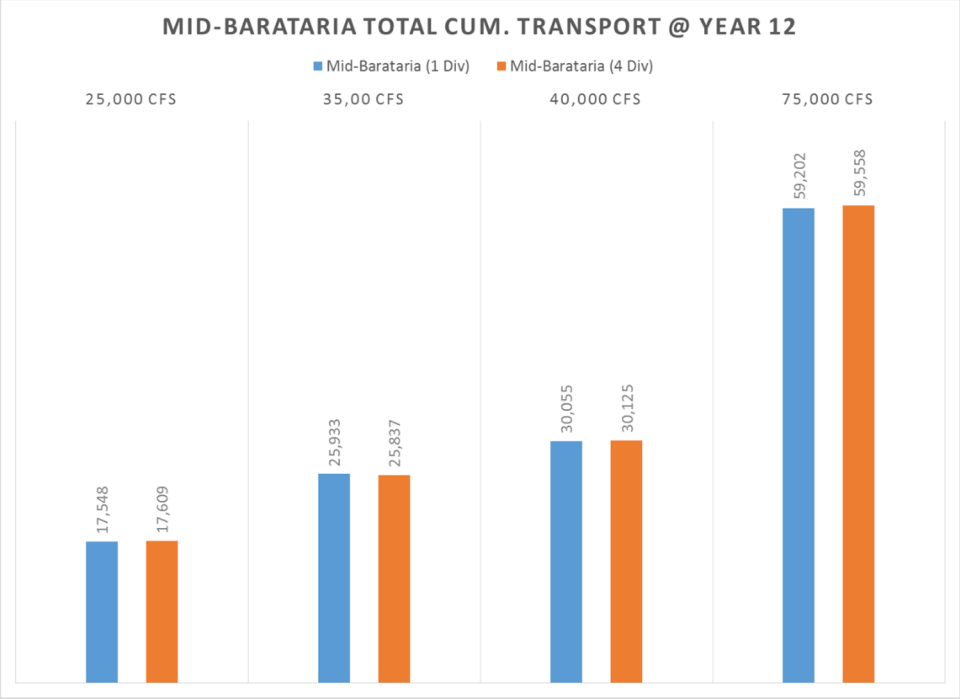

Figure 6.3.9: Comparison of Cumulative. Total Transport through Mid-Barataria Diversion for Individual and Multiple Operations

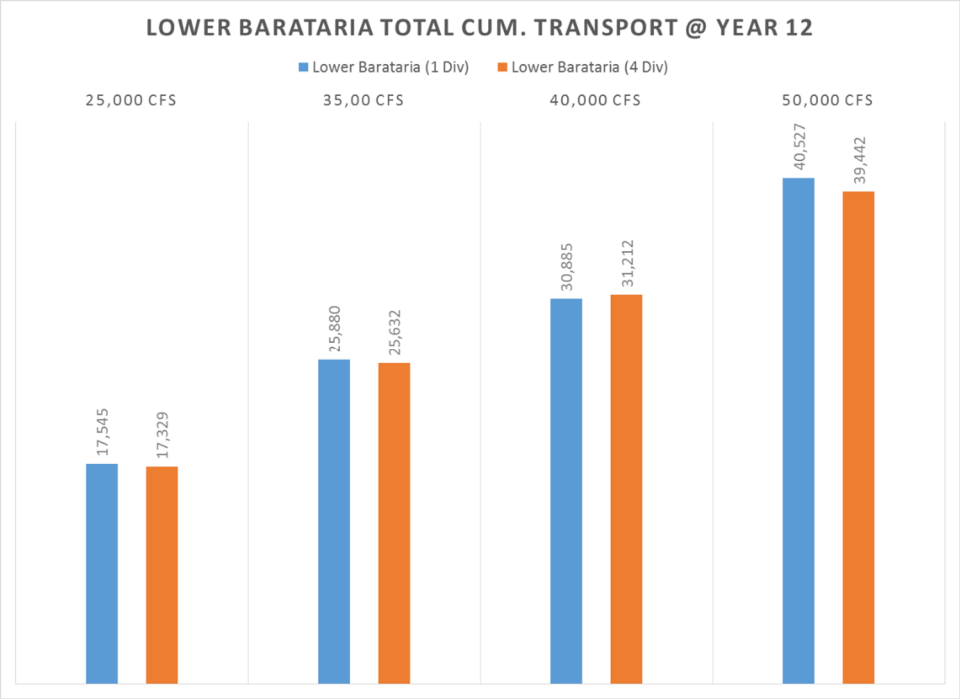

Figure 6.3.10: Comparison of Cumulative. Total Transport through Lower Barataria Diversion for Individual and Multiple Operations

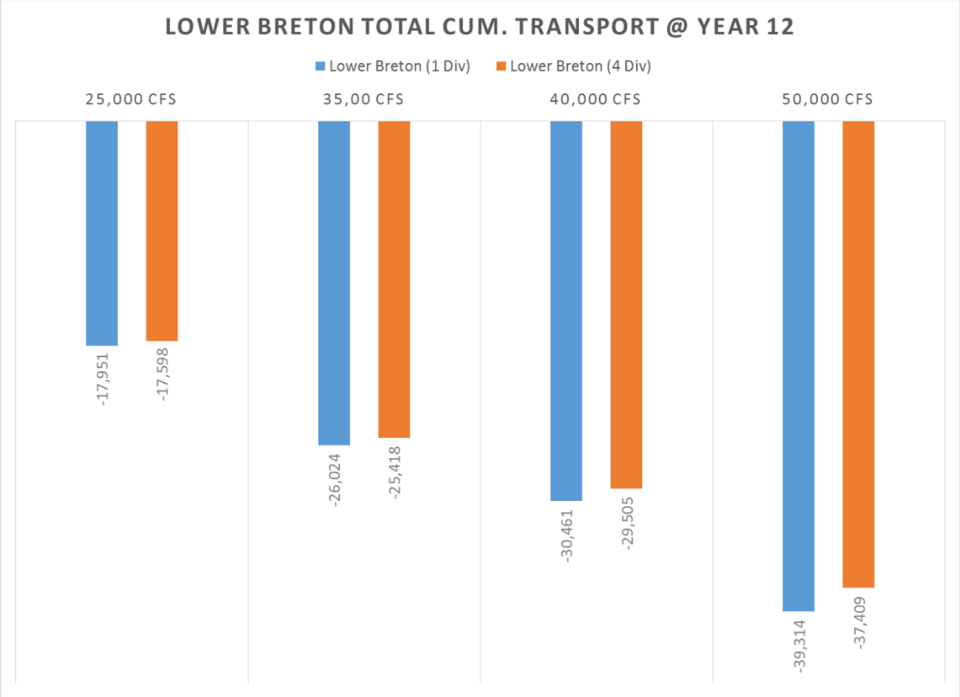

Figure 6.3.11: Comparison of Cumulative Total Transport through Lower Breton Diversion for Individual and Multiple Operations

6.4 DISCUSSION

The cumulative laterally averaged deposition analysis by reach clearly shows that while influences from some diversions are minimal in some reaches, especially further upstream, in most cases the diversion impacts span multiple reaches and trigger deposition near Venice and HOP. Especially high diversions flows, as proposed for Mid-Barataria Diversion (75,000cfs), cause depositional changes that are significant, especially in the lower reaches.

Figure 6.4.1 depicts the 12-Year cumulative total transport difference, obtained by subtracting the diverted total transport for the 1 diversion case from the 4 diversion case for the same diverted discharge flow (i.e. 25,000cfs for Mid-Breton).

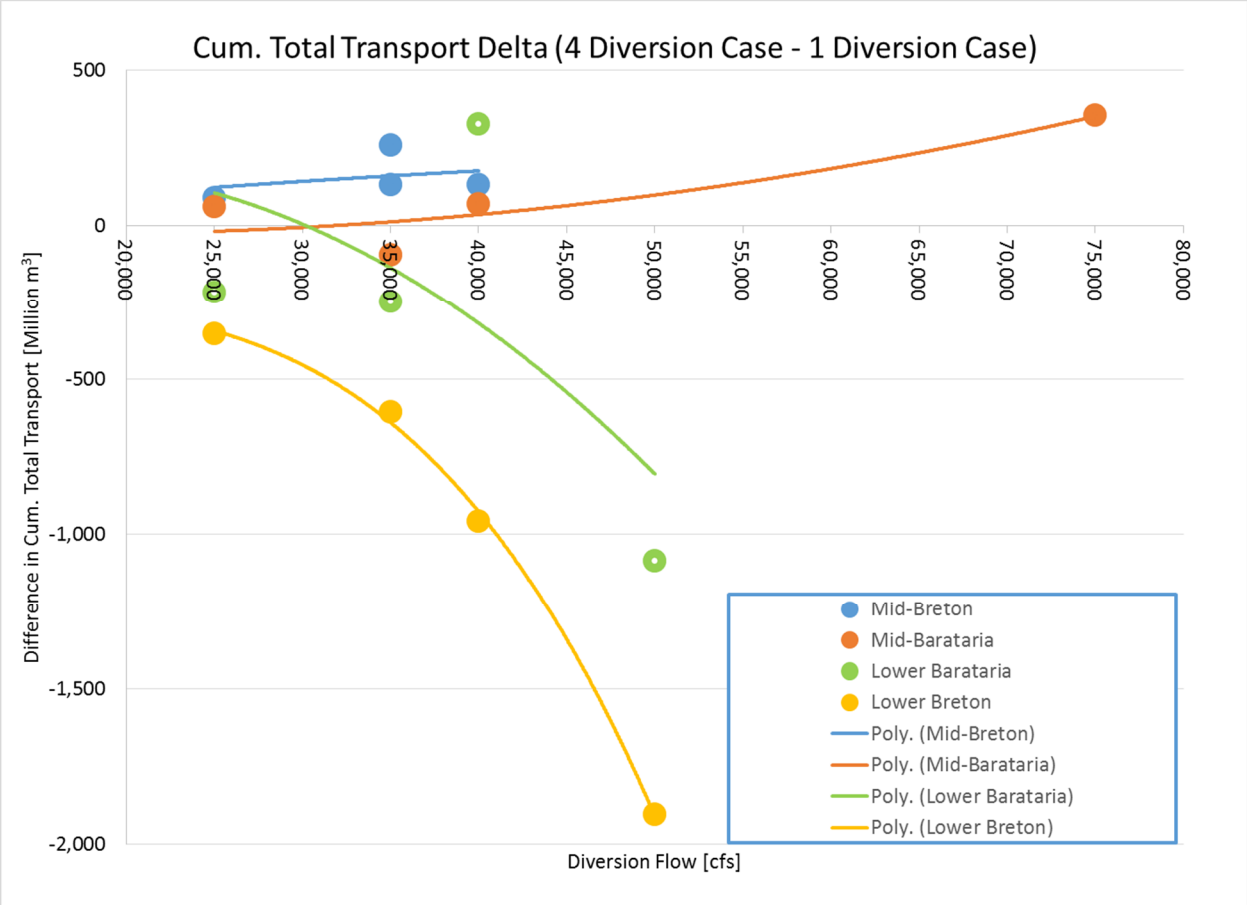

Figure 6.4.1: Difference in 12-Year Cumulative Total Transport measured in Million m^3 versus Individual Diversion Flows
(4 Diversion Case – 1 Diversion Case)

The increase in individual diversion flow tends to increase the difference in cumulative transport of sand between single diversion and multiple diversion scenarios. This is highlighted by the Mid-Breton case, which had two results for a 35,000cfs diversion flow. The difference in cumulative sand transport for the scenario diverting more flow (210,000cfs total flow diverted) overall over 4 diversions is greater than for the other case (140,000cfs total flow diverted).

The Lower Breton Diversion appears to follow an increasing trend in the difference between the individual and multiple diversion transport values. A similar trend can be observed for the Lower Barataria, while in general having a smaller difference in diverted cumulative transport between the 4 diversion case and the 1 diversion case. Furthermore, the Lower-Diversions appear to have greater differences than the Mid-Diversions.

Figure 6.4.2 shows the difference in cumulative transport as a percentage of the single diversion transport. This indicates that the Lower Breton Diversion, which is the diversion closest to HOP, has the largest difference in cumulative sand transport followed by the Lower-Barataria Diversion. The negative percentage indicates that when only 1 diversion is operated the cumulative total sand transport through the diversion is larger than when all 4 diversions are operated. For Lower Breton and Lower Barataria the difference increases with increase in overall flow for the 4 diversion cases.

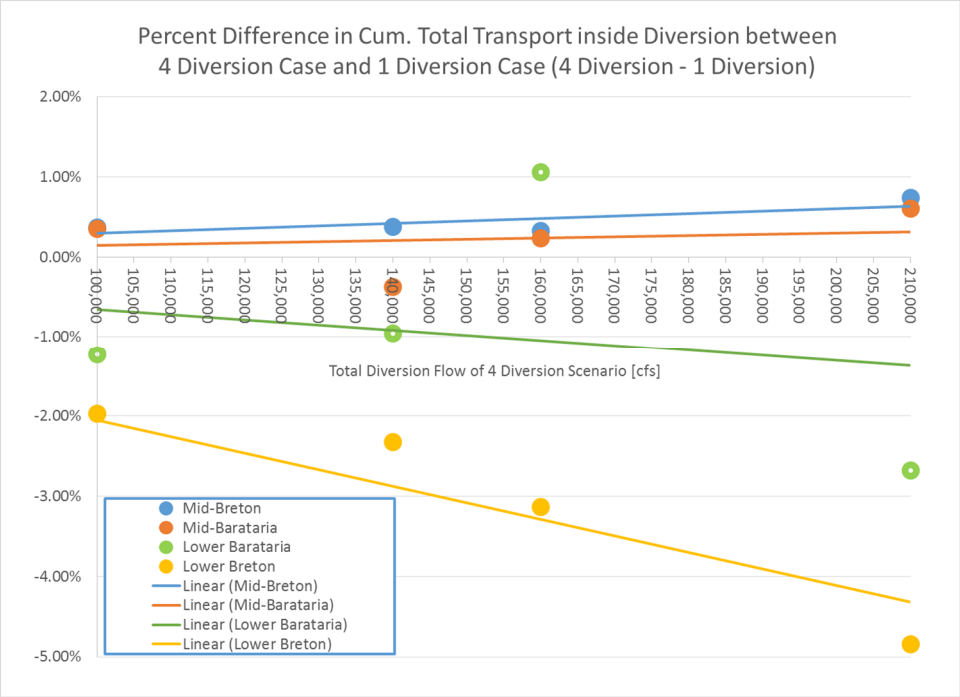

Figure 6.4.2: 12-Year Percent Change in Cumulative Total Transport between the Multiple Scenario and Single Diversion Case
(4 Diversion Case – 1 Diversion Case)

The Mid-Breton and Mid-Barataria Diversions on the other hand appear to divert slightly more when all diversions are in operation, when compared to the operation of a single diversion. The difference is the greatest for Mid-Breton, which is the most upstream diversion proposed. To investigate this effect for Mid-Breton, the water levels were extracted for the no diversion, one diversion and four diversions (Scenario 1). Figure 6.4.3 depicts the change in water surface level at river centerline for the operation of the Mid-Breton Diverison at 35,000cfs (Run 12, 1 Diversion) and the operation of the Mid Breton Diversion at 35,000cfs in conjunction with Mid-Barataria at 75,000cfs, Lower Barataria at 50,000cfs and Lower Breton at 50,000cfs (Run 15, 4 Diversions), as well as the no diversion water levels.

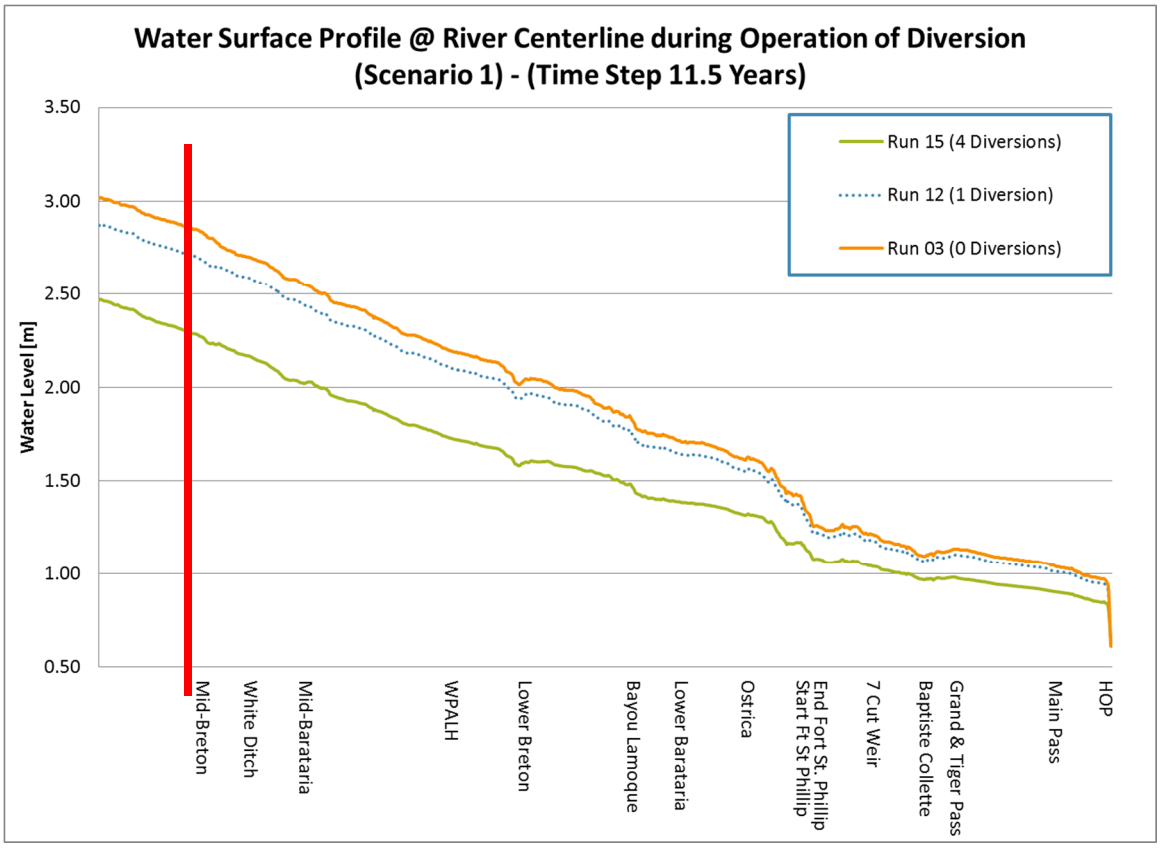

Figure 6.4.3: Water Surface Profile at River Centerline during Operation of Diversion (Scenario 1) – (Time Step 11.5 Years)

For the 4 Diversion case the water level difference between Belle Chasse and Mid – Breton is -0.0227m, while the water level difference for the 1 Diversion case is -0.213m, indicating that the 4 diversion case has a steeper slope (0.0020%) than the 1 diversion case (0.0019%). Similarly, the 1 diversion case (0.0019%) has a steeper slope than the no diversion case (0.0018%). This observation is consistent with the gradually varied flow analysis (Chaudhry 1993), which shows that an M-2 curve can be expected upstream of a diversion, which implies that the water surface slope is steeper than the normal flow. The steeper slope will increase the stream power and results in more in-river transport of sand and consequently greater availability of sand for greater extractions. Similar slope patterns were observed for the reach upstream of Mid-Barataria.

6.5 CONCLUSIONS

The hypothesis regarding the independence of morphological changes due to single and multiple diversions is not accepted since each diversion does not function independent in terms of local and regional deposition within the Mississippi River. The largest dependencies are on the most downstream diversions, which increase with the total diverted flow.

The hypothesis regarding sediment capture interdependencies is accepted within limits. For example, if the total diversion flow is less than 140,000cfs, the percent difference in diverted sand between the single and the multiple diversion case is less than 3% (see Figure 6.4.2. Except for the Lower Breton Diversion, a total diversion flow of less than 140,000cfs would generate a difference of less than 1%. The critical flow for interdependency with regard to the diversion capture rate appears to be approximately 140,000cfs.

As Mid-Barataria and Mid-Breton diversion undergo design and permitting, their impacts have to be analyzed as individual structures as well as their cumulative impacts due to other diversions that are operated simultaneously.

7.0 CHAPTER 7: RESEARCH QUESTIONS

7.1 RESEARCH QUESTION 1

Research Question 1:

Does the river have sufficient energy to divert the targeted discharges for the four (4) main diversion locations?

7.1.1 METHODOLOGY

The model runs summarized in Table 7.1.1.1 were set-up to obtain data in support of an evaluation of this question:

Table 7.1.1.1: Model Runs for Research Question 1:

#	Hydrograph		Years	Diversions	Diversion Info	Other
	U	V				
6		X	1-12	1	Mid-Barataria = 75,000cfs	
9		X	1-12	1	Mid-Barataria = 75,000 cfs	Gulf Stage Boundary @ Diversions
8		X	1-12	2	Mid-Breton = 35,000 cfs & Mid-Barataria = 75,000cfs	
10		X	1-12	2	Mid-Breton = 35,000 cfs & Mid-Barataria = 75,000 cfs	Gulf Stage Boundary @ Diversions
15		X	1-12	4	Mid-Breton = 35,000 cfs & Mid-Barataria = 75,000 cfs, Lower Barataria = 50,000 cfs & Lower Breton = 50,000 cfs	
11		X	1-12	4	Mid-Breton = 35,000 cfs & Mid-Barataria = 75,000 cfs, Lower Barataria = 50,000 cfs & Lower Breton = 50,000 cfs	Gulf Stage Boundary @ Diversions

All runs cover a 12 year computational run and utilize the variable hydrograph. Three diversion cases were set up, one with 1 diversion, which includes Mid-Barataria at 75K, one with 2 diversions, which includes Mid Breton at 35K and Mid-Barataria at 75K and one with 4 diversions, which includes Mid Breton at 35K, Mid-Barataria at 75K, Lower Barataria at 50K and Lower Breton at 50K. Each diversion case was run with a pre-

calculated, enforced extraction based on the desired diversion flow as well as an open boundary / gulf-stage condition. For the open boundary / gulf stage condition, the prescribed boundary condition at the outflow of each diversion is replaced by the stage, which is based on the water level in the Gulf of Mexico.

The diversion channels in the open boundary runs were the same as those used in the runs with prescribed discharge boundary conditions, which are the same as utilized in the long model (McCorquodale et al. 2017), which are summarized in Table 7.1.1.2. The only modification was, that the runs for Mid-Breton conducted as part of this study were not limited to March and April only as indicated below the table (**). The diversion widths provided in Table 7.1.1.2 are based on an invert of -40ft and a non-depositional velocity of 2m/s as provided by the Water Institute of the Gulf (TWIG) (McCorquodale et al. 2017). The model runs assume that the full width of the diversion is available for flow.

Table 7.1.1.2 Diversion Plan for PR #2 (McCorquodale et al. 2017 – Table 5.2)

	Qmax cfs (m^3/s)	Invert ft (m)	Width ft (m)	Remarks
1. Master Plan Mid-Barataria Sediment Diversion at RM 60.7 – Right Descending Bank (RDB) Case 1	**75,000 (2125)***	-40 ft (-12.2)	**330 (100t)**	**Myrtle Grove**
2. Master Plan Mid-Breton Sediment Diversion at RM 68.6 – LDB	**35,000 (992)****	-40 (-12.2)	**165 (50)**	**White Ditch**
3. Master Plan Lower Barataria Sediment Diversion at RM 29.5 – RDB	**50,000 (1416)***	-40 (-12.2)	**165 (50)**	**Empire**
4. Master Plan Lower Breton Sound Sediment Diversion at RM 42.8 – LDB	**50,000 (1416)***	-40 (-12.2)	**165 (50)**	**Black Bay**

* *Only open when Tarbert Flow > 600,000 cfs*

** *Only open when Tarbert Flow > 600,000 cfs and March and April only.*

It is assumed that there are no energy losses due to the control structure, which implies a wide channel opening. In addition, the Water Institute recommended a diversion channel velocity of 2m/s to prevent sand deposition in the delivery channel.

7.1.2 RESULTS

The Figures 7.1.2.1 to 7.1.2.4 show the results for the worst case scenario, which is the operation of four diversions at river flows exceeding 600,000 cfs. The results for the 1 diversion and 2 diversion runs are included in Appendix R1.

When running all four diversions at a river flow trigger point of 600,000 cfs, all diversions except the Lower Breton Diversion can divert the respective target flows, which are: 75,000 cfs for the Mid-Barataria Diversion, 50,000 cfs for the Lower Barataria and the Lower Breton Diversions and 35,000 cfs for the Mid-Breton Diversion. The Lower Breton Diversion is the most downstream diversion and therefore, has the lowest river energy with respect to the Gulf of Mexico stage for diversion of discharge. Over the 12-year period modeled, the Lower Breton Diversion falls short by 0.5% of the target discharge, when all diversions are in operation at > 600,000 cfs river flows. The selection of the 600,000 cfs mark for diversion activation is based on the value established during the development of the original regional 3-D Model for the Lower Mississippi River (McCorquodale et al. 2017, Master Plan 2012).

The 1 and 2 diversion cases similarly divert the target flows for the respective diversions, which means the blue line, representing the open flow condition always exceeds the red line, representing the forced flow. Negative discharge numbers represent discharge to the east side of the Mississippi River, as diverted by Mid-Breton and Lower Breton Diversions, while positive discharge numbers represent flow to the west of the Mississippi River, as diverted by the Mid-Barataria and the Lower Barataria Diversions.

All model runs utilized for this research question are based on keeping the geometry of the diversions the same for the two discharge boundary conditions. The fact that the instantaneous discharge for the stage-based open boundary conditions almost always exceeds the forced extractions shows that the geometry of the diversion can divert more flow than the design flow, which means that the diverted flow would have to be managed by a gated structure to the desired maximum discharge condition.

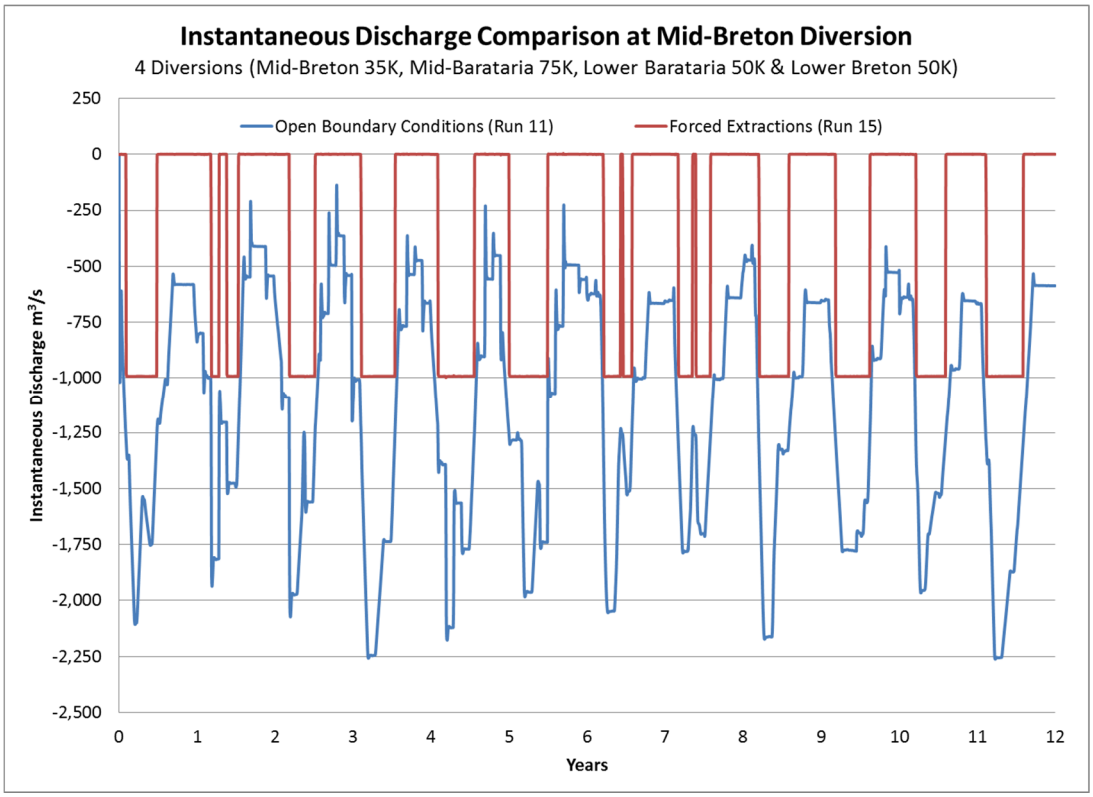

Figure 7.1.2.1: Instantaneous Discharge Comparison at Mid-Breton Diversion

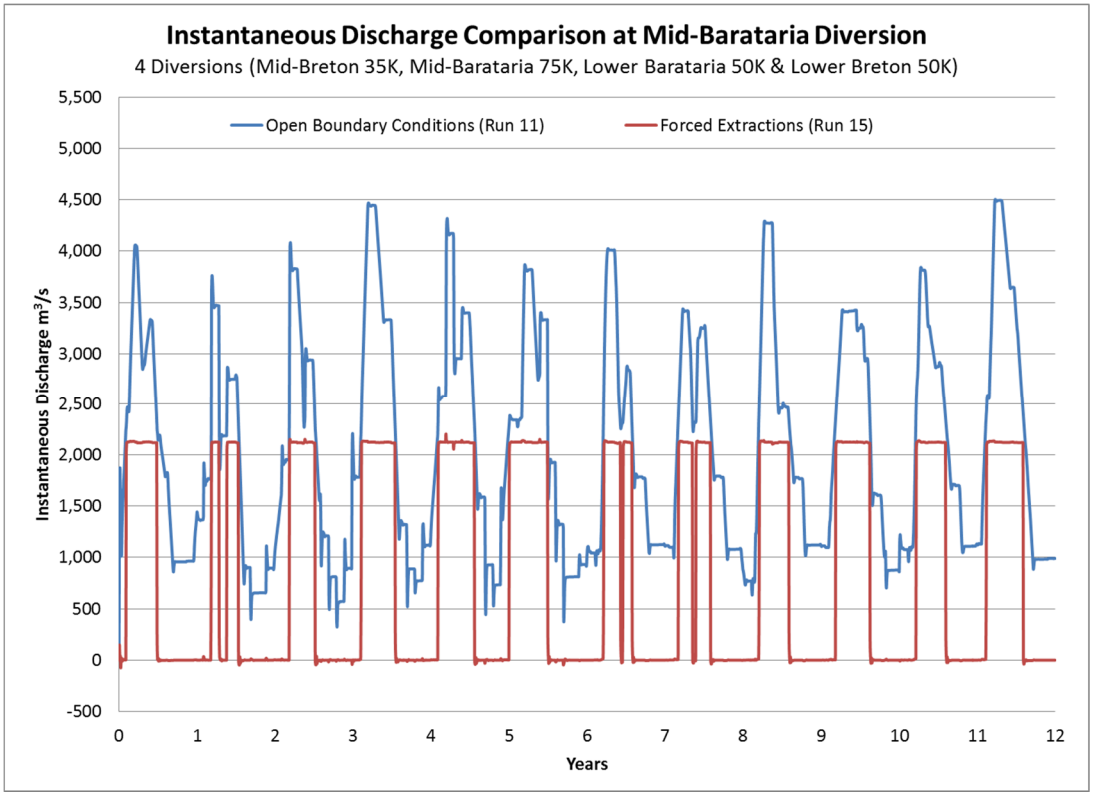

Figure 7.1.2.2: Instantaneous Discharge Comparison at Mid-Barataria Diversion

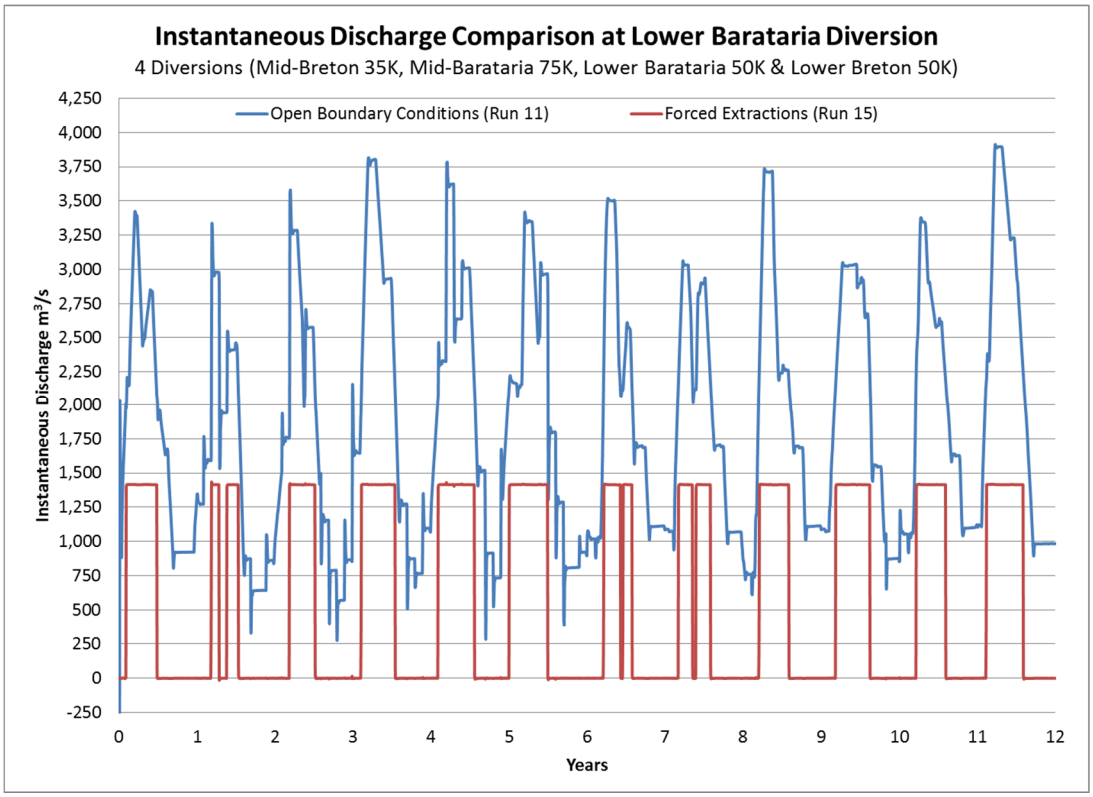

Figure 7.1.2.3: Instantaneous Discharge Comparison at Lower Barataria Diversion

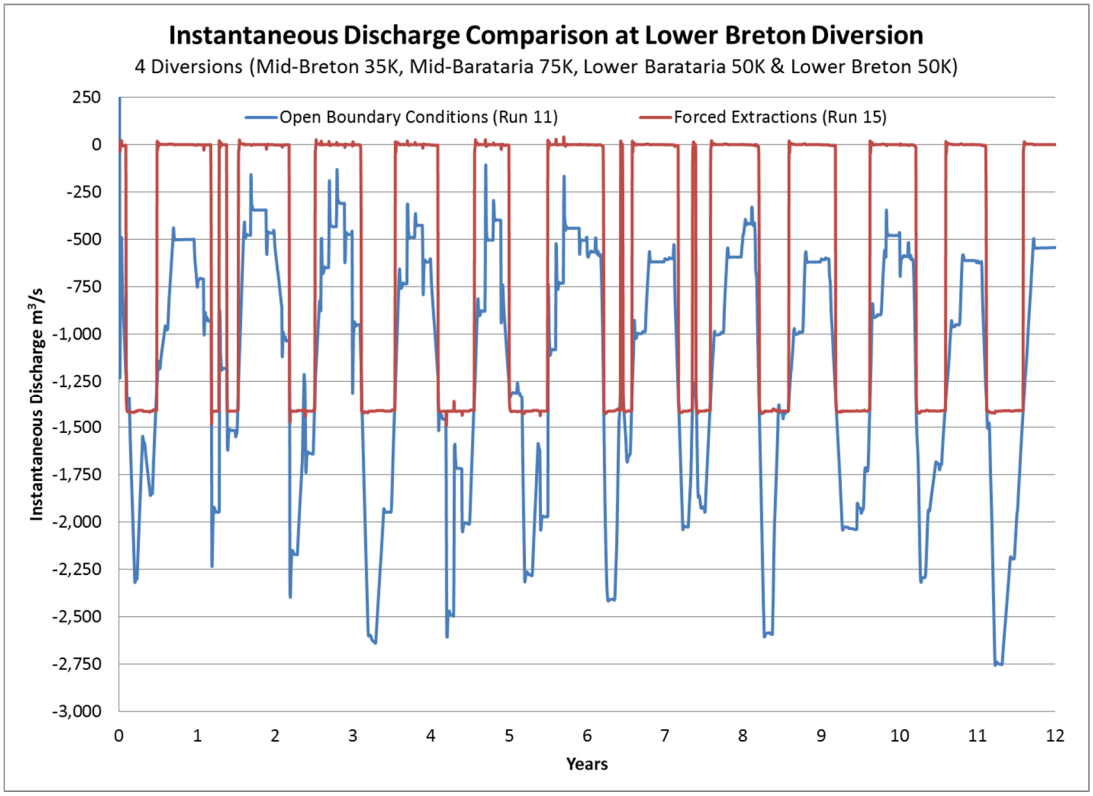

Figure 7.1.2.4: Instantaneous Discharge Comparison at Lower Breton Diversion

7.1.3 DISCUSSION

Utilizing the variable hydrograph offers a wider range of Mississippi River discharges, and includes a realistic variety of flow durations as well as a variety of peak flows. The model runs were based on the assumption that the diversions would be opened at Mississippi River flows exceeding 600,000 cfs, and therefore, the results are related to this specific operational point. It appears that only once in 12 years, with 4 diversions in operation, the Lower Breton did not divert 100% of the design flow. Therefore, running all 4 diversions at a total of 210,000 cfs, resulted in one of the diversions (Lower Breton) discharging only 99.5% of the target discharge, while the others discharged at 100% of the target discharge.

In all cases where the instantaneous discharge for the open boundary conditions exceeds the design flow (forced extractions) a gate would need to be operated to allocate the desired maximum flow amount, especially during peak flows.

If operation at a lower flow than 600,000 cfs in the Mississippi River is considered, a new evaluation would need to be generated, with the applicable diversion runs. At less than 600,000 cfs there could be a deficit between the desired flow (forced flow) and the open flow (open Gulf-stage boundary) due to the loss of flow and stream power. Similarly, if a constrictive structure is imposed on the channel, it is necessary to repeat this energy study.

7.1.4 CONCLUSIONS

At a river flow at or greater than 600,000 cfs there is only 0-0.5% probability that the diversion flows will be restricted by the availability of an energy differential between the River and the Gulf of Mexico.

The operational trigger point of Mississippi River flow directly impacts the diversion efficiency. If a value lower than 600,000 cfs is considered or an increase in diversion flow, change of diversion location or the diversion geometry, a new evaluation should be conducted to verify that the expected design flow (forced extraction) can physically be obtained at all times when the diversion is opened.

7.2 RESEARCH QUESTION 2

Research Question 2:

How does the change in spatially variable Eddy Viscosity impact the outcomes for cumulative sedimentation/erosion?

7.2.1 METHODOLOGY

In order to identify the impact of Eddy Diffusivity and Eddy Viscosity on the cumulative deposition within bends a sensitivity analysis was conducted by modifying the calibrated base values for Eddy Diffusivity and Eddy Viscosity. See Figures 7.2.1.1 to 7.2.1.3 for a visual representation of the base values as established for the original, long model (McCorquodale et al. 2017). A 20% increase and 20% decrease were applied to the base values in the calibrated ".edy" file.

The eddy viscosity and diffusivity were assumed to be equal in the base runs. The sensitivity assumes that they remain equal. However, one run was made to test this assumption, in which only the eddy diffusivity was decreased without changing the calibrated values for the eddy viscosity.

The ".edy" file is set up where the first part of the file is representing eddy viscosity and the second, lower portion, eddy diffusivity.

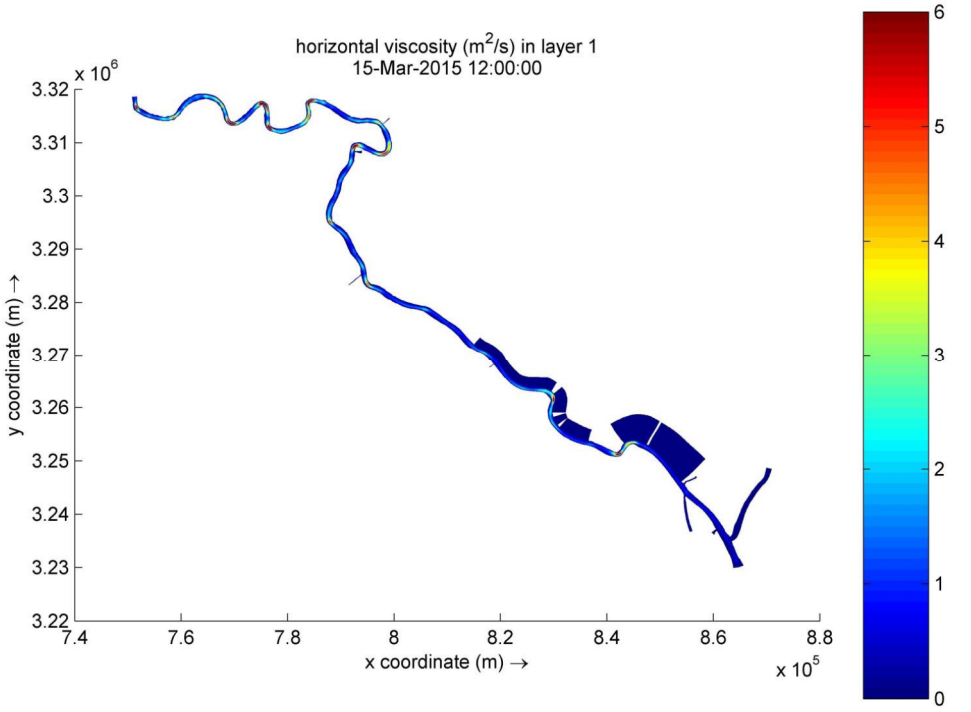

Figure 7.2.1.1: Calibrated Eddy Viscosity (and Eddy Diffusivity) in m2/s (Domain)

(Source: McCorquodale et al. 2017, Appendix I, Figure 1-2a)

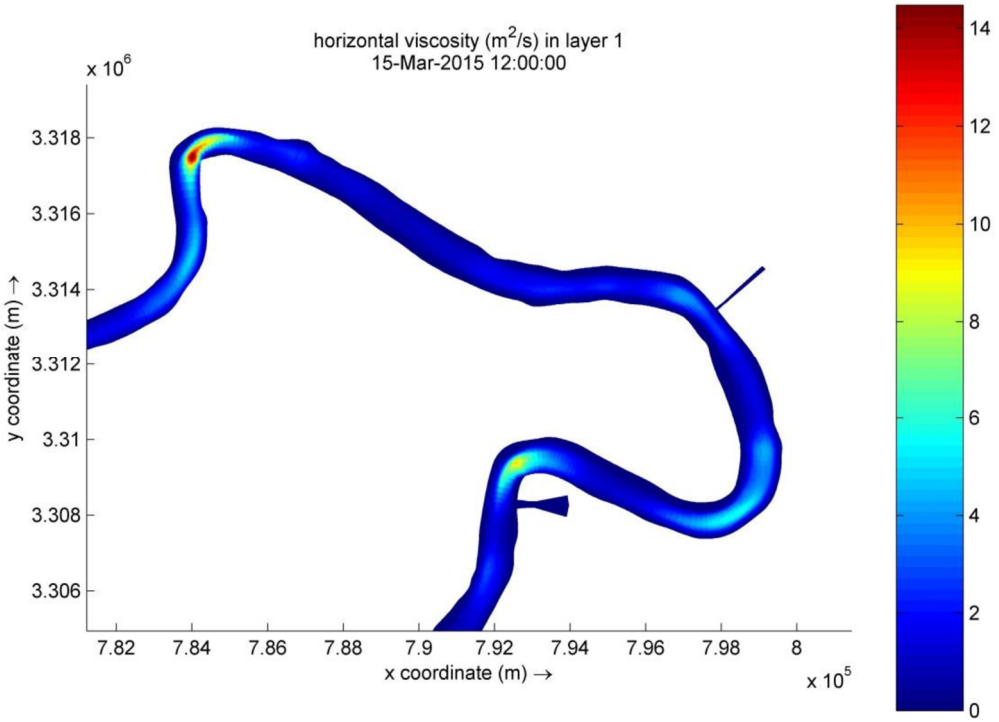

Figure 7.2.1.2: Calibrated Eddy Viscosity (and Eddy Diffusivity) in m2/s (Domain)

(Source: McCorquodale et al. 2017, Appendix I, Figure 1-2b)

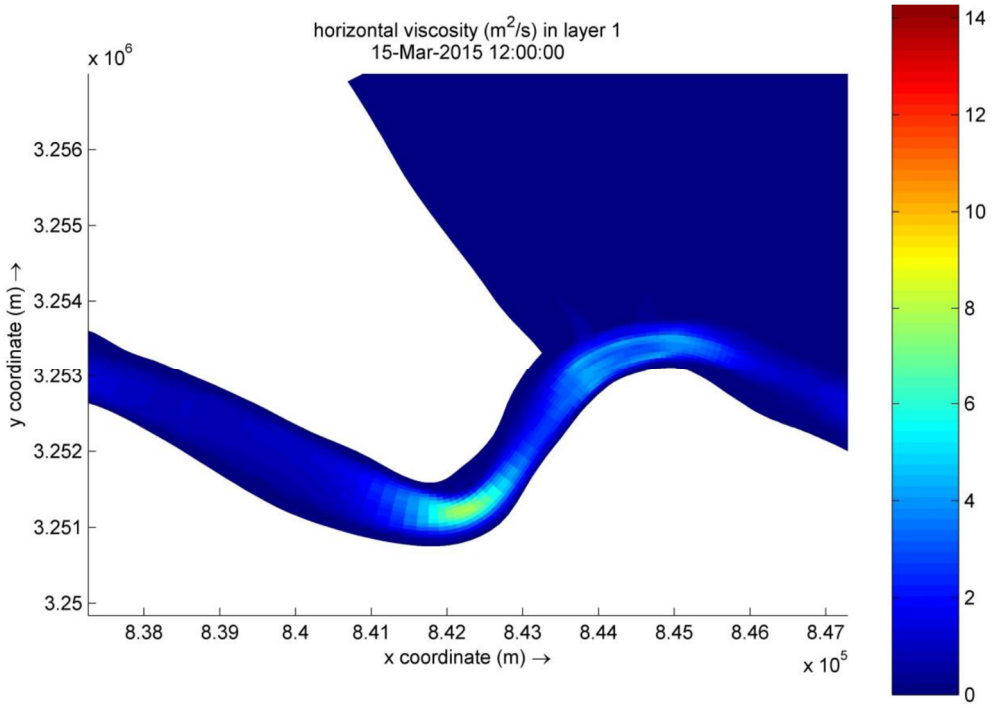

Figure 7.2.1.3: Calibrated Eddy Viscosity (and Eddy Diffusivity) in m2/s (Domain) (Source: McCorquodale et al. 2017, Appendix I, Figure 1-2c)

The model runs in Table 7.2.1.1 were set-up to obtain data in support of the evaluation:

Table 7.2.1.1: Model Runs for Research Question 2:

#	Hydrograph		Years	Diversions	Diverions Info	Other
	U	V				
3		X	1-12	None		
30		X	1-12	None		20% Decrease Eddy Diffusivity & Eddy Viscosity
30a		X	1-12	None		20% Decrease Eddy Diffusivity Only
32		X	1-12	None		20% Increase Eddy Diffusivity & Eddy Viscosity
8		X	1-12	2	Mid-Breton = 35,000 cfs & Mid-Barataria = 75,000cfs	
31		X	1-12	2	Mid-Breton = 35,000 cfs & Mid-Barataria = 75,000cfs	20% Decrease Eddy Diffusivity & Eddy Viscosity
33		X	1-12	2	Mid-Breton = 35,000 cfs & Mid-Barataria = 75,000cfs	20% Increase Eddy Diffusivity & Eddy Viscosity

7.2.2 RESULTS

The Laterally Averaged Cumulative Erosion/Sedimentation was computed and exported for the model runs completed for this evaluation and the deposition in meters was plotted along the river domain from River Mile 75.5 to 0. All 4 cases are depicted in each graph (Figures 7.2.2.1 to 7.2.2.4) and listed below:

1. Base Case = same Eddy Diffusivity & Eddy Viscosity as Original Model
2. 20% Decrease = 20% Decrease in Eddy Diffusivity & Eddy Viscosity
3. 20% Decrease (Partial) = 20% Decrease in Eddy Diffusivity Only
4. 20% Increase = 20% Increase in Eddy Diffusivity & Eddy Viscosity

Figure 7.2.2.1 depicts the laterally averaged cumulative deposition at year 12 for the various eddy diffusivity / eddy viscosity cases for the no diversion scenario, while Figure 7.2.2.2 depicts the results for the two diversion case (Mid-Breton and Mid-Barataria).

Overall the results appear similar for the 4 different cases. The largest areas of change were in the stronger bend regions. The main consistent trend is that a decrease in diffusivity results in less deposition, which is highlighted in Figures 7.2.2.3 and 7.2.2.4. The increase or decrease in both, eddy diffusivity and eddy viscosity, does not have a consistent trend.

A close-up at Myrtle Grove Bend (see Figure 7.2.2.3) indicates that a decrease in eddy diffusivity only is in good agreement with the calibrated base case but results in less deposition within Myrtle Grove Bend, while a decrease of both, eddy viscosity and diffusivity, increases the deposition within the bend. However, an increase in both, eddy viscosity and diffusivity results in a depositional shift of the peak deposition in an upstream direction, while reducing deposition downstream of the bend and increasing deposition upstream of the proposed Mid-Barataria Diversion. A close-up at the bend upstream of Fort St. Philip (see Figure 7.2.2.4) indicated that an increase in eddy viscosity and diffusivity results in increased deposition, while a decrease in both results only in a minor reduction in deposition. On the contrary, a decrease in eddy diffusivity only results in a more significant depositional reduction within the bend region.

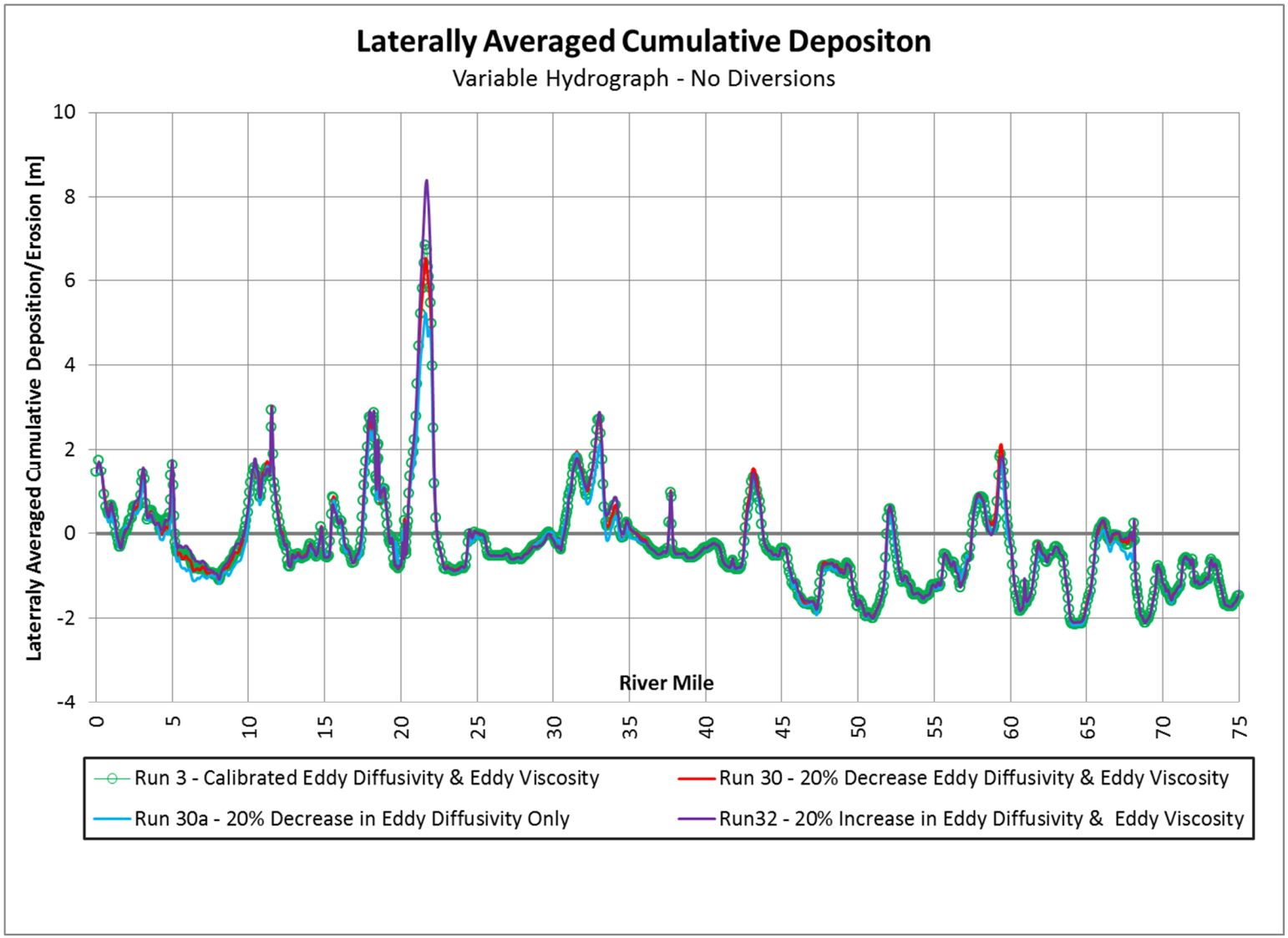

Figure 7.2.2.1: Laterally Averaged Cumulative Deposition for Various Eddy Diffusivity / Eddy Viscosity Cases No Diversions

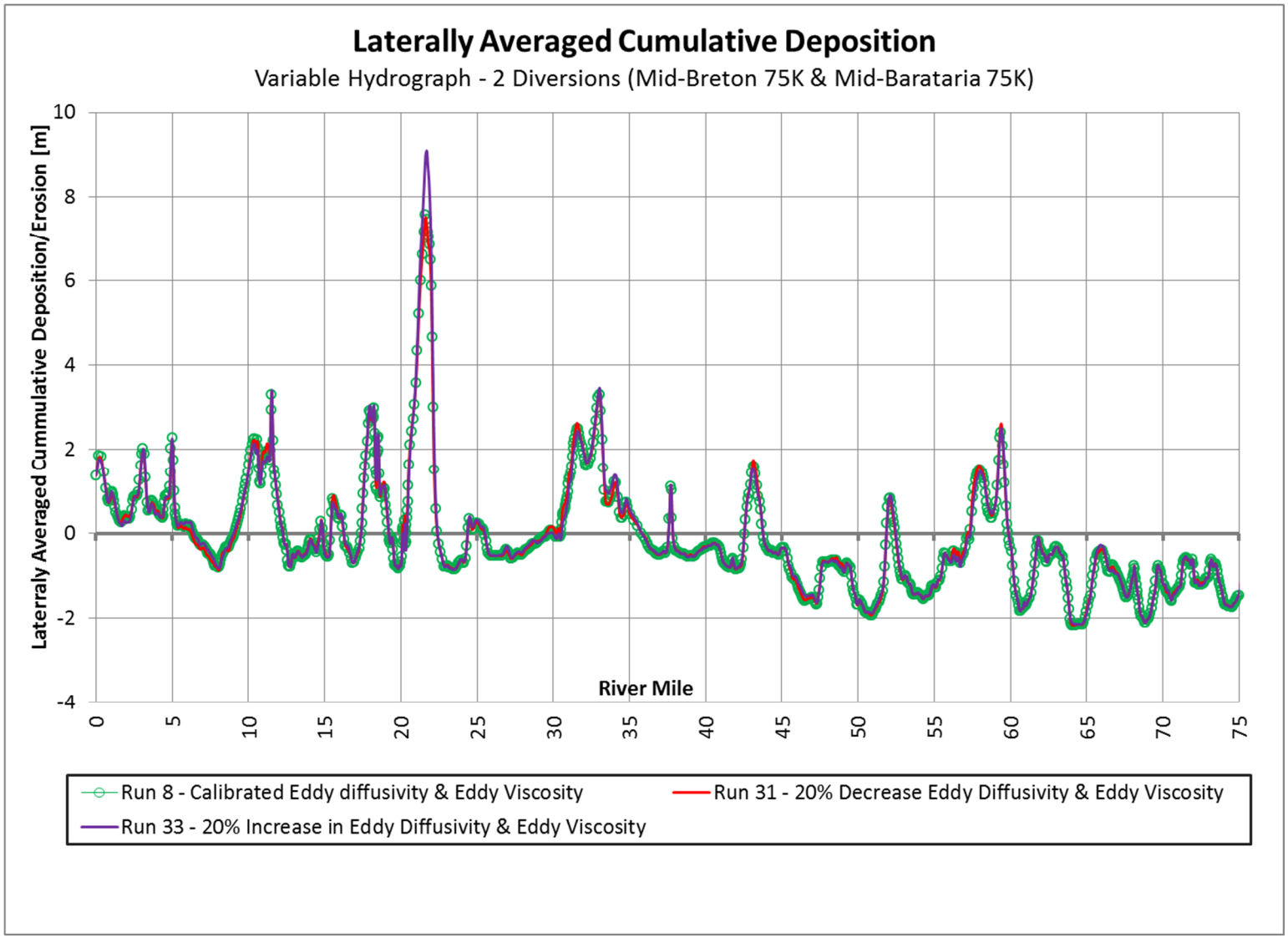

Figure 7.2.2.2: Laterally Averaged Cumulative Deposition for Various Eddy Diffusivity / Eddy Viscosity Cases 2 Diversions (Mid-Breton 35K & Mid-Barataria 75K)

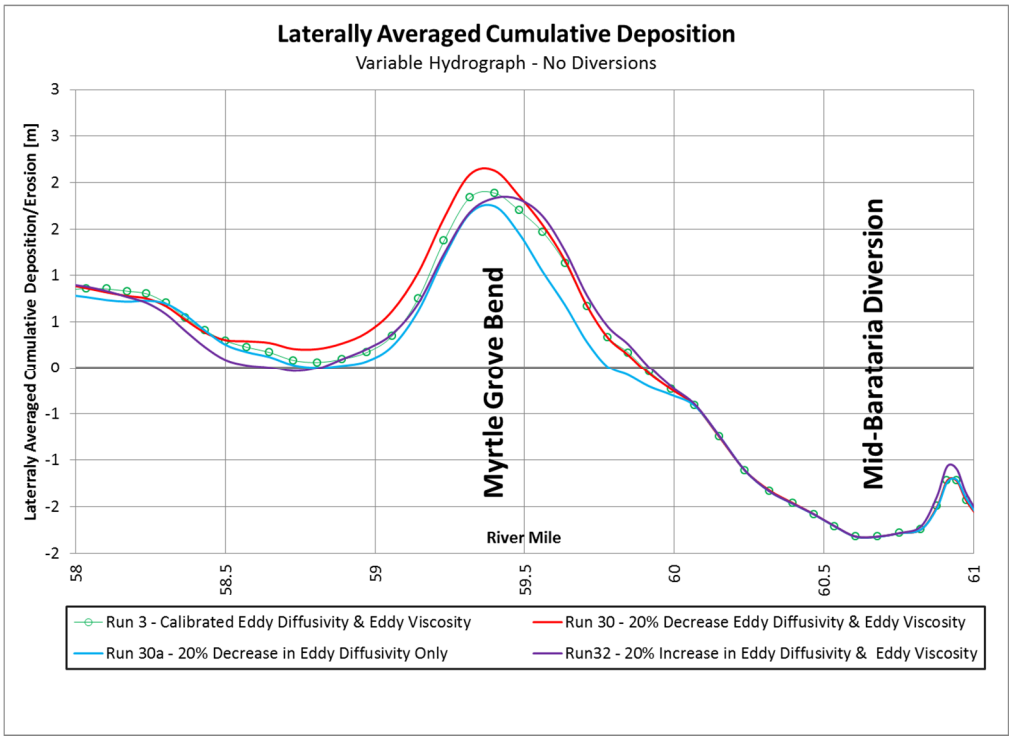

Figure 7.2.2.3: Laterally Averaged Cumulative Deposition for Various Eddy Diffusivity / Eddy Viscosity Cases – No Diversions (River Miles 58-61)

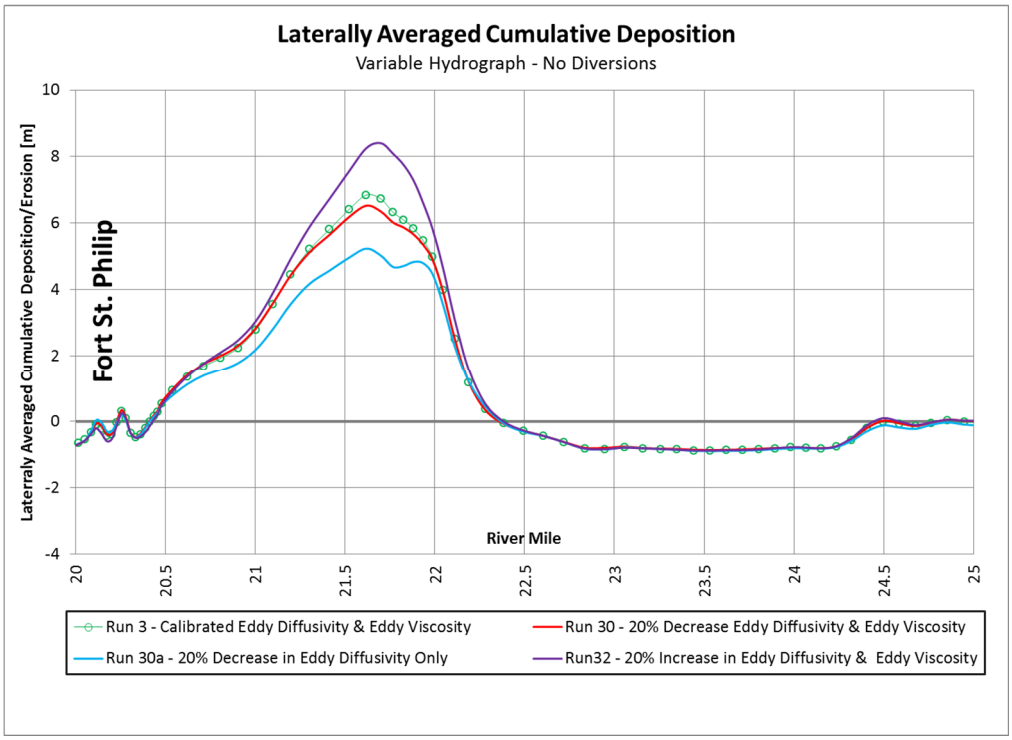

Figure 7.2.2.4: Laterally Averaged Cumulative Deposition for Various Eddy Diffusivity / Eddy Viscosity Cases – No Diversions (River Miles 20-25)

7.2.3 DISCUSSION

Changing Eddy Viscosity and Eddy Diffusivity in the ".edy" file had the greatest impact on the deposition at bends. The no diversion case (see Figure 7.2.1) and the 2 diversion case (see Figure 7.2.2) follow the same pattern at the bends. The higher the bend curvature, the greater was the change in calculated deposition. The changes observed at two significant bends in the river are illustrated in Figure 7.2.3, which highlights the bend at Myrtle Grove, downstream from the proposed Mid-Barataria Diversion, as well as Figure 7.2.4, which highlights the bend upstream of Fort St. Philip, which has the highest curvature within the model domain.

Changing the Eddy Diffusivity by a certain percentage alone had a greater effect than changing both Eddy Viscosity and Diffusivity by the same percentage (see Figure 7.2.4). The change in eddy diffusivity changes the lateral diffusion of sand while eddy viscosity affects the lateral momentum transfer. Since the highest concentration of suspended sand is near the thalweg, an increase in diffusivity will have more direct effect on the lateral transfer of suspended sand and vice versa for a decrease in diffusivity. Changing Eddy Viscosity and Diffusivity appears to partially nullify the effect of changing Eddy Diffusivity only. There appears to be a dependence of deposition in bends on the turbulent Prandtl-Schmidt Number [Momentum Transfer Coefficient/Diffusivity] (Cengel & Cimbala 2006).

7.2.4 CONCLUSIONS

Based on the model simulations it is suggested that reducing the Eddy Diffusivity only, would result in a reduction of predicted deposition at bends. Therefore, if a model output is generating depositions, which appear high based on observation, the model can be adjusted by decreasing the Eddy Diffusivity relative to the Eddy Viscosities. Similarly, if results appear to underestimate deposition within the bends, the Eddy Diffusivity and Eddy Viscosity should be increased.

In summary, it is recommended, to first calibrate the Eddy Diffusivity and Eddy Viscosity as being equal to each other for a general calibration of a model, followed by a fine-tuning for the bend regions, by adjustment of Eddy Diffusivity only

It is recommended to further analyze the effect of the turbulent Prandtl-Schmidt Number on deposition in bends.

.

7.3 RESEARCH QUESTION 3

Research Question 3:

How does system with no diversions, 1 diversion and 2 diversions respond to sea level rise (NRCIII Curve)?

How does the response for a system with no diversions vary depending on annual hydrograph variability?

7.3.1 METHODOLOGY

The model runs summarized in Table 7.3.1.1 were set-up to obtain data in support of an evaluation of this question. All runs are covering a 48 year computational run.

Table 7.3.1.1: Model Runs for Research Question 3:

#	Hydrograph		Years	Diversions	Diverions Info	Other
	U	V				
40		X	1-48	None		
45		X	1-48	None		NRC III - Increase in Stage
41	X		1-48	None		
42	X		1-48	None		NRC III - Increase in Stage
43	X		1-48	1	Mid-Barataria = 75,000cfs	
44	X		1-48	1	Mid-Barataria = 75,000cfs	NRC III - Increase in Stage
47		X	1-48	1	Mid-Barataria = 75,000cfs	
46		X	1-48	1	Mid-Barataria = 75,000cfs	NRC III - Increase in Stage
48		X	1-48	2	Mid-Breton = 35,000 cfs & Mid-Barataria = 75,000cfs	
50		X	1-48	2	Mid-Breton = 35,000 cfs & Mid-Barataria = 75,000cfs	NRC III - Increase in Stage

There are five different base cases to identify the differences between, variable and uniform hydrograph cases as well as no-diversion and diversion cases. There is one no-diversion run for a uniform hydrograph (Run 41) and one no-diversion run for the variable hydrograph (Run 40). Similarly, there is a one-diversion run for a uniform hydrograph (Run 43) and a one-diversion run for a variable hydrograph (Run 47). Only the variable hydrograph was analyzed for the two-diversion case (Run 48).

For each of the base cases a corresponding run with sea-level adjusted stage boundaries was developed. The stage elevations were adjusted in the bct-file for sea level rise (SLR) by applying the NRC III Eustatic Sea Level Rise (ESLR), developed by the National Research Council (NCR), which represents the upper limit of the ESRL values used by McCorquodale et al (2017). NRC III was also the least optimistic case in the 2012 State Master Plan published by CPRA (CPRA 2012). Figure 7.3.1.1 depicts the utilized NRC III Curve and the associated stage increase.

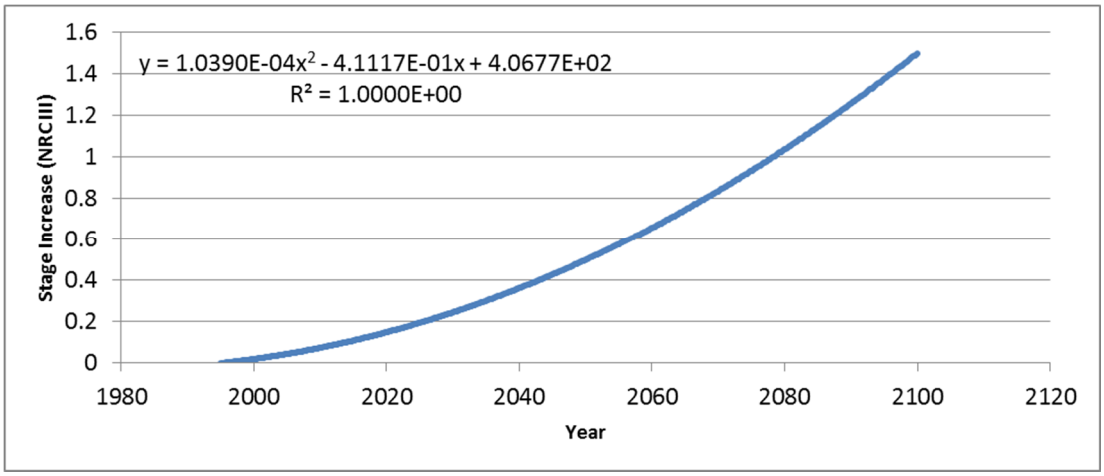

Figure 7.3.1.1: Predicted Stage Increase (NRC III Curve)

ESLR does not include predictions for local subsidence. Relative Sea Level Rise (RSLR), which includes the local subsidence rate (LSR) and ESLR, was not applied in this research (RSLR = ESLR + LSR). Utilization of RSL would accelerate the trends observed for ESLR. The LSR varies along the Mississippi River and is of the order of 0.5 m in 50 years, which is similar in magnitude to the ESLR over 50 years (McCorquodale et al 2017).

The Laterally Averaged Cumulative Erosion/ Sedimentation for the entire domain (N = 1130) from Belle Chasse to HOP was computed for the established model runs (Table 7.3.1.1). The depositional data have been extracted for the main river channel (M 77:95) and a 3-point filter was applied to eliminate data scatter/noise while providing a smoother representation of the data trends.

Domain average annual change will be determined and represented by plotting the average and standard deviation of the laterally averaged cumulative erosion/ sedimentation changes between periods over time.

7.3.2 RESULTS

7.3.2.1 Laterally Averaged Cumulative Deposition

The laterally averaged cumulative deposition was extracted at the end of 48 years and plotted for all 10 cases listed in Table 7.3.1.1. Appendix R3.1 includes one graph per run depicting the laterally averaged deposition along the river reach (Belle Chasse to HOP). Figures 7.3.2.1.1 and 7.3.2.1.2 are a representation of these plots for the no diversion case utilizing the uniform hydrograph without SLR (Run 41) and with SLR (Run 42). Each graph includes three trendlines (Year 24, Year 30 & Year 48) to reflect the overall depositional trends.

The changes over time are predominantly depositional, with the most deposition occurring within the first 24 years. In addition, the deposition is mostly occurring within the bends (in point bars). When comparing the with-SLR and without-SLR graphs, it can be noted that the deposition increases due to SLR.

To better review the results and compare individual cases the trendlines were plotted without the deposition data. Figure 7.3.2.1.3 depicts all trendlines for the 10 cases, while Figures 7.3.2.1.4 to 7.3.2.1.7 depict specific trendlines for comparison.

Figure 7.3.2.1.3 shows that overall the introduction of SLR resulted in an increase of deposition of 0.5 m near HOP over 48 years, while the upstream increase in deposition is in the order of 0.1 m.

Figure 7.3.2.1.4 is a comparison between the uniform and the variable hydrograph runs for no-diversion and one-diversion scenarios without SLR. Overall the utilization of the uniform hydrograph yields more deposition than the runs utilizing the variable hydrograph. In the no-diversion case the peak deposition is the same but slightly shifted, which generates slightly less deposition near HOP, while the overall domain remains predominantly depositional. In the one-diversion scenario, the utilization of the

uniform hydrograph yields larger deposition consistently over the entire river domain (Belle Chasse to HOP).

Figure 7.3.2.1.5 is a comparison between the uniform and the variable hydrograph runs for the no-diversion and the one-diversion scenarios with SLR. Overall the utilization of the uniform hydrograph yields more deposition than the runs utilizing the variable hydrographs. In contrast to the results of the 'without-SLR' cases depicted in Figure 7.3.2.1.4, the 'with-SLR' scenarios yield consistently larger deposition over the entire river domain (Belle Chasse to HOP). In addition, the deposition difference between the uniform and the variable hydrograph run increases from the no-diversion case to the one-diversion case. The depositional trendline peak for the no-diversion case is similar for the uniform and the variable hydrograph runs, while the one-diversion case, which has a larger peak for the uniform hydrograph run than the variable run, varies.

Figure 7.3.2.1.6 is a comparison between the with-SLR and without-SLR cases for the uniform hydrograph runs with no-diversion and one-diversion. Overall, the depositional increase due to SLR is similar, with the majority of depositional increase occurring below Lower Breton, an area impacted by multiple natural Gulf of Mexico stage impacted outlets. The deposition increase due to SLR is slightly larger for the no-diversion case. The one-diversion case results in some erosion near the upstream boundary when compared to the no-diversion case.

Figure 7.3.2.1.7 is a comparison between the with-SLR and without-SLR cases for the variable hydrograph runs with no-diversion, one-diversion and two-diversions. Overall, the depositional increase due to SLR is similar for the no-diversion and diversion cases. The majority of depositional increase occurs below Lower Breton and decreases as one progresses upstream. The deposition increase due to SLR is slightly increasing from no-diversion case to the one diversion case and the two-diversion case. The erosional trend from upstream of White Ditch increased with increase in diversions, while the impact of SLR in this area appears fairly consistent.

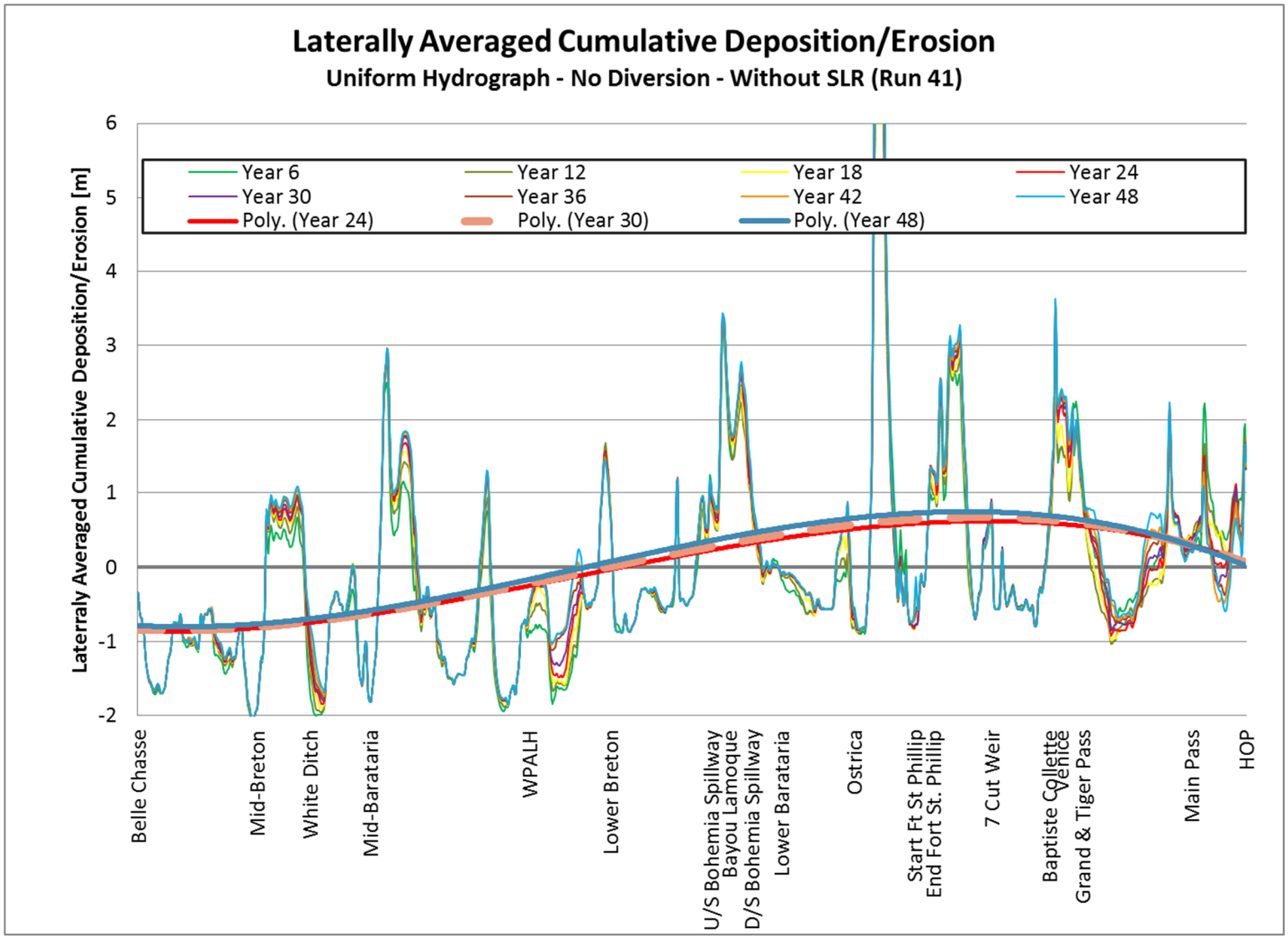

Figure 7.3.2.1.1: Laterally Average Cumulative Deposition/Erosion due to SLR – Uniform Hydrograph No Diversion – Without Sea Level Rise (Run 41)

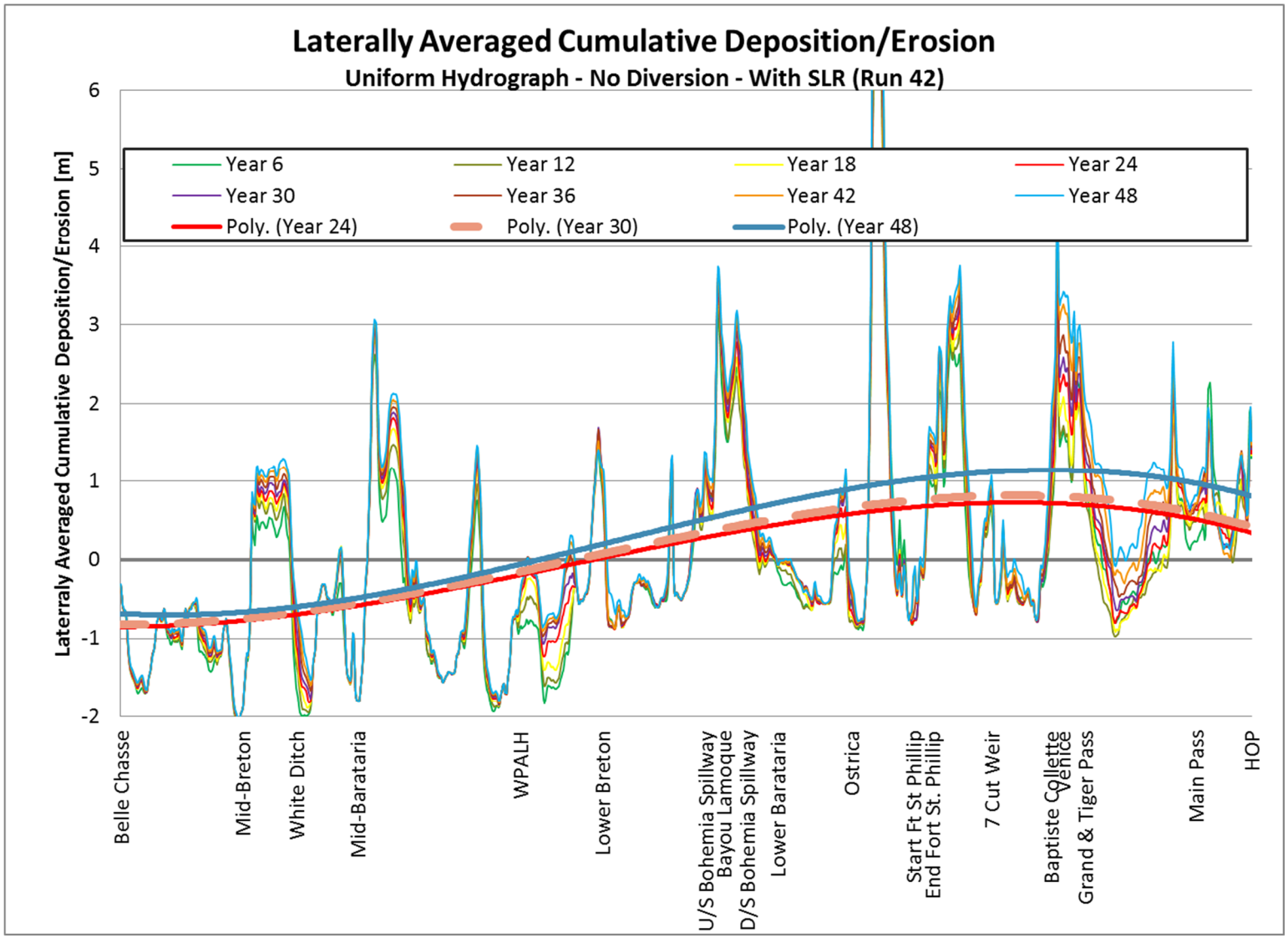

Figure 7.3.2.1.2: Laterally Average Cumulative Deposition/Erosion due to SLR – Uniform Hydrograph No Diversion – With Sea Level Rise (Run 42)

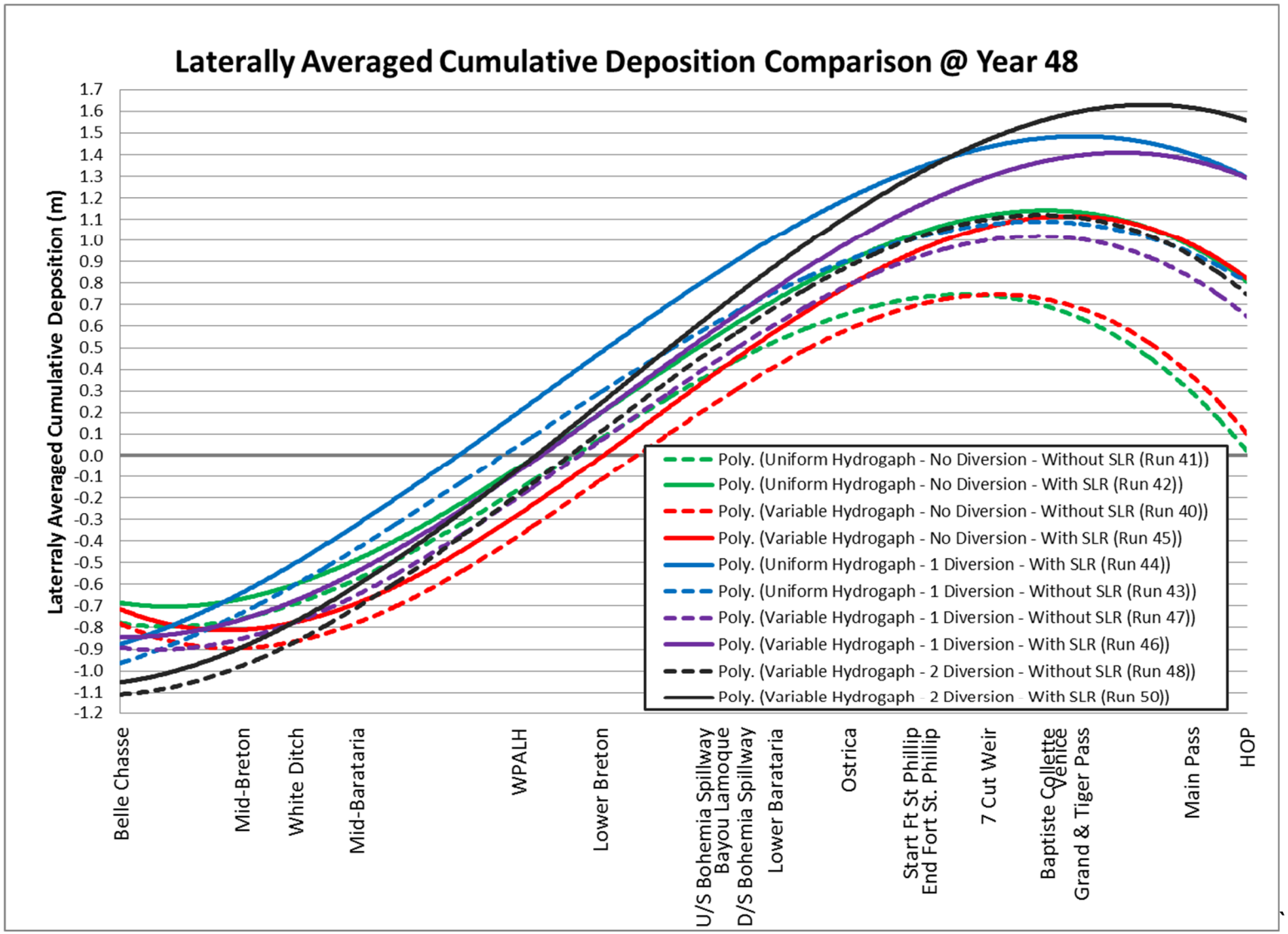

Figure 7.3.2.1.3: Laterally Averaged Cumulative Deposition Comparison (With & Without Sea Level Rise)

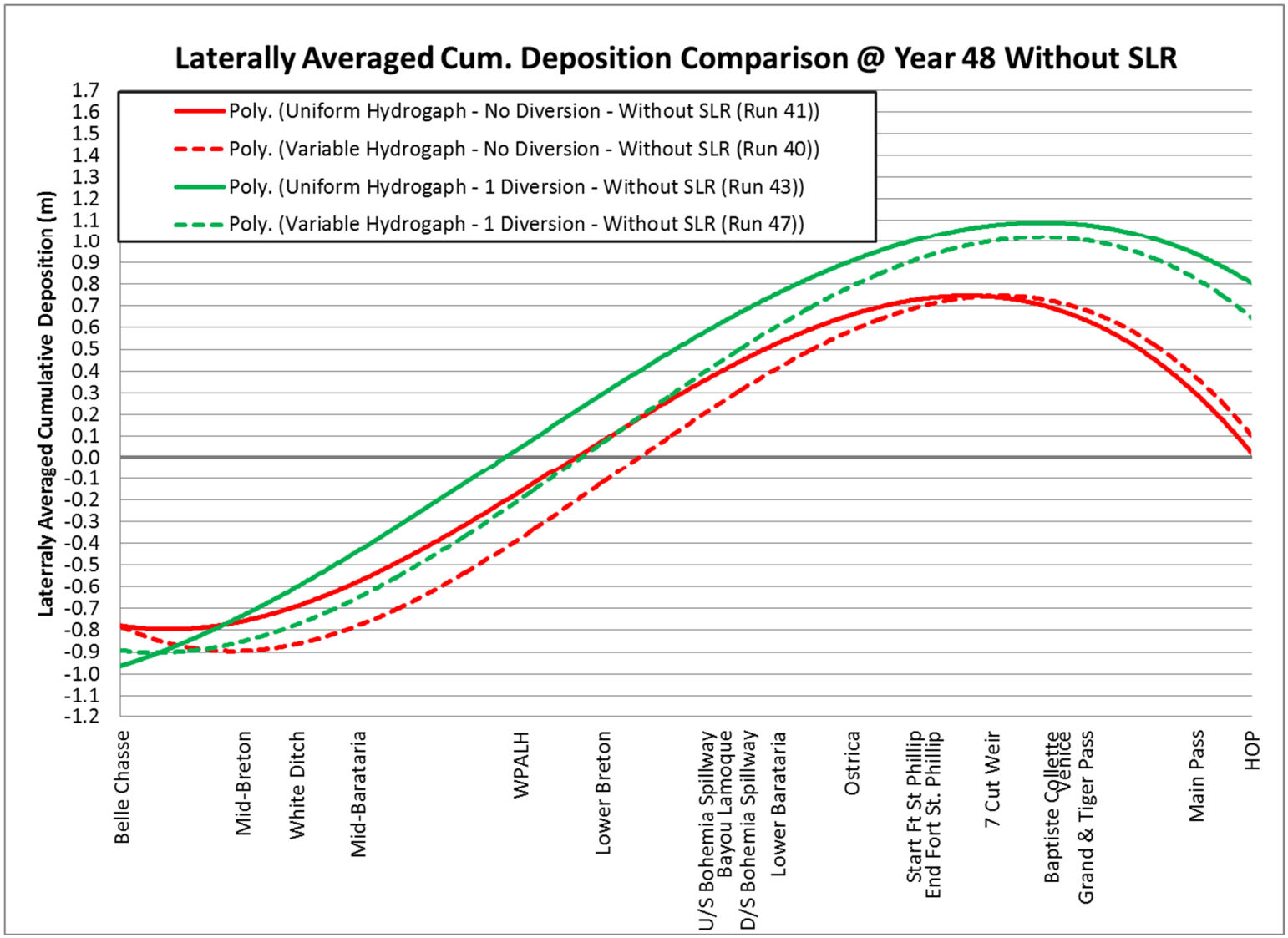

Figure 7.3.2.1.4: Laterally Averaged Cumulative Deposition Comparison (Without Sea Level Rise Only)

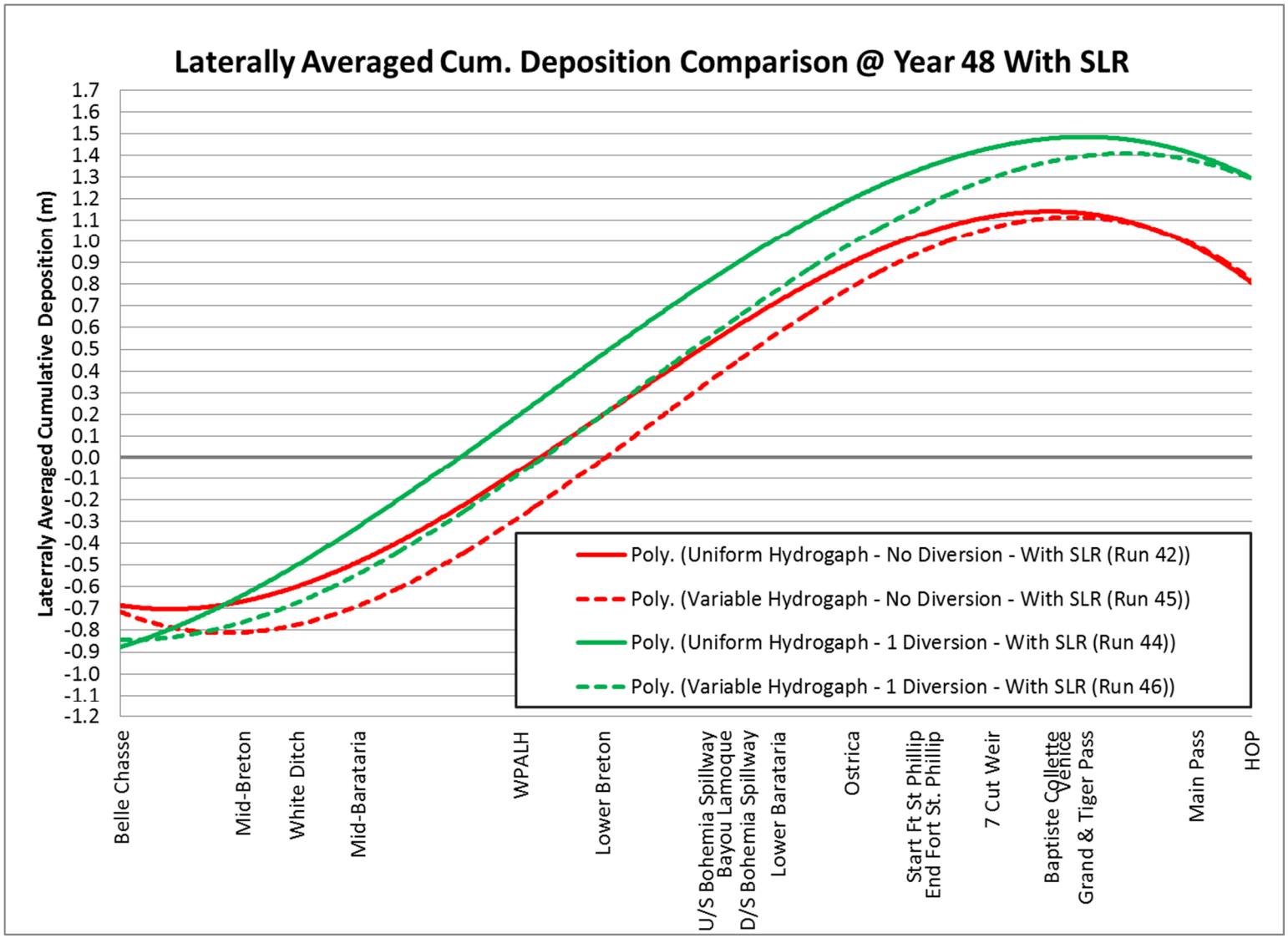

Figure 7.3.2.1.5: Laterally Averaged Cumulative Deposition Comparison (With Sea Level Rise Only)

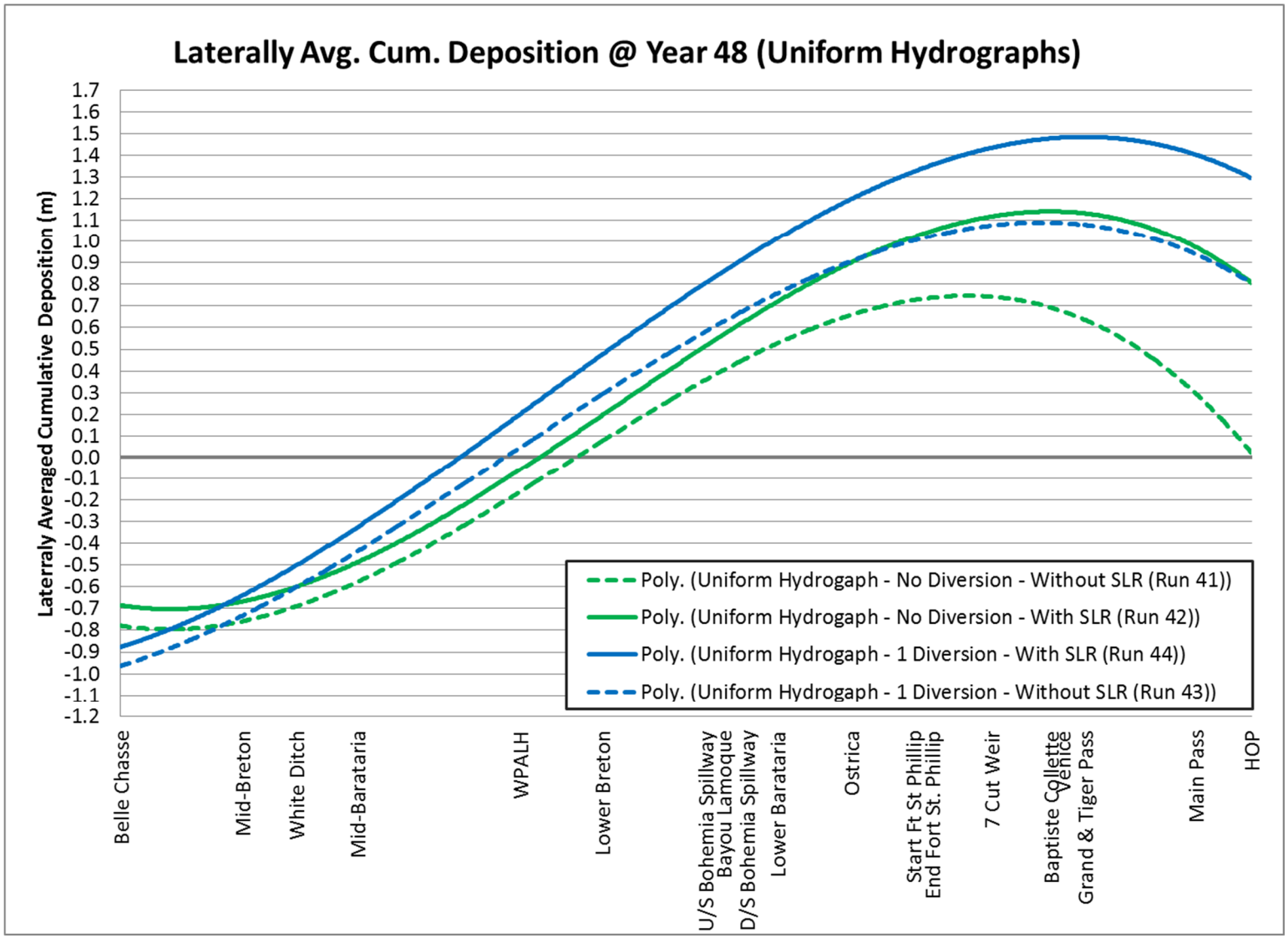

Figure 7.3.2.1.6: Laterally Averaged Cumulative Deposition Comparison (With Sea Level Rise Only)

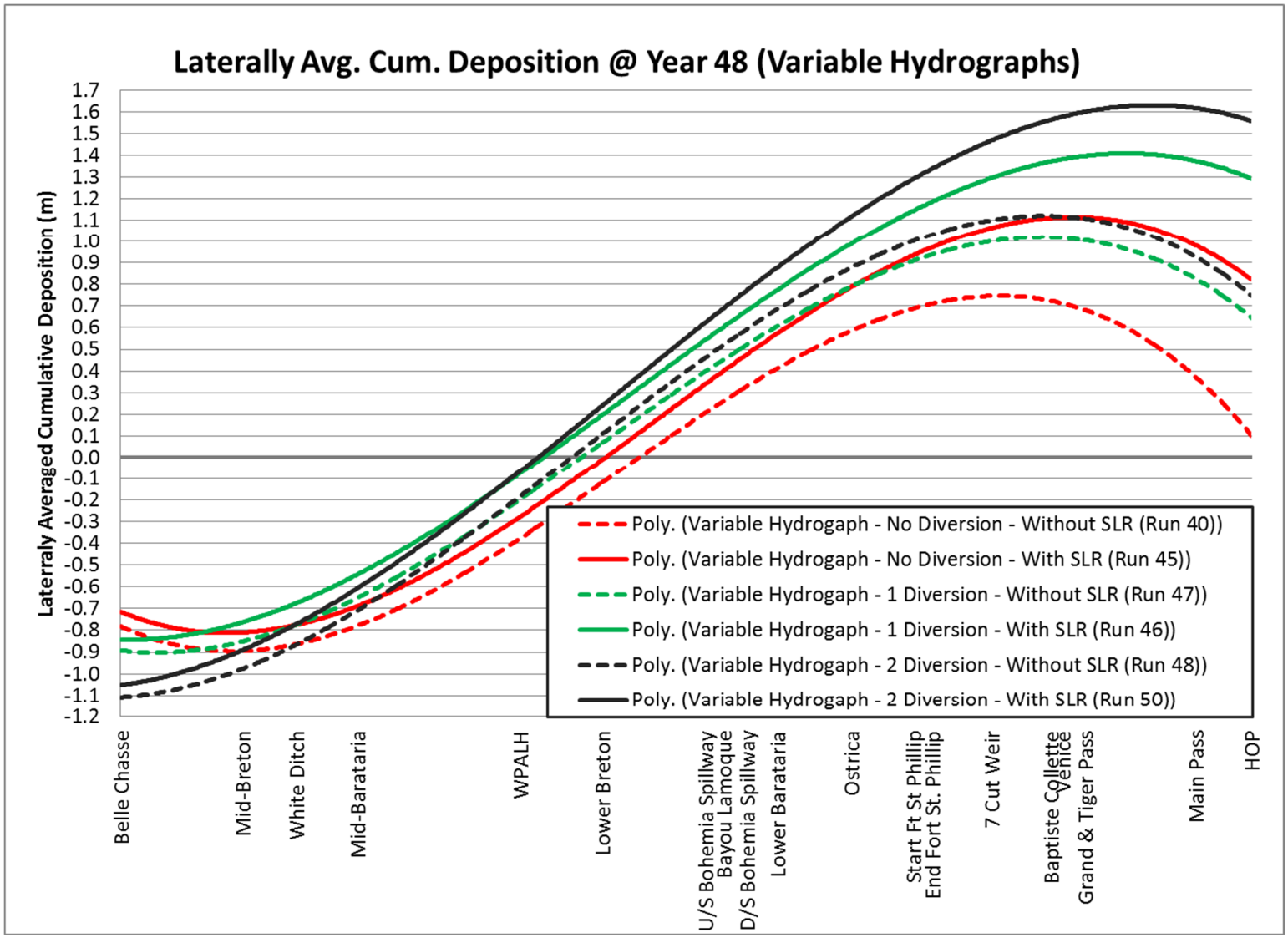

Figure 7.3.2.1.7: Laterally Averaged Cumulative Deposition Comparison (With Sea Level Rise Only)

7.3.2.2 3-Year Changes in Laterally Averaged Cumulative Deposition

The laterally averaged cumulative deposition was extracted at 3-year increments between year 3 and year 48, which represents the end of the simulation. The 3-year changes in laterally averaged deposition were calculated by subtracting the laterally averaged deposition of the previous increment from the next, for example subtracting values for year 6 from year 9. The 3-point filter was applied to the deposition data by river mile (RM). The deposition data were plotted along the river reach (Belle Chasse to HOP) for all 10 runs listed in Table 7.3.1.1. The graphs depicting the 3-Year Changes (time derivatives) along the river domain are shown in Appendix R3.2. The 3-Year Changes are obtained by subtracting the deposition data of year x from the deposition data of the year x+3, for example subtracting deposition data of year 12 from the deposition data of year 15.

For plot clarity only selected 3-Year periods within the 48-Year computational time were depicted in Figures 7.3.2.2.1a – 7.3.2.2.10a. To further simplify observation of trends, the associated trendlines derived from the 3-Year plots were depicted separately in Figures 7.3.2.2.1b – 7.3.2.2.10b

In general, the observed trend is a decrease in magnitude of the erosion and deposition rate; however a true equilibrium is not reached within the 48-year duration of the simulation. For a true equilibrium the change over time should approach zero.

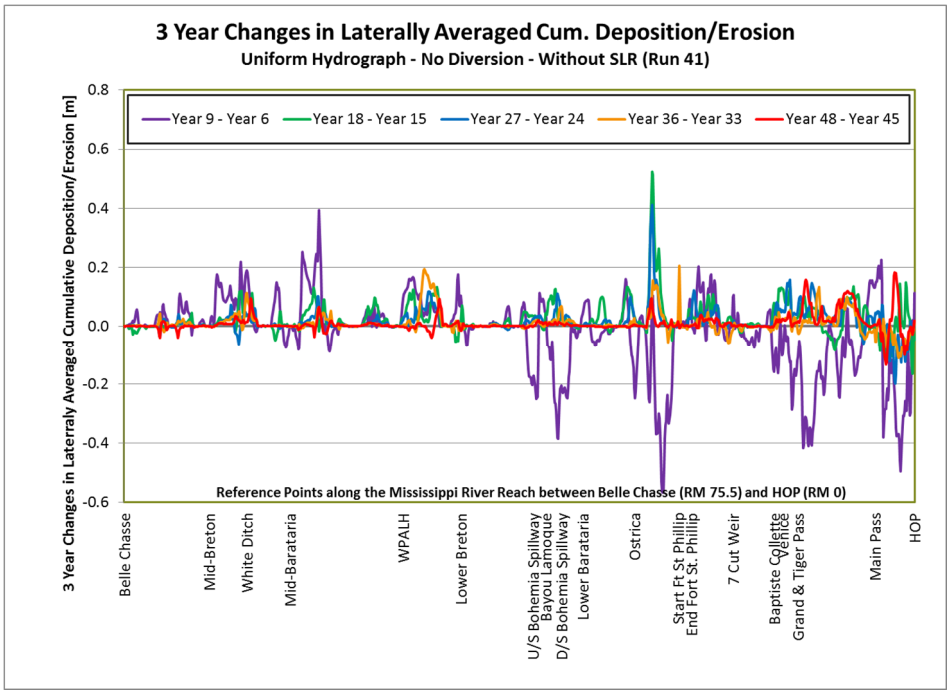

Figure 7.3.2.2.1a: 3-Year Changes in Laterally Averaged Cumulative Deposition Uniform Hydrograph, No Diversion and Without SLR (Run 41)

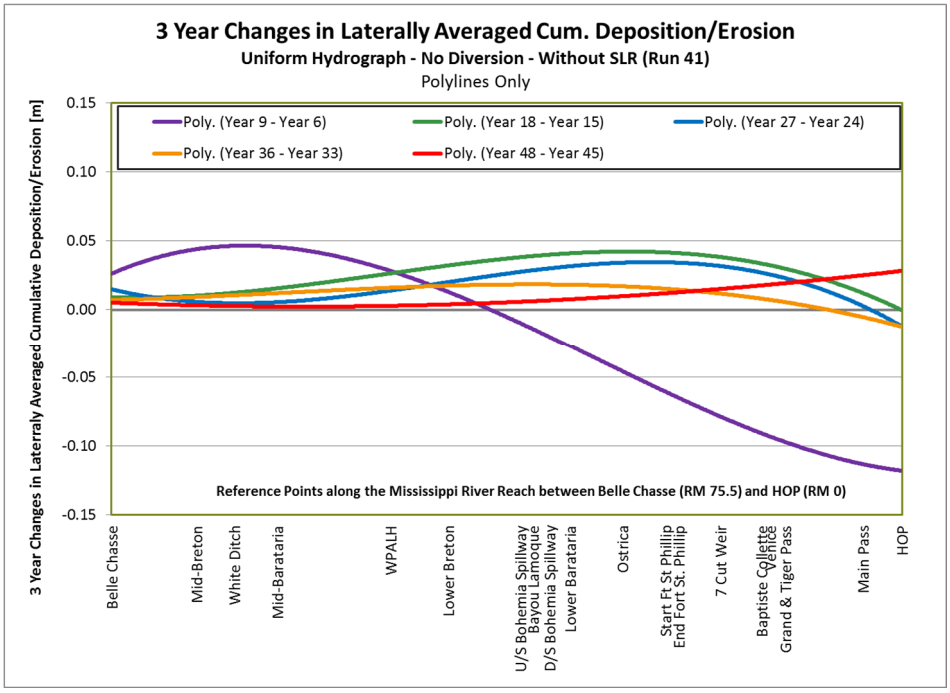

Figure 7.3.2.2.1b: 3-Year Changes in Laterally Averaged Cumulative Deposition Uniform Hydrograph, No Diversion and Without SLR (Run 41) – Polylines Only

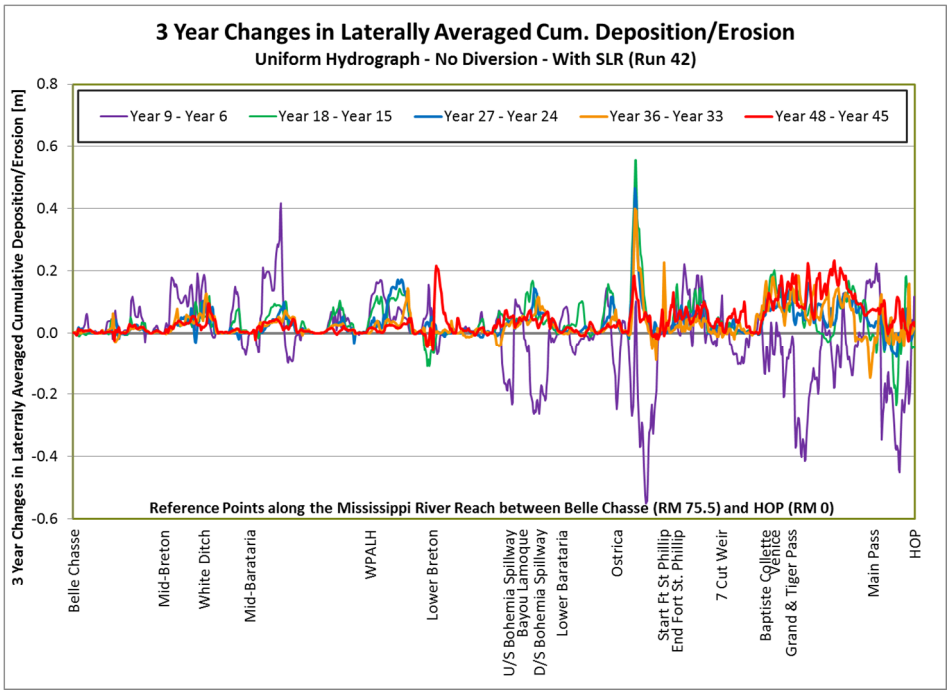

Figure 7.3.2.2.2a: 3-Year Changes in Laterally Averaged Cumulative Deposition Uniform Hydrograph, No Diversion and With SLR (Run 42)

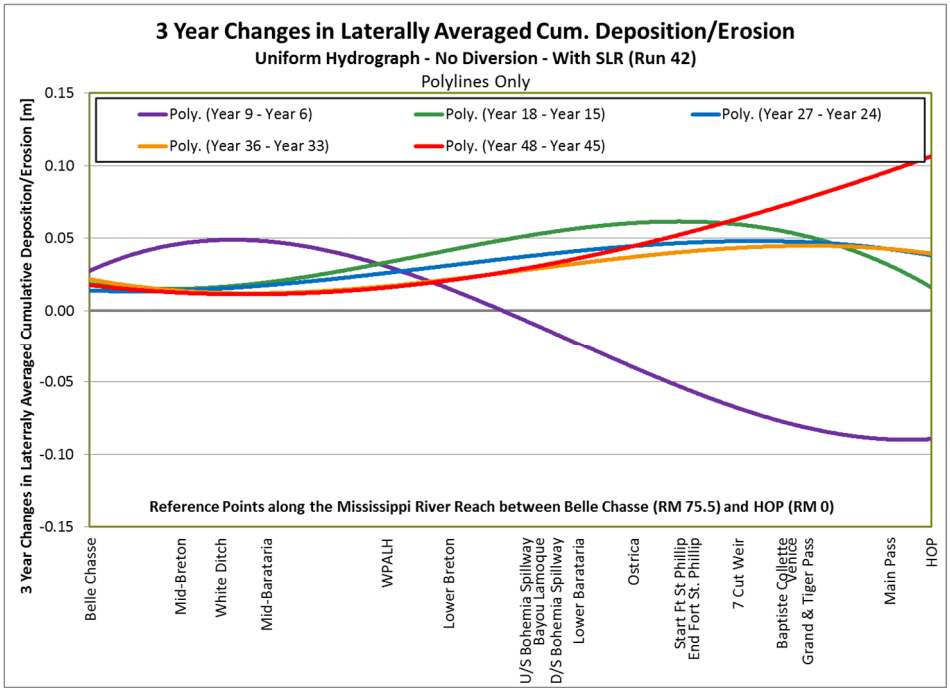

Figure 7.3.2.2.2b: 3-Year Changes in Laterally Averaged Cumulative Deposition Uniform Hydrograph, No Diversion and With SLR (Run 42) – Polylines Only

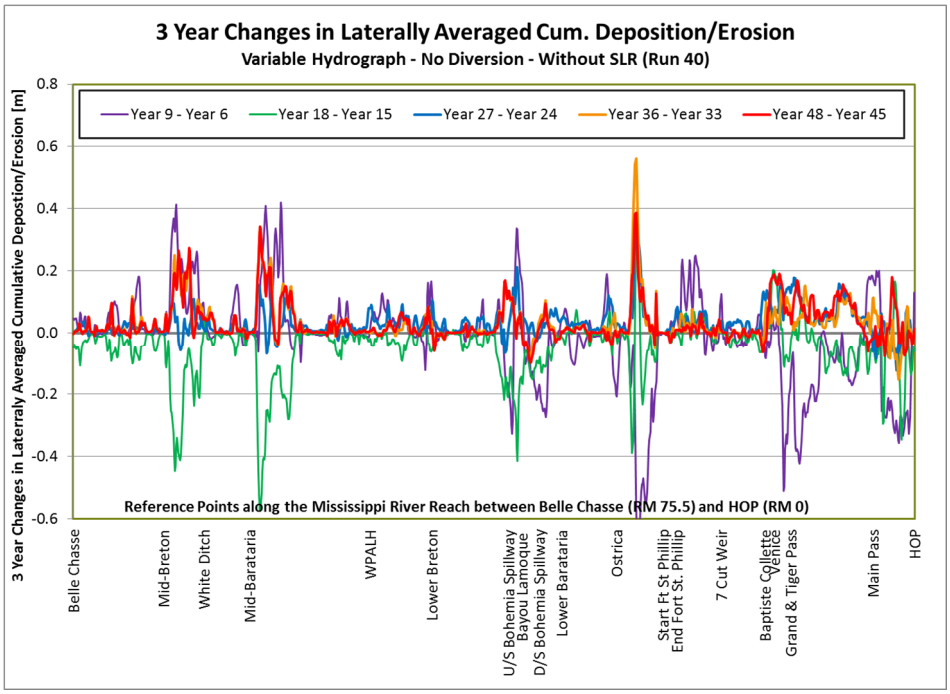

Figure 7.3.2.2.3a: 3-Year Changes in Laterally Averaged Cumulative Deposition Variable Hydrograph, No Diversion and Without SLR (Run 40)

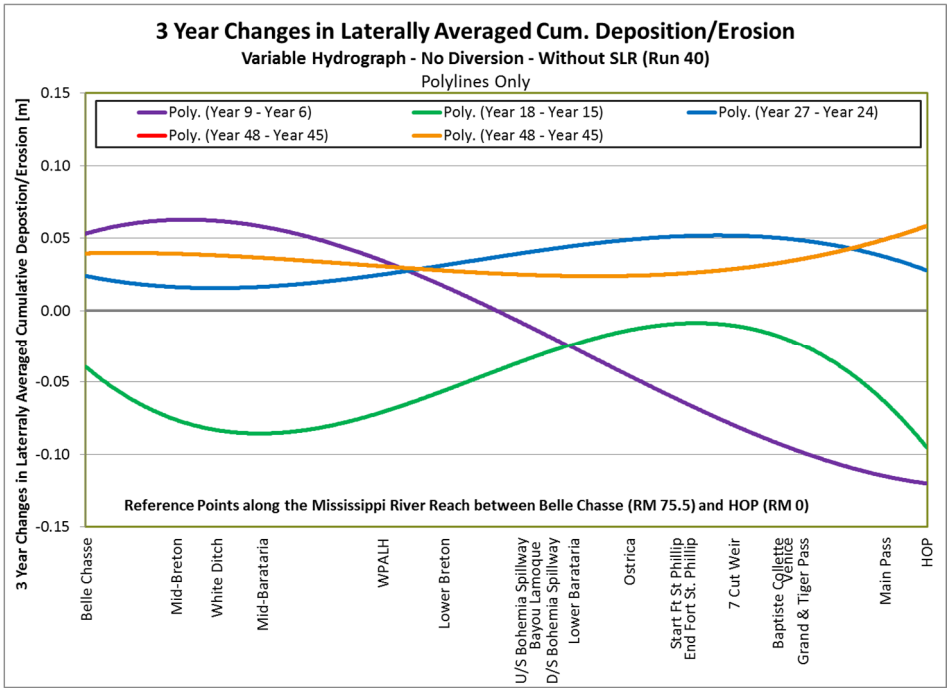

Figure 7.3.2.2.3b: 3-Year Changes in Laterally Averaged Cumulative Deposition Variable Hydrograph, No Diversion and Without SLR (Run 40) – Polylines Only

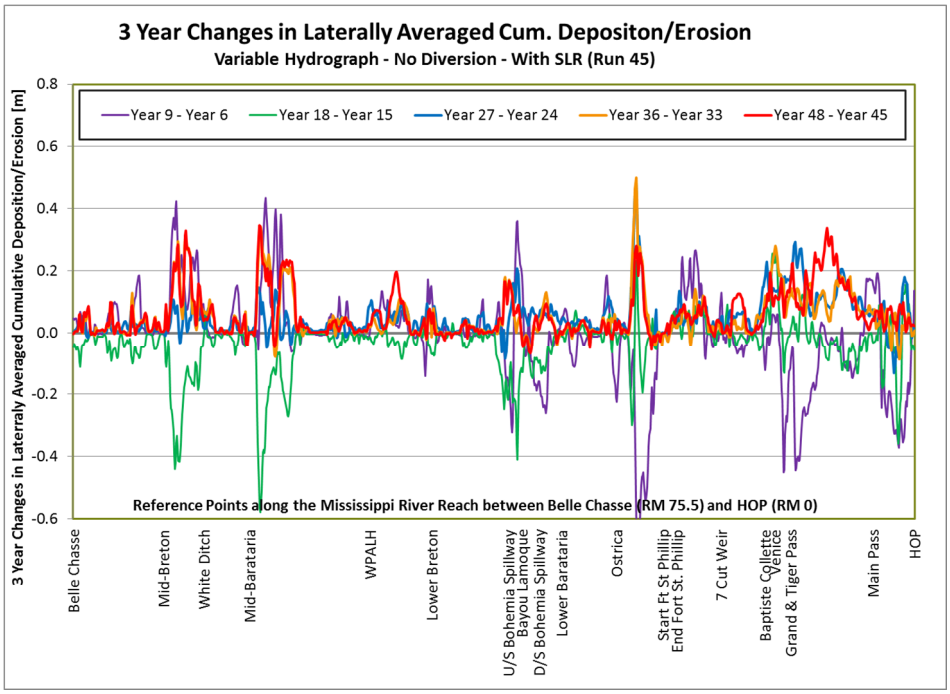

Figure 7.3.2.2.4a: 3-Year Changes in Laterally Averaged Cumulative Deposition Variable Hydrograph, No Diversion and With SLR (Run 45)

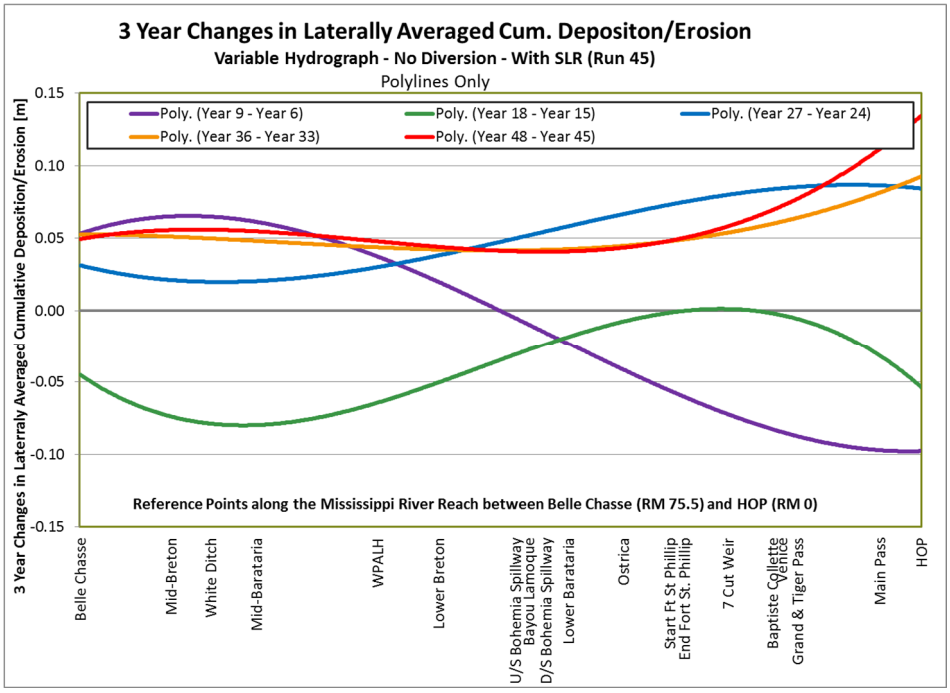

Figure 7.3.2.2.4b: 3-Year Changes in Laterally Averaged Cumulative Deposition Variable Hydrograph, No Diversion and With SLR (Run 45) – Polylines Only

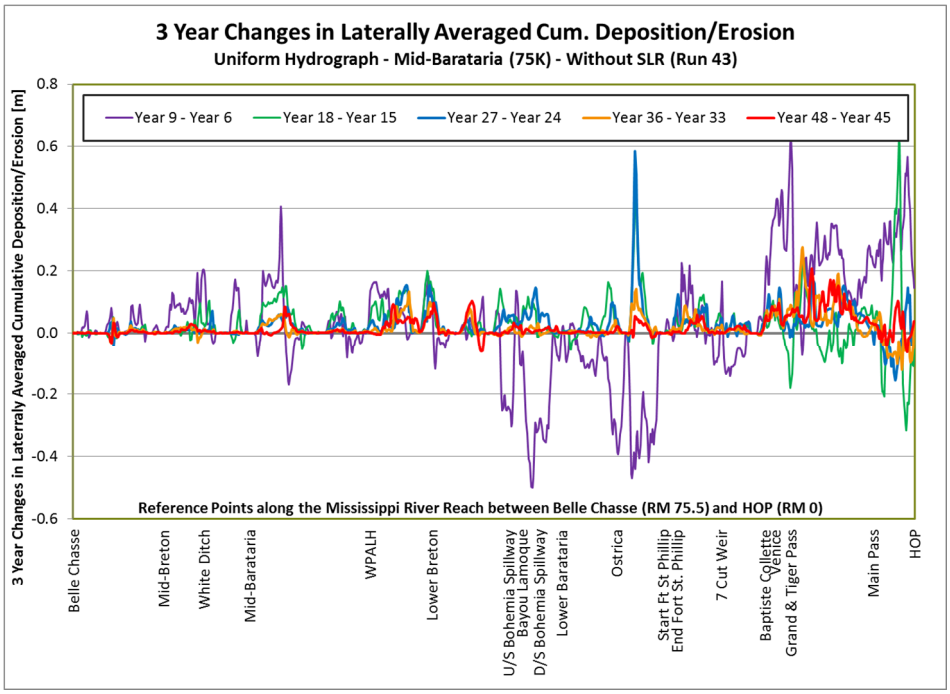

Figure 7.3.2.2.5a: 3-Year Changes in Laterally Avg. Cumulative Deposition, Uniform Hydrograph, 1 Diversion (Mid-Barataria 75K) and Without SLR (Run 43)

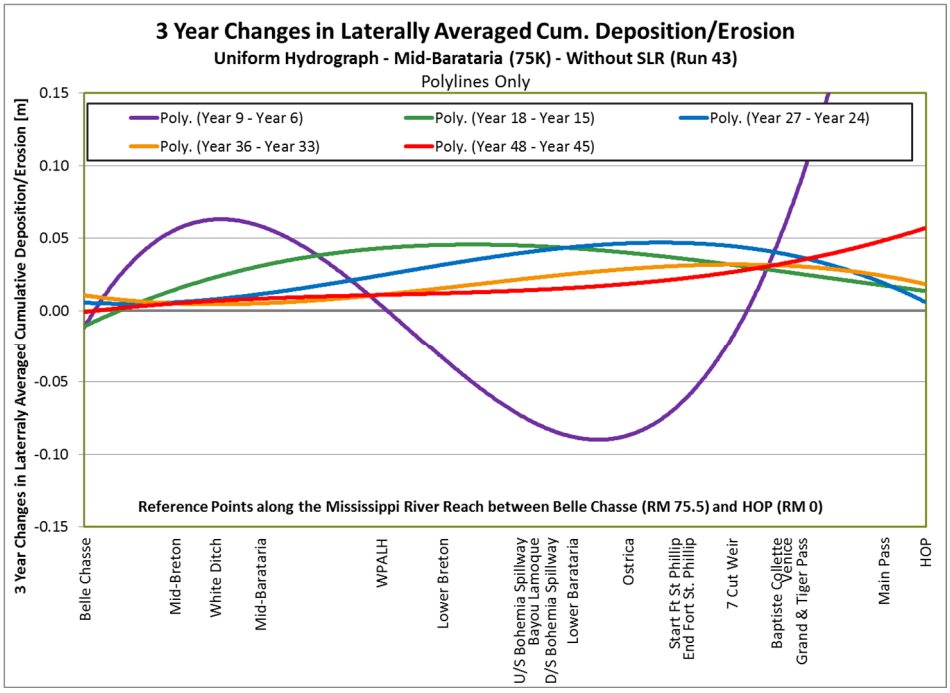

Figure 7.3.2.2.5b: 3-Year Changes in Laterally Averaged Cumulative Deposition, Uniform Hydrograph, 1 Diversion (Mid-Barataria 75K) and Without SLR (Run 43) – Polylines Only

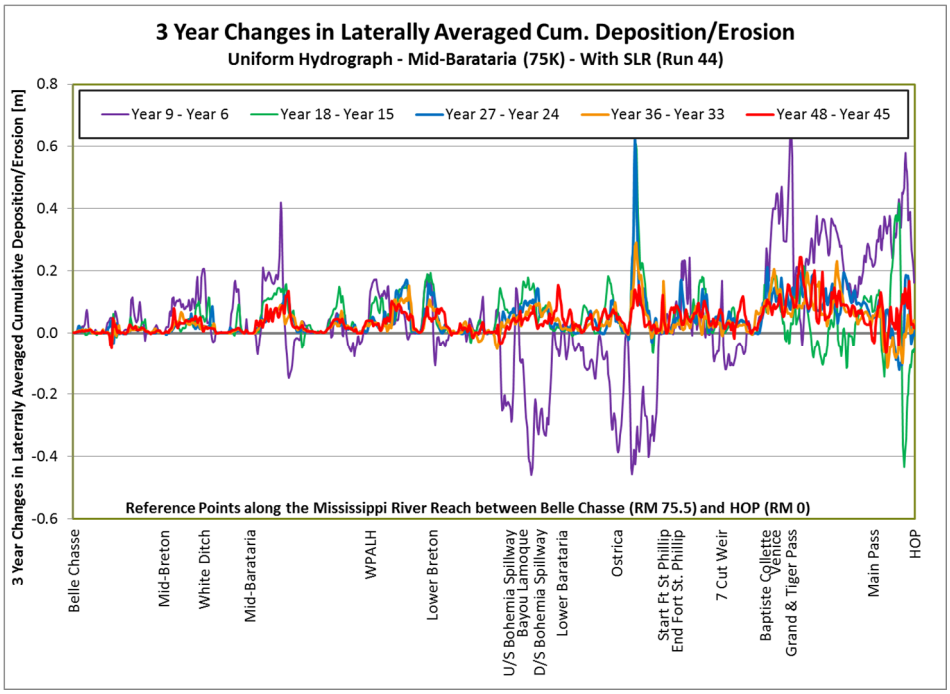

Figure 7.3.2.2.6a: 3-Year Changes in Laterally Average Cumulative Deposition, Uniform Hydrograph, 1 Diversion (Mid-Barataria 75K) and With SLR (Run 44)

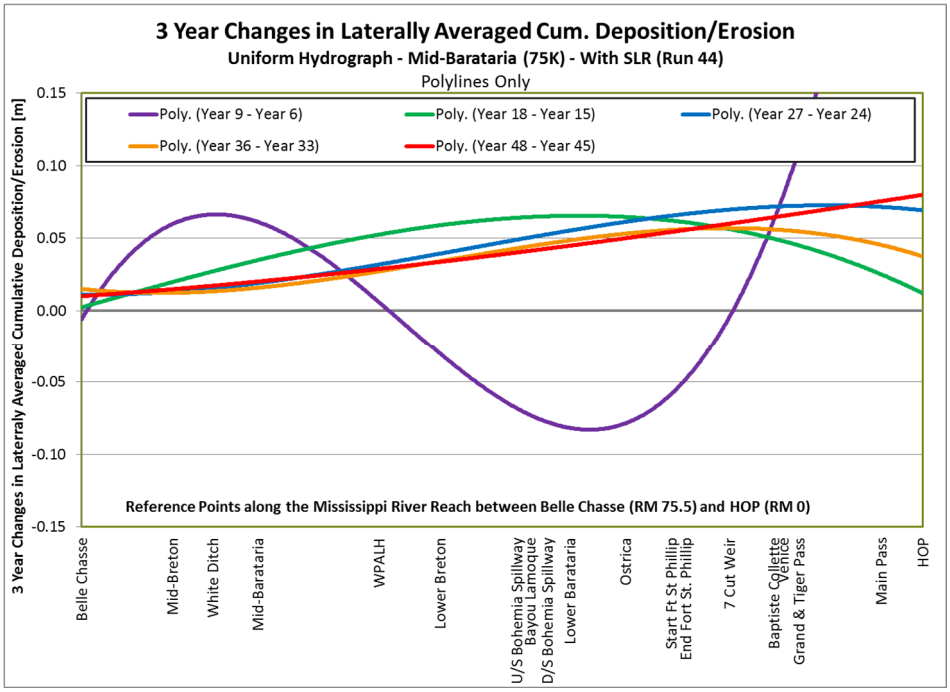

Figure 7.3.2.2.6b: 3-Year Changes in Laterally Average Cumulative Deposition, Uniform Hydrograph, 1 Diversion (Mid-Barataria 75K) and With SLR (Run 44) – Polylines Only

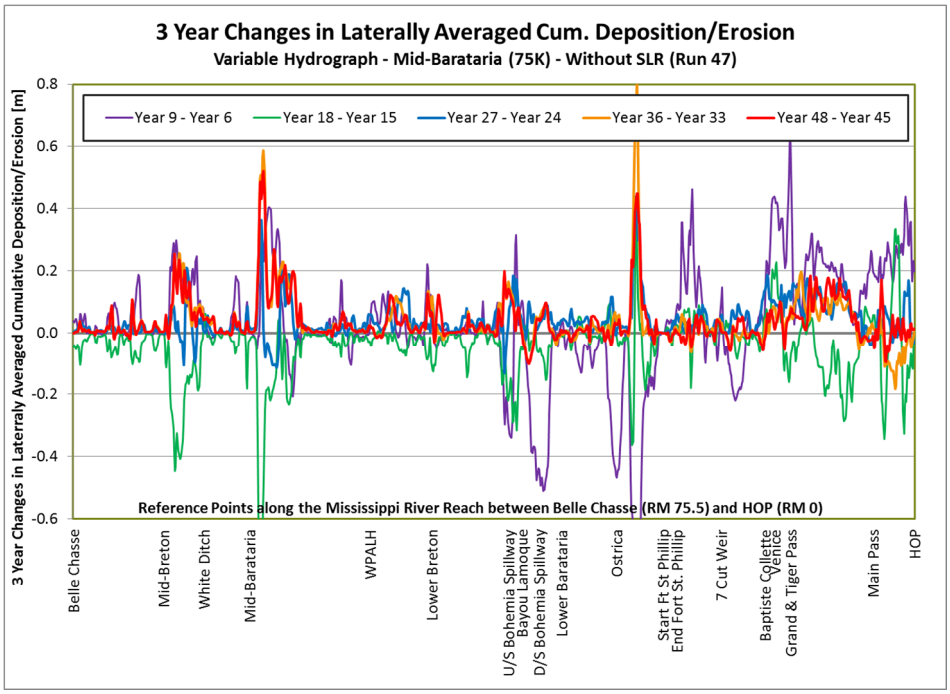

Figure 7.3.2.2.7a: 3-Year Changes in Laterally Average Cumulative Deposition, Variable Hydrograph, 1 Diversion (Mid-Barataria 75K) and Without SLR (Run 47)

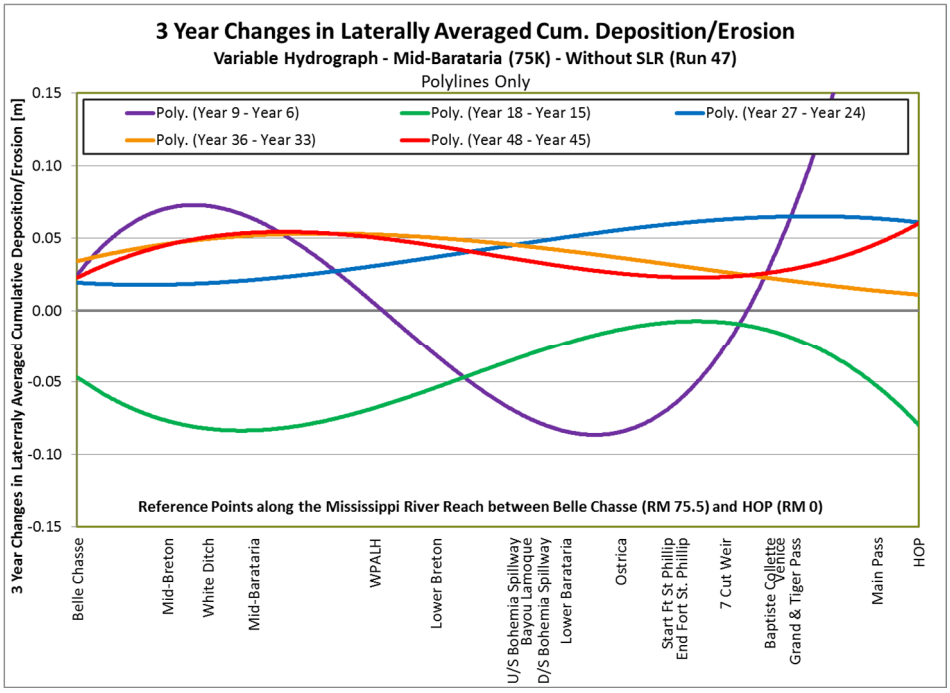

Figure 7.3.2.2.7b: 3-Year Changes in Laterally Average Cumulative Deposition, Variable Hydrograph, 1 Diversion (Mid-Barataria 75K) and Without SLR (Run 47) – Polylines Only

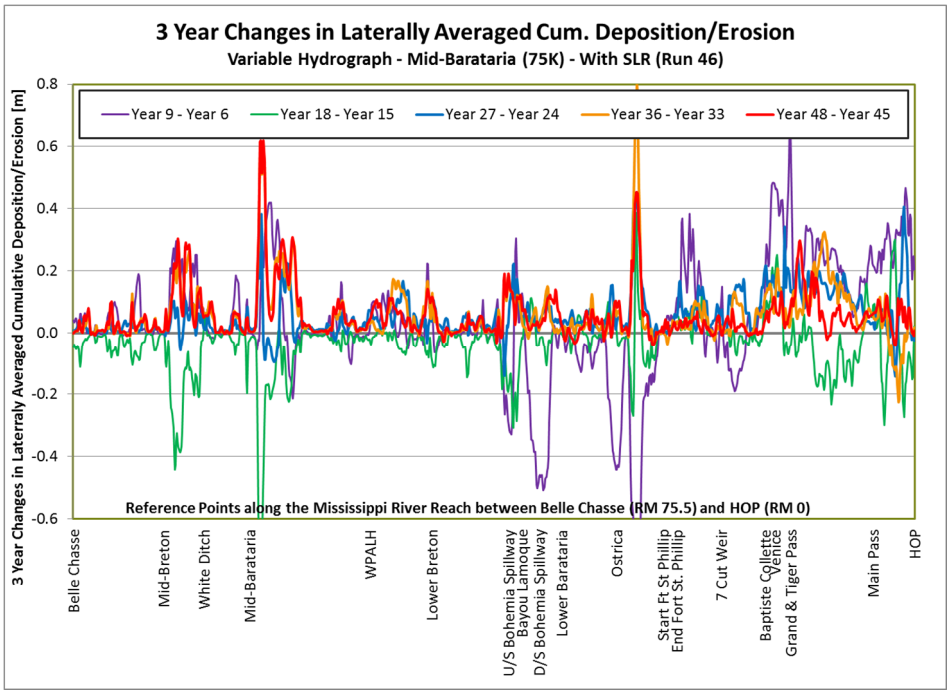

Figure 7.3.2.2.8a: 3-Year Changes in Laterally Averaged Cumulative Deposition, Variable Hydrograph, 1 Diversion (Mid-Barataria 75K) and With SLR (Run 46)

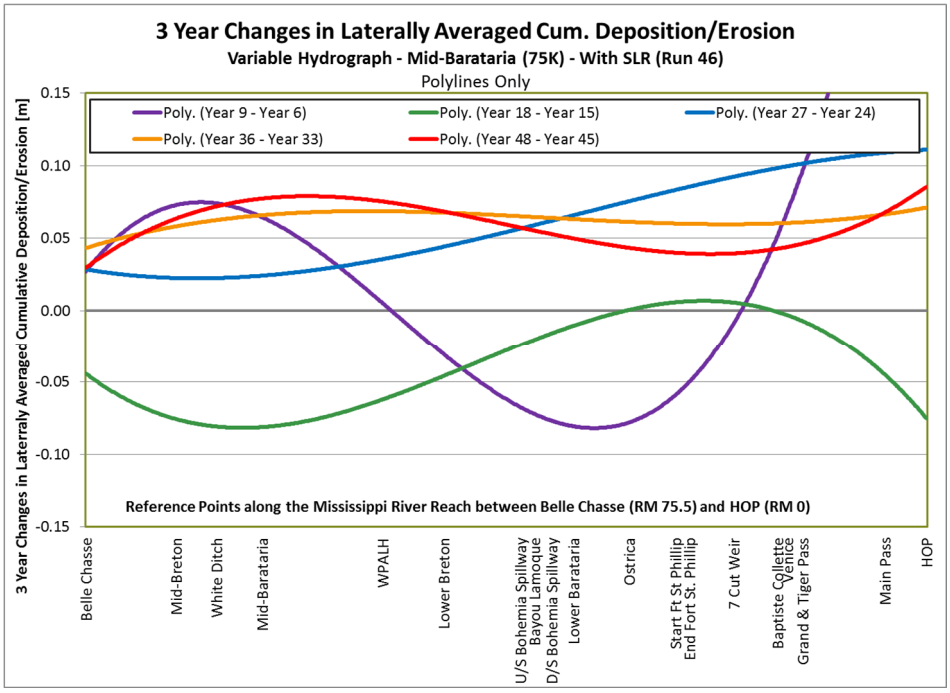

Figure 7.3.2.2.8b: 3-Year Changes in Laterally Averaged Cumulative Deposition, Variable Hydrograph, 1 Diversion (Mid-Barataria 75K) and With SLR (Run 46) – Polylines Only

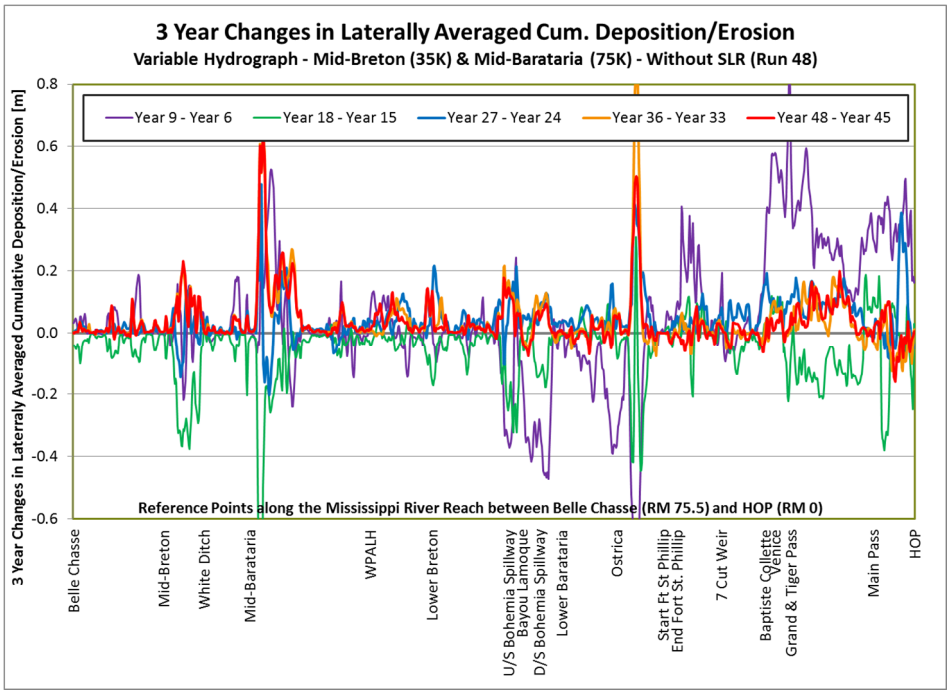

Figure 7.3.2.2.9a: 3-Year Changes in Laterally Average Cumulative Deposition, Variable Hydrograph, 2 Diversions (Mid-Breton & Mid-Barataria) and Without SLR (Run 48)

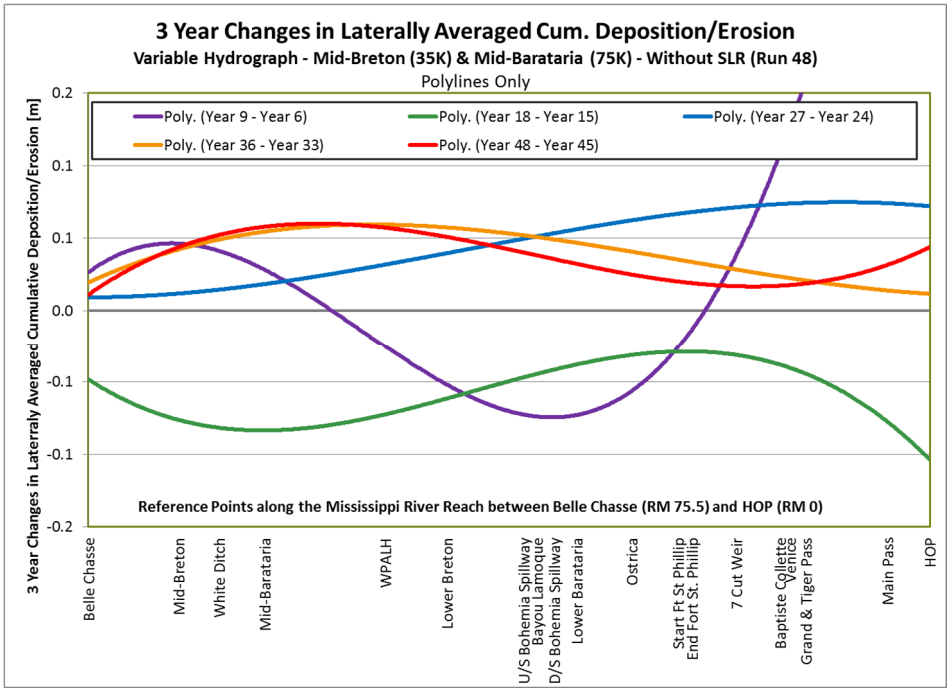

Figure 7.3.2.2.9b: 3-Year Changes in Laterally Averaged Cumulative Deposition, Variable Hydrograph, 2 Diversions (Mid-Breton & Mid-Barataria) and Without SLR (Run 48) – Polylines Only

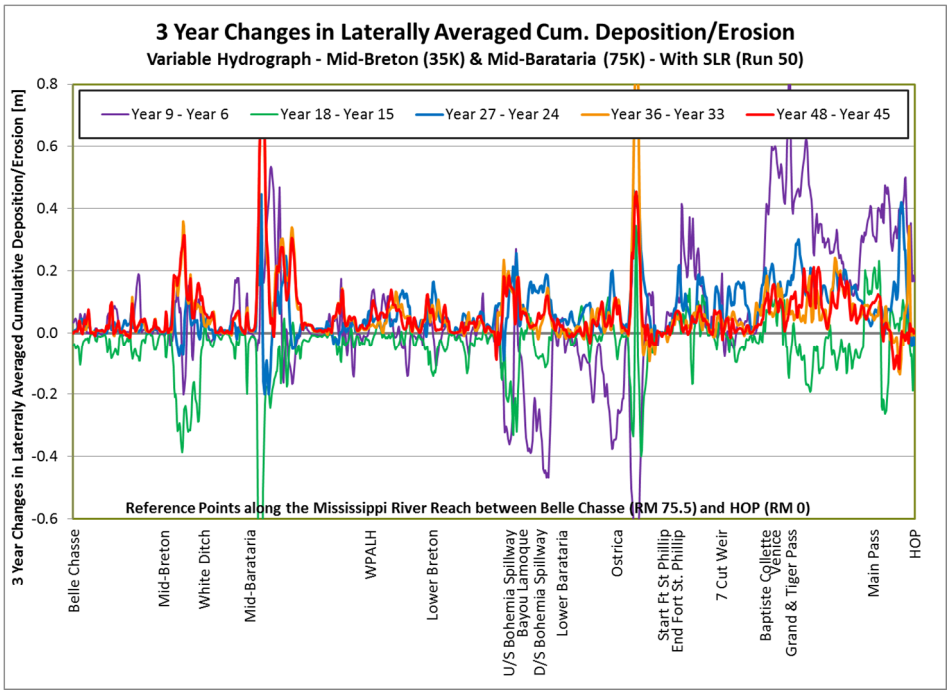

Figure 7.3.2.2.10a: 3-Year Changes in Laterally Averaged Cumulative Deposition, Variable Hydrograph, 2 Diversions (Mid-Breton & Mid-Barataria) and With SLR (Run 50)

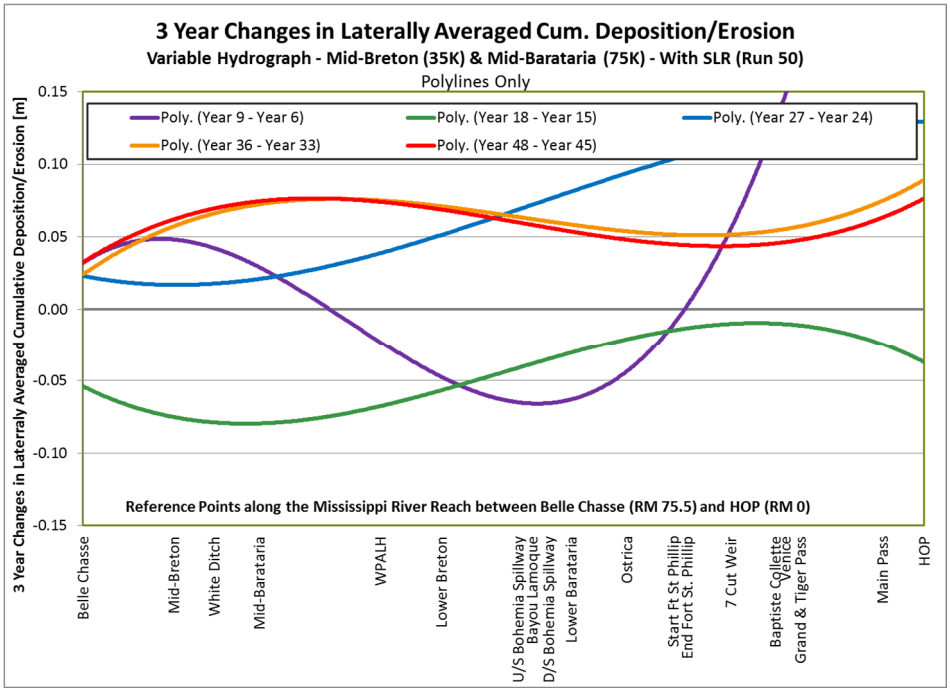

Figure 7.3.2.2.10b: 3-Year Changes in Laterally Averaged Cumulative Deposition, Variable Hydrograph, 2 Diversions (Mid-Breton & Mid-Barataria) and With SLR (Run 50) - Polylines Only

7.3.3 DISCUSSION

7.3.3.1 Deposition Correlation to 48-Year Sea Level Rise

To evaluate the change in laterally averaged cumulative deposition due to SLR the data from the run without SLR was deducted from the data of the run with SLR to obtain the change in deposition. This change was depicted in 6-year intervals with added trendlines for years 24, 30 and 48 (see Appendix R3.3.1). Additional figures were developed from the data to only depict the change in laterally averaged cumulative deposition along the river domain at year 24 and year 48 (see Appendix R3.3.2).

To further analyze the deposition due to SLR the figures listed in Table 7.3.3.1.1 were developed by calculating the deposition change [m] (deposition with SLR – deposition without SLR) and normalizing it by dividing by the SLR to be experienced over the 48 year modeled period (deposition change [m]/SLR over 48 years [m]) to obtain a non-dimensional factor representing depositional trends. SLR in meters for the 48 years was calculated at 0.602m.

Table 7.3.3.1.1: Index of Figures for Deposition Trends due to SLR:

Hydrograph	Diversion	Figure
Uniform	No Diversion	7.3.3.1.1
Variable	No Diversion	7.3.3.1.2
Uniform	1 Diversion	7.3.3.1.3
Variable	1 Diversion	7.3.3.1.4
Variable	2 Diversions	7.3.3.1.5

All Figures (7.3.3.1.1 to 7.3.3.1.5) follow a similar trend where the deposition between RM 40 and 75.5 (Belle Chasse), which is the upstream portion of the domain, has a uniform increase of the deposition over time, while the deposition between RM 40 and HOP (RM 0) increases more rapidly at the HOP and asymptotically approaches the uniform deposition rate at RM 40. This reach also increases in deposition over time.

When comparing the no-diversion cases (Figure 7.3.3.1.1 and 7.3.3.1.2) the uniform hydrograph case generates larger deposition between RM 40 and HOP while the values between RM 40 and Belle Chasse are comparable. The maximum difference of the trendlines at HOP at year 48 between the two cases is approximately 0.15.

When comparing the 1-diversion cases (Figure 7.3.3.1.3 and 7.3.3.1.4) to the no diversion cases, both maximum depositional values are less than in their no diversion counterpart. Also, contrary to the no diversion case, the uniform hydrograph case yields a smaller maximum value at HOP than the variable case, 0.81 for uniform and 1.05 for the variable case trendline. However, overall the deposition along the domain in the uniform case is higher than in the variable case, especially between RM 40 and RM 55, and a general shift in the location of the transition between the asymptotic and the uniform portion of the depositional trendline. The shift is from RM 40 to approximately RM 60.

When comparing all variable hydrograph cases (Figure 7.3.3.1.2, 7.3.3.1.4 and 7.3.3.1.5), the 2 diversion case results in larger deposition than the no diversion case but follows the same pattern. The maximum difference at HOP at year 48 between the no diversion and the 2 diversion cases is approximately 0.15. The one and two diversion cases indicate a smaller increase in deposition between year 42 and 48 than in earlier periods. In addition the 12-year period between years 24 and 36 appears to have a larger increase than the 12-year period between years 0 to 12 or the 12-year period between years 36 and 48.

Overall it is interesting to observe the slightly different overall depositional behavior for the 1 diversion case, which has a smaller maximum deposition at HOP than the no-diversion case but the 2-diversion case exceeds the maximum of the no-diversion case. This drop in maximum deposition between the no-diversion and the 1-diversion case at HOP can be observed in both hydrograph cases. A possible explanation is the increased impacts at Fort St. Phillip with the 2-diversion case.

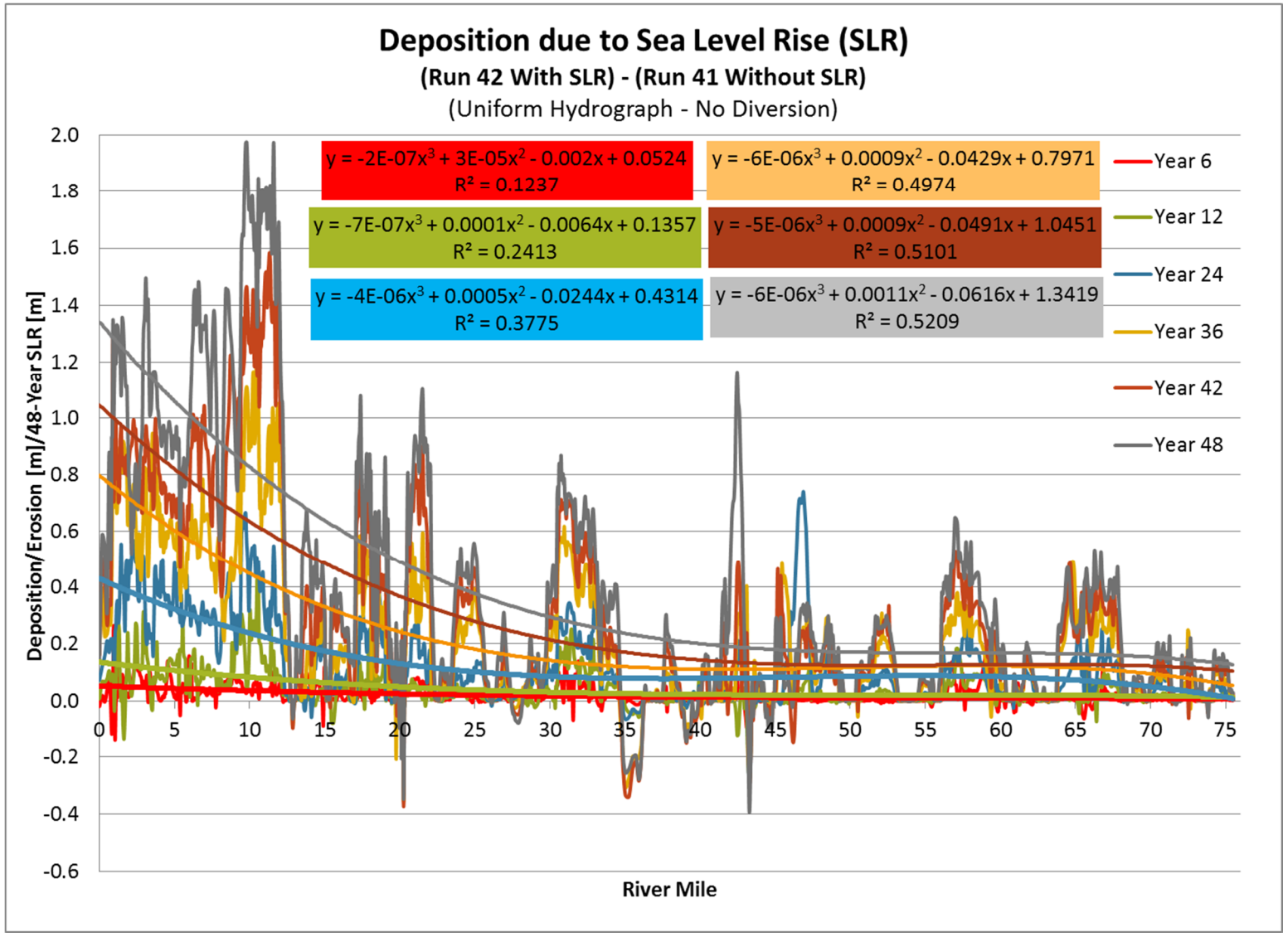

Figure 7.3.3.1.1: Deposition due to SLR – Uniform Hydrograph - No Diversion)

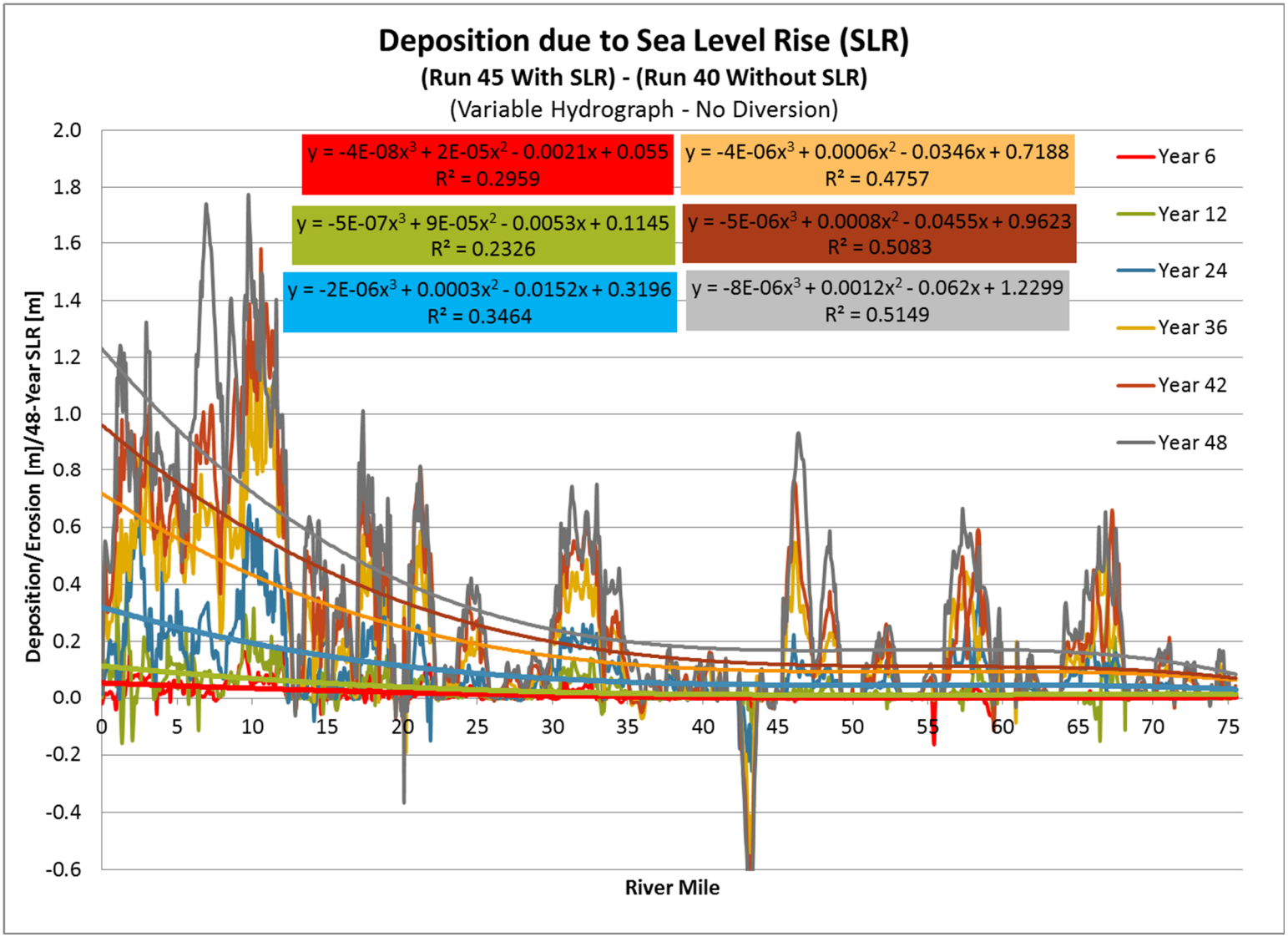

Figure 7.3.3.1.2: Deposition due to SLR – Variable Hydrograph - No Diversion)

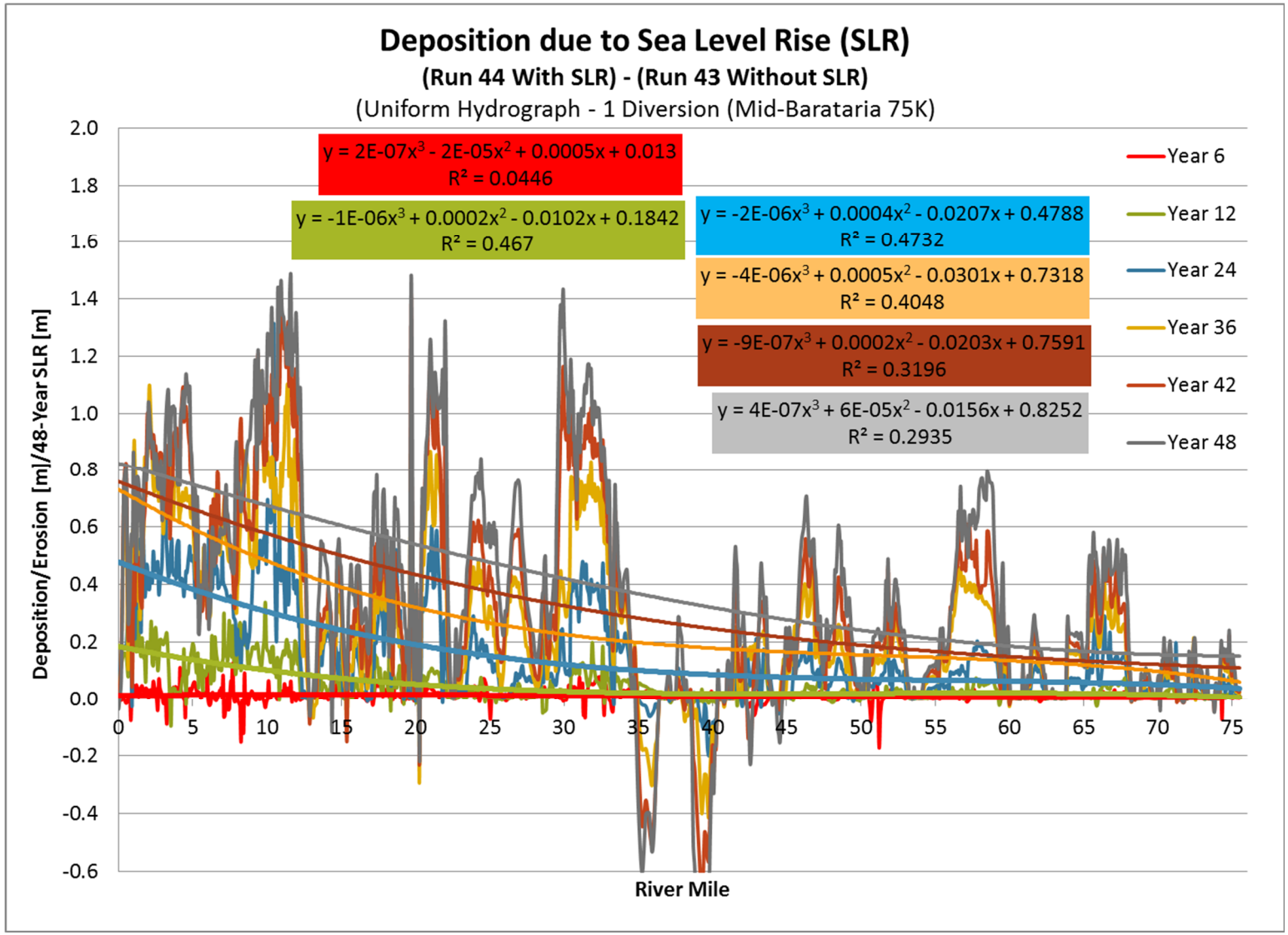

Figure 7.3.3.1.3: Deposition due to SLR – Uniform Hydrograph - 1 Diversion (Mid-Barataria 75K)

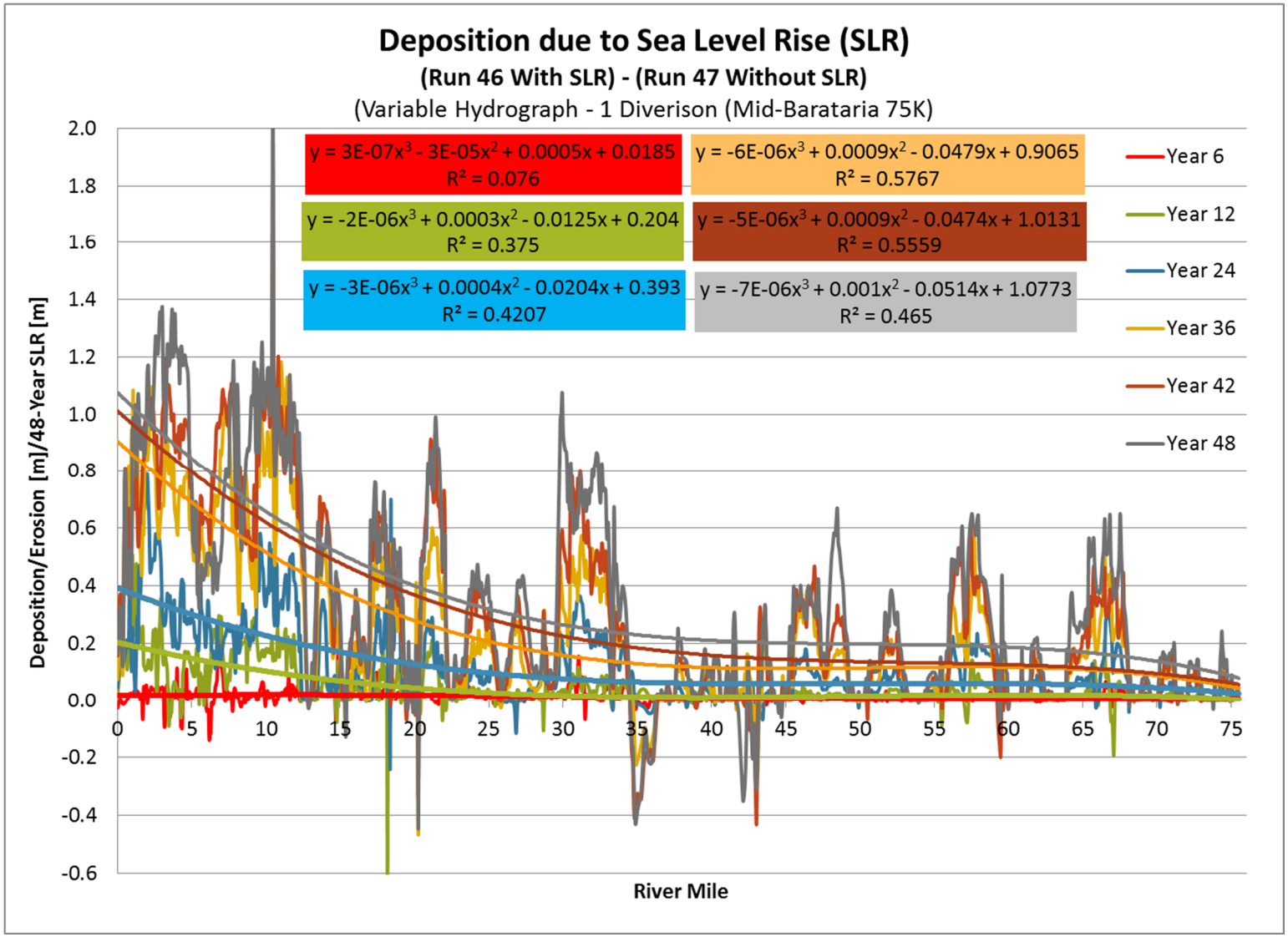

Figure 7.3.3.1.4: Deposition due to SLR – Variable Hydrograph - 1 Diversion (Mid-Barataria 75K)

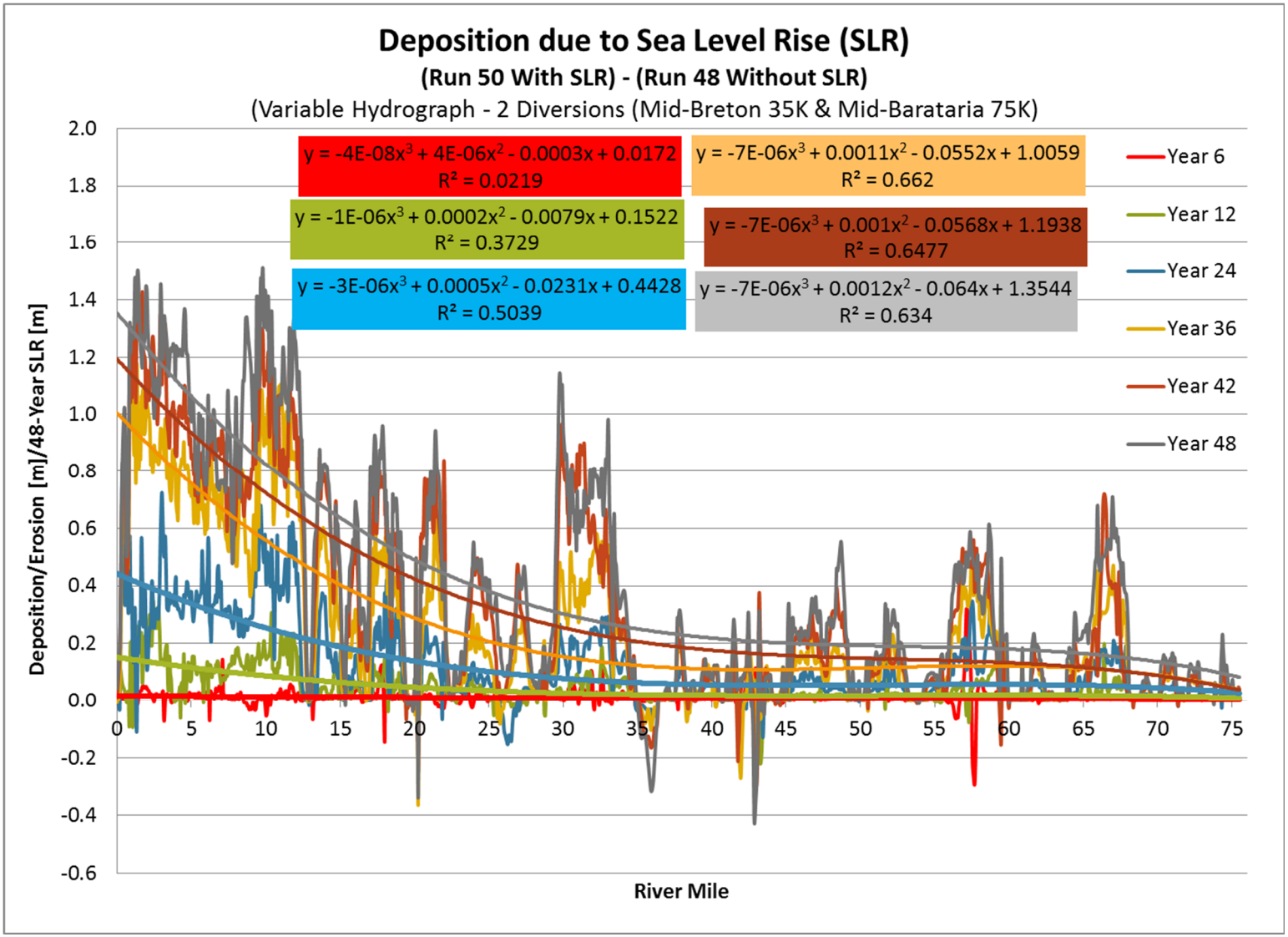

Figure 7.3.3.1.5: Deposition due to SLR – Variable Hydrograph - 2 Div. (Mid-Breton 35K & Mid-Barataria 75K)

7.3.3.2 Domain Averaged Cumulative Deposition due to SLR (3-Year Change):

Figures 7.3.3.2.1 through 7.3.3.2.10 depict the domain averaged cumulative deposition for the model runs identified in Table 7.3.1.1. The average and the standard deviation were developed for each 3-year period. For example, the value for laterally averaged cumulative deposition of year 3 was subtracted from the laterally averaged cumulative deposition of year 6 to determine the 3-Year Change between Years 3 and 6. The average and the standard deviation were developed longitudinally for each 3-Year interval up to 48 years.

The following trends can be observed:

- Periodicity in the variable hydrograph case is equal to the reoccurring period of the variable hydrograph, which is 12 years.
- Uniform Hydrograph: In both scenarios, with and without sea level rise, the 1-diversion case has a higher average deposition than the no-diversion case. Also, the standard deviation is slightly higher in the 1-diversion case versus the no-diversion case.
- Variable Hydrograph: In both scenarios, with and without sea level rise, the 1-diversion case has a higher average deposition than the no-diversion case. Also, the standard deviation is slightly higher in the 1-diversion case versus the no-diversion case.
- For the no-diversion case, with no sea level rise, both hydrograph cases (uniform and variable) result in a similar average in deposition, which is approaching zero with a slight increase in the last 2 years. This increase may indicate changes in the deposition pattern in the river downstream of Fort St. Phillip.
- For the no-diversion case, with sea level rise, both hydrograph cases (uniform and variable) result in a similar trend as the without sea level rise cases but remains above zero, except the variable case has an oscillating approach to the mean value of the uniform case over time.
- For the 1-diversion case, without and with sea level rise, the average deposition of the variable case is oscillating about a mean value that is slightly less than the

uniform case. In general, the standard deviation of the variable case is higher than the standard deviation of the uniform case, which is to be expected.

- Variable Hydrograph: Between the 2-diversion case and the 1-diversion case, there is a very slight increase in deposition average, for the no sea level rise scenario. The increase is even less for the with sea level rise scenario. The introduction of the second diversion (Mid-Breton) increases the erosion between Mid-Breton and Belle Chasse due to the M2-backwater effect (Chow 1959)

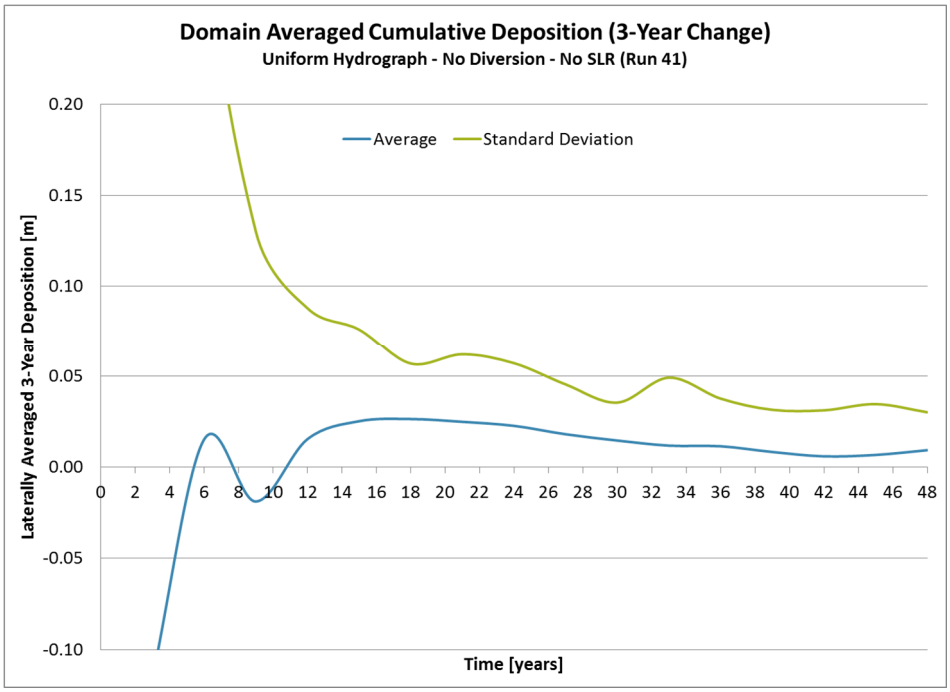

Figure 7.3.3.2.1: Domain Averaged Cumulative Deposition (3-Year Change) Uniform Hydrograph, No Diversion and No Sea Level Rise (Run 41)

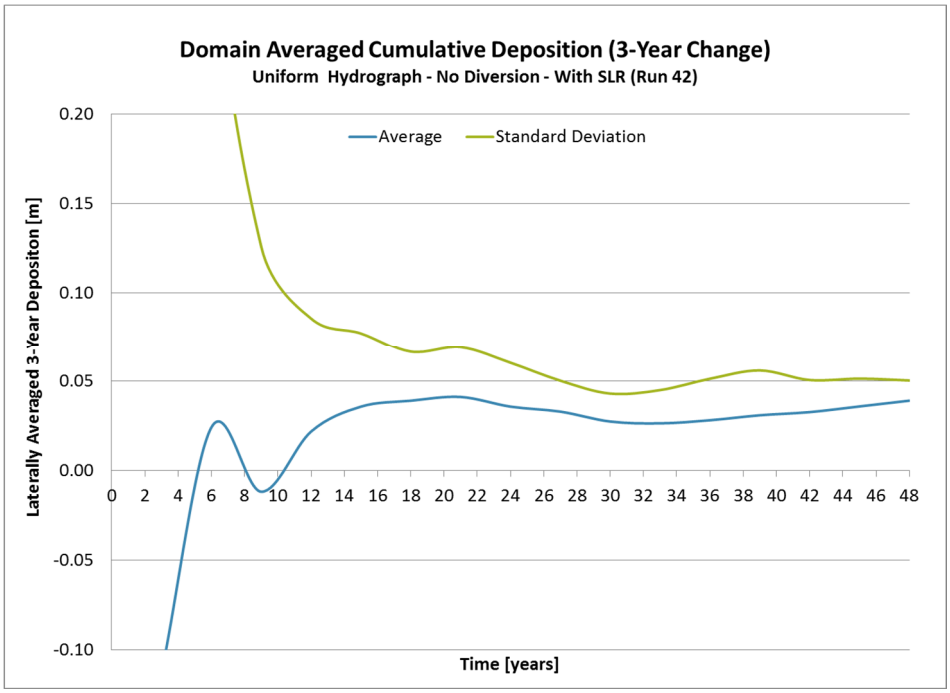

Figure 7.3.3.2.2: Domain Averaged Cumulative Deposition (3-Year Change) Uniform Hydrograph, No Diversion and With Sea Level Rise (Run 42)

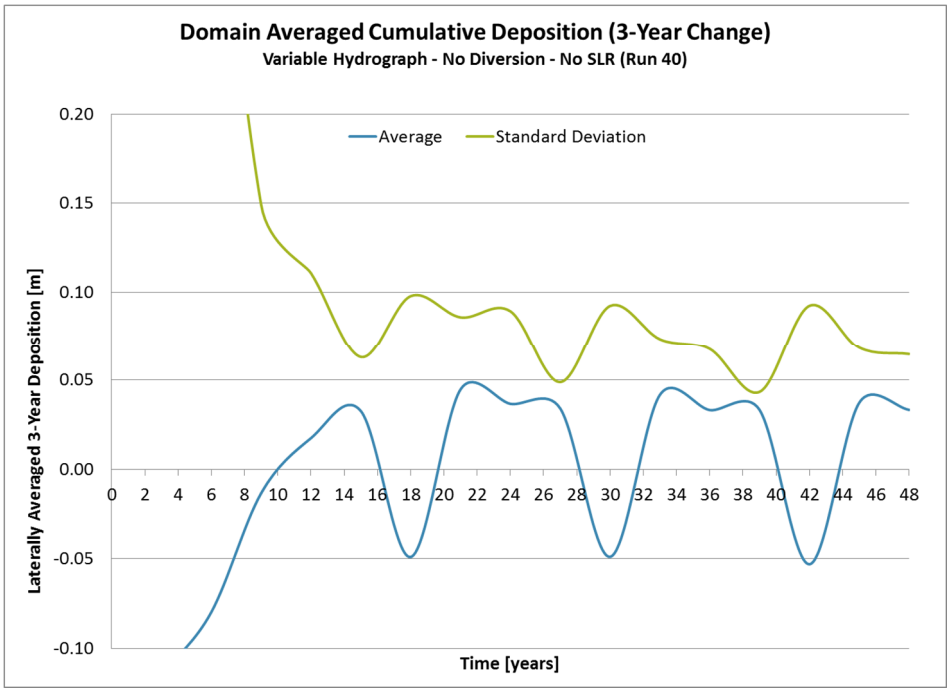

Figure 7.3.3.2.3: Domain Averaged Cumulative Deposition (3-Year Change) Variable Hydrograph, No Diversion and No Sea Level Rise (Run 40)

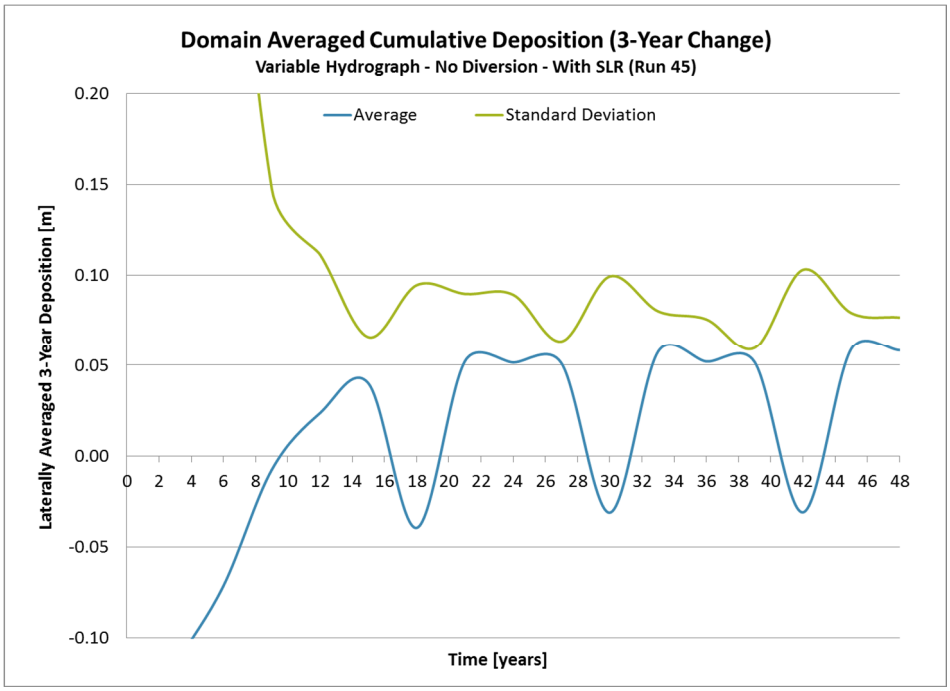

Figure 7.3.3.2.4: Domain Averaged Cumulative Deposition (3-Year Change) Variable Hydrograph, No Diversion and With Sea Level Rise (Run 45)

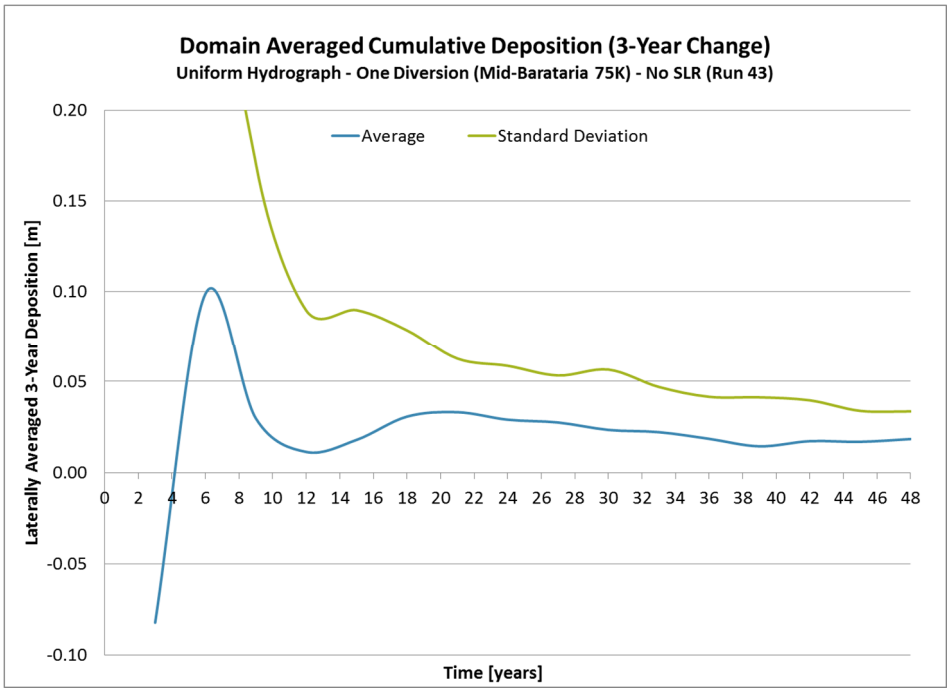

Figure 7.3.3.2.5: Domain Averaged Cumulative Deposition (3-Year Change) Uniform Hydrograph, One Diversion (Mid-Barataria 75K) and No Sea Level Rise (Run 43)

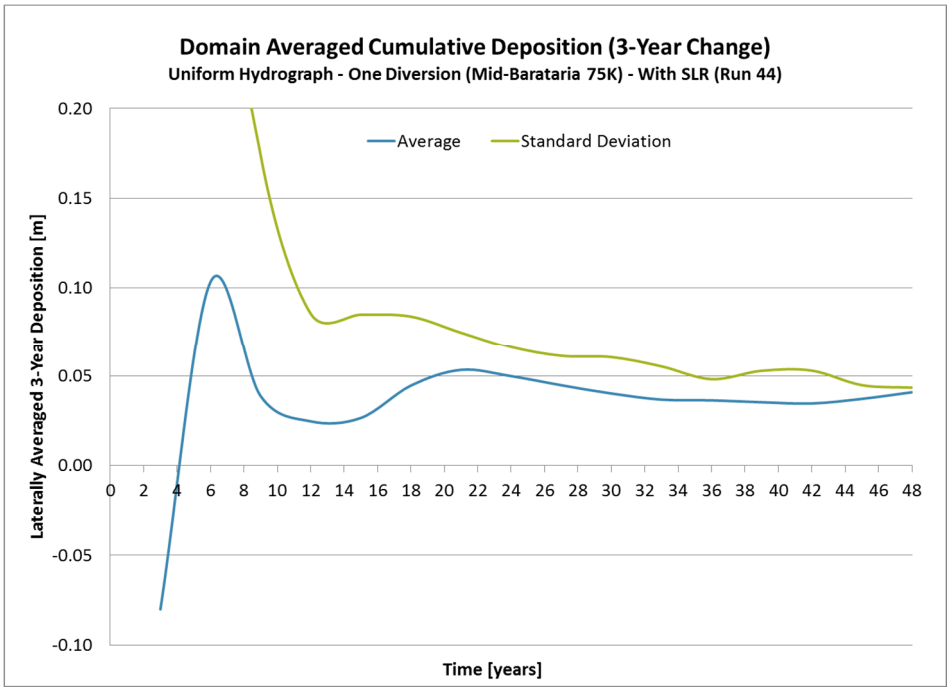

Figure 7.3.3.2.6: Domain Averaged Cumulative Deposition (3-Year Change) Uniform Hydrograph, One Diversion (Mid-Barataria 75K) and With Sea Level Rise (Run 44)

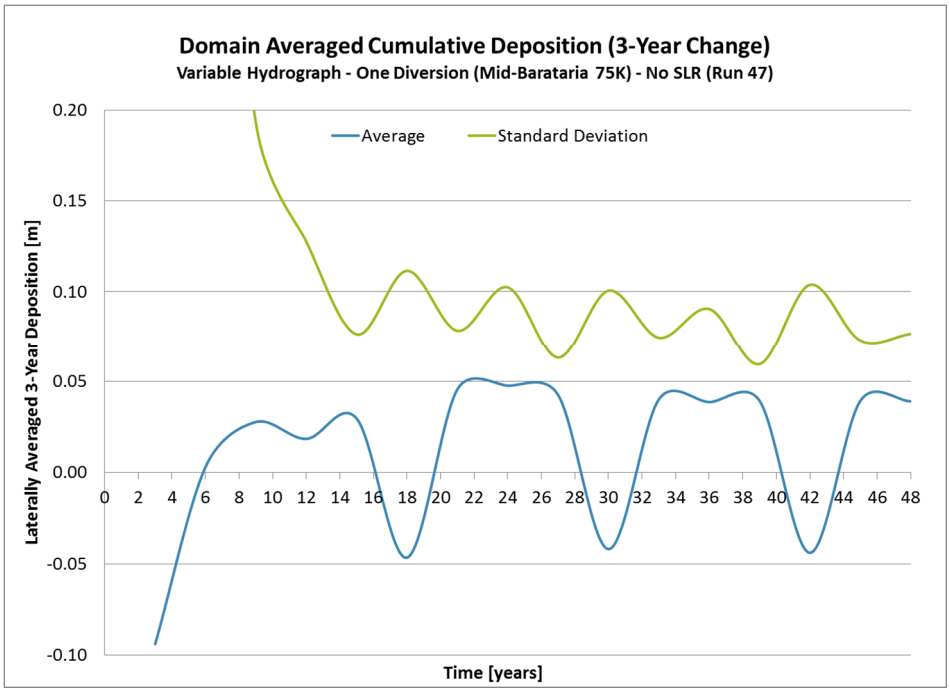

Figure 7.3.3.2.7: Domain Averaged Cumulative Deposition (3-Year Change) Variable Hydrograph, One Diversion (Mid-Barataria 75K) and No Sea Level Rise (Run 47)

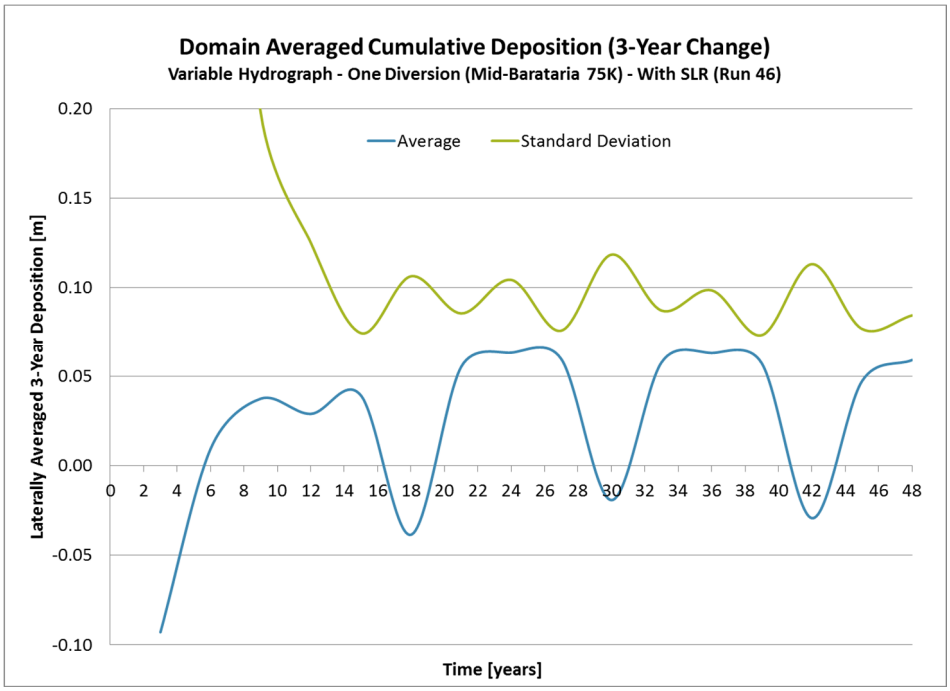

Figure 7.3.3.2.8: Domain Averaged Cumulative Deposition (3-Year Change) Variable Hydrograph, One Diversion (Mid-Barataria 75K) and With Sea Level Rise (Run 46)

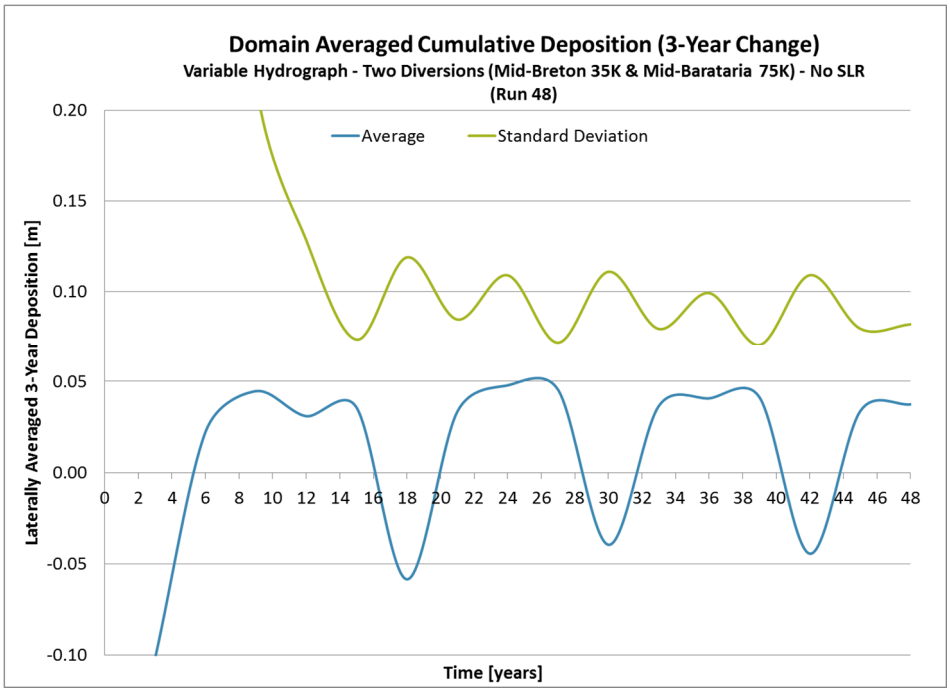

Figure 7.3.3.2.9: Domain Averaged Cumulative Deposition (3-Year Change) Variable Hydrograph, Two Diversions (Mid-Breton 35K & Mid-Barataria 75K) and No Sea Level Rise (Run 48)

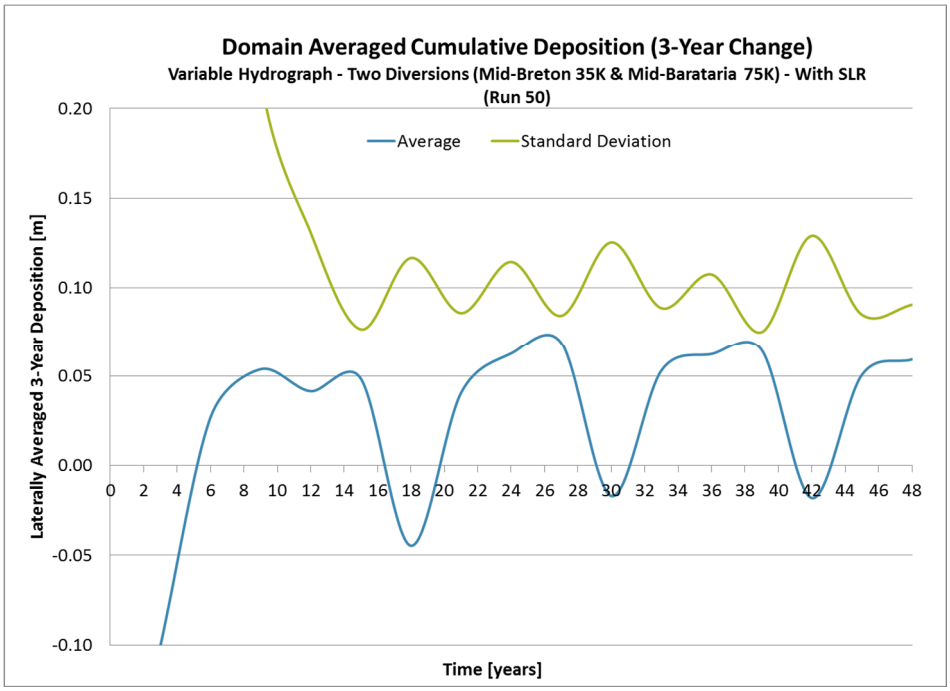

Figure 7.3.3.2.10: Domain Averaged Cumulative Deposition (3-Year Change) Variable Hydrograph, Two Diversions (Mid-Breton 35K & Mid-Barataria 75K) and With SLR (Run 50)

To further analyze the trends in depositional behavior, the domain averaged cumulative deposition due to SLR was calculated for 3-Year periods. The average and standard deviation was calculated for the 3-Year changes and plotted over time. Figures 7.3.3.2.11 to 7.3.3.2.15 depict these calculated domain values for the various diversion and hydrograph cases. See Table 7.3.3.2.1 for a figure index.

Table 7.3.3.2.1: Index of Figures for Domain Averaged Cumulative Deposition [m] due to SLR (3-Year Change):

Hydrograph	Diversion	Figure
Uniform	No Diversion	7.3.3.2.11
Variable	No Diversion	7.3.3.2.12
Uniform	1 Diversion	7.3.3.2.13
Variable	1 Diversion	7.3.3.2.14
Variable	2 Diversion	7.3.3.2.15

For all five cases (Figure 7.3.3.2.11 to 7.3.3.2.15) neither the average nor the standard deviation approach equilibrium or indicate a trend towards equilibrium. The depicted averages and standard deviations rather continue to increase with oscillating values and are not approaching zero.

When comparing the uniform hydrograph non-diversion case to the variable hydrograph non-diversion case, the average for the variable hydrograph case is slightly higher overall while the uniform case reaches a higher maximum average at year 48 of 0.03m. The standard deviation reaches a higher maximum in the variable hydrograph case, which is approximately 0.055m. Both cases reach an initial peak in standard deviation near year 16/17, with the variable hydrograph cases generating the larger peak in standard deviation.

When comparing the uniform hydrograph 1-diversion case to the variable hydrograph 1-diversion case the average in both cases only surpasses 0.02m in 3 occasions during the 48 year period, with the uniform hydrograph case reaching the first passing of 0.02m at year 22 and the variable hydrograph case reaching the first passing of 0.02m around

year 28. The standard deviation for the variable hydrograph case is predominantly above 0.04m while the uniform hydrograph case standard deviation only surpasses 0.04 bear year 38.

When comparing the variable hydrograph cases for no-diversion, 1-diversion and 2-diversion, the average rate over time slightly increases from the no-diversion to the 1-diversion and the 2-diversion case. The standard deviation appears to oscillate more with increase in diversions. For the no-diversion case the initial peak in standard deviation around year 18 is followed by a period of more or less consistent standard deviation until year 40, from where another incline starts until year 48, the end of the computational runs. The 1-diversion case standard deviation has a more consistent incline while the 2-diverision case standard deviation also has a consistent incline but with oscillating values. These trends as described further support the observation of not achieving equilibrium in the modeled 48 years.

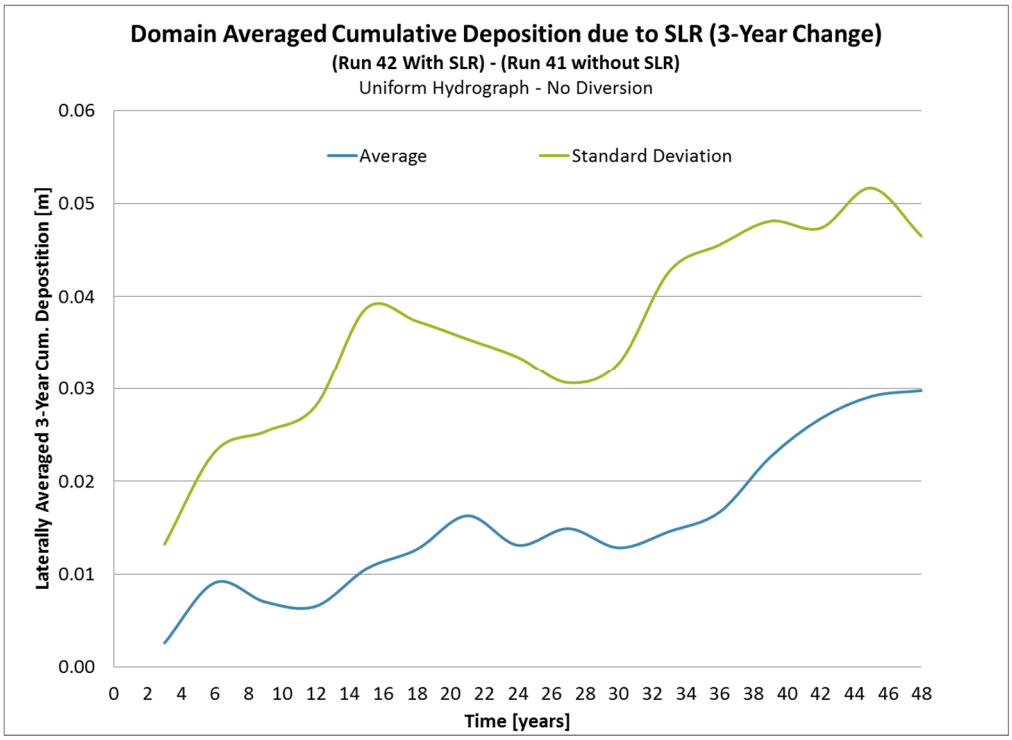

Figure 7.3.3.2.11: Domain Averaged Cumulative Deposition due to SLR (3-Year Change) Uniform Hydrograph, No Diversion

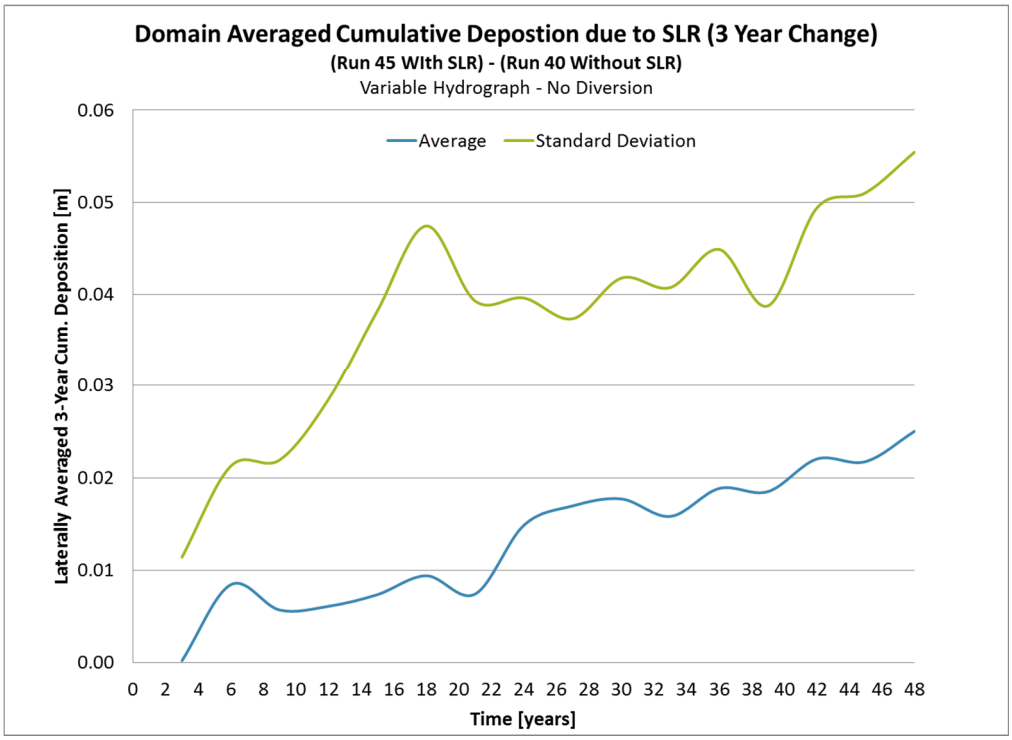

Figure 7.3.3.2.12: Domain Averaged Cumulative Deposition due to SLR (3-Year Change) Variable Hydrograph, No Diversion

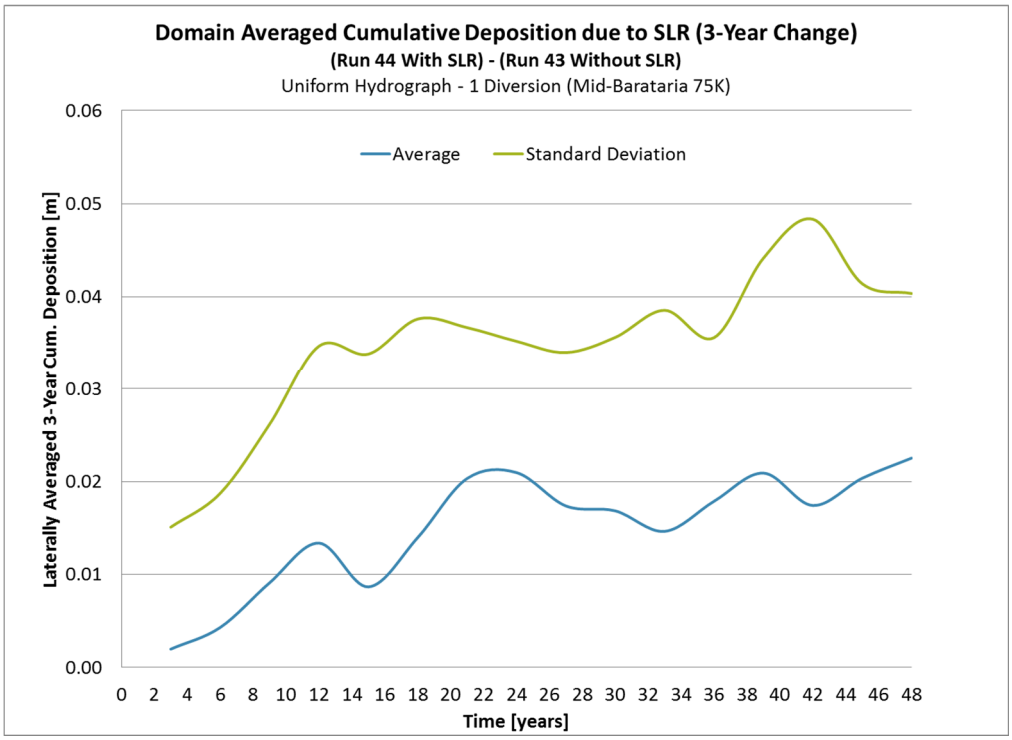

Figure 7.3.3.2.13: Domain Averaged Cumulative Deposition due to SLR (3-Year Change) Uniform Hydrograph, 1 Diversion (Mid-Barataria 75K)

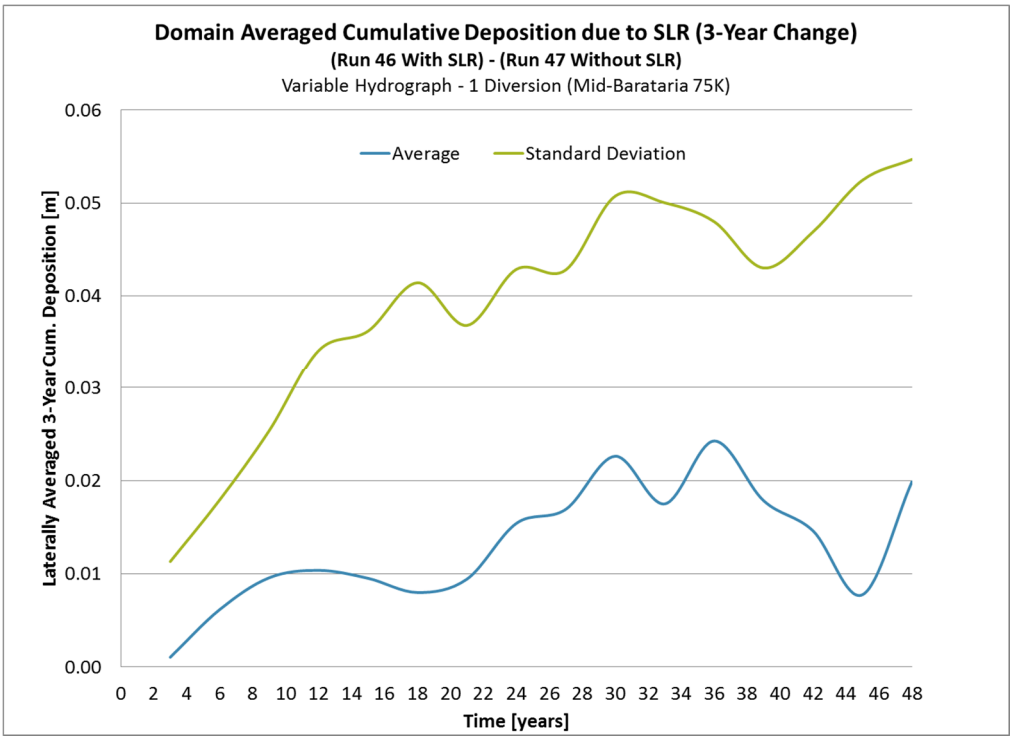

Figure 7.3.3.2.14: Domain Averaged Cumulative Deposition due to SLR (3-Year Change) Variable Hydrograph, 1 Diversion (Mid-Barataria 75K)

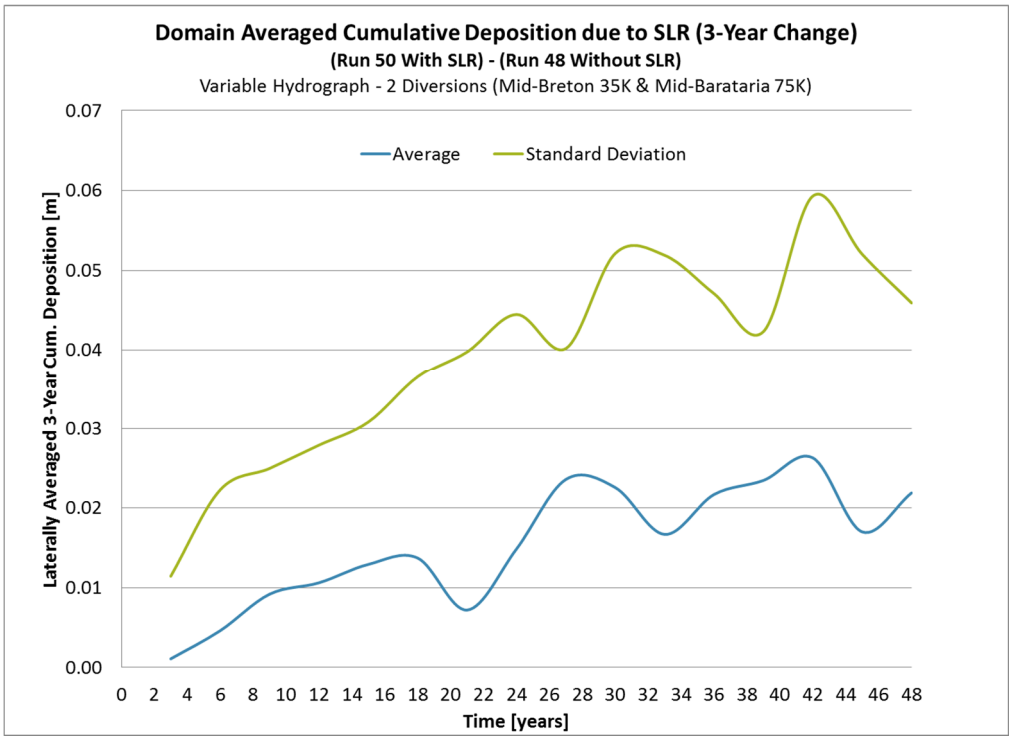

Figure 7.3.3.2.15: Domain Averaged Cumulative Deposition due to SLR (3-Year Change) Variable Hydrograph, 2 Diversions (Mid-Breton 35K & Mid-Barataria 75K)

7.3.3.3 Loss of Flow with Sea Level Rise:

To compare flows in a no diversion scenario with and without SLR, the instantaneous discharges at Venice were plotted for the 48 year time period (Figures 7.3.3.3.1). Variable hydrograph runs with (Run 45) and without SLR (Run 40) were utilized for this comparison. It is observed that the discharge peaks with SLR decline over time as SLR increases.

To further compare impacts in flow between no diversion and a one diversion case, Figure 7.3.3.3.2 and 7.3.3.3.3 were developed, which add the instantaneous discharge for the variable hydrograph runs with SLR (Run 46) and without SLR (Run 47) to the data from Figure 7.3.3.3.1, while zooming into peak flows between 5 year intervals. Figure 7.3.3.3.2 highlights the peaks in years 15-20 while Figure 7.3.3.3.3 focuses on years 38-43.

It is observed that the no diversion case without SLR (Run 40) has the largest discharge at Venice, while the 1 diversion case with SLR (Run 46) has the smallest discharge at the same location. The two cases without SLR, one no diversion (Run 40) and one with one diversion (Run 47) show a continuous difference between peak flows, with the one diversion cases having the lower flows of the two. However, the no diversion case with SLR (Run 45) starts at higher peak discharges than the one diversion case without SLR (Run 47), but over time declines in peak discharge until it eventually drops below the peak discharge values of Run 47.

The increased deposition in the Fort St. Phillip (FSP) to Head of Passes (HOP) reach resulted in an increased stage (energy) at upstream distributaries relative to the Gulf of Mexico. This in turn reduced the streampower and caused more deposition, i.e. there was a positive feedback that accelerated the impacts of SLR in this reach.

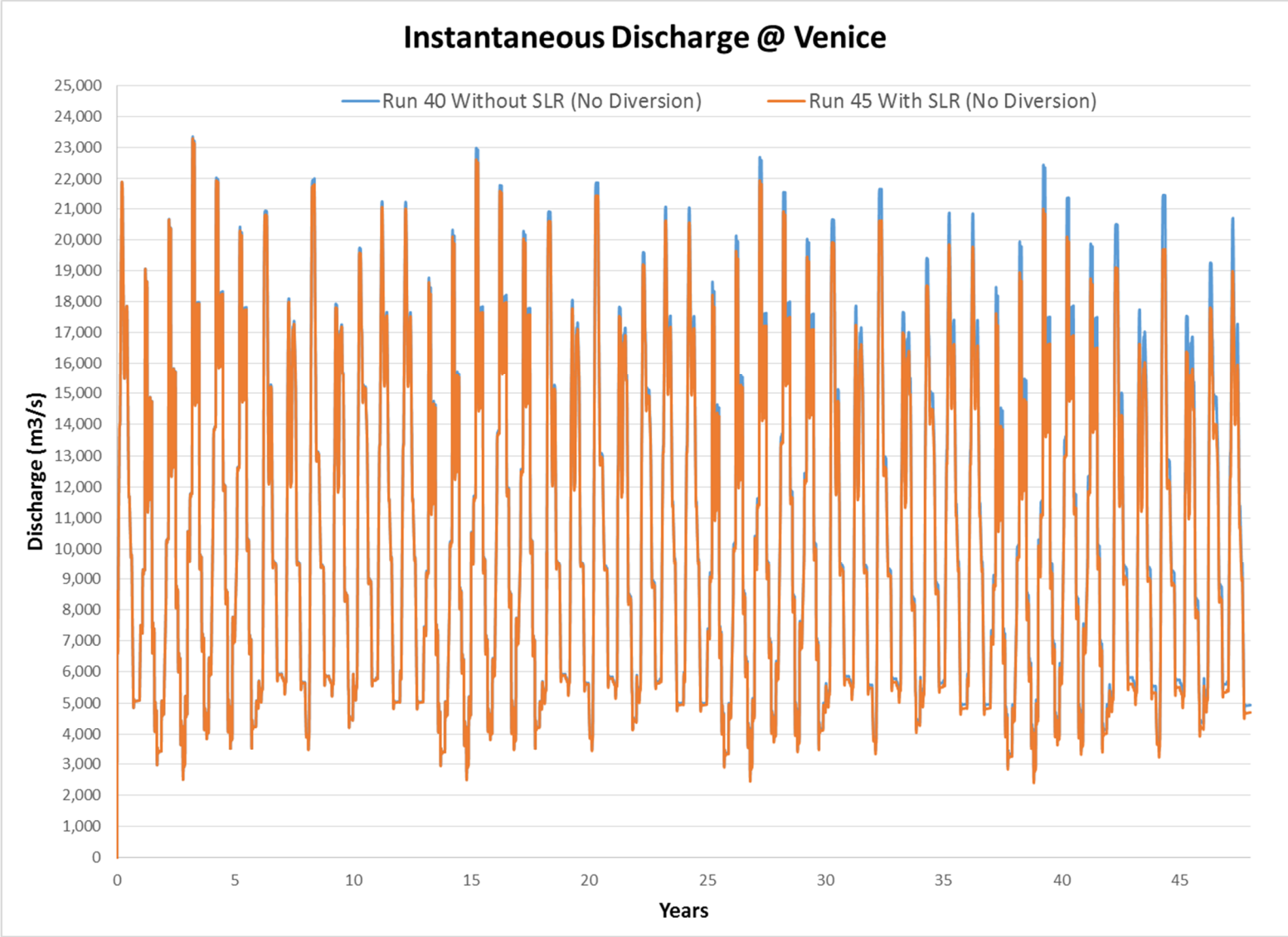

Figure 7.3.3.3.1: Changes in Instantaneous Discharge at Venice due to SLR No Diversion

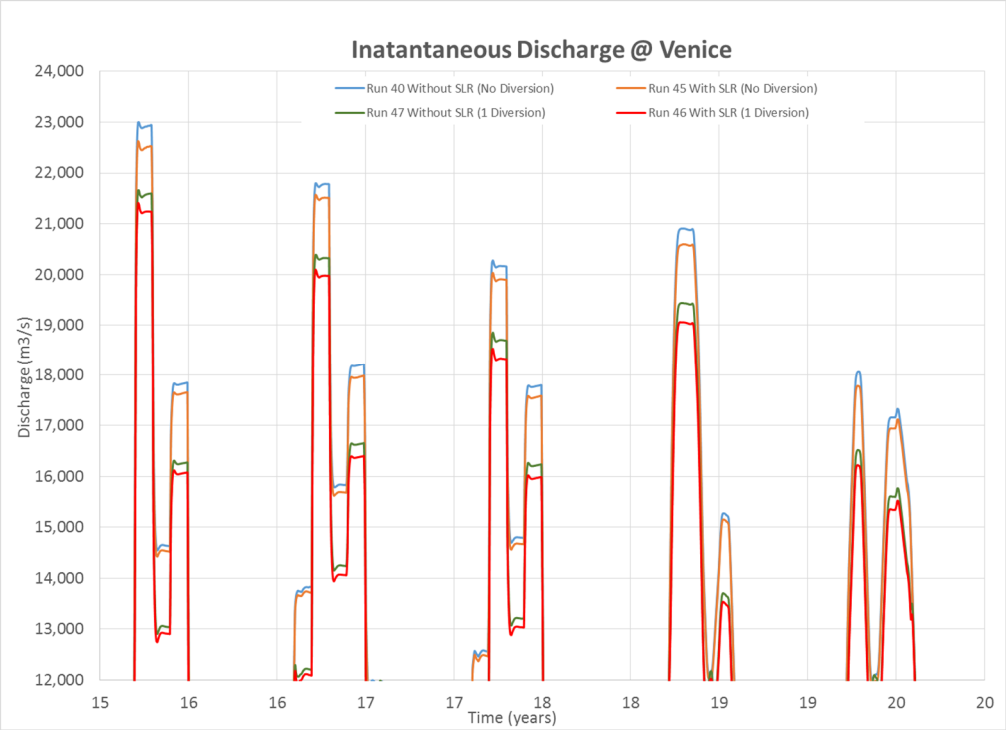

Figure 7.3.3.3.2: Peak Changes in Instantaneous Discharge at Venice due to SLR No Diversion & 1 Diversion (Mid-Barataria 75K), Year 15-20

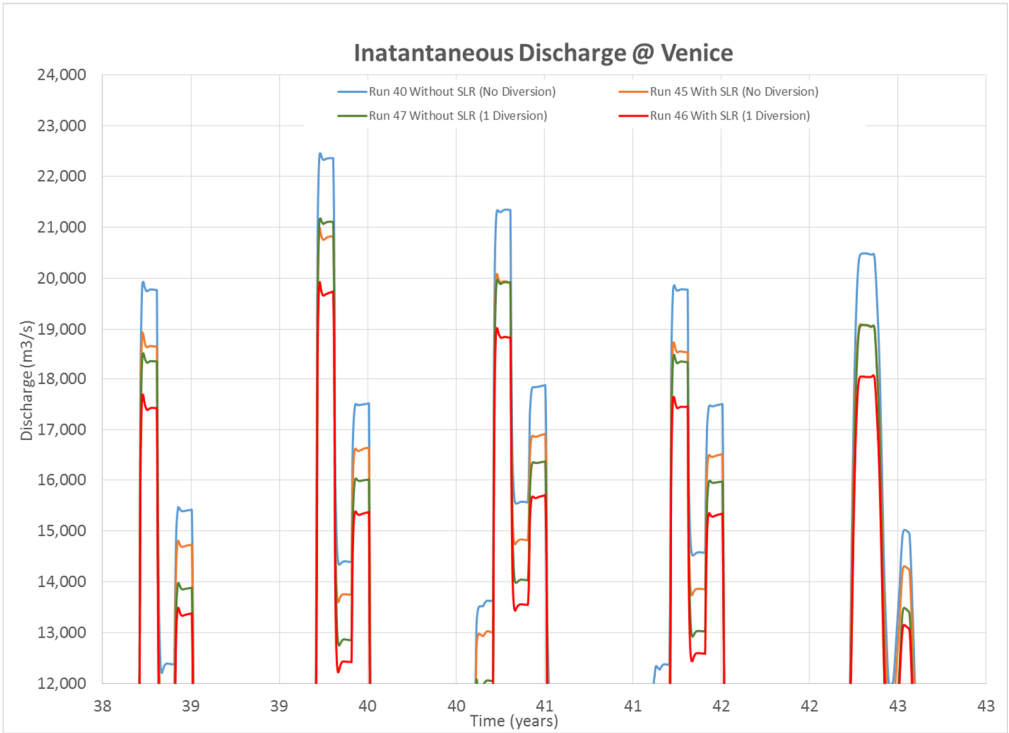

Figure 7.3.3.3.3: Peak Changes in Instantaneous Discharge at Venice due to SLR No Diversion & 1 Diversion (Mid-Barataria 75K), Year 38-43

7.3.3.4 Streampower:

Streampower is sometimes used as an index of the potential sand transport capacity of a river, since the sediment transported is dependent on the available streampower. Streampower is defined in this research as the discharge (Q) times the bed shear stress (τ_o). There is no sand movement below approximately 8,000m^3/s (McCorquodale et al. 2017). A reduction in streampower has a direct correlation to the sand movement and deposition.

The relationship of sand discharge to streampower can be simplified as follows:

[7.1] $$Q_{Sand} \propto Streampower$$

[7.2] $$Q_{Sand} \propto Q\ \tau_o$$

[7.3] $$\tau_o = \Upsilon\ \mathrm{R}\ S_f$$

[7.4] $$S_f \propto \left\{\frac{n^2\ Q^2}{R^{10/3}}\right\}$$

Assuming Υ, R and n are nearly constant the following simplification can be made:

[7.5] $$\tau_o \propto Q^2$$

[7.6] $$Q_{Sand} \propto QQ^2$$

[7.7] $$Q_{Sand} \propto Q^3$$

$Where\ \tau_o = Bed\ Shear$; $Q = Mississippi\ River\ Discharge$;

$Q_{Sand} = Sediment\ (Sand)\ Discharge$; $\Upsilon =$ Specific $Weight\ of\ Fluid;$

$\mathrm{R} = Hydraulic\ Radius;\ and\ S_f =$ F$riction\ Slope.$

To identify the streampower loss in the FSP-HOP reach of the Mississippi River, instantaneous discharge data were extracted at Venice (RM 11.2). Only values exceeding the 8,000m^3/s threshold were plotted. The results show an accelerated loss of stream power (see Figure 7.3.3.4.1 below) with time. The maximum loss of streampower plotted is 24% for high flow events, which contributes to accelerated deposition. The average loss at year 48 is approximately 18%.

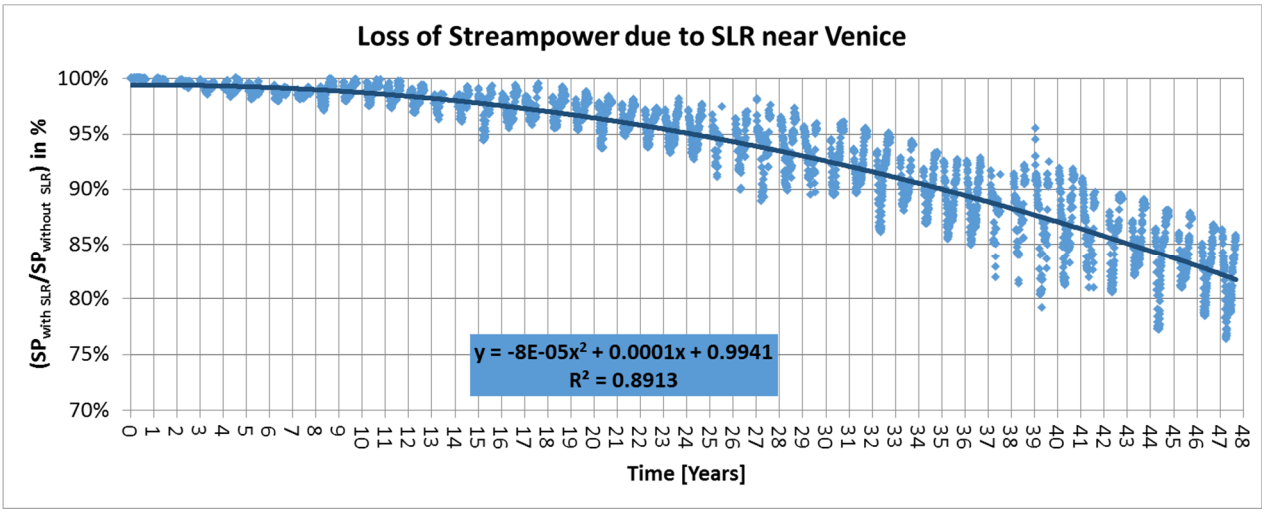

Figure 7.3.3.4.1: Loss of Streampower due to Sea Level Rise near Venice

In 2009, an analysis of West Bay Sediment Diversion Effects was published by Paul Kemp in the form of a Memorandum to the WFF Science Team. The summary of this memorandum also highlights the importance of regional factors that are driving the deposition upstream and increasing flow through the upstream distributaries. The presented findings in relation to deposition changes due to SLR near HOP and streampower loss in the same region support Kemp's statement that observed long-term trends clearly establish the importance of regional adjustment to sea level rise, subsidence and upstream shift of the depocenter. Kemp further states that these regional drivers will favor enlargement and sustained maintenance of upstream distributaries, and new diversions like West Bay, at the expense of downstream ones. This is in agreement with the described findings of this research.

7.3.4 CONCLUSIONS

It was observed that the system with no diversions, 1 diversion and 2 diversions respond to sea level rise (NRCIII Curve) by an increase in deposition. The depositional effects downstream of Fort St. Phillip are accelerated and decrease asymptotically from HOP to approximately RM 40. The addition of the Mid-Barataria diversion resulted in an upstream shift of the depocenter.

The introduction of a diversion results in a decrease in streampower, which in combination with the streampower loss generated by sea level rise, results in overall increase in deposition. Therefore, any analysis of diversion impacts needs to include sea level rise as a component of the analysis to estimate a range of expected deposition and streampower loss.

A true equilibrium was neither achieved for the without sea level rise nor the with sea level rise scenario evaluated by the 48 year model runs.

When comparing results for the no-diversion case for the uniform hydrograph and the variable hydrograph without sea level rise, it can be observed that location of maximum deposition of 0.75m occurs further upstream for the uniform hydrograph run, just downstream of Fort St. Philip. Upstream of the maximum deposition location, the deposition for the uniform hydrograph is higher than for the variable hydrograph all the way to Belle Chasse; this results in less erosion between Belle Chasse and Lower Breton and more deposition between Lower Breton and the downstream end of Fort St. Philip. Between the downstream end of Fort St. Philip and HOP the uniform case yields a slightly smaller deposition than the variable case. However, overall the uniform case results in higher depositional predictions for the system as a whole.

Similarly, with sea level rise, the uniform case yields higher deposition than the variable case for almost the entire domain. This proportional increase remains similar when introducing diversions, while the deposition overall increases with the addition of diversions, as previously concluded.

7.4 RESEARCH QUESTION 4

Research Question 4:

How does change in sediment load at upstream boundary (Belle Chase) impact morphologic changes?

7.4.1 METHODOLOGY

Four model runs were completed using the variable hydrograph with a 12 year duration, which represents 1 cycle of the established variable hydrograph. Two base runs were made: one no-diversion case (Run 3) and one two-diversion case (Run 8). The diversions introduced were the currently proposed Mid-Breton Diversion at 35,000 cfs and Mid-Barataria at 75,000 cfs.

The next two runs represent the same conditions as the base cases, which include a no-diversion run (Run 36) and a two-diversion run (Run 37), but include an increase in sand input at the upstream boundary (Belle Chasse). The increase in sediment was established by taking the input concentration for very fine, fine and medium Sand (VF, F & M) in the input-file (bcc-file) and increasing them by 50%. This increase was selected because it is representative of the uncertainty in the upstream sand concentration. Table 7.4.1.1 summarizes the model runs, which were set-up in support of this research question.

Table 7.4.1.1: Model Runs for Research Question 4:

#	Hydrograph		Years	Diversions	Diversion Info	Other
	U	V				
3		X	1-12	None		
8		X	1-12	2	Mid-Breton = 35,000 cfs & Mid-Barataria = 75,000cfs	
36		X	1-12	None		50% Increase in Sediment (VF, F, M)
37		X	1-12	2	Mid-Breton = 35,000 cfs & Mid-Barataria = 75,000cfs	50% Increase in Sediment (VF, F, M)

7.4.2 RESULTS

The cumulative erosion/sedimentation as function of time and space can be obtained from the map file (trim-file). To quantify the changes in deposition between the base case and the increased sand input case, the cumulative erosion/sedimentation of each run was extracted at the final computational step, which represents the end of year 12.

The extracted values for cumulative erosion/sedimentation from the no-diversion Base Case (Run 3) were subtracted from the extracted values for cumulative erosion/sedimentation from the no-diversion modified case (Run 36). The modified case was subject to the established 50% increase of sand at the Upstream Boundary (Belle-Chasse).

{Run 36 No Diversion Base Case +50% Increase} – {Run 3 No Diversion Base Case]

The calculated difference in cumulative deposition between the increased sediment case (Run 36) and the base case (Run3) was plotted for the no-diversion scenario to identify the overall magnitude and location of the depositional impacts as shown in Figures 7.4.2.1a to 7.4.2.9a.

In addition, cross-sections at key sand bars and crossings, which coincide with the anticipated depositional zones, were developed by extracting bed level in water level points from the map file (trim-file). These cross sections depict the bathymetry at the

beginning of the computational runs as well as the end of the 12-year computational period. The end bathymetry for the base case (Run 3) and the bathymetry for the increased sediment case (Run 36) are included. Figures 7.4.2.1 (b/c/d) to 7.4.2.9 (b/c/d) depict corresponding cross sections selected for the respective map images Figures 7.4.2.1a to 7.4.2.9a.

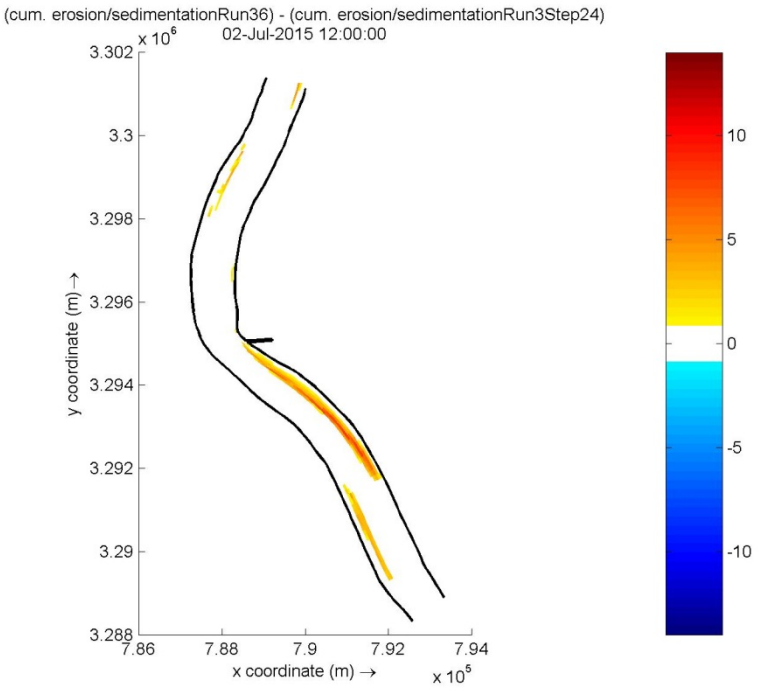

Figure 7.4.2.1a: Difference (Run 36 - Run3) in Cumulative Deposition due to Sediment Increase (Mid-Breton Area - RM 72.4 to RM 63.3) at t= 12 years

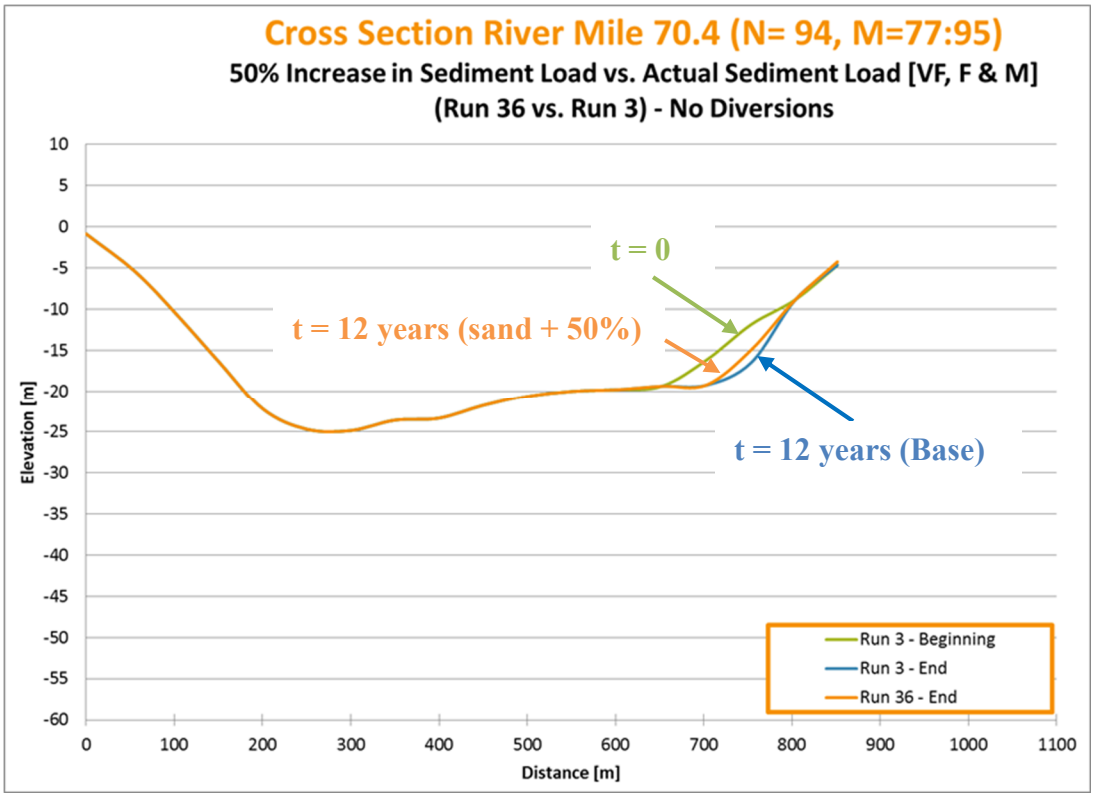

Figure 7.4.2.1b: Cross Section River Mile 70.4 (U/S Mid-Breton)

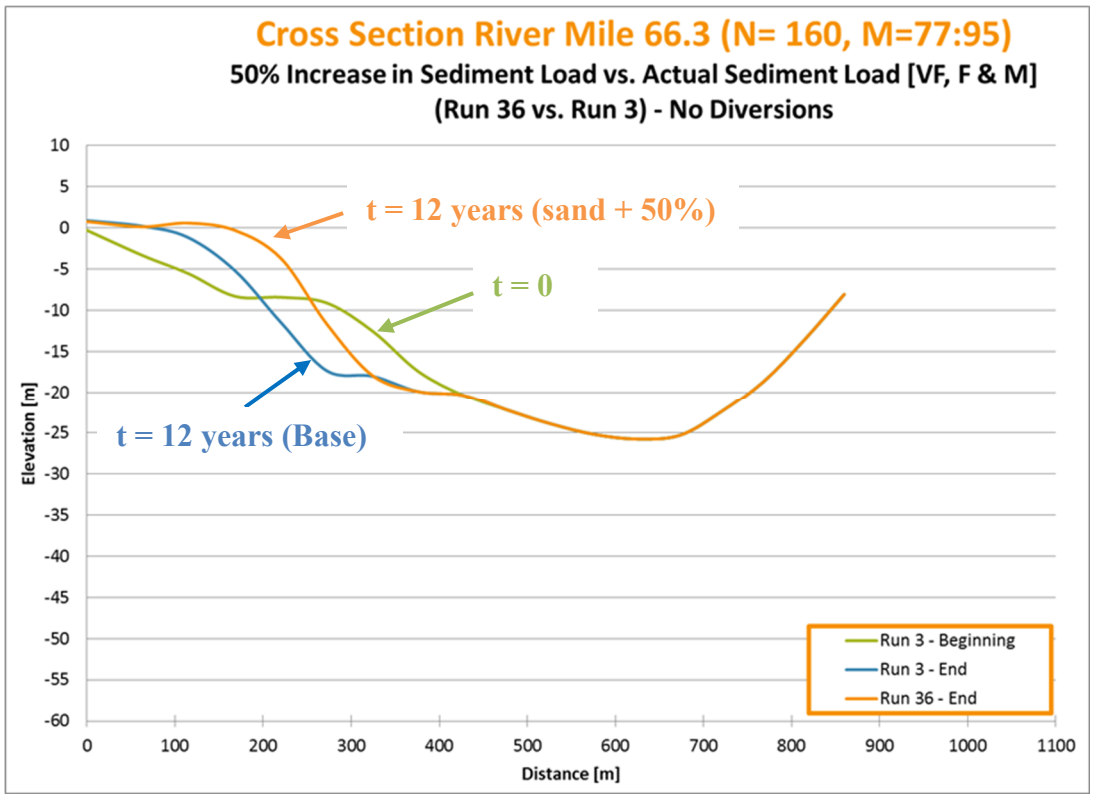

Figure 7.4.2.1c: Cross Section River Mile 66.3 (D/S Mid-Breton)

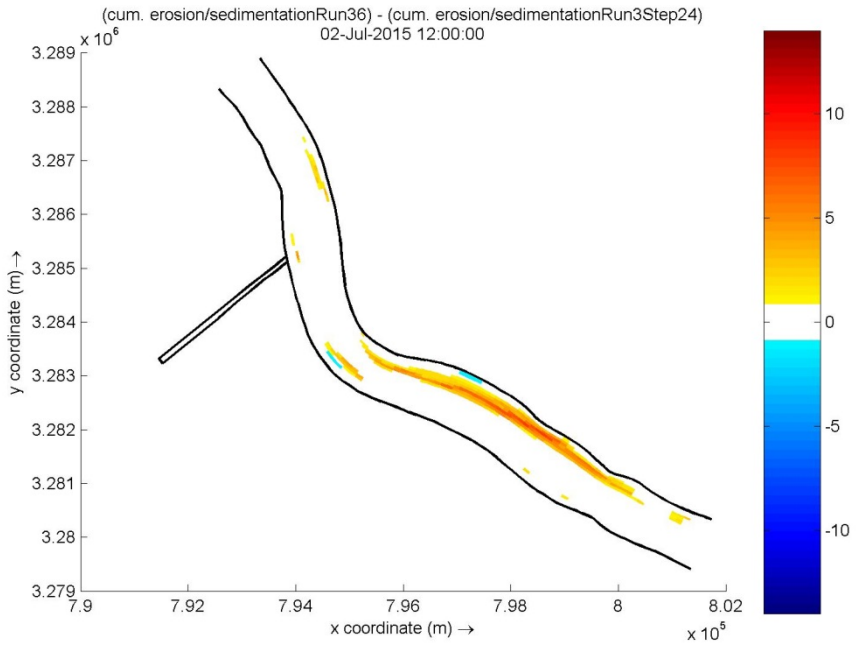

Figure 7.4.2.2a: Difference (Run 36 - Run3) in Cumulative Deposition due to Sediment Increase (Mid-Barataria Area - RM 63.3 to RM 55.1) at t= 12 years

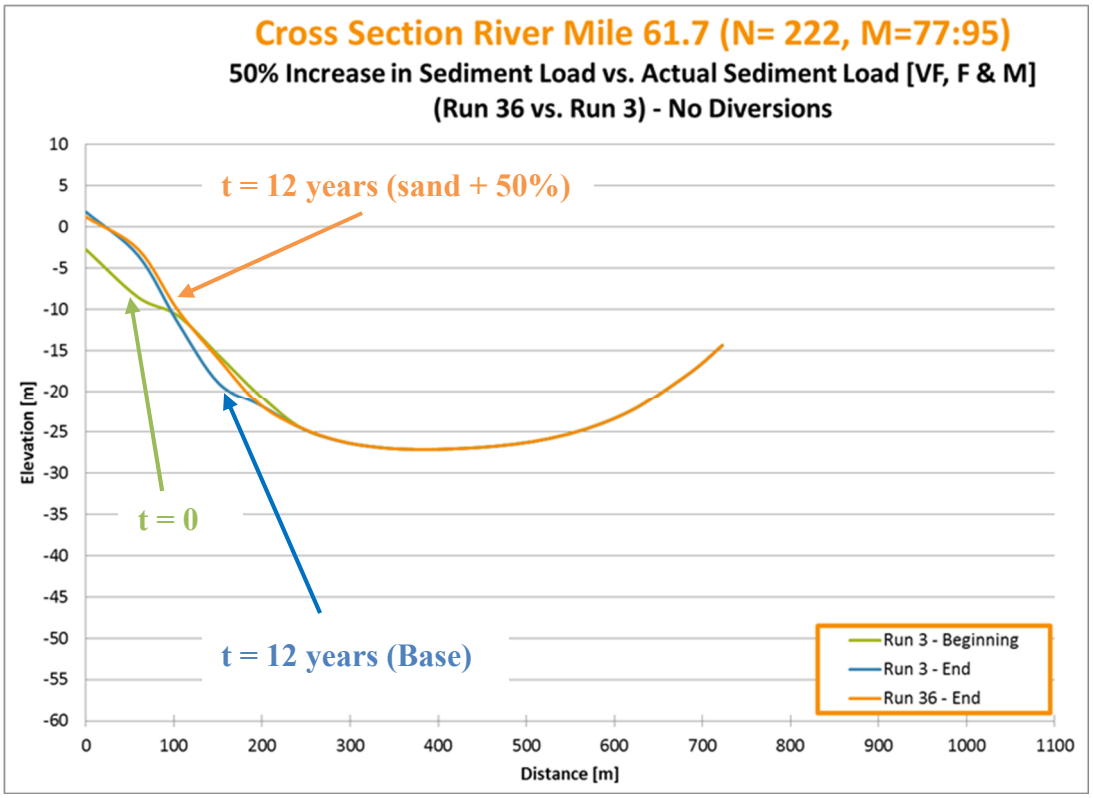

Figure 7.4.2.2b: Cross Section River Mile 61.7 (U/S Mid-Barataria)

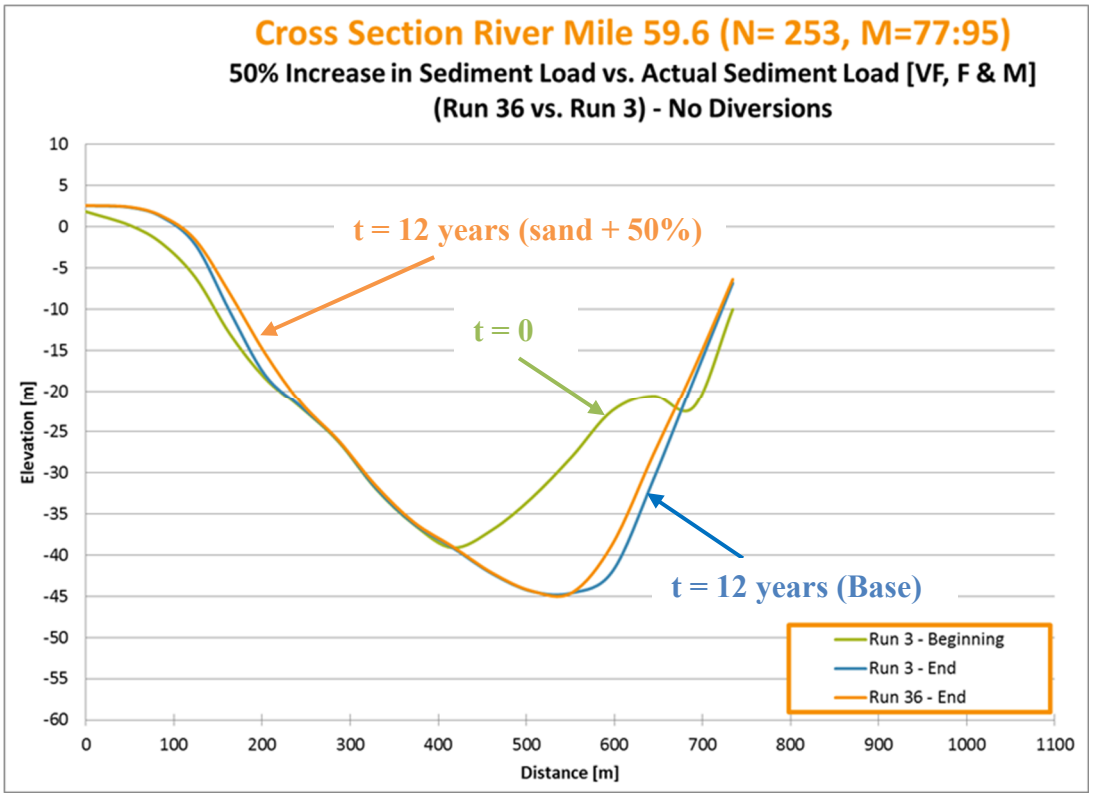

Figure 7.4.2.2c: Cross Section River Mile 59.6 (D/S Mid-Barataria)

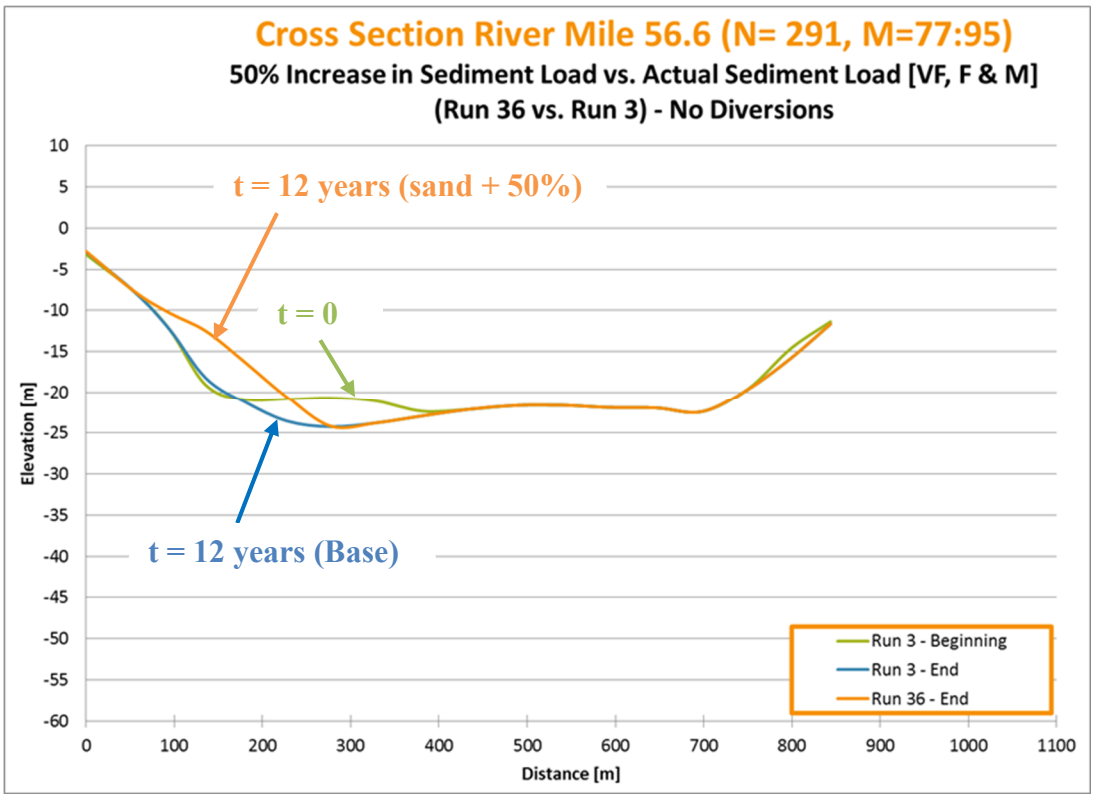

Figure 7.4.2.2d: Cross Section River Mile 56.6 (Crossing D/S Mid-Barataria)

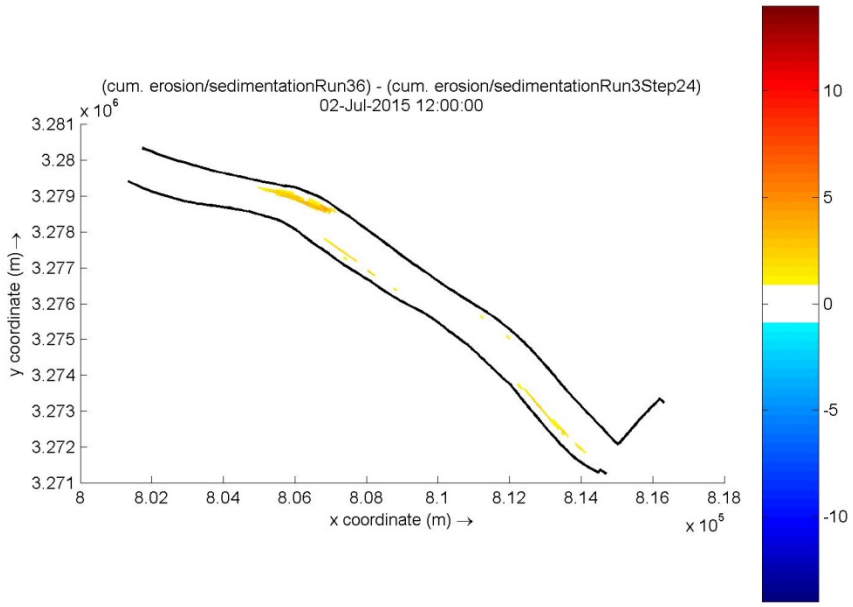

Figure 7.4.2.3a: Difference (Run 36 - Run3) in Cumulative Deposition due to Sediment Increase (WPAH to U/S Bohemia Area - RM 55.1 to RM 45.2) at t= 12 years

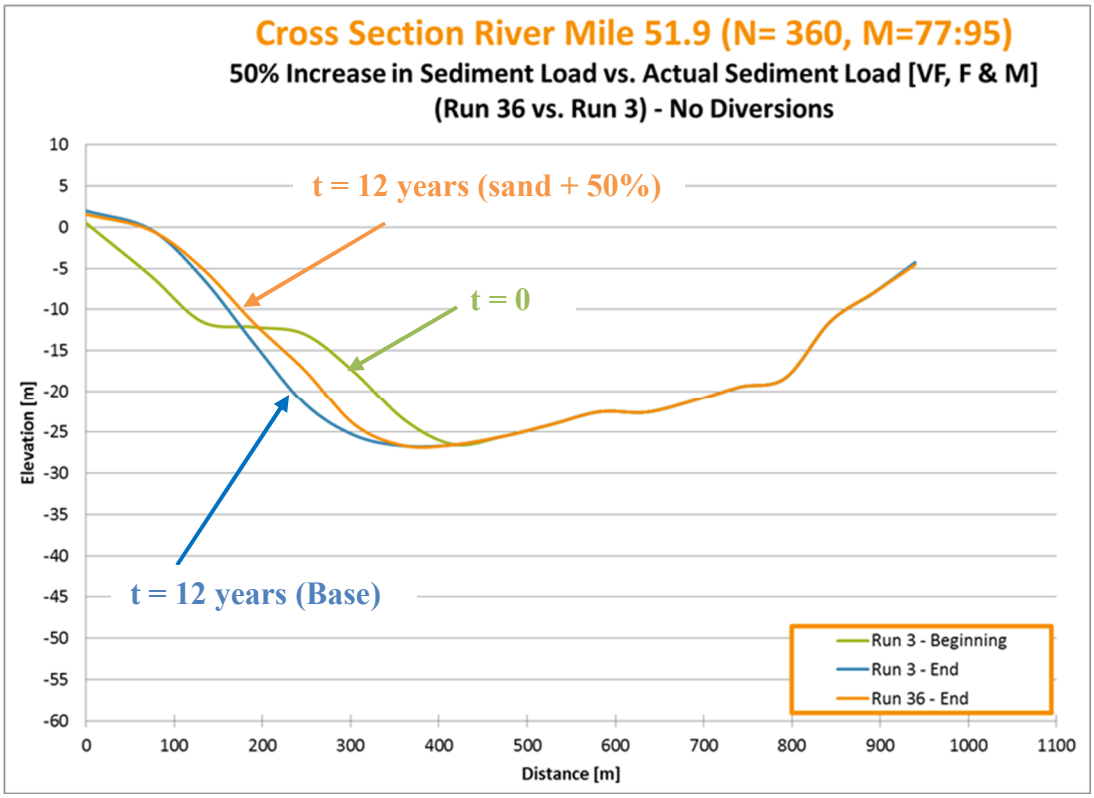

Figure 7.4.2.3b: Cross Section River Mile 51.9 (U/S Bohemia)

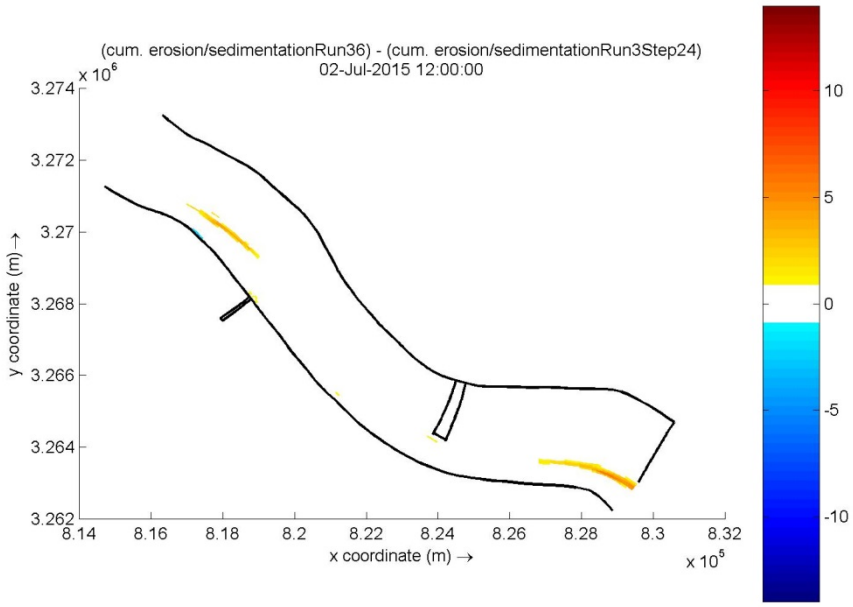

Figure 7.4.2.4a: Difference (Run 36 - Run3) in Cumulative Deposition due to Sediment Increase (Lower Barataria & Lower Breton Area – RM 45.2 to RM 34.2) at t= 12 years

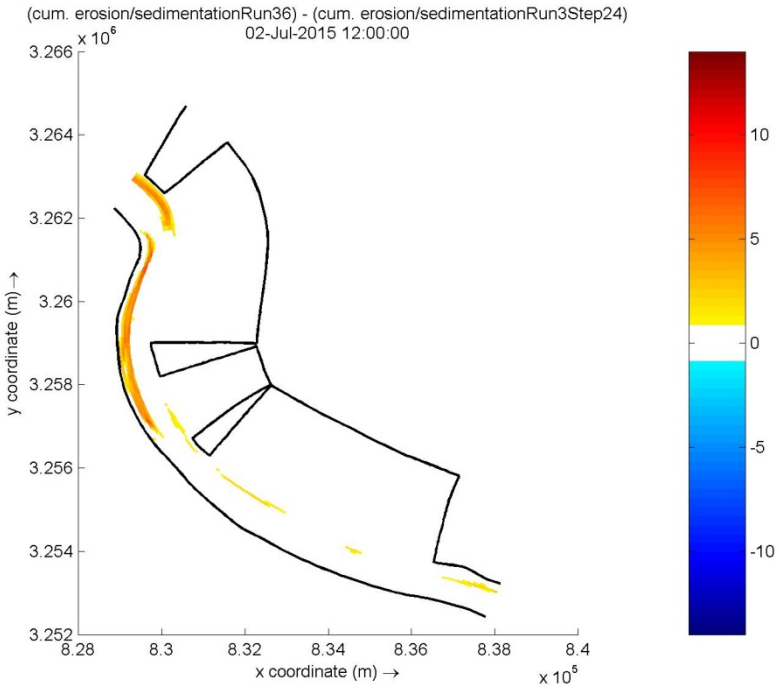

Figure 7.4.2.5a: Difference (Run 36 - Run3) in Cumulative Deposition due to Sediment Increase (Bayou Lamoque Area – RM 34.2 to RM 24.8) at t= 12 years

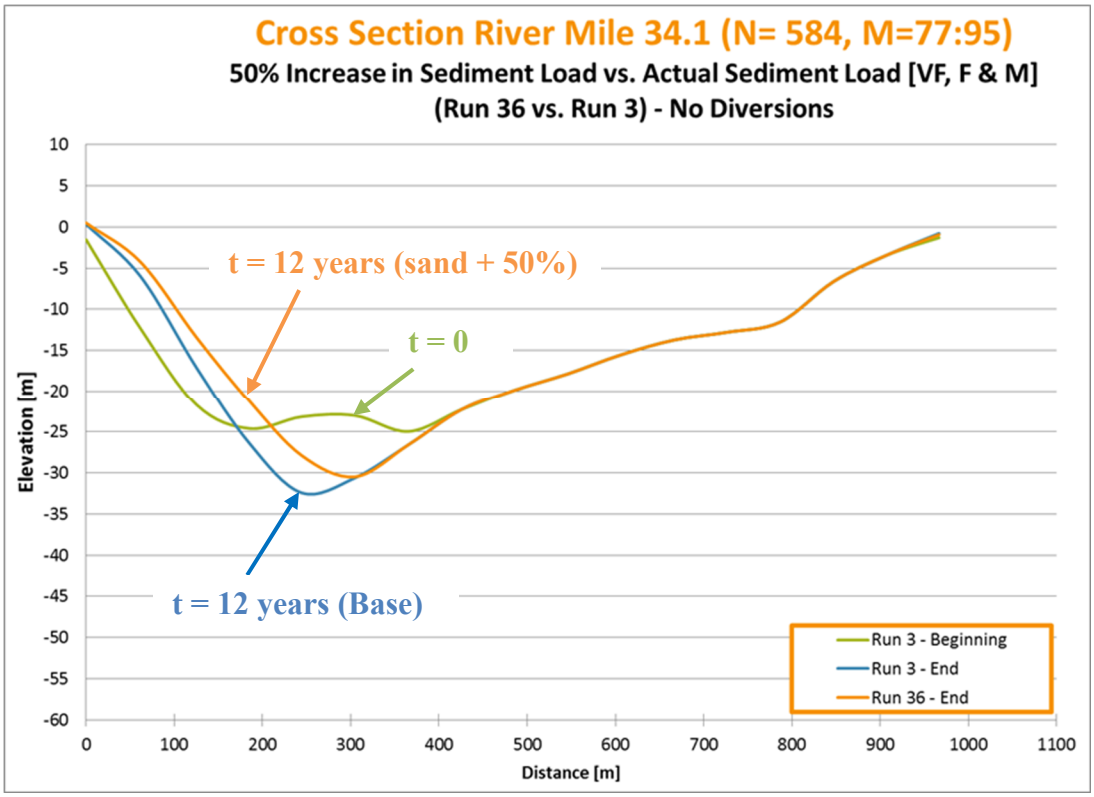

Figure 7.4.2.5b: Cross Section River Mile 34.1 (Bend U/S Bayou Lamoque)

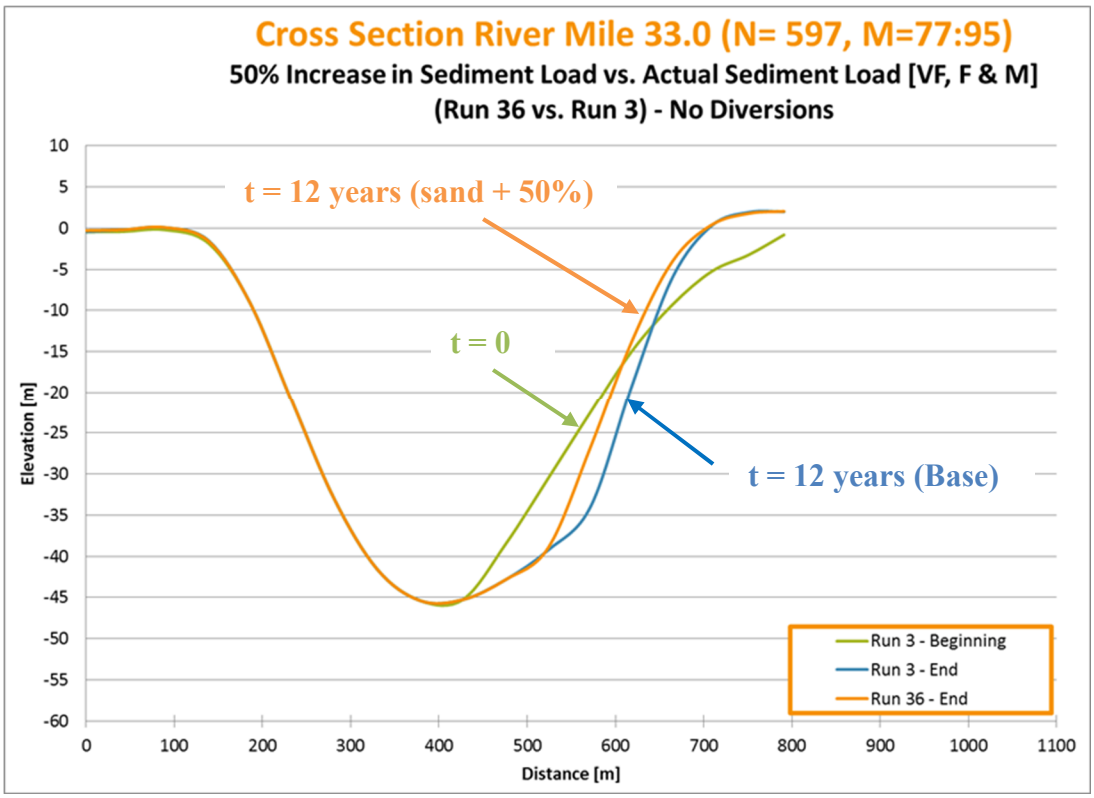

Figure 7.4.2.5c: Cross Section River Mile 33.0 (Bend at Bayou Lamoque)

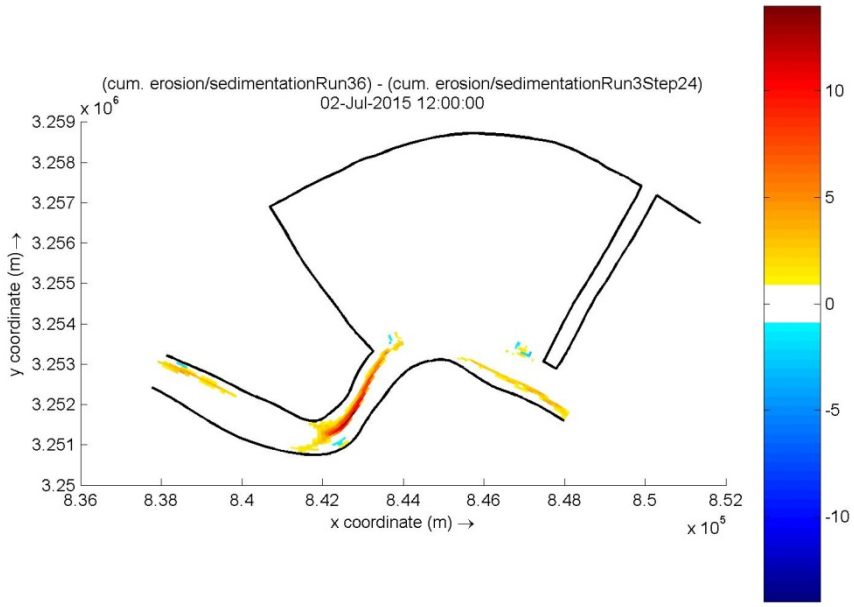

Figure 7.4.2.6a: Difference (Run 36 - Run3) in Cumulative Deposition due to Sediment Increase (Fort St. Philip Area – RM 24.8 to RM 17.3) at t= 12 years

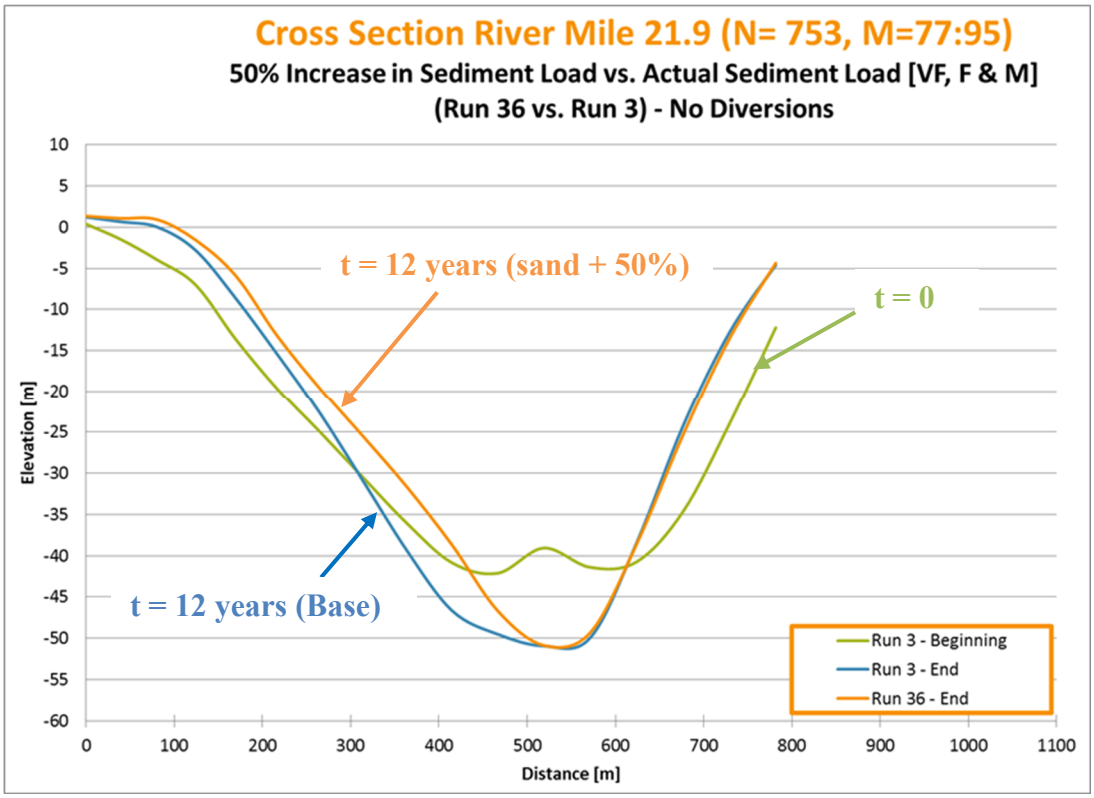

Figure 7.4.2.6b: Cross Section River Mile 21.9 (U/S Fort St. Philip)

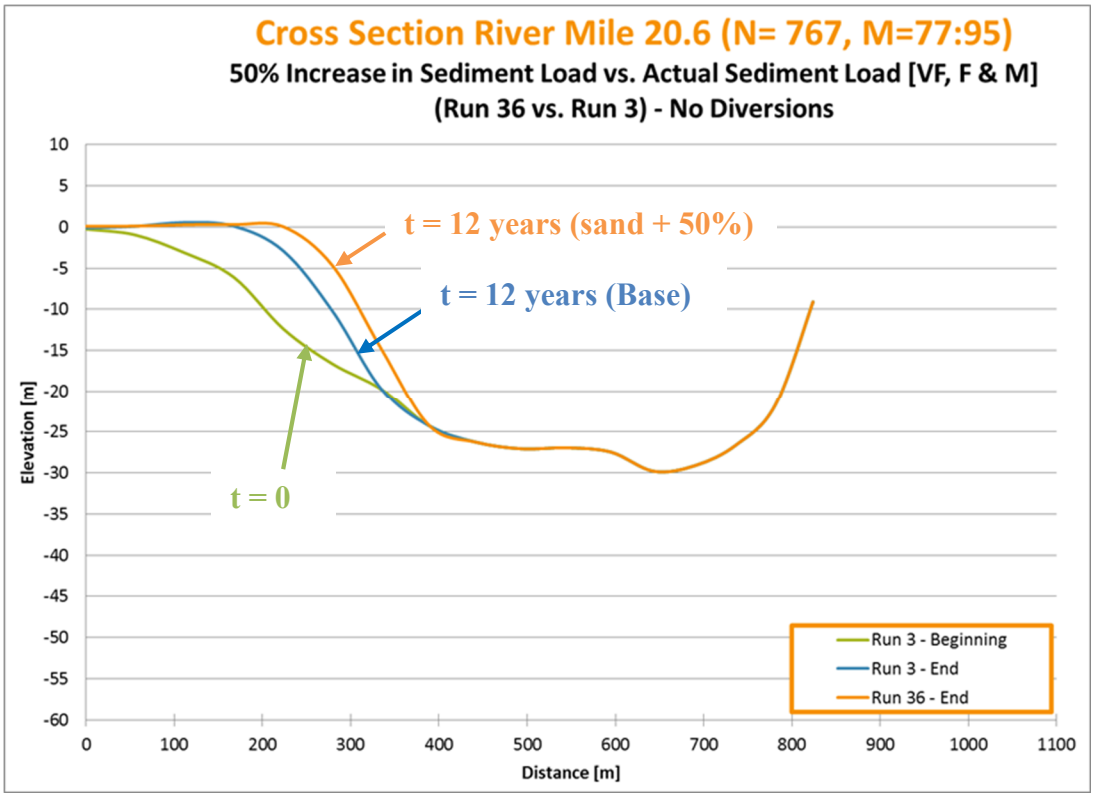

Figure 7.4.2.6c: Cross Section River Mile 20.6 (at Fort St. Philip)

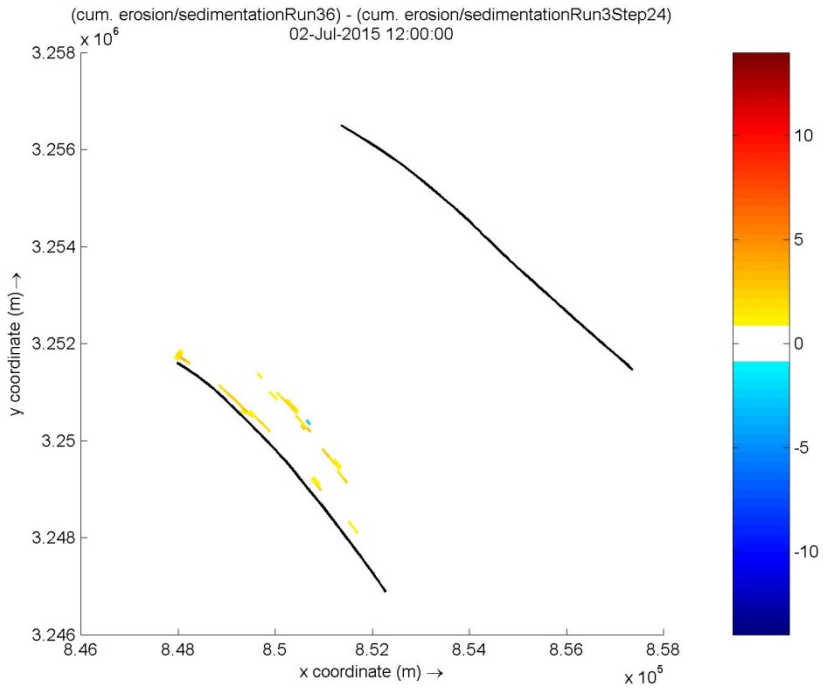

Figure 7.4.2.7a: Difference (Run 36 - Run3) in Cumulative Deposition due to Sediment Increase (D/S Fort St. Philip Area – RM 17.3 to RM 13.2)

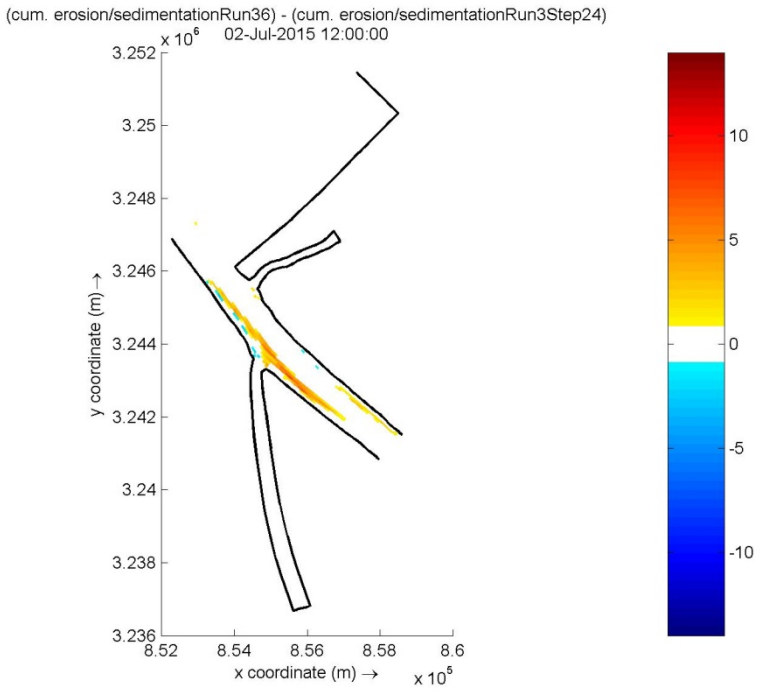

Figure 7.4.2.8a: Difference (Run 36 - Run3) in Cumulative Deposition due to Sediment Increase (Venice Area – RM 13.2 to RM 8.0) at t= 12 years

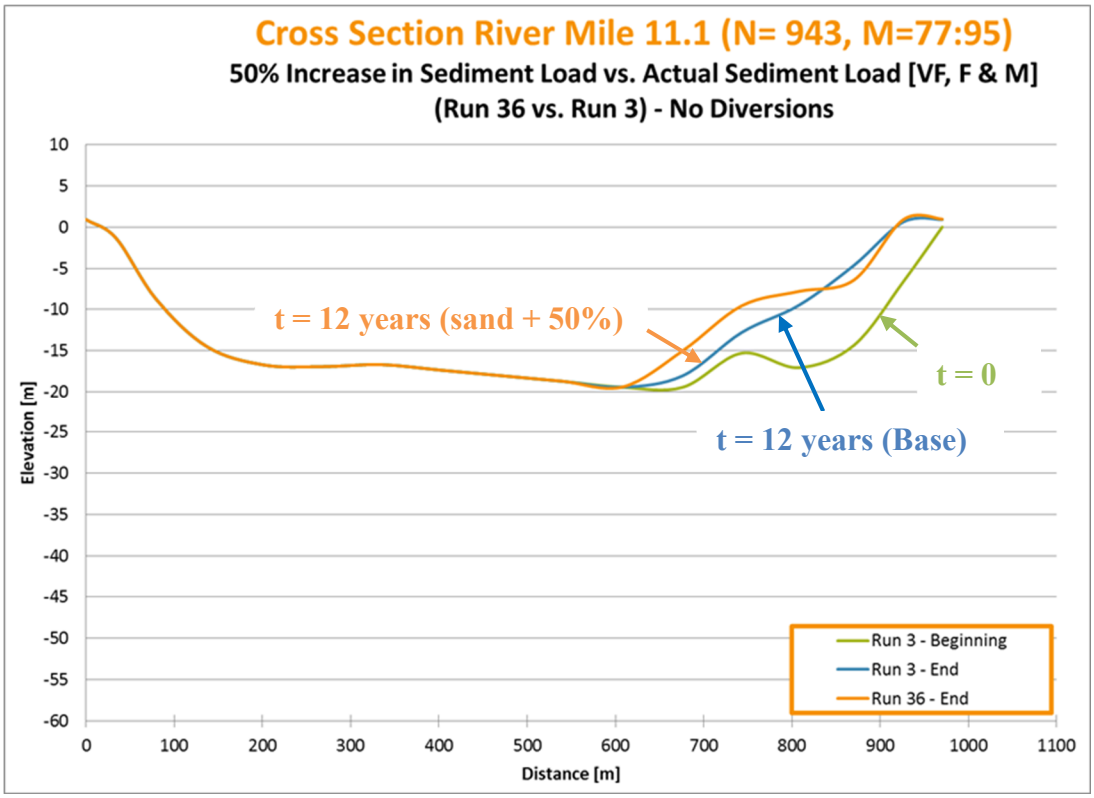

Figure 7.4.2.8b: Cross Section River Mile 11.1 (U/S Tiger & Grand Pass)

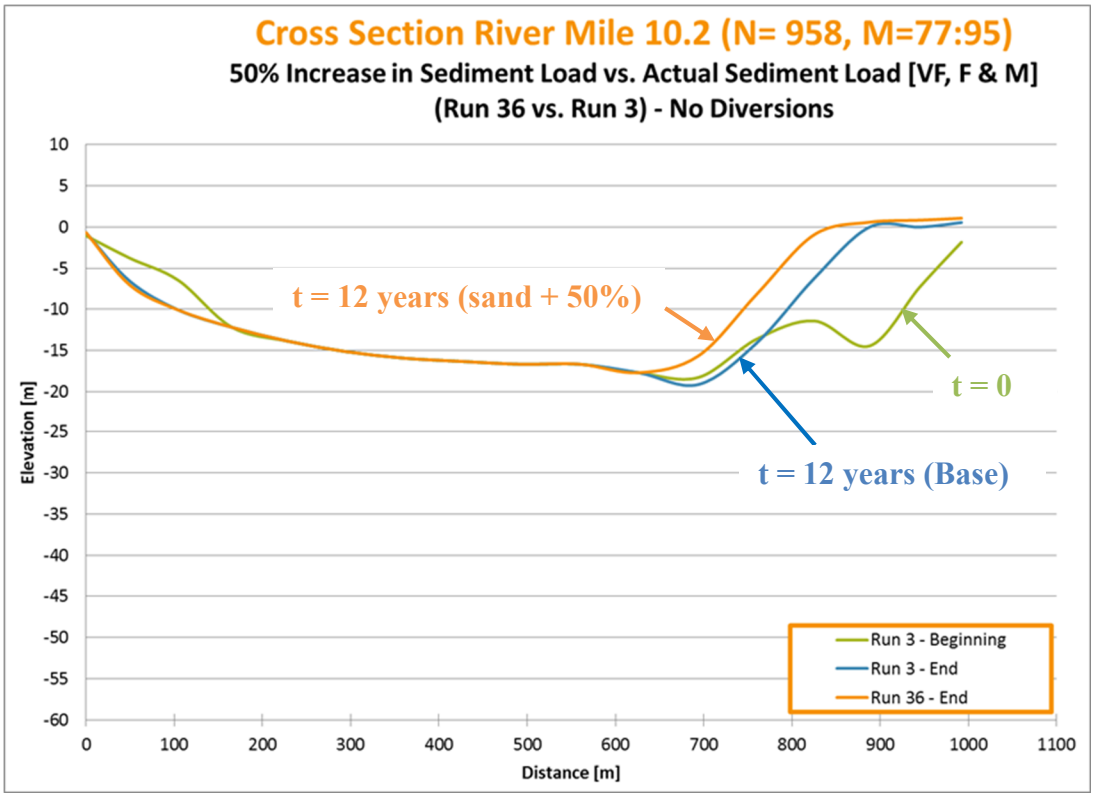

Figure 7.4.2.8c: Cross Section River Mile 10.2 (U/S Tiger & Grand Pass)

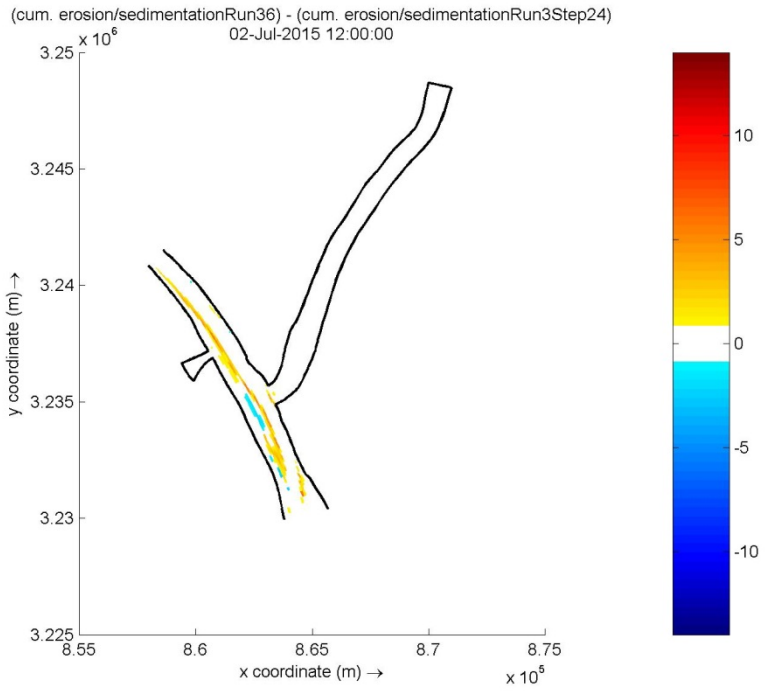

Figure 7.4.2.9a: Difference (Run 36 - Run3) in Cumulative Deposition due to Sediment Increase (HOP Area – RM 8.0 to RM 0.0) at t= 12 years

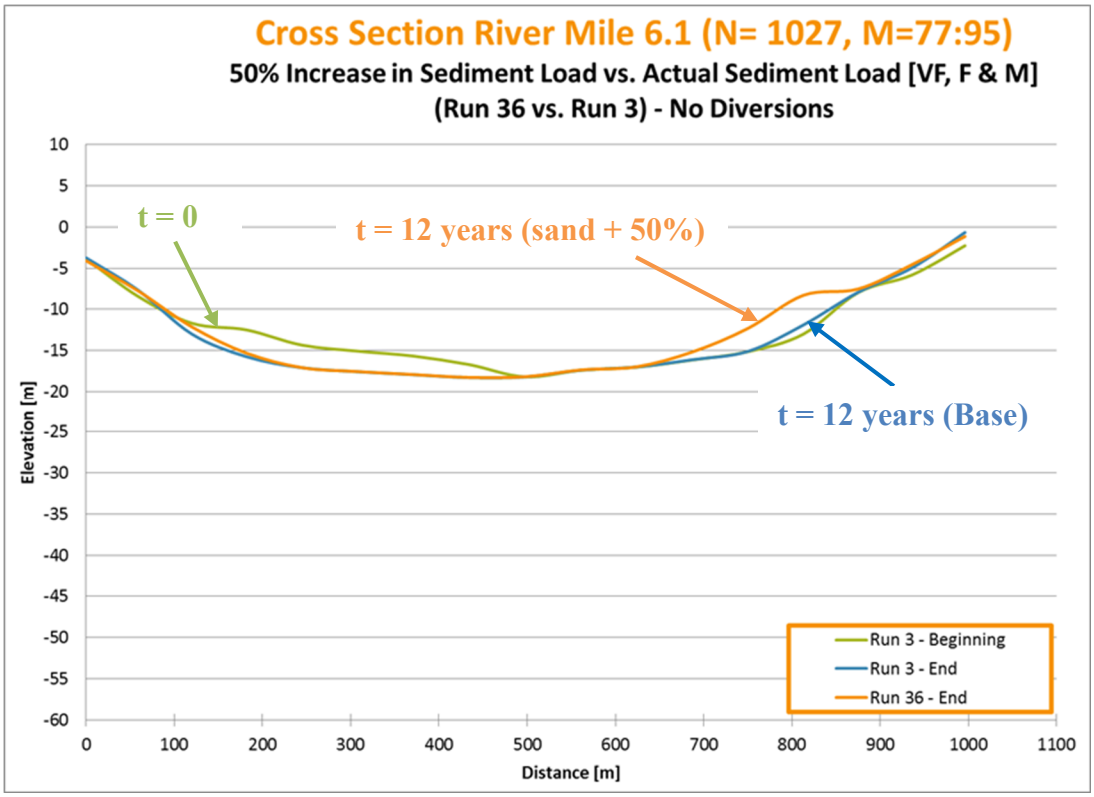

Figure 7.4.2.9b: Cross Section River Mile 6.1 (U/S West Bay)

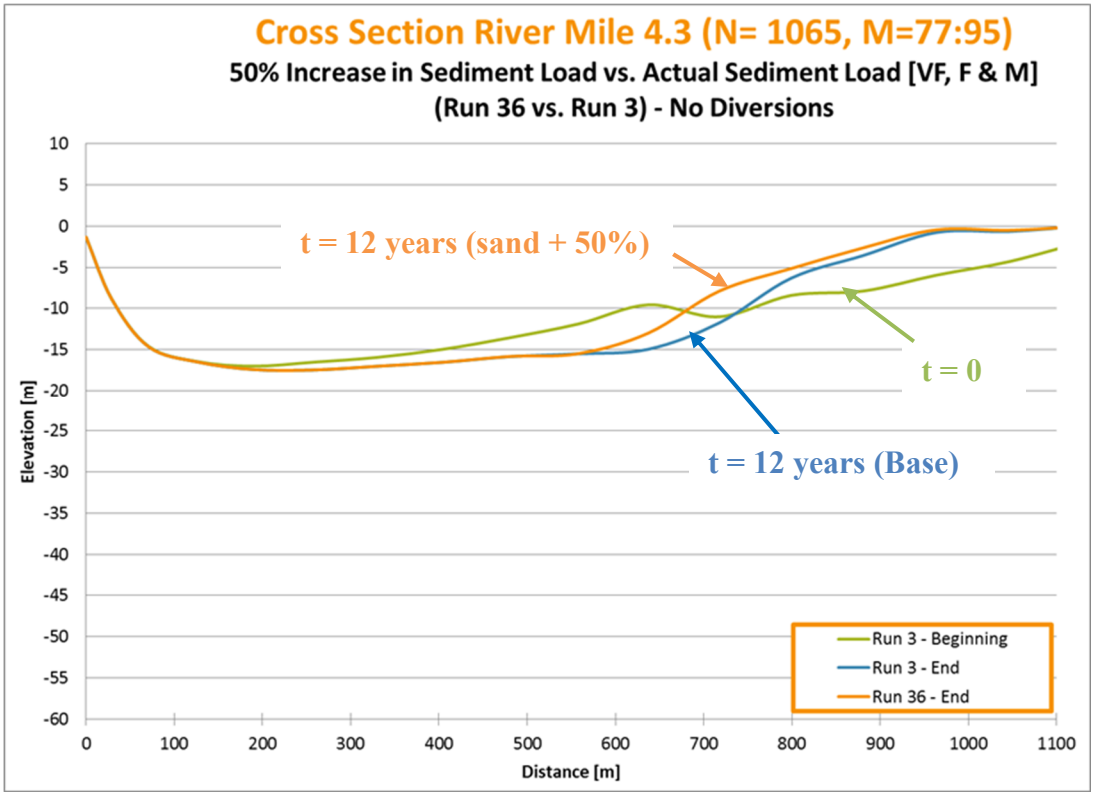

Figure 7.4.2.9c: Cross Section River Mile 4.3 (West Bay – U/S Cubits Gap)

To obtain the deposition within the river channel, the laterally averaged cumulative erosion/sedimentation was extracted. Based on the established grid, the longitudinal cells most representative of the Mississippi River channel are in the range M 77:95 laterally along the Mississippi River between Belle Chasse (Upstream Boundary) and Head of Passes (Downstream Boundary).

The laterally averaged cumulative erosion/sedimentation values at year 12 were extracted from the map (trim-file) for all four runs listed in Table 7.4.1.1 and plotted against the river miles to depict the depositional trends (see Figure 7.4.2.10). The red lines indicate the two no-diversion cases (Run 3 & 36) while the blue lines indicate both two-diversion cases (Run 8 & 37).

The plotted deposition in meters has a maximum deposition of 10 m near River Mile 20 and maximum erosion of -2 m upstream of River Mile 50.

Figure 7.4.2.10 depicts greater values for deposition with the increase of sand load introduced at Belle Chasse for the no diversion and the two diversion cases. The peak depositional areas show the greatest magnitudes in deposition change.

In addition, the introduction of the Mid-Breton (RM 68.6) and Mid-Barataria (RM 60.7) Diversions, result in an increased deposition downstream, especially near Venice and HOP, while more erosion appears to occur upstream of the diversions compared to the cases with no diversions.

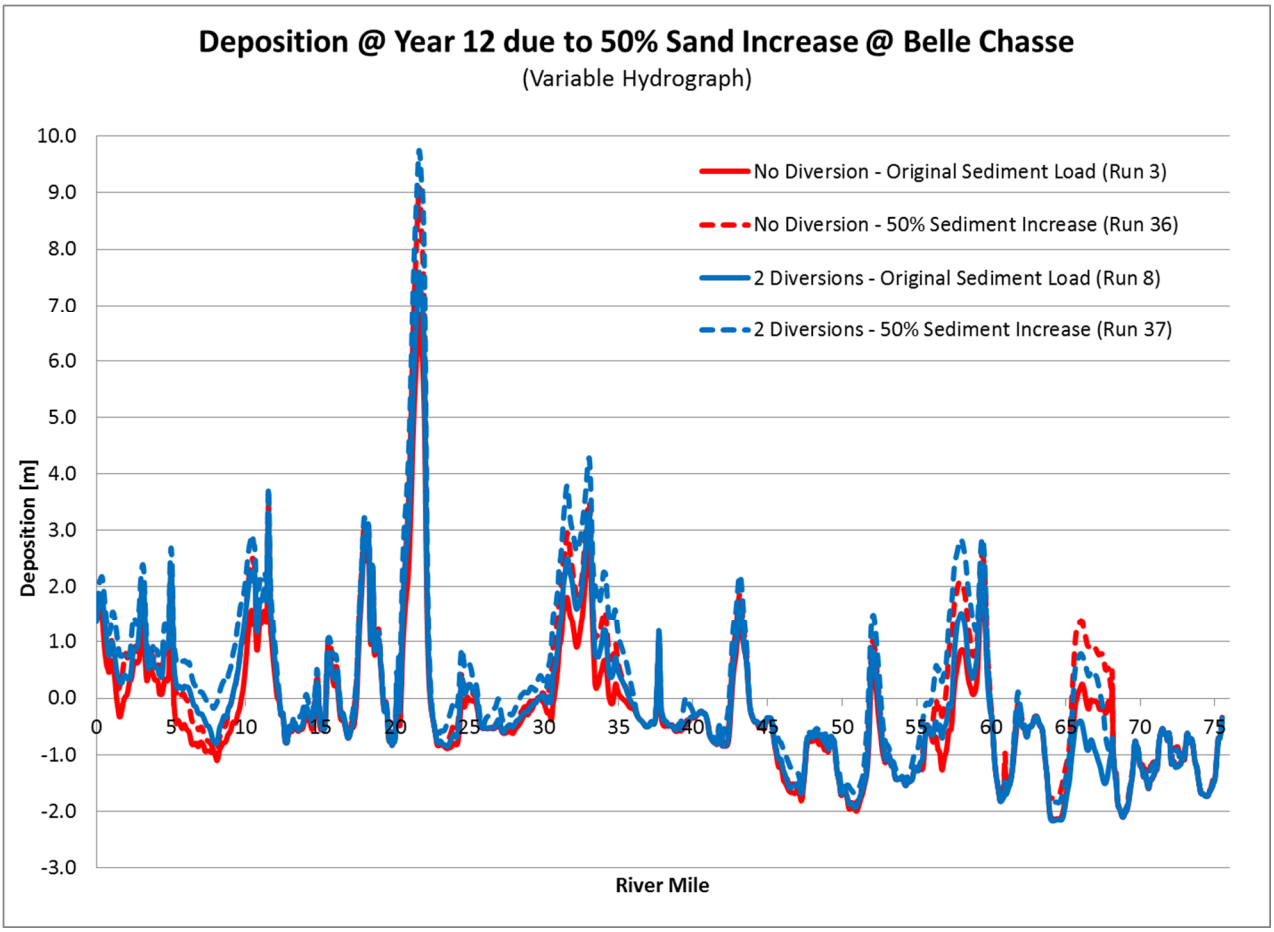

Figure 7.4.2.10: Deposition at Year 12 due to 50% Sand Increase at Belle Chasse

To identify the sand transport changes in a diversion due to an increase in sand load in the river, the instantaneous suspended and bed load for sand (VF, F & M) was extracted in the river, upstream of the proposed Mid-Barataria Diversion, as well as within the diversion. The data obtained from the map file (trim-file) are depicted in Figures 7.4.2.11 and 7.4.2.12 below. The blue lines in both figures depict the Base Case (Run 8) within the river (Figure 7.4.2.11) and the diversion (Figure 7.4.2.12) while the red line represents the modified case (Run 37), with the increased sand load introduced at the upstream boundary (Belle Chasse).

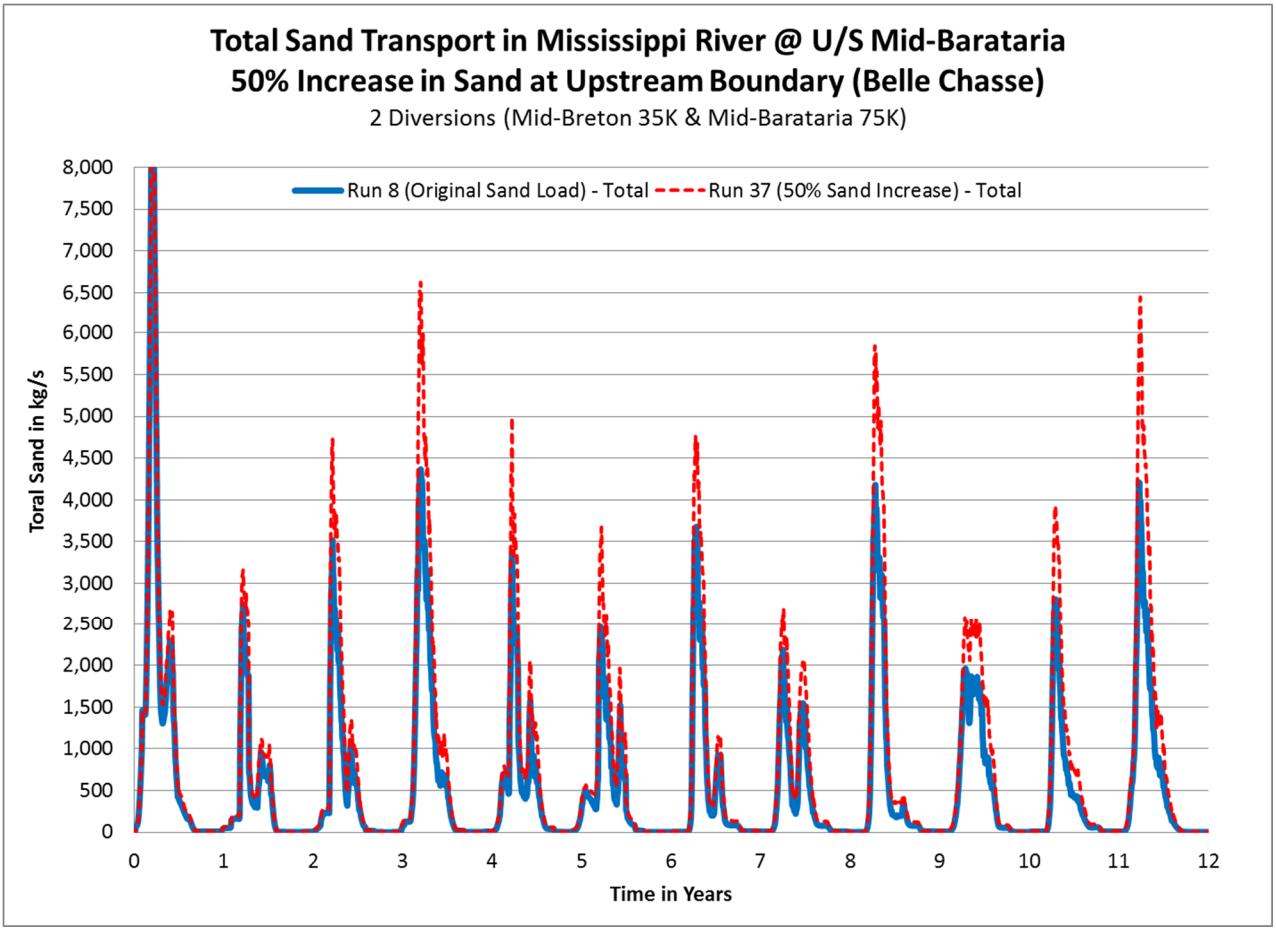

Figure 7.4.2.11: Total Sand Transport in Mississippi River at U/S Mid-Barataria due to 50% Sand Increase at Belle Chasse (Run 8 & Run 37)

The case with the increase in sand at the upstream boundary results in an increase of sand load in the river, particularly at the peaks. Maximum sand load in the river for the base case (Run3) is approaching 4,500 kg/s while the maximum sand load for the modified case (Run 37) is approximately 6,500 kg/s, when neglecting the transient effect of the first year, which is less than the 50% increase in sand load at the upstream boundary (Belle Chasse).

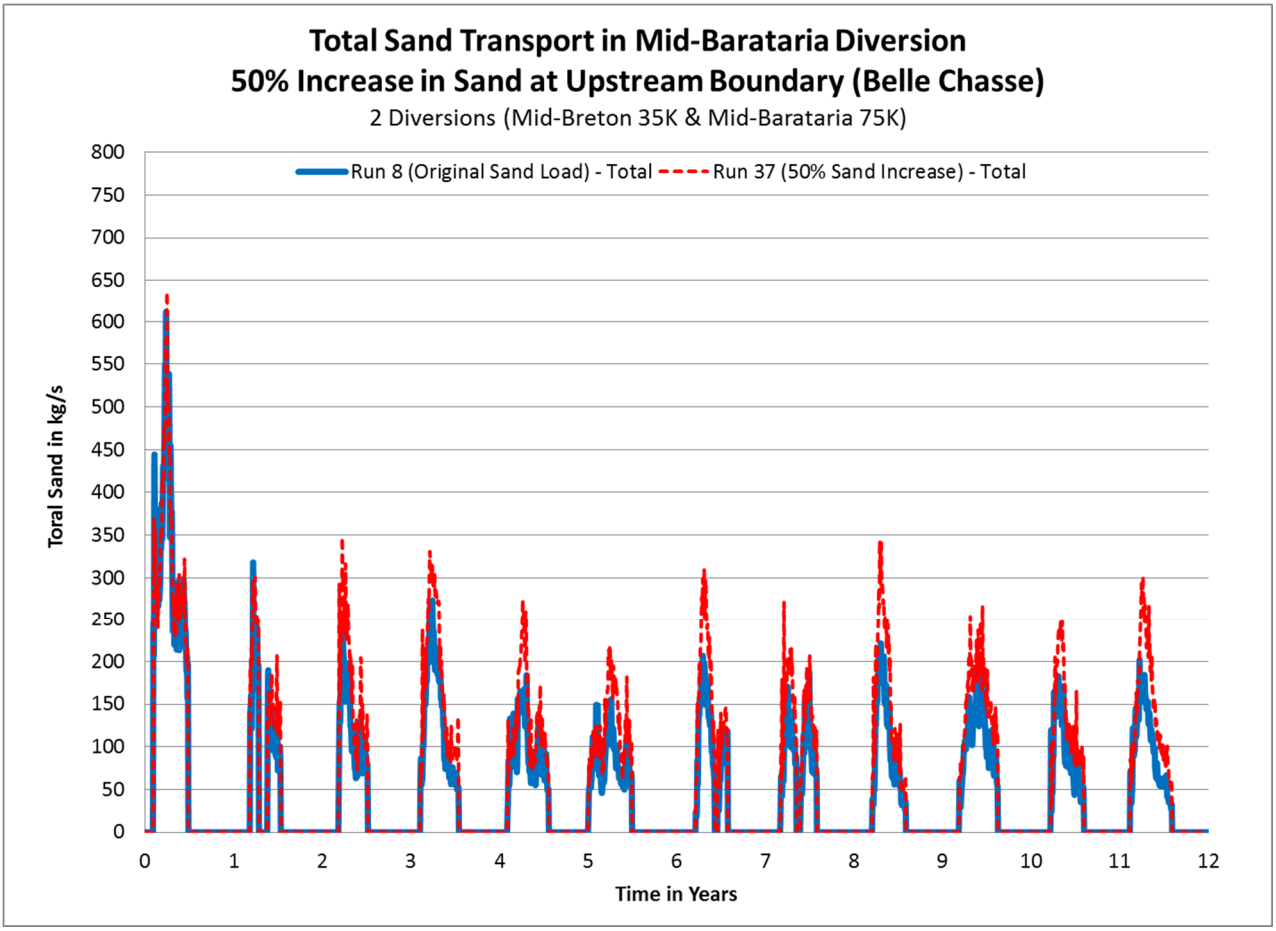

Figure 7.4.2.12: Total Sand Transport in Mid-Barataria Diversion due to 50% Sand Increase at Belle Chasse (Run 8 & Run 37)

The case with the increase in sand at the upstream boundary results in a proportionally smaller increase of sand load in the diversion, while the peaks remain the main area of increase. Maximum sand load in the diversion for the base case (Run 8) is approximately 300 kg/s while the maximum sand load for the modified case (Run 37) is approximately 350 kg/s, when neglecting the transient effect of the first year.

The actual values extracted from the map file (trim-file) for the bed load and the suspended sand load within the river, upstream of Mid-Barataria, and inside the Mid-Barataria diversion are summarized in Table 7.4.2.1 for the no-diversion base case (Run 8) and the no-diversion modified case (Run 37), representing the 50% sand increase at Belle Chasse.

Table 7.4.2.1: Average Annual Load Analysis at Mid-Barataria Diversion

Location	Description	Average Annual Load Run 8 [kg/s]	Average Annual Load Run 37 [kg/s]	**Run 8** (Base)	**Run 37** (50% Sediment Increase)	**Change** between Run 8 and Run 37
River	Bed Load	4.3	7.3	0.7%	0.9%	70.5%
	Suspended Load	584.6	815.2	99.3%	99.1%	39.4%
	Total	588.8	822.5	100.0%	100.0%	39.7%
Diversion	Bed Load	0.8	1.3	1.6%	1.9%	59.3%
	Suspended Load	48.7	64.5	98.4%	98.1%	32.5%
	Total	49.5	65.8	100.0%	100.0%	32.9%

Table 7.4.2.1 shows that the river and the diversion loads are dominated by the suspended load, which is approximately 99% of the total sand load. The increase in sand load at the upstream boundary resulted in a 70% increase in river bedload and only a 60% increase in the diversion bedload. However, the suspended load in the river increases by nearly 39.4%, while the suspended load in the diversion increases by only 32.5%. Overall, the total sand load increases approximately 40% in the river and only 33% in the diversion itself.

7.4.3 DISCUSSION

Based on the results obtained from comparing the cumulative deposition at year 12 from a base case with the deposition of the case with increased sand load at Belle Chasse, it was observed that the increase in available sand resulted in deposition of material within existing sand bars and on the channel edges. Therefore, additional sand in the system is less likely to impact the existing ship channel with in the Mississippi River.

In order to quantify the depositional trends due to change in sand input at the upstream boundary and the introduction of two diversions trendlines were added to the deposition plots (see Figure 7.4.3.1).

The difference between the 50% increase at Belle Chasse and the 40% in the downstream reach (Mid-Barataria) is due to its storage in low shear stress zones e.g. point bars. For these (12 year) runs a morphological equilibrium has not been achieved. A morphological equilibrium appears to be only possible for a simple riverine system

with no significant distributaries, since the flows in these are sensitive to local deposition and may in turn affect the streampower in the river.

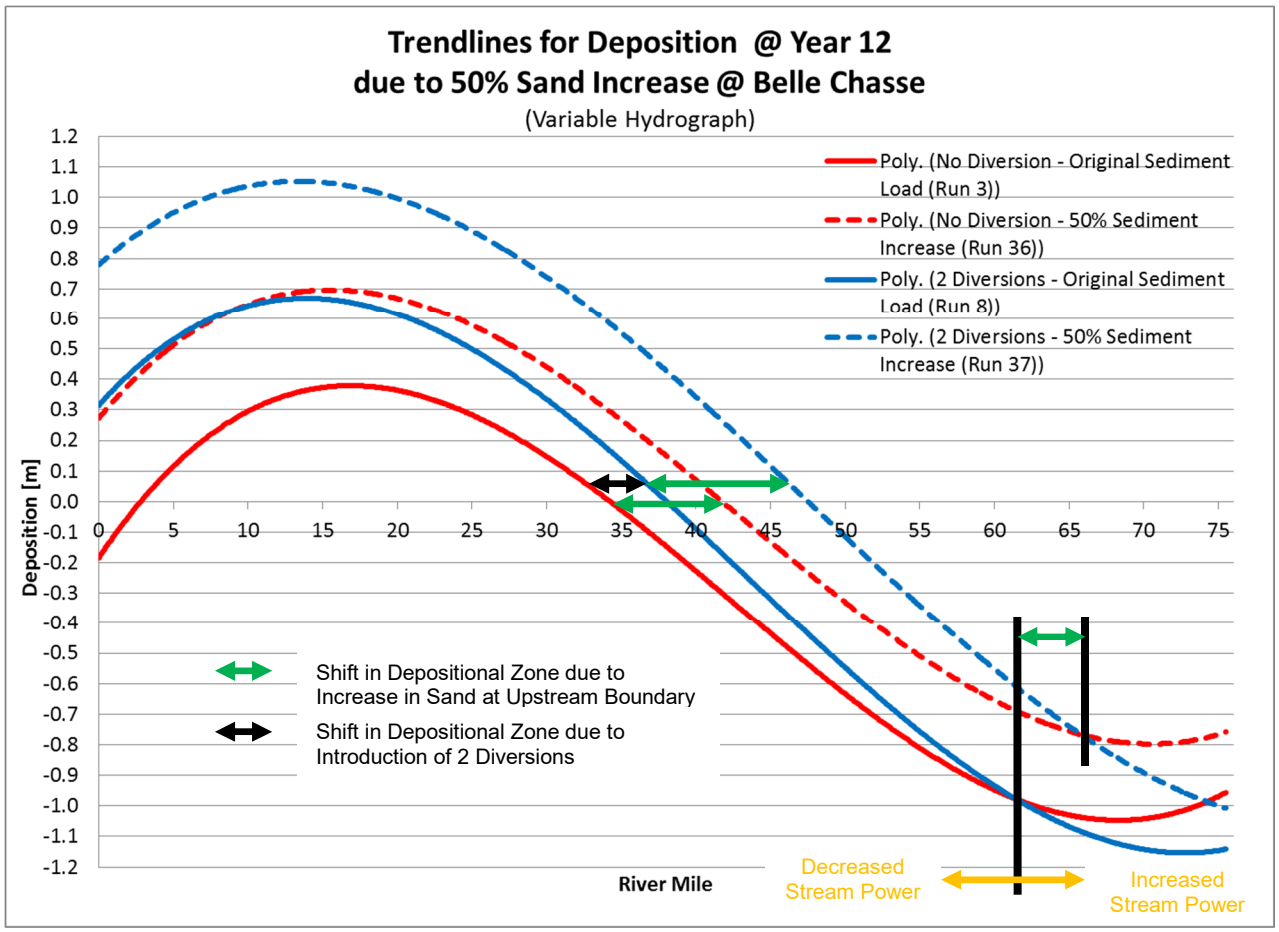

Figure 7.4.3.1: Trendlines for Deposition at Year 12 due to 50% Sand Increase at Belle Chasse

The domain average change in deposition for the non-diversion case due to the applied 50% increase of sand at the upstream boundary was calculated to be 0.307m, while the average change in deposition for the two diversion case is 0.379m, or a 23% increase due to the diversions.

In addition, the increase in sand in the system results in a shift of the depositional zone towards the upstream. The introduction of the two diversions increases this trend. The

added sand sediment also decreases the erosional zone for both cases, no diversion and with two diversions.

The shift of the depositional zone due to the increase in sand concentration at the upstream boundary is consistent in magnitude for the no diversion and the two diversion scenarios. However, the introduction of the two diversions caused the development of a transition point near the diversions. The transition point is where there is a change from erosional to depositional. Upstream of the transition point stream power is increased resulting in increased erosion and downstream of the transition point the stream power decreases resulting in increased deposition. This transition point is shifted upstream when increasing the sand load at the upstream boundary.

For further analysis, the laterally averaged cumulative sedimentation/erosion difference was calculated for the no-diversion case, which was obtained by laterally averaging the difference between the cumulative sedimentation/erosion for the increased sediment case (Run 36) and the base case (Run 3). In addition, the laterally averaged cumulative sedimentation/erosion difference was calculated for the two-diversion case (Run 37 – Run 8). Figure 7.4.3.2 depicts the results of the change in deposition and associated trendlines. Red depicts the change in deposition for the no-diversion case and the associated trendline, while blue depicts the change in deposition for the two-diversion case and the associated trendline.

The depositional change for the no-diversion case peaks at approximately 2.2 m, which is higher than the peak for the two-diversion case at 2.1m, while overall the trend shows more deposition in the two-diversion case, indicated by the trendline being above the trendline for the no-diversion case for the majority of the domain.

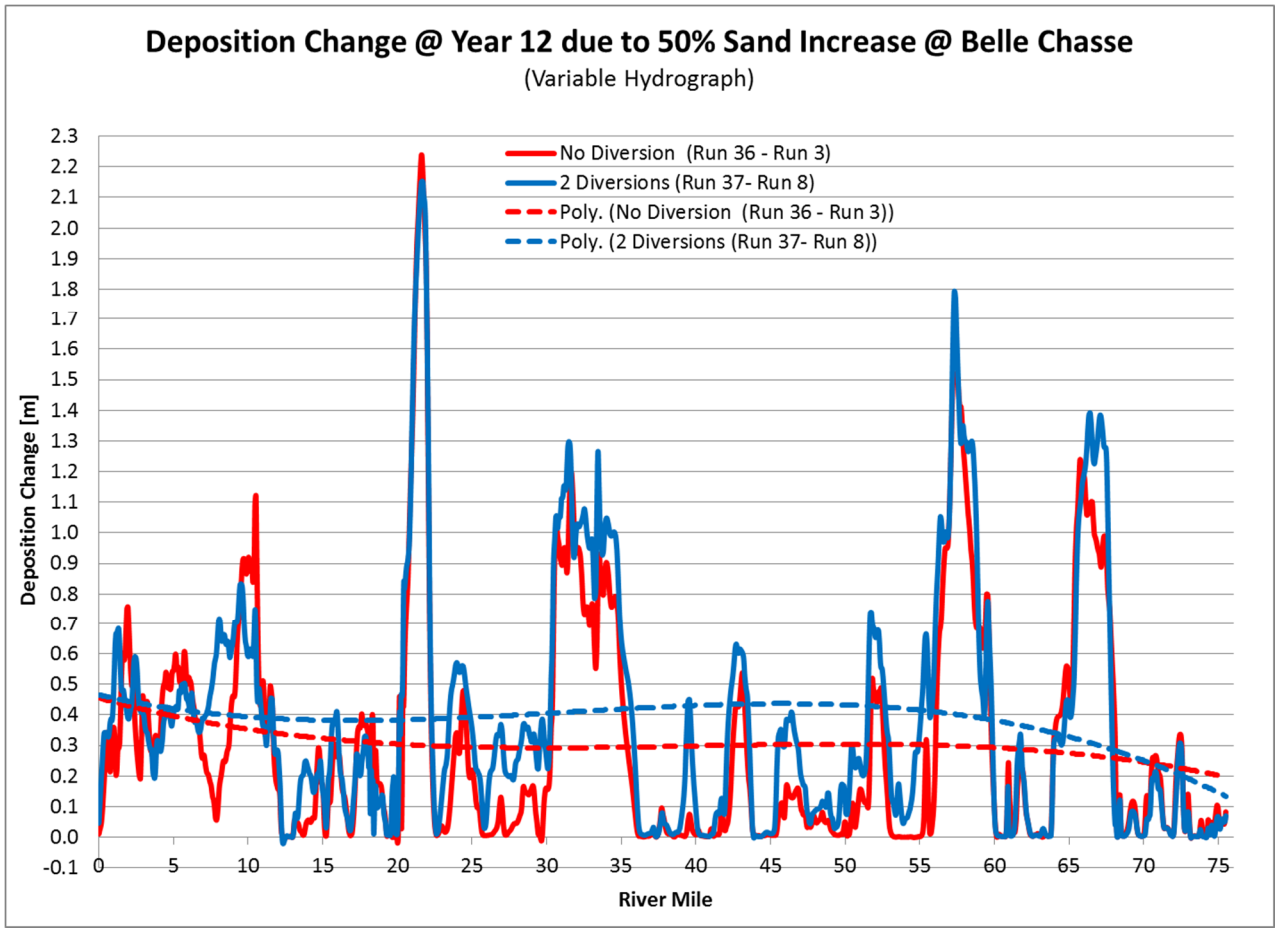

Figure 7.4.3.2: Deposition Change at Year 12 due to 50% Sand Increase at Belle Chasse

7.4.4 CONCLUSIONS

When the sand load in the system is increased by 50% by increasing the boundary condition at Belle Chasse, then the 12 year changes in terms of sand load in the river compared to the diversion can be described as follows:

- Bed Load in the River is less than 1% of the Total Load but increases with increase in average annual load at Belle Chasse. Bed Load in the Diversion also increases with increase in average annual load at Belle Chasse but constitutes >1% but less than 2% of the Total Load of the Diversion. Therefore, the increase in Bed Load within the diversion is less than within the river.
- Suspended Load in the River is >99% of the Total Load and decreases with increase in average annual load at Belle Chasse. Suspended Load in the Diversion also decreases with increase in average annual load at Belle Chasse but constitutes approximately 98% of the Total Load of the Diversion. Therefore, the decrease in Suspended Load within the diversion is less than within the river.

Similarly, the 12 year changes in terms of deposition in the river can be described as follows:

- The depositional peaks are located in river bend (e.g. point bars).
- Increase in overall deposition by approximately 0.3m on average without diversions and by approximately 0.4m on average with 2 diversions (Mid-Breton 35,000 cfs and Mid-Barataria 75,000 cfs).
- In both cases, no-diversion and 2-diversions, result in a trendline with a maximum deposition change at HOP, of approximately 0.45m.

The differences resulting from the 50% increase in sand concentration are an indication of the uncertainties of the sediment transport and morphological results. Therefore, the results of the cases with the increased sand concentrations reflect an upper limit of the range to be expected as a result of the uncertainties in sand concentration at the upstream boundary (Belle Chasse).

The overall effect of the 50% increase of sand input was an average change in deposition of 0.307m for the non-diversion case and 0.379m for the two-diversion case, or a 23% increase due to the diversions.

The effect on the deposition zone due to the increase of sand input for both cases, the no-diversion and the two-diversion, is similar. Both cases incur an upstream shift of the deposition zone, while the two diversion case further accelerates this shift.

Proportionally, the diversions do not capture the same increase in bed and suspended load as experienced in the river. Even though the river is experiencing a large increase (70%) of the bedload due to the sand increase at the upstream boundary, the bed-load is only a small percentage (1-2%) of the total sand load.

8.0 CHAPTER 8: GENERAL CONCLUSIONS

Bathymetric equilibrium is considered to occur when the rate of change of deposition or erosion is zero. A near equilibrium is reached upstream of Fort St. Philip, where only minor distributaries influence the river dynamics; however, downstream of Fort St. Philip, where nearly 50% of the river flow is discharged to the distributaries, no equilibrium occurred within the 48 year period of the simulation. The variable hydrograph results showed a dynamic equilibrium upstream of Fort. St. Philip, while the uniform hydrograph results showed an absolute equilibrium upstream of Fort St. Philip. The dynamic equilibrium in the upstream reach had the periodicity of the variable hydrograph record, i.e. 12 years. In summary, the absolute bathymetry equilibrium is not independent of the annual variability of the hydrograph, even if the flow duration curves are the same.

Utilizing a uniform hydrograph results in a more conservative approach to evaluating diversion efficiency and sand capture, since utilizing a uniform hydrograph is resulting in a smaller fraction of sand diverted from the river into the diversion. The fraction of sediment captured by the diversion depends on the availability of sand in the system as well as the flow hydrograph pattern. Therefore, utilizing a more realistic, variable hydrograph pattern, will result in more accurate sand load volumes captured by the diversion.

This study shows that morphological changes are dependent on the number and location of multiple diversions. The largest interdependencies occur for the most downstream diversions, which increase with the total diverted flow. Sediment capture showed only minor interdependencies amongst multiple diversions. For example, if the total diversion flow is less than 140,000 cfs, the percent difference in diverted sand between the single and the multiple-diversion case is less than 3%.

At a river flow at or greater than 600,000 cfs there is only 0-0.5% probability that the diversion flows will be restricted by the availability of an energy differential between the River and the Gulf of Mexico, if the geometry of the diversion remains as modeled

(Table 7.1.1.2). The operational trigger point of Mississippi River flow directly impacts the diversion efficiency. Values lower than 600,000 cfs or an increase in total diverted flow, change of diversion location or the diversion geometry, would impact the possible diversion flow and sediment capture.

Based on the Eddy Viscosity/Diffusivity sensitivity analysis it was observed that reducing the Eddy Diffusivity only, results in a reduction of predicted deposition at bends. If Eddy Viscosity and Diffusivity are modified together the changes in deposition or erosion in bends are less than if Diffusivity is changed by itself.

A true equilibrium was neither achieved within 48 years with or without sea level rise. It was observed that the system with no diversions, 1 diversion and 2 diversions responds to sea level rise (NRCIII Curve) by an increase in deposition. The deposition increases with the total diverted flow. The increase in deposition is related to the loss of streampower generated by sea level rise and additionally by diverted flow. The depositional effects downstream of Fort St. Phillip are accelerated and decrease asymptotically from HOP to approximately RM 40. Especially the introduction of larger diversions, like the Mid-Barataria diversion, result in an upstream shift of the depocenter. Furthermore, the utilization of a uniform hydrograph increases the predicted deposition within the Mississippi River domain.

The differences resulting from the 50% increase in sand concentration at Belle Chasse are an indication of the uncertainties of the sediment transport and morphological results. Therefore, the results of the cases with the increased sand concentrations reflect an upper limit of the range to be expected as a result of the uncertainties in sand concentration at the upstream boundary (Belle Chasse). The increase in sand concentration did not significantly impact the sand capture rate of the diversion over the 12-year simulation. However, the increase did have an impact on the morphological changes in the Mississippi River, with an increase in depositional trend throughout the domain.

9.0 CHAPTER 9: RECOMMENDATIONS

It is recommended to develop a 48-Year variable hydrograph, which incorporates the mean rate of increase in flow over the past 50 years. This would eliminate the periodicity observed from repeating a 12-year variable hydrograph over a 48 year run time.

A higher sea level rise scenario should be evaluated, for example the high scenario from the 2017 Master Plan (CPRA 2017). In addition, the inclusion of tides would be beneficial, to evaluate the full range of potential impacts. The entire domain of the shortmodel is within the tidal influence, even at high flows.

While an increase in sand concentration of 50% was evaluated a potential reduction in sand concentration was not considered as part of this research. It would be beneficial to not only model a decrease in sand concentration, e.g. by 1/3 but also perform a sensitivity analysis for sand load increase required at the upstream boundary to offset the erosional feature in the upstream reach of the domain. As part of this sensitivity analysis it should include an analysis of appropriate upstream boundary conditions, especially in cases utilizing a uniform hydrograph.

As Mid-Barataria and Mid-Breton diversion undergo design and permitting, their impacts have to be analyzed as individual structures as well as their cumulative impacts when operated at the same time or both are operated at different times. The actual structures, diversion opening trigger points, and maximum flow considered for the Mid-Breton and Mid-Barataria Diversions should be modeled for a morphologic change analysis within the river and to evaluate diversion sand capture and efficiency.

Furthermore, the model should be expanded into the adjacent receiving basins to evaluate sediment deposition in the wetlands, especially sand. TWIG has conducted some recent research in this regard and the model modifications should be coordinated

to implement any lessons learned. This should be extended to the ‘natural’ passes since these will evolve morphologically over several decades.

Based on the Eddy Viscosity/Diffusivity sensitivity analysis it is recommended, to first calibrate the Eddy Diffusivity and Eddy Viscosity as being equal to each other for a general calibration of a model, followed by a fine-tuning for the bend regions, by adjustment of Eddy Diffusivity only. It would be beneficial to tweak the calibration of the model once the 48-year hydrograph is established and a focus should be given to the bend regions. In general, it is recommended to further analyze the effect of the turbulent Prandtl-Schmidt Number on deposition in bends.

The van Rijn (1984) sand transport model tends to over-scour the deepest parts of the channel. In the current version of Delft3D-Flow it was not possible to modify the sand transport exponent (2.1 at present) on the excess shear term in van Rijn without a code change. Sensitivity studies should be made to determine the best exponent that would reduce this excessive incising effect.

The current model does not account for sediment dredged within the domain for navigation or sand mining. To incorporate annual dredging, the model would need to be stopped and re-started frequently, which could introduce errors. Therefore, it may be useful to continue in 12-year patterns, and account for any sediment removal within that period for a re-start bathymetry.

As a final recommendation it should be considered to focus on morphologic changes at point bars and erosional hotspots anticipated from Mid-Breton and Mid-Barataria diversions (independent and together). The first step would be to fine-tune calibration to best represent accurate point bar geometry and erosional “holes” followed by a long term analysis of morphological impacts from diversion operation.

REFERENCES

Ayres, Steven 2015. *A Simulation of the Mississippi River Salt Wedge Estuary Using a Three-Dimensional Cartesian Z Coordinate Model*. Ph.D. Dissertation, University of New Orleans, Louisiana.

Bos, Matthijs 2011. *The Morphological Effects of Sediment Diversions of the Lower Mississippi River*. Delft, Netherlands.

Cengel, Yunus A. & Cimbala, John M. 2006. *Fluid Mechanics – Fundamentals and Applications*. McGraw Hill, New York, NY.

Chaudhry, M Hanif 1993, *Open-Channel Flow*, Prentice-Hall Inc., Englewood Cliffs, New Jersey (ISBN 0-13-637141-8)

Coastal Protection and Restoration Authority (CPRA) – (formerly OCPR), 2007. *Louisiana's Comprehensive Master Plan for a Sustainable Coast*. Baton Rouge, Louisiana.

Coastal Protection and Restoration Authority (CPRA), 2012. *Louisiana's Comprehensive Master Plan for a Sustainable Coast*. Baton Rouge, Louisiana.

Coastal Protection and Restoration Authority (CPRA), 2017. *Louisiana's Comprehensive Master Plan for a Sustainable Coast.* Baton Rouge, Louisiana.

Copeland, Ronald & Thomas, William A. 1992. *Lower Mississippi River Tarbert Landing to East Jetty Sedimentation Study – Numerical Model Investigation*, New Orleans, Louisiana

Cornelissen, Sander C. 2004. Numerical Modellin of Stratified Flows – Comparison of the Sigma and Z Coordinate Systems. M.Sc. Thesis, TU Delft, Deft, Neterlands

Davis, Mallory 2010. *Numerical Simulation of Unsteady Hydrodynamics in the Lower Mississippi River*. M.Sc. Thesis, University of New Orleans, Louisiana.

Deltares 2011. Delft3D-FLOW User Manual. *Simulation of multi-dimensional hydrodynamic and transport phenomena, including sediments.* Delft, Netherlands

Kemp, Paul 2009. *Memorandum Regarding ERDC West Bay Sediment Diversion Effects (November 2009) dated December 13, 2009*, Vicksburg, Mississippi.

Louisiana Department of Natural Resources (LDNR) 1998. *Coast 2050: Towards a Sustainable Coastal Louisiana,* Baton Rouge, Louisiana

McCorquodale, Alex et al. 2017. *Development of a Regional 3-D Model for the Lower Mississippi River – Final Report* submitted to CPRA Baton Rouge, Louisiana

Meselhe, E.A., Georgiou, I., Allison, M.A., and McCorquodale, J.A. (2012). *Numerical modeling of hydrodynamics and sediment transport in lower Mississippi at a proposed delta building diversion*, Journal of Hydrology, Volumes 472–473, November, Pages 340-354.

NOAA: Tides&Currents. (2012). Tides&Currents. Retrieved from Tides&Currents: http://tidesandcurrents.noaa.gov/

Papanicolauo, Athanasios N. (Thanos) et al. 2008. *Sediment Transport Modeling Review – Current and Future Developments*, Journal of Hydraulic Engineering, ASCE

Partheniades, E., 1965. *"Erosion and Deposition of Cohesive Soils.*" Journal of the Hydraulics Division, ASCE 91 (HY 1): 105–139. 79, 329, 571

Pavlykova, Tatiana, *A 3-D Hydrodynamic Modeling at Head of Passes of the Mississippi River.* M.Sc. Thesis, University of New Orleans, Louisiana

Pereira, Joao 2011. *Numerical Modeling of River Diversions in the Lower Mississippi River*. Ph.D. Dissertation, University of New Orleans, Louisiana

Pratt, Thad 2009. "*West Bay Sediment Diversion Work Plan Task 1: Data Collection and Analysis".* Public Presentation. USACE-ERDC, Vicksburg, Mississippi

Reins, Nina 2005. *Sediment Investigations in the Vicinity of the Old River Control Complex: Red River above Old River Outflow Channel*. M.Sc. Thesis, Tulane University, New Orleans, Louisiana

Richards, Carol Parsons 2014. *Restoration in the Mississippi River Delta: Old River Control Structure to the Gulf of Mexico*. Public Presentation at the CEER Conference, July 31, 2014, Vicksburg, Mississippi

Spasojevic & Holly 1994. *Three-Dimensional Numerical Simulation of Mobile-Bed Hydrodynamics.* Iowa Institute of Hydraulic Research, The University of Iowa, Iowa City, Iowa

Terán González, Grecia 2014. *3-D Hydrodynamic and Non-Cohesive Sediment Transport Modeling in the Lower Mississippi River*. M.Sc. Thesis, University of New Orleans, New Orleans, Louisiana

United States Army Corps of Engineers (USACE) 2004. *Louisiana Coastal Study (LCA), Louisiana – Ecosystem Restoration Study, Final Volume 1: LCA Study – Main Report*, New Orleans, Louisiana

United States Army Corps of Engineers (USACE): Rivergages. (2012). RiverGages. Retrieved from www.rivergages.com

United States Army Corps of Engineers (USACE): MRHDM (2017). http://www.mvn.usace.army.mil/Missions/Environmental/ Louisiana-Coastal-Area/Mississippi-River-Hydrodynamic-and-Delta-Managemen/

United States Army Corps of Engineers (USACE): MRT (2017). http://www.mvd.usace.army.mil/About/Mississippi-River-Commission-MRC/Mississippi-River-Tributaries-Project-MR-T/

Rijn, L. (1984a). Sediment transport, Part I: bed load transport. Journal of Hydraulics Engineering, 1431-1456.

Rijn, L. (1984b). Sediment transport, Part II: suspended load transport. Journal of Hydraulic Engineering, 1613-1640.

Rijn, L. (1984c). Sediment transport, Part III: bed form and alluvial roughness. Journal of Hydraulic Enginnering, 1733-1754.

APPENDIX R1

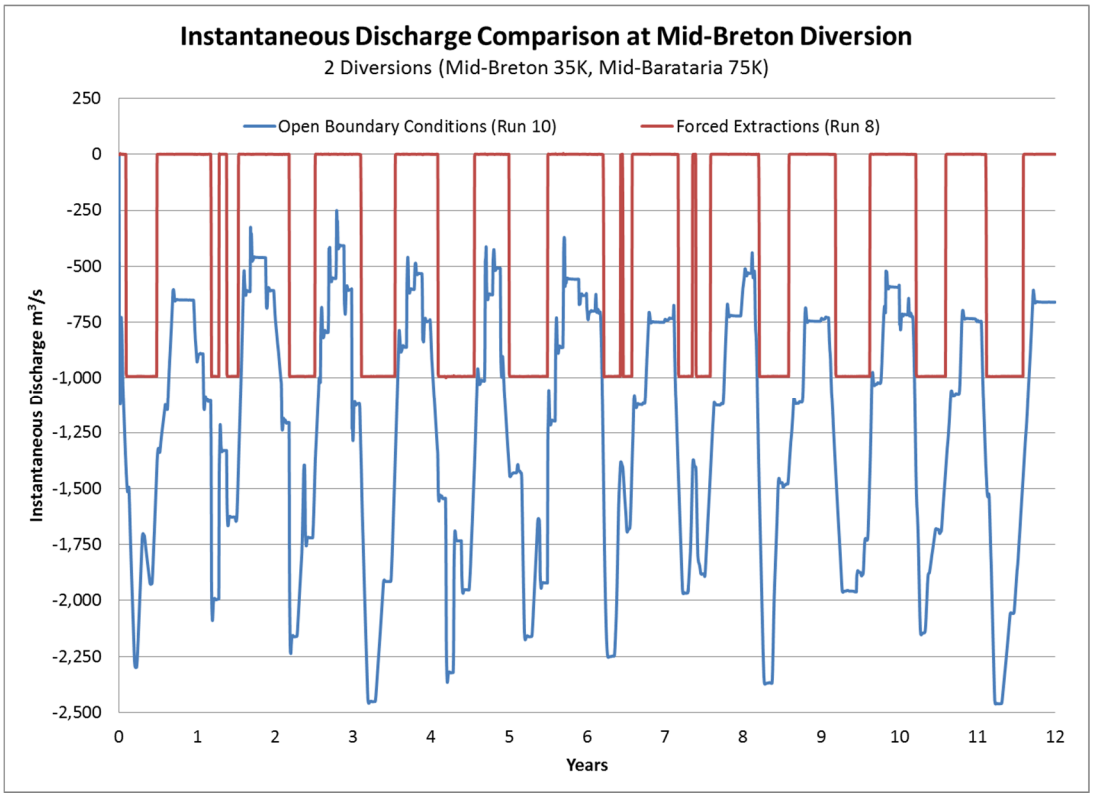

Figure R1.1: Instantaneous Discharge Comparison at Mid-Breton Diversion (2 Diversion Case)

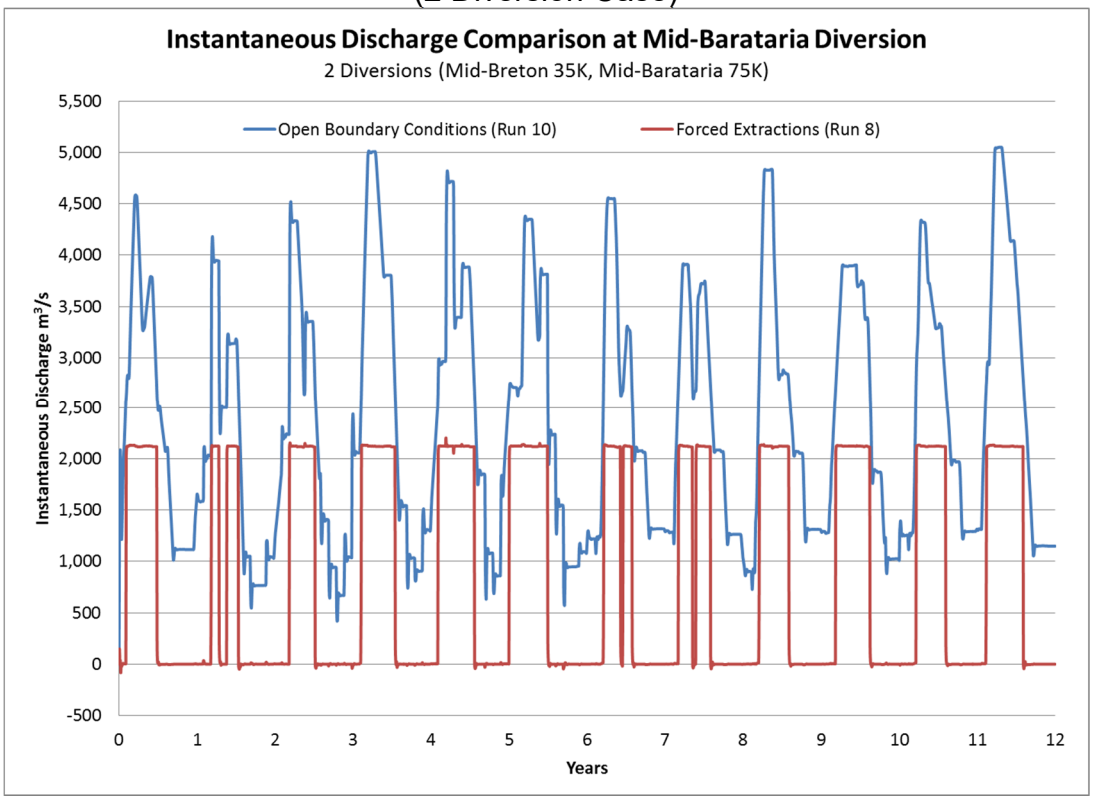

Figure R1.2: Instantaneous Discharge Comparison at Mid-Barataria Diversion (2 Diversion Case)

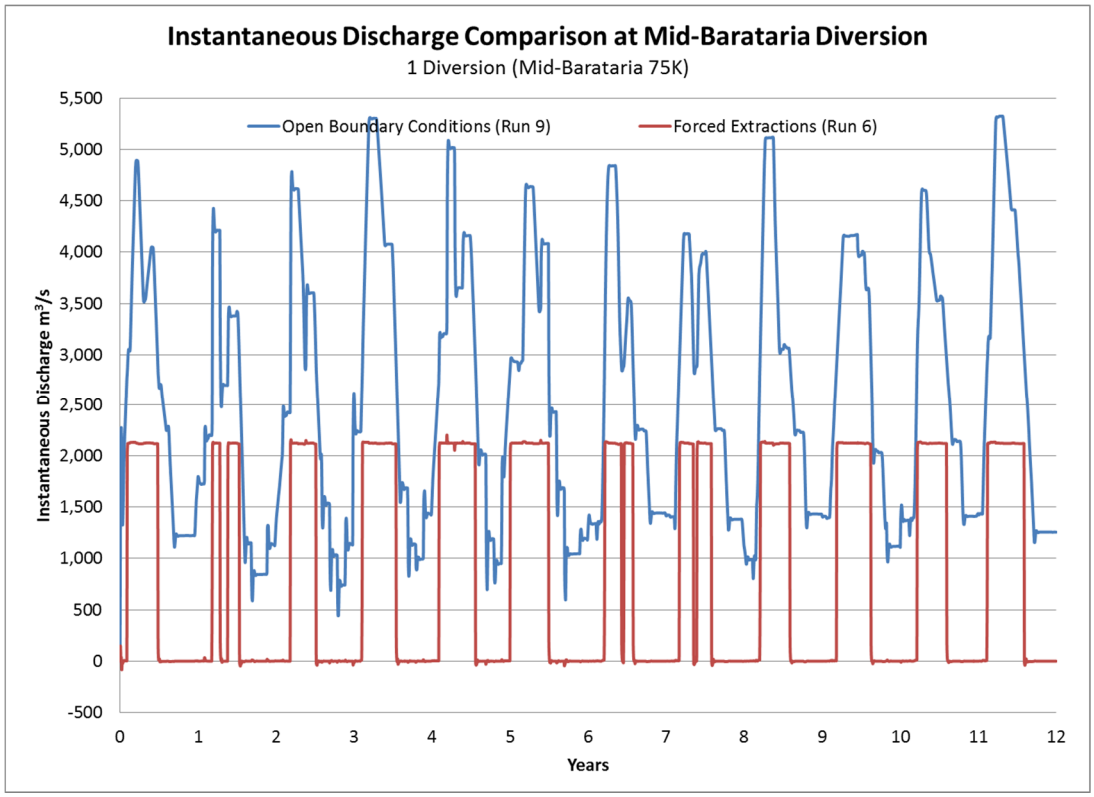

Figure R1.3: Instantaneous Discharge Comparison at Mid-Barataria Diversion (1 Diversion Case)

APPENDIX R3.1

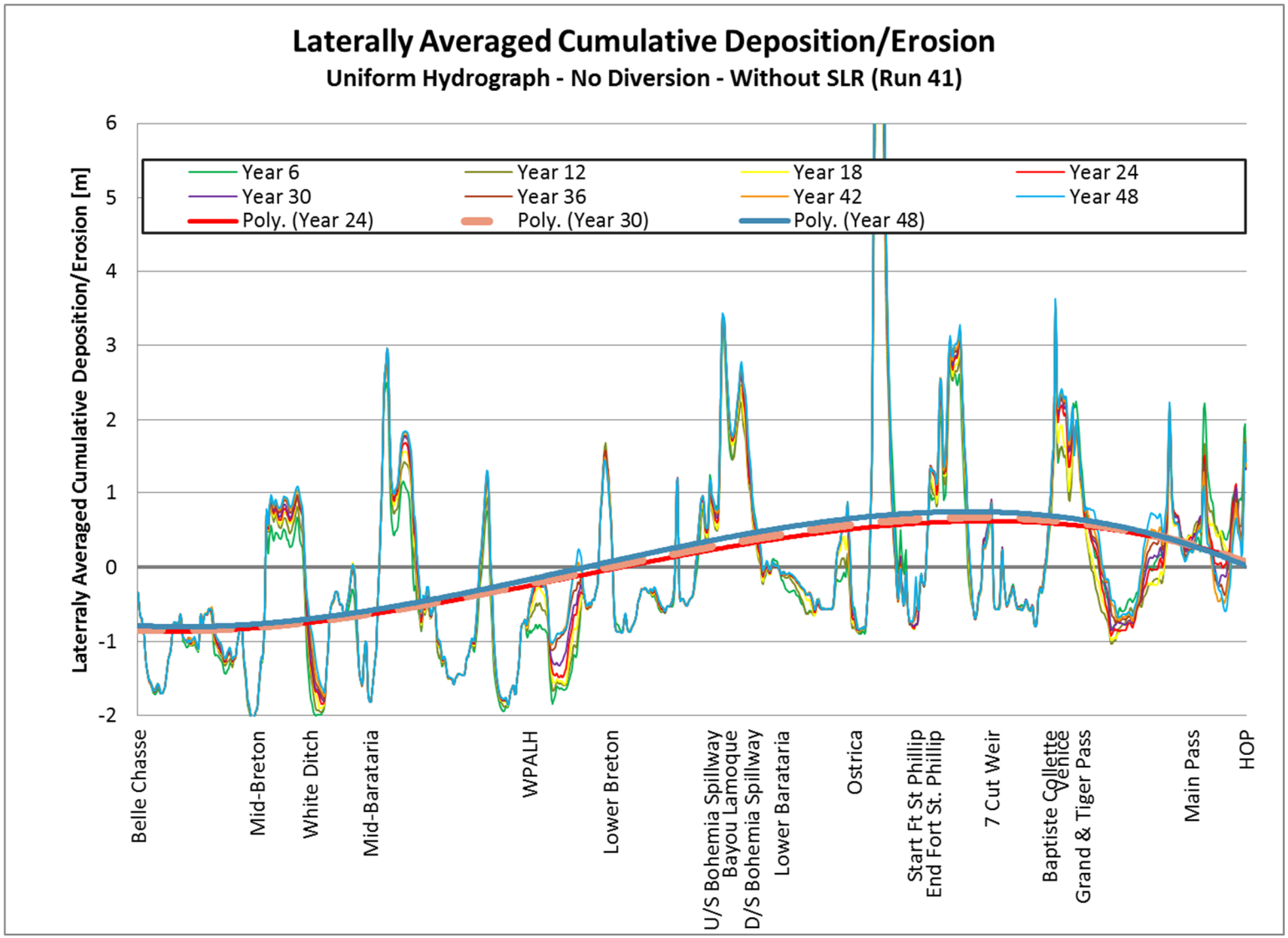

Figure R.3.1.1: Laterally Average Cumulative Deposition/Erosion due to SLR – Uniform Hydrograph No Diversion – Without Sea Level Rise (Run 41)

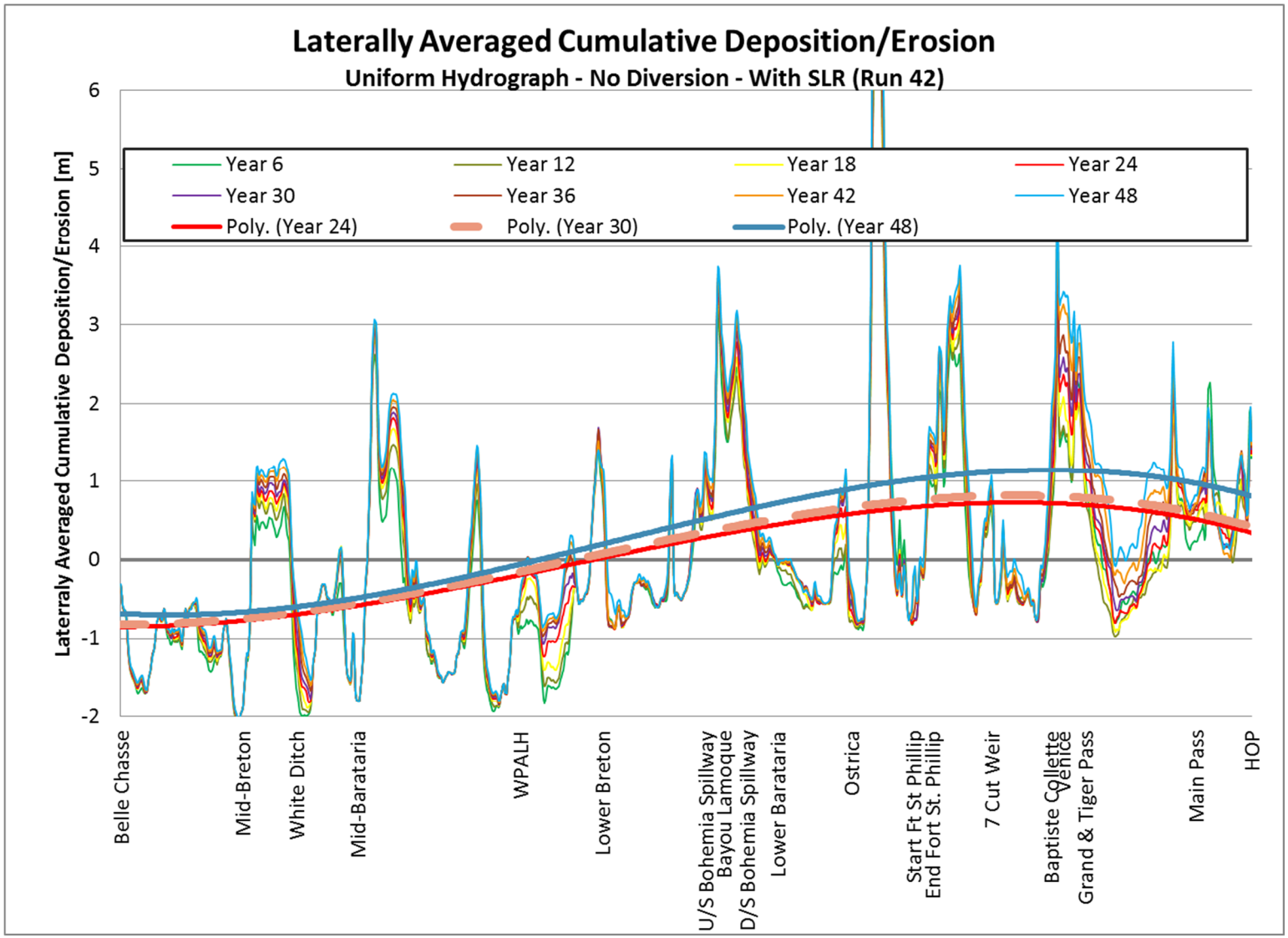

Figure R.3.1.2: Laterally Average Cumulative Deposition/Erosion due to SLR – Uniform Hydrograph No Diversion – With Sea Level Rise (Run 42)

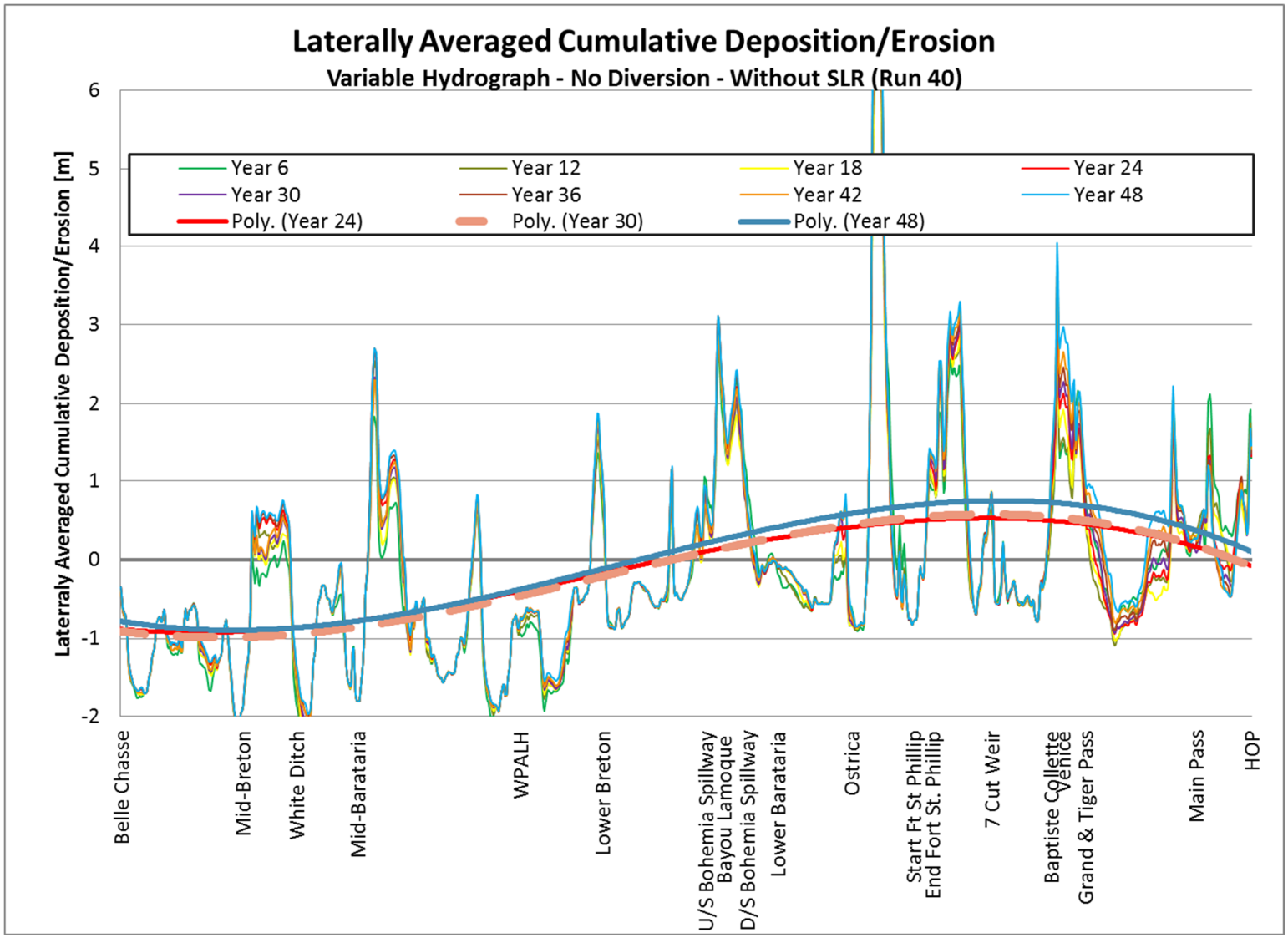

Figure R.3.1.3: Laterally Average Cumulative Deposition/Erosion due to SLR – Variable Hydrograph No Diversion – Without Sea Level Rise (Run 40)

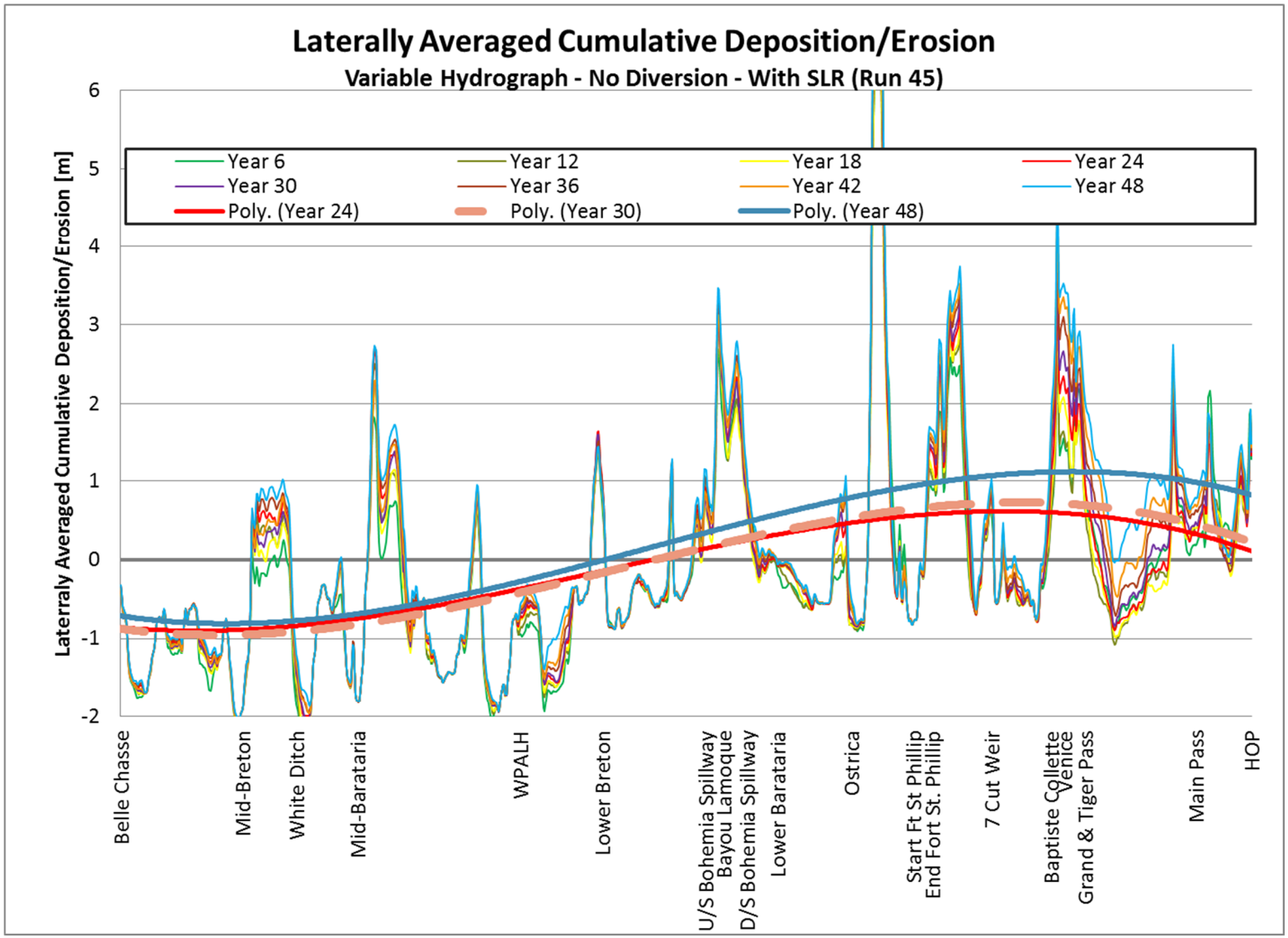

Figure R.3.1.4: Laterally Average Cumulative Deposition/Erosion due to SLR – Variable Hydrograph No Diversion – With Sea Level Rise (Run 45)

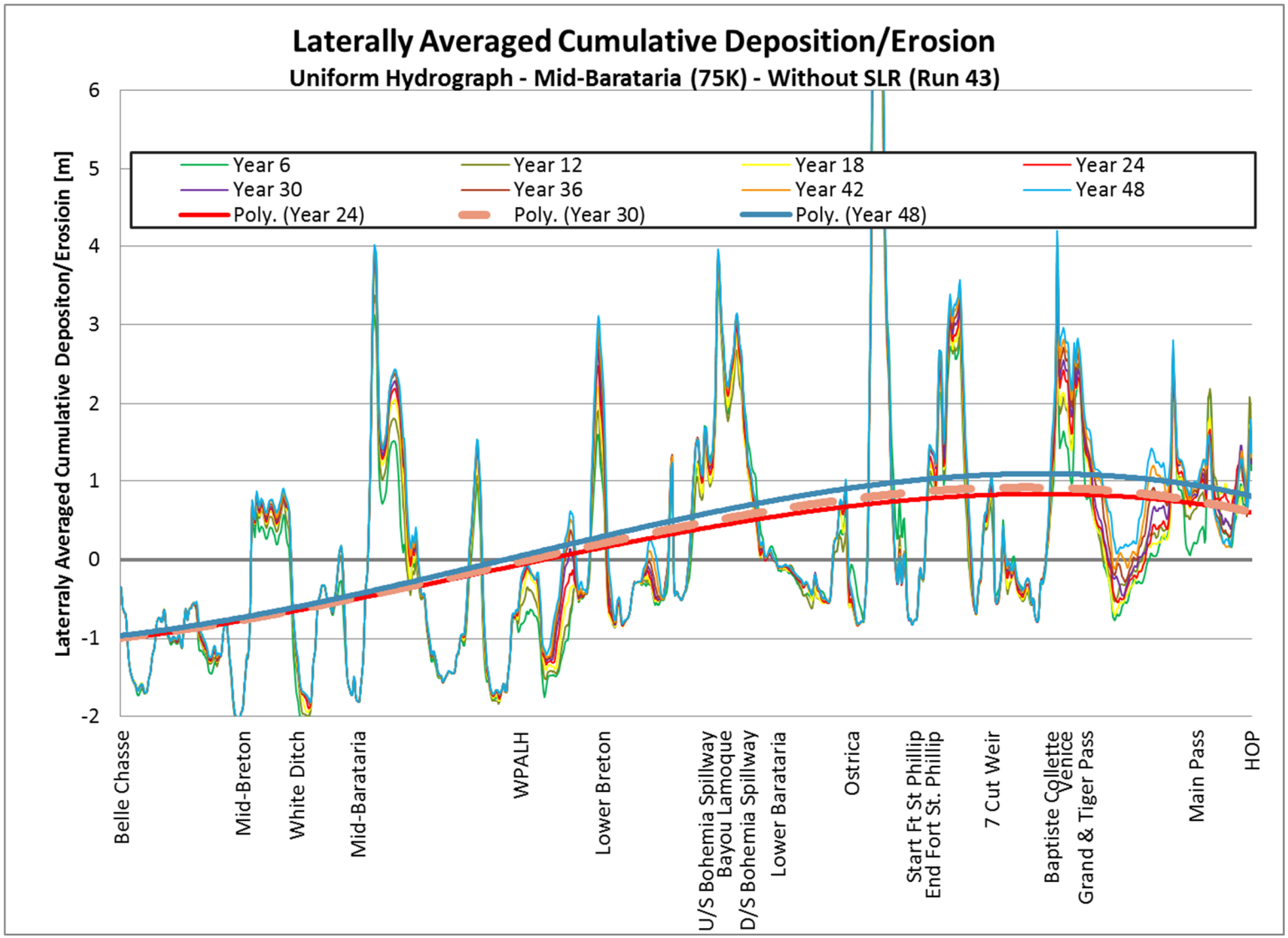

Figure R.3.1.5: Laterally Average Cumulative Deposition/Erosion due to SLR – Uniform Hydrograph 1 Diversion (Mid-Barataria 75K) – Without Sea Level Rise (Run 43)

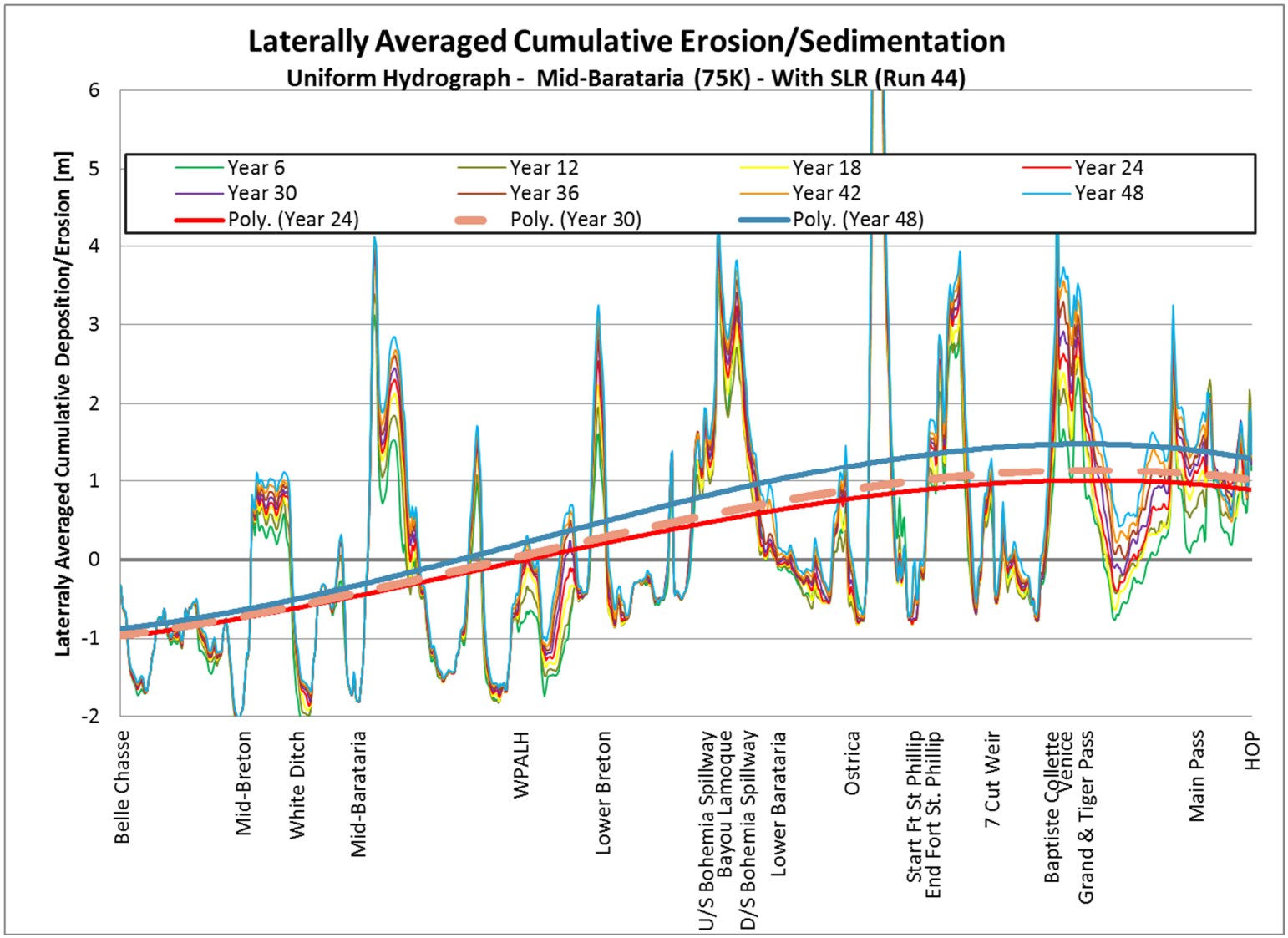

Figure R.3.1.6: Laterally Average Cumulative Deposition/Erosion due to SLR – Uniform Hydrograph 1 Diversion (Mid-Barataria 75K) – With Sea Level Rise (Run 44)

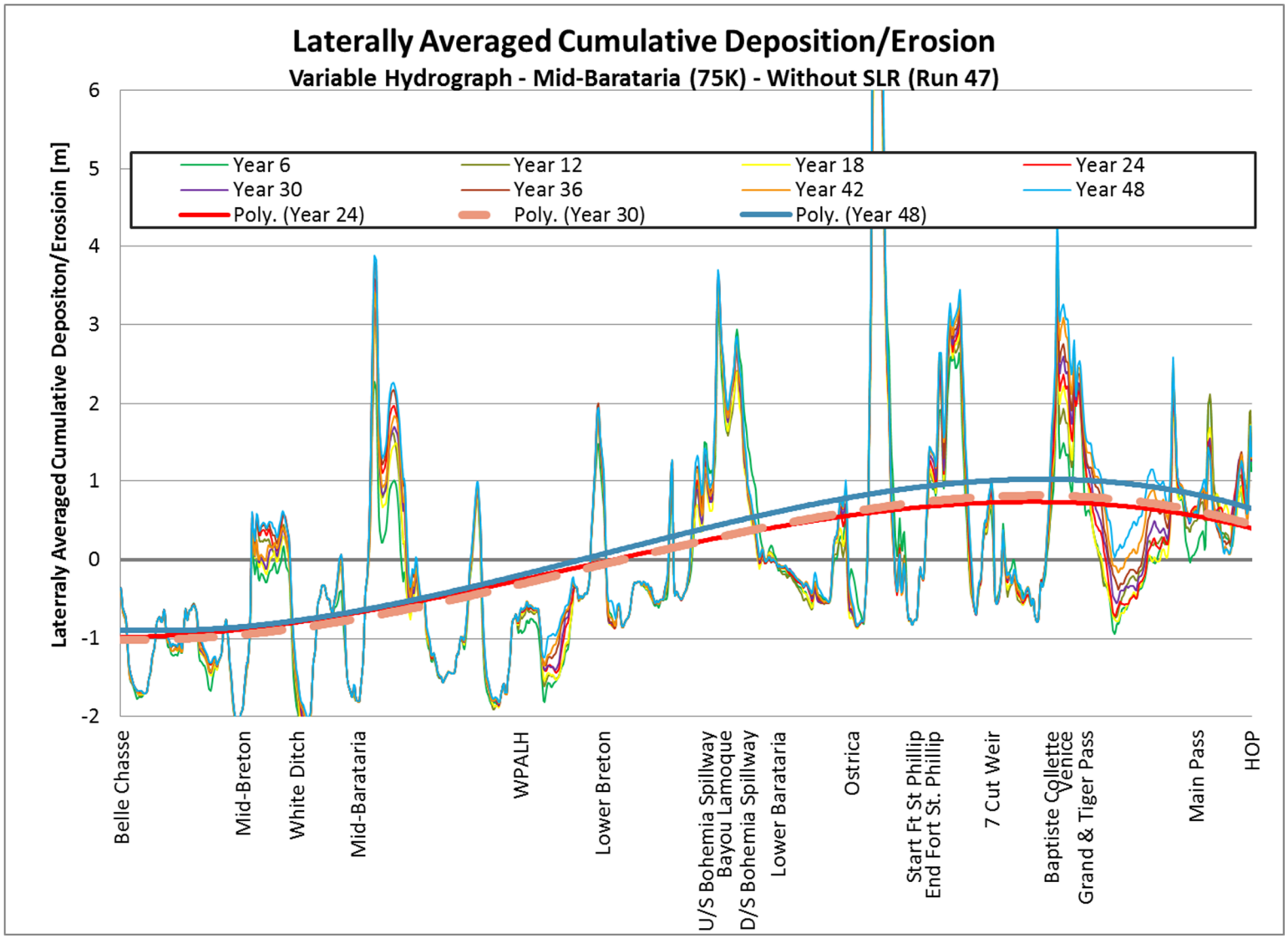

Figure R.3.1.7: Laterally Average Cumulative Deposition/Erosion due to SLR – Variable Hydrograph 1 Diversion (Mid-Barataria 75K) – Without Sea Level Rise (Run 47)

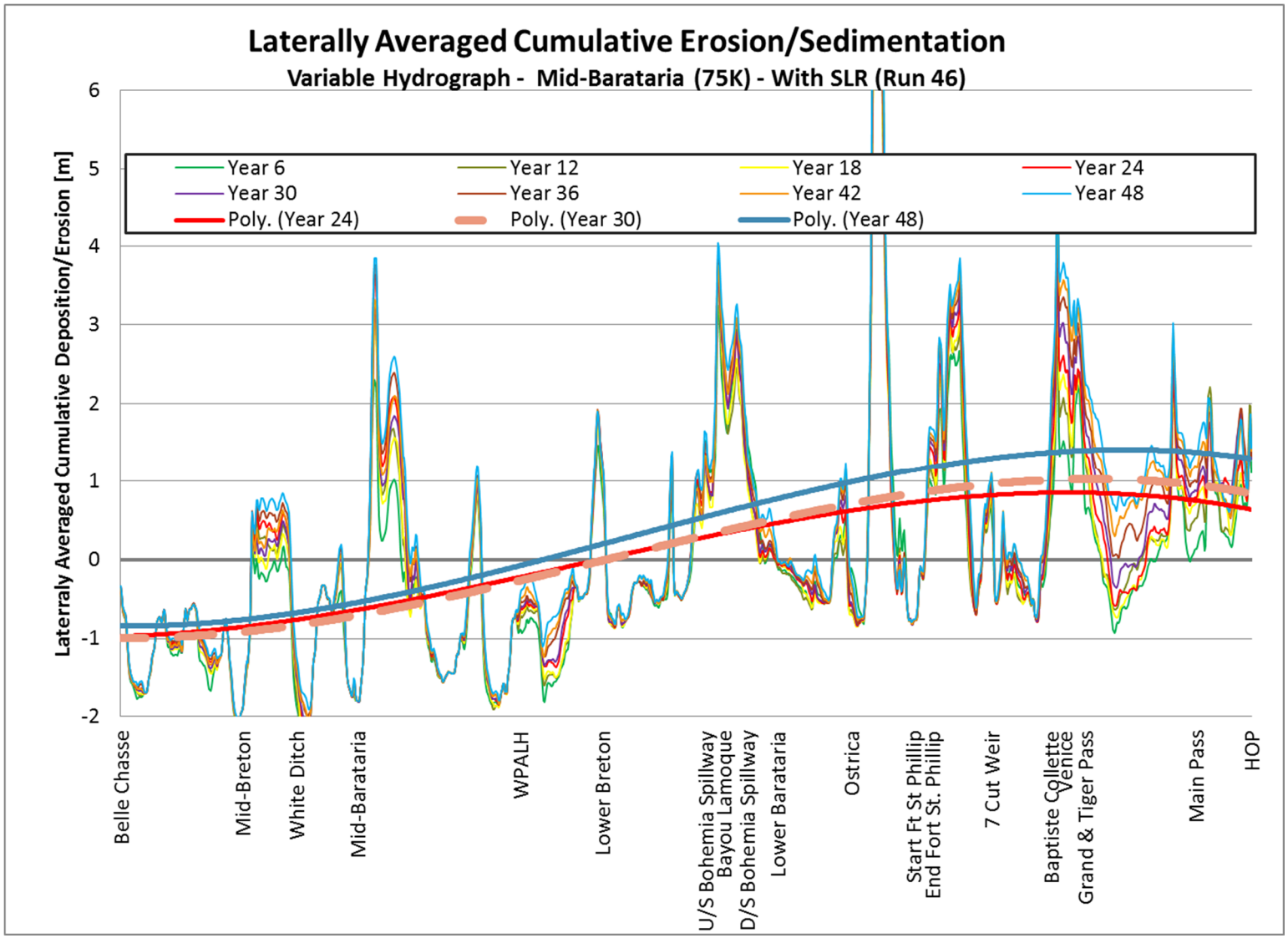

Figure R.3.1.8: Laterally Average Cumulative Deposition/Erosion due to SLR – Variable Hydrograph 1 Diversion (Mid-Barataria 75K) – With Sea Level Rise (Run 46)

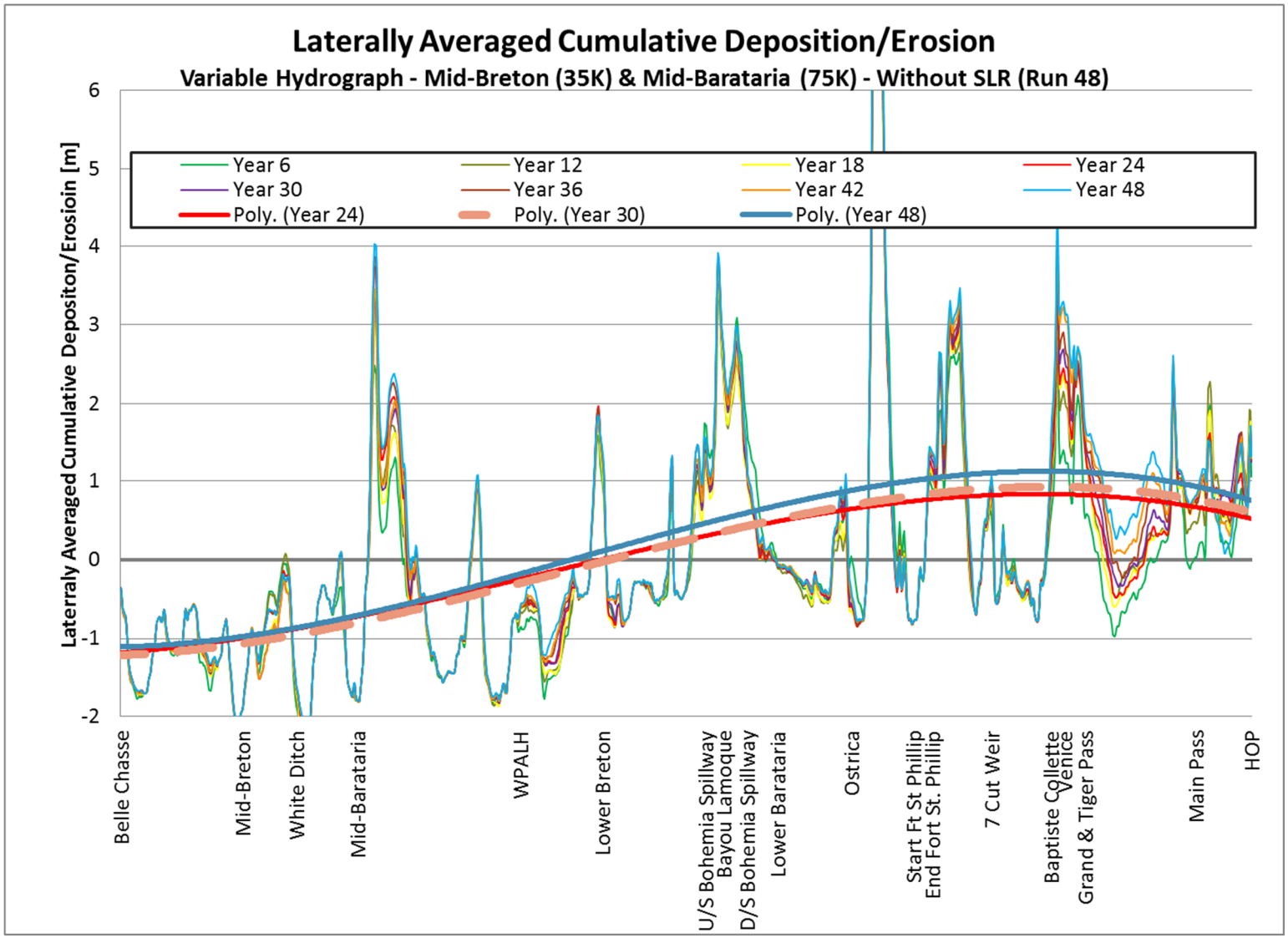

Figure R.3.1.9: Laterally Average Cumulative Deposition/Erosion due to SLR – Variable Hydrograph 2 Diversions (Mid-Breton 35K & Mid-Barataria 75K) – Without Sea Level Rise (Run 48)+

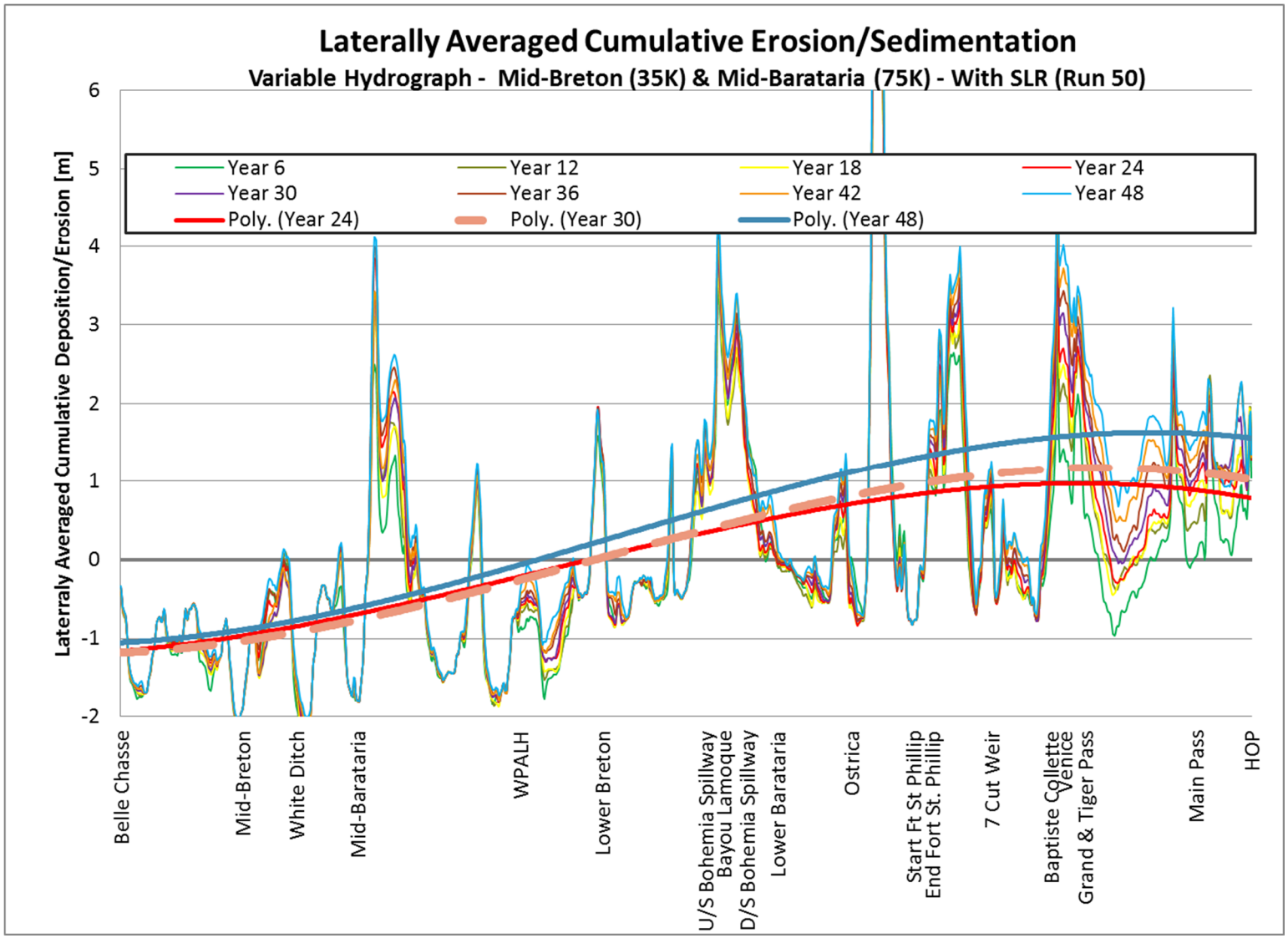

Figure R.3.1.10: Laterally Average Cumulative Deposition/Erosion due to SLR – Variable Hydrograph 2 Diversions (Mid-Breton 35K & Mid-Barataria 75K) – With Sea Level Rise (Run 50)

APPENDIX R3.2

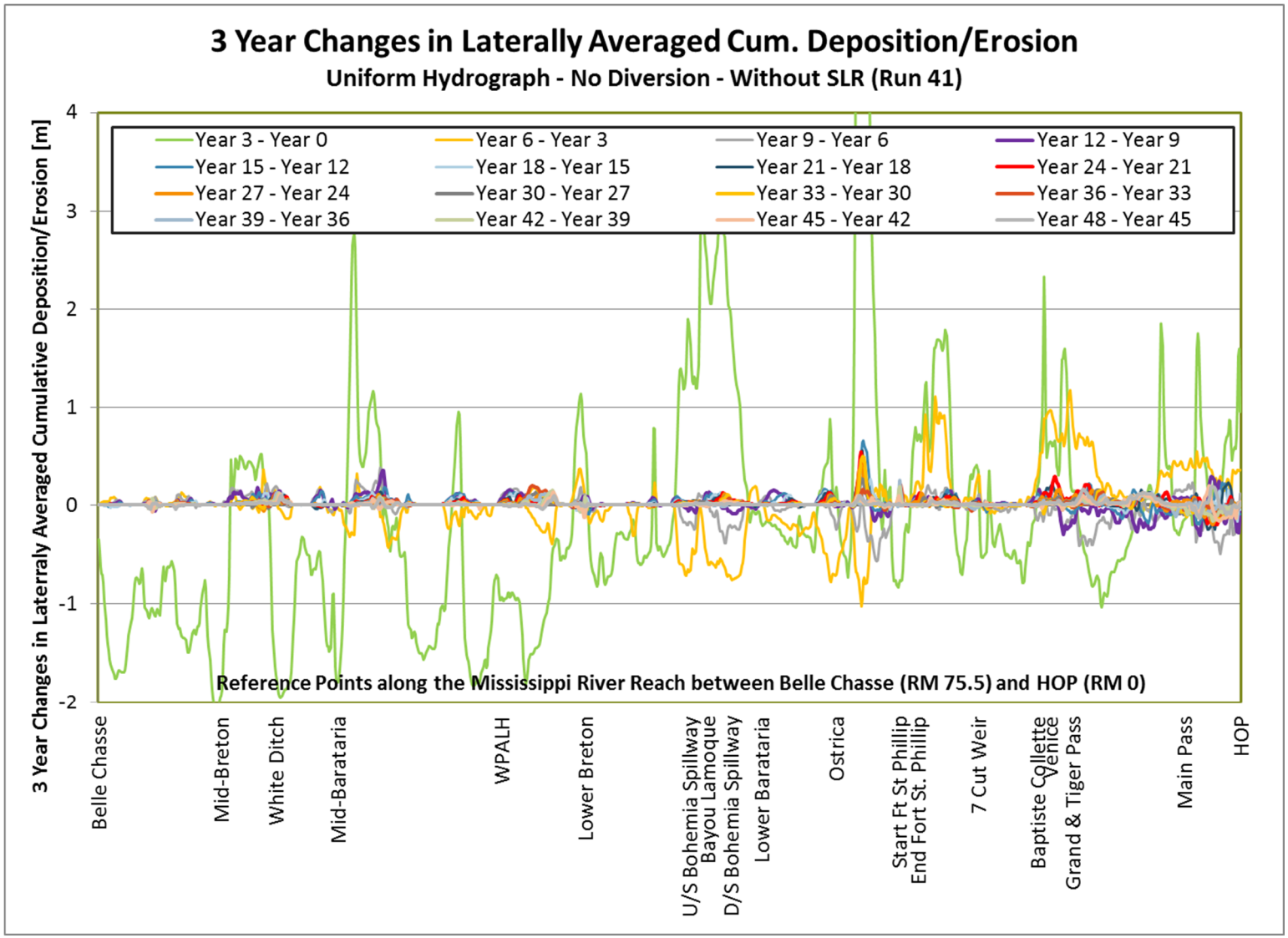

Figure R.3.2.1: 3- Year Changes in Laterally Average Cumulative Deposition/Erosion due to SLR – Uniform Hydrograph, No Diversion – Without Sea Level Rise (Run 41)

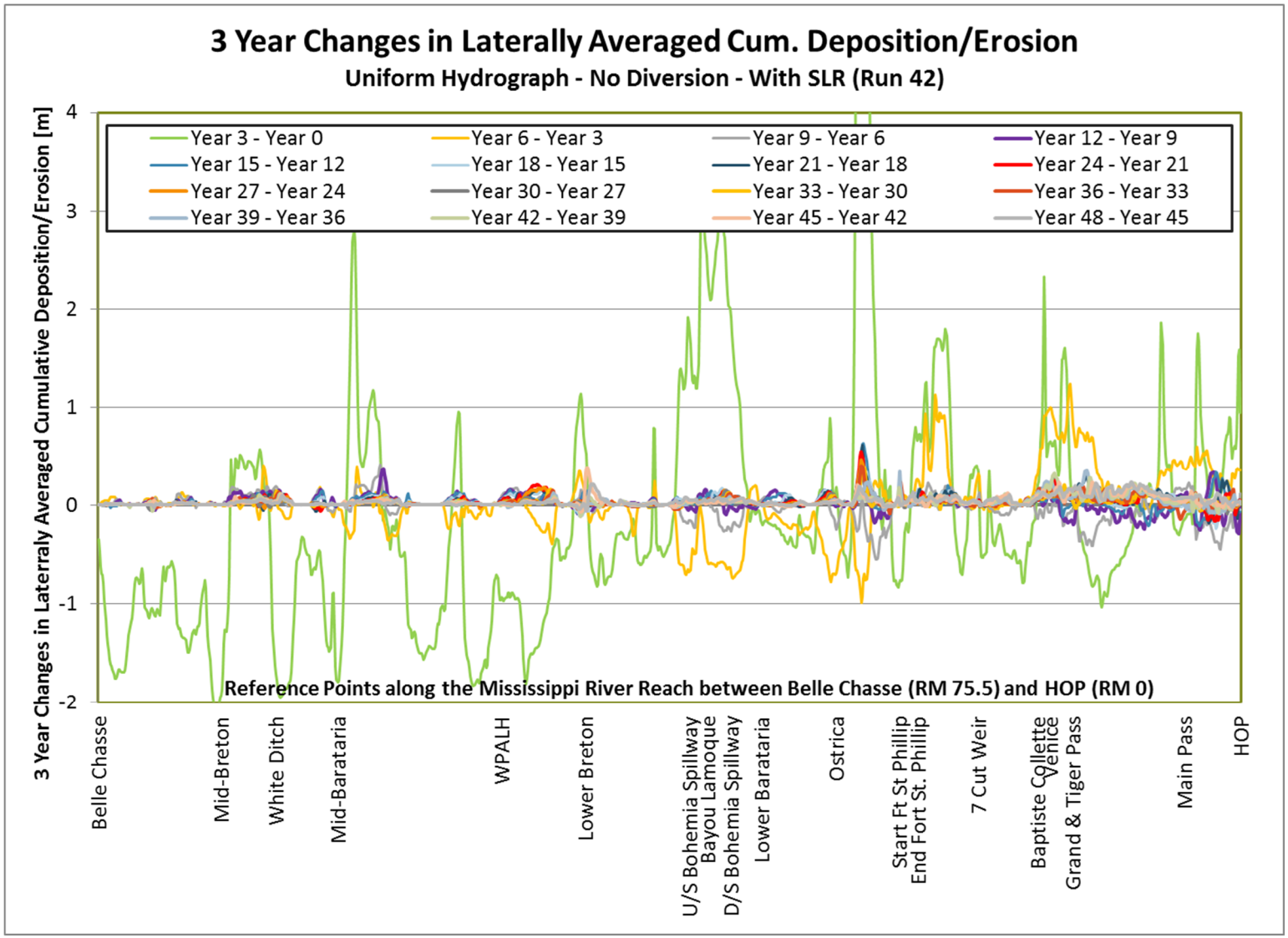

Figure R.3.2.2: 3- Year Changes in Laterally Average Cumulative Deposition/Erosion due to SLR – Uniform Hydrograph, No Diversion – With Sea Level Rise (Run 42)

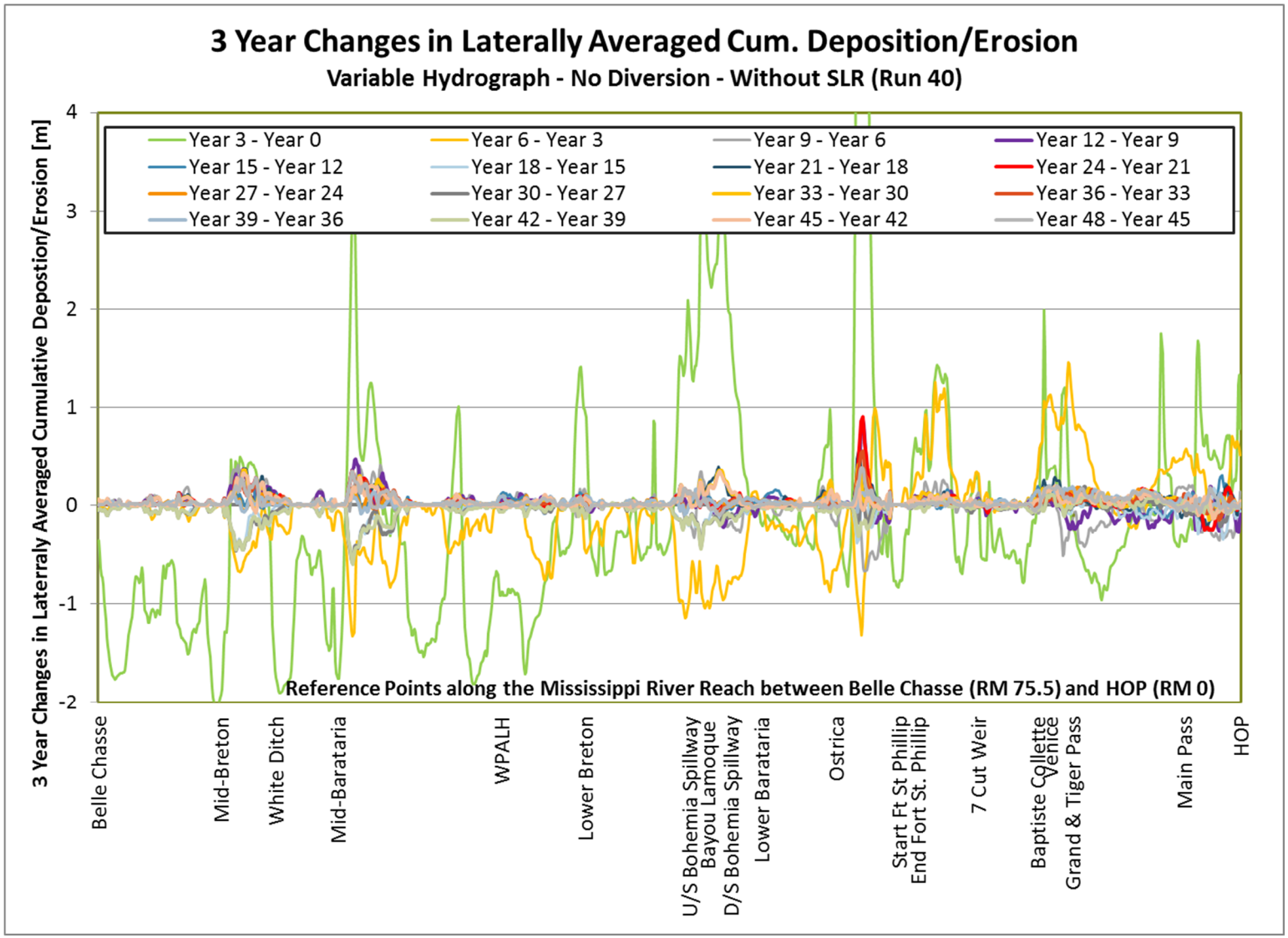

Figure R.3.2.3: 3- Year Changes in Laterally Average Cumulative Deposition/Erosion due to SLR – Variable Hydrograph, No Diversion – Without Sea Level Rise (Run 40)

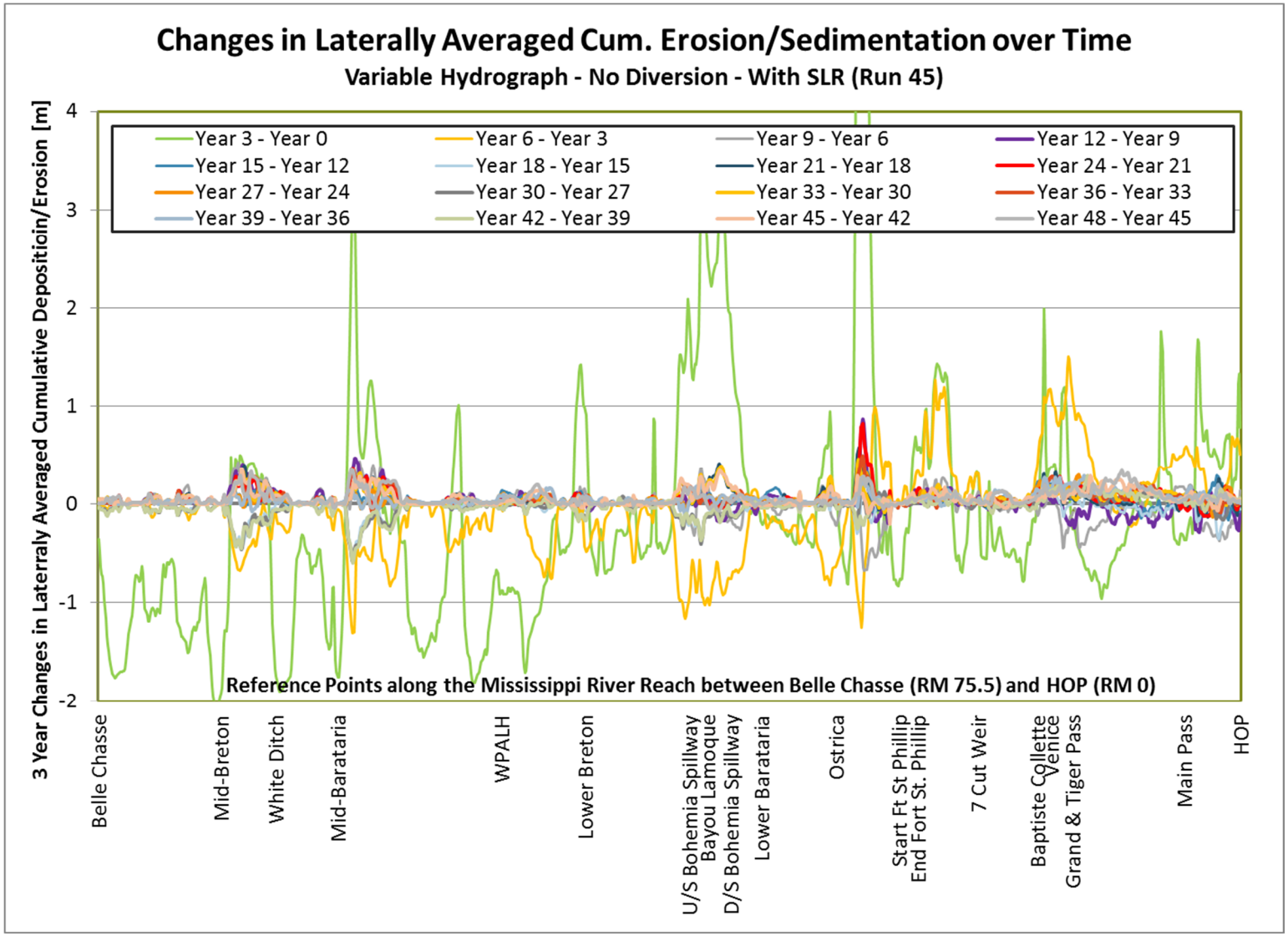

Figure R.3.2.4: 3- Year Changes in Laterally Average Cumulative Deposition/Erosion due to SLR – Variable Hydrograph, No Diversion – With Sea Level Rise (Run 45)

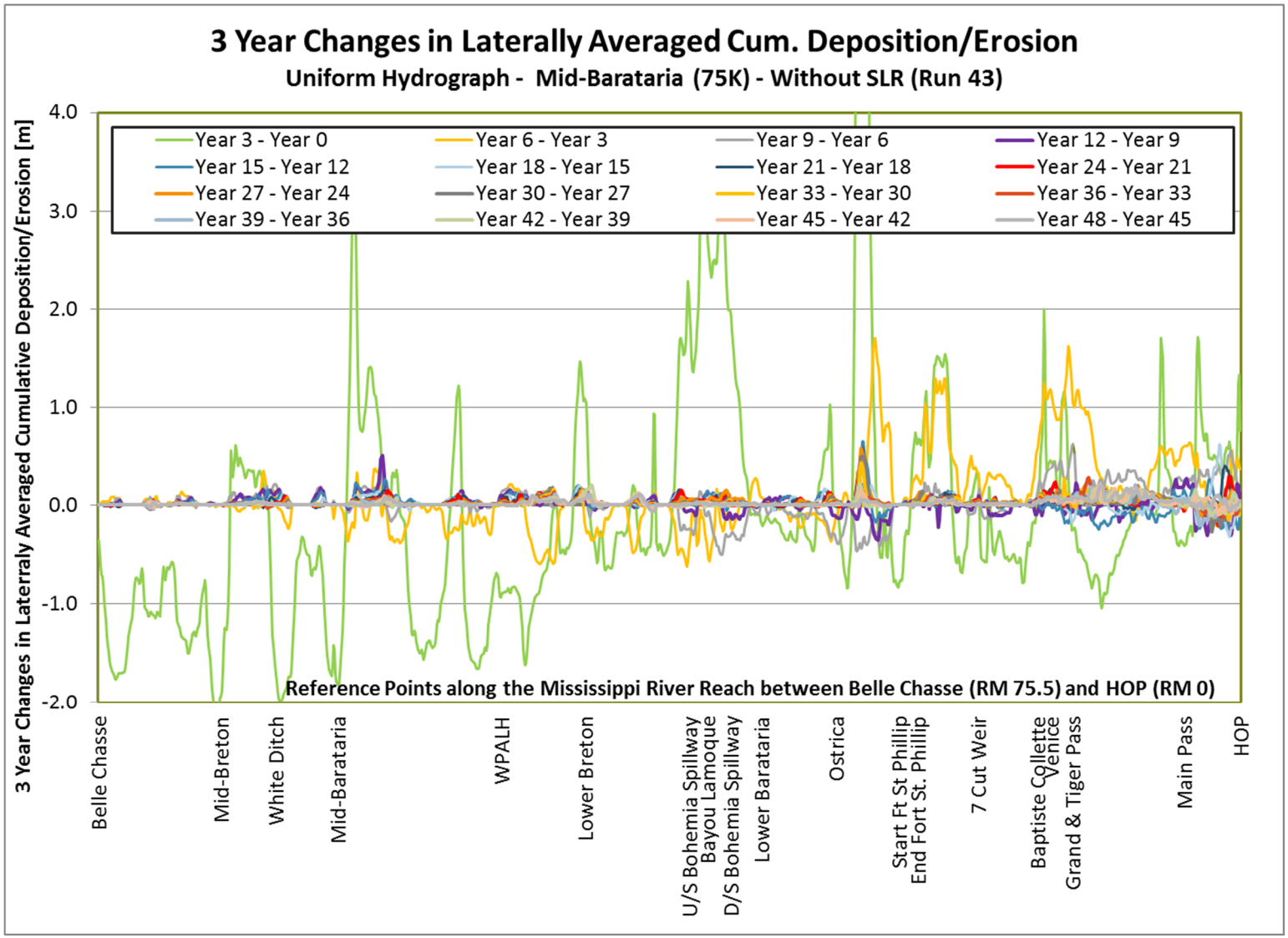

Figure R.3.2.5: 3- Year Changes in Laterally Average Cumulative Deposition/Erosion due to SLR – Uniform Hydrograph, 1 Diversion (Mid-Barataria 75K) – Without Sea Level Rise (Run 43)

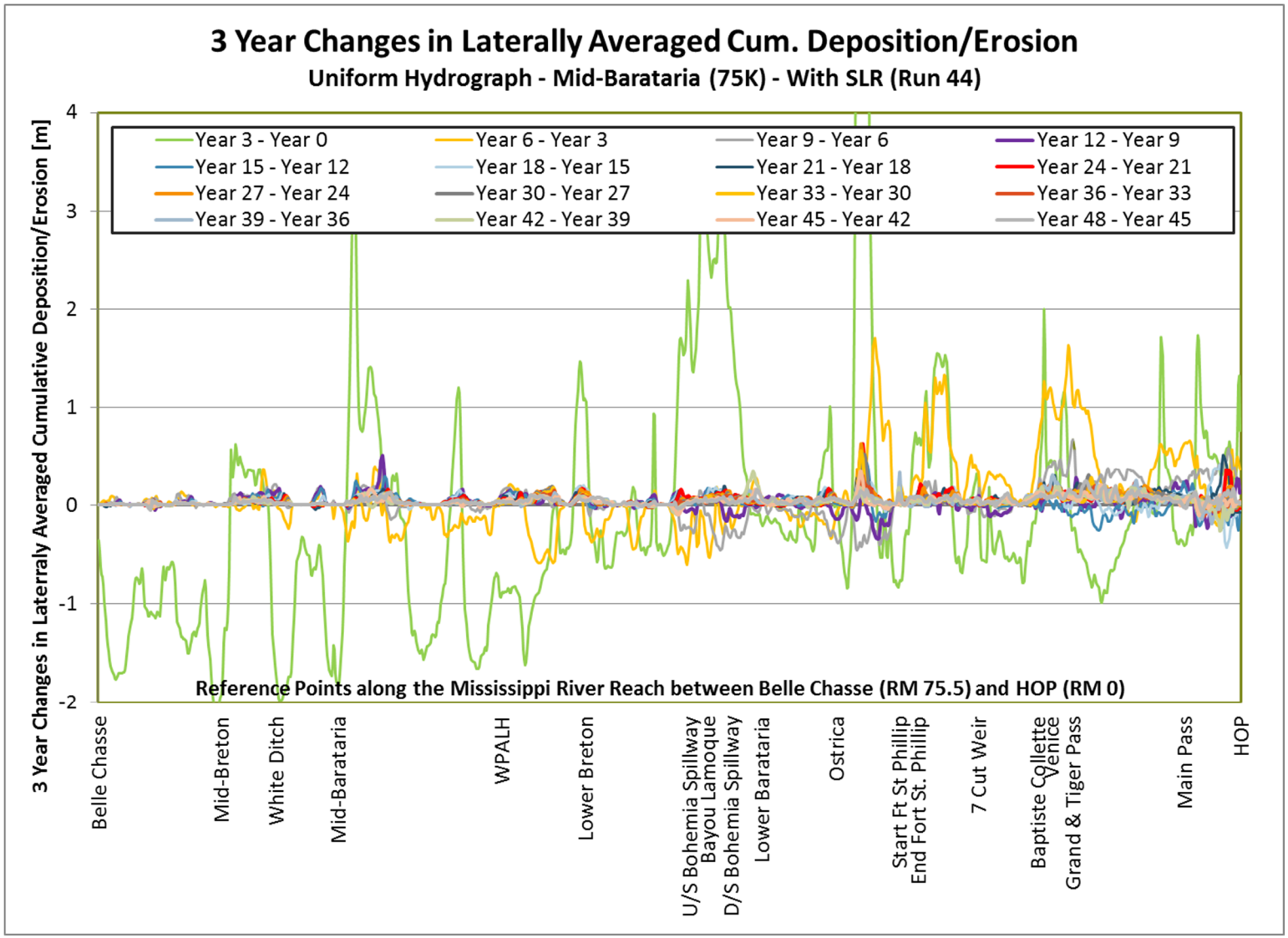

Figure R.3.2.6: 3- Year Changes in Laterally Average Cumulative Deposition/Erosion due to SLR – Uniform Hydrograph, 1 Diversion (Mid-Barataria 75K) – With Sea Level Rise (Run 44)

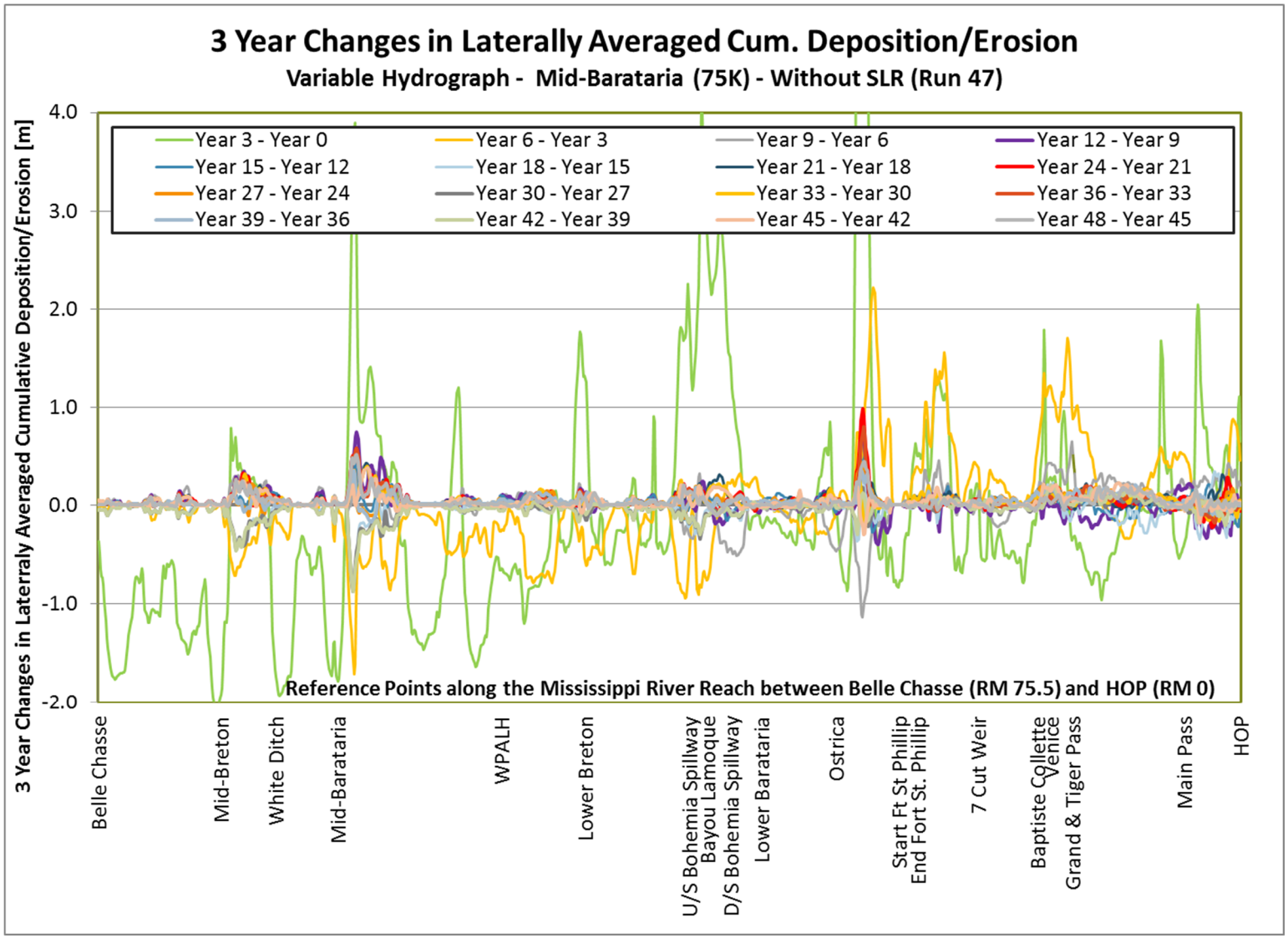

Figure R.3.2.7: 3- Year Changes in Laterally Average Cumulative Deposition/Erosion due to SLR – Variable Hydrograph, 1 Diversion (Mid-Barataria 75K) – Without Sea Level Rise (Run 47)

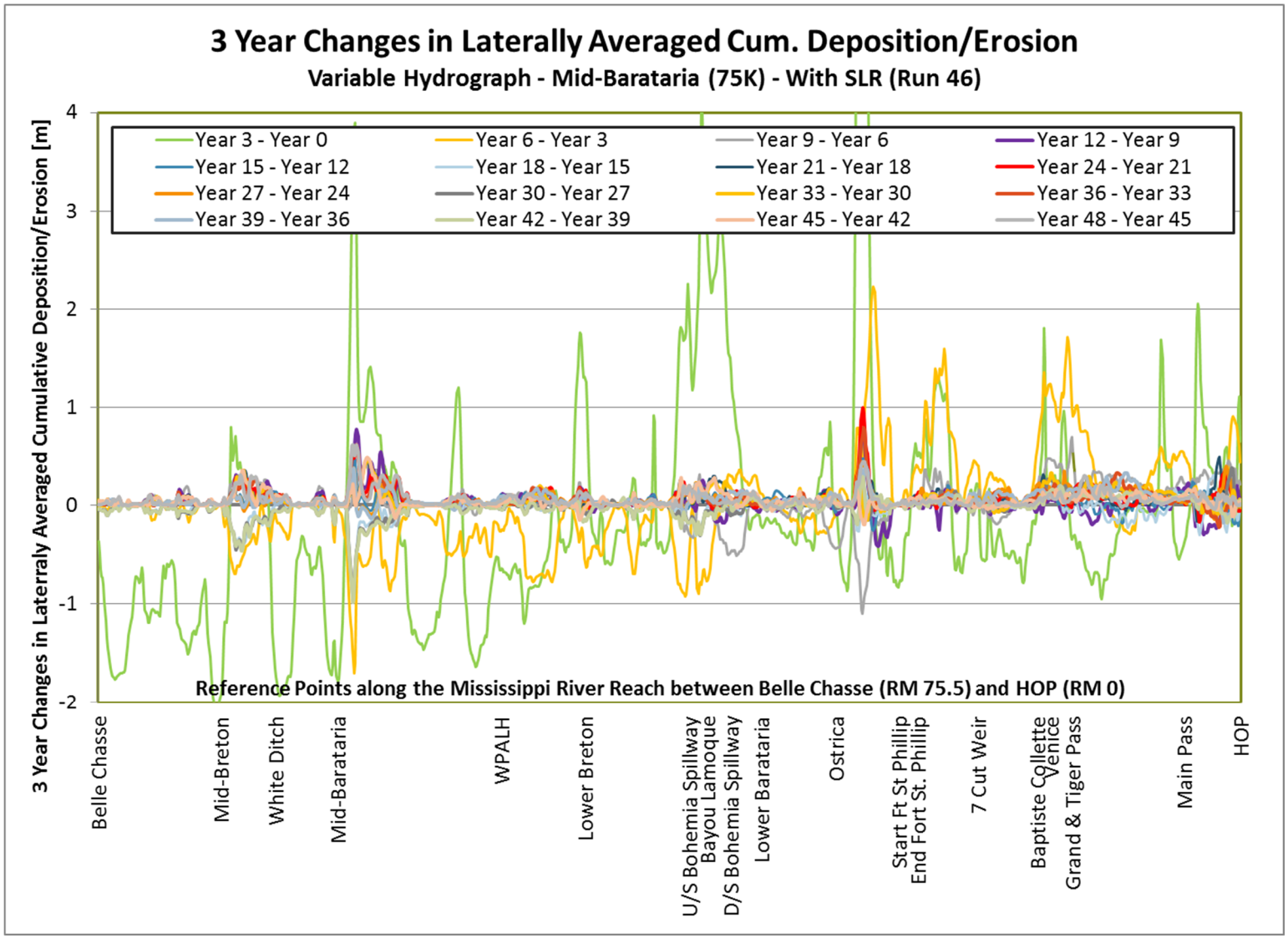

Figure R.3.2.8: L3- Year Changes in Laterally Average Cumulative Deposition/Erosion due to SLR – Variable Hydrograph, 1 Diversion (Mid-Barataria 75K) – With Sea Level Rise (Run 46)

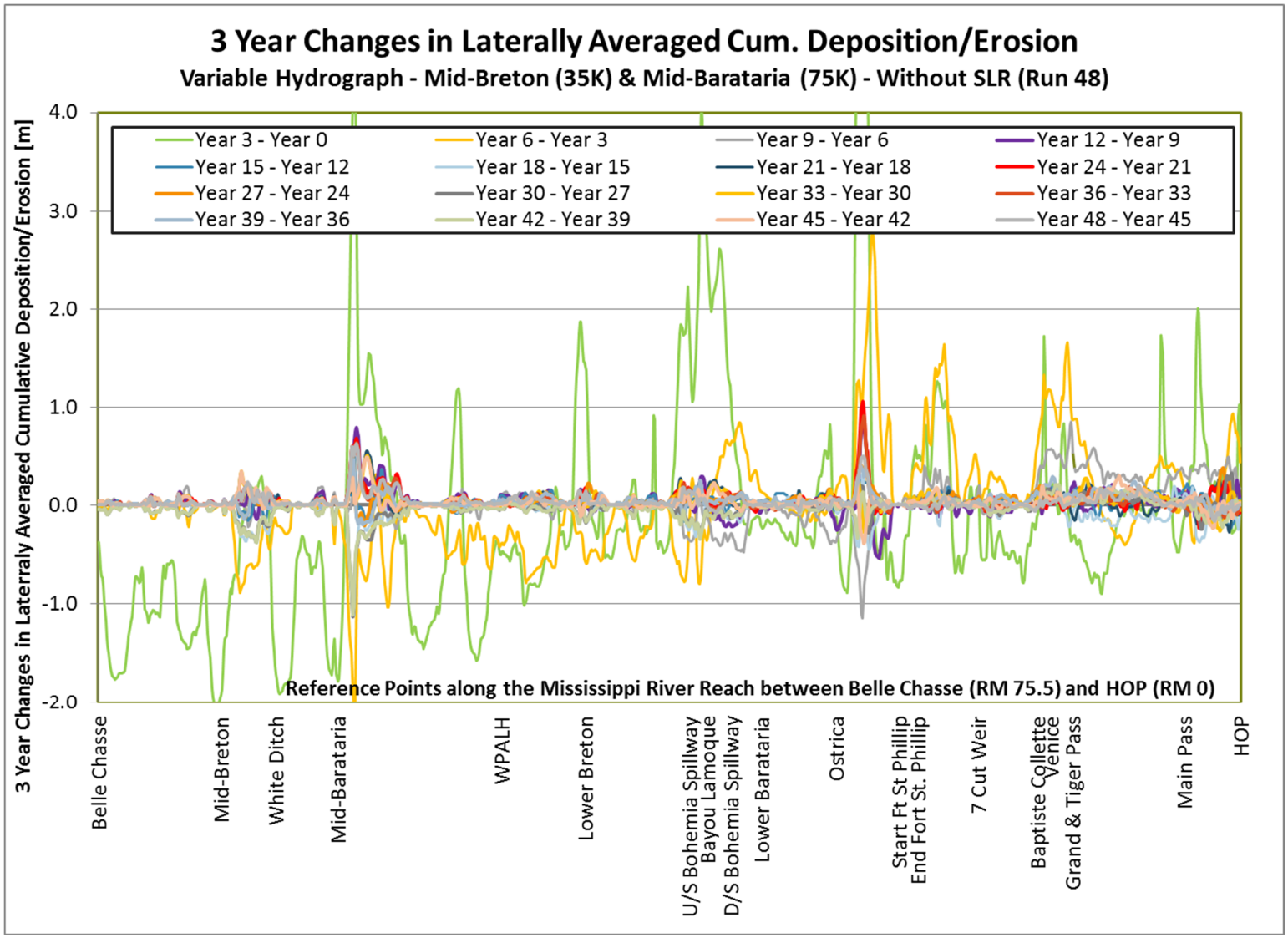

Figure R.3.2.9: 3- Year Changes in Laterally Average Cumulative Deposition/Erosion due to SLR – Variable Hydrograph, 2 Diversions (Mid-Breton 35K & Mid-Barataria 75K) – Without Sea Level Rise (Run 48)

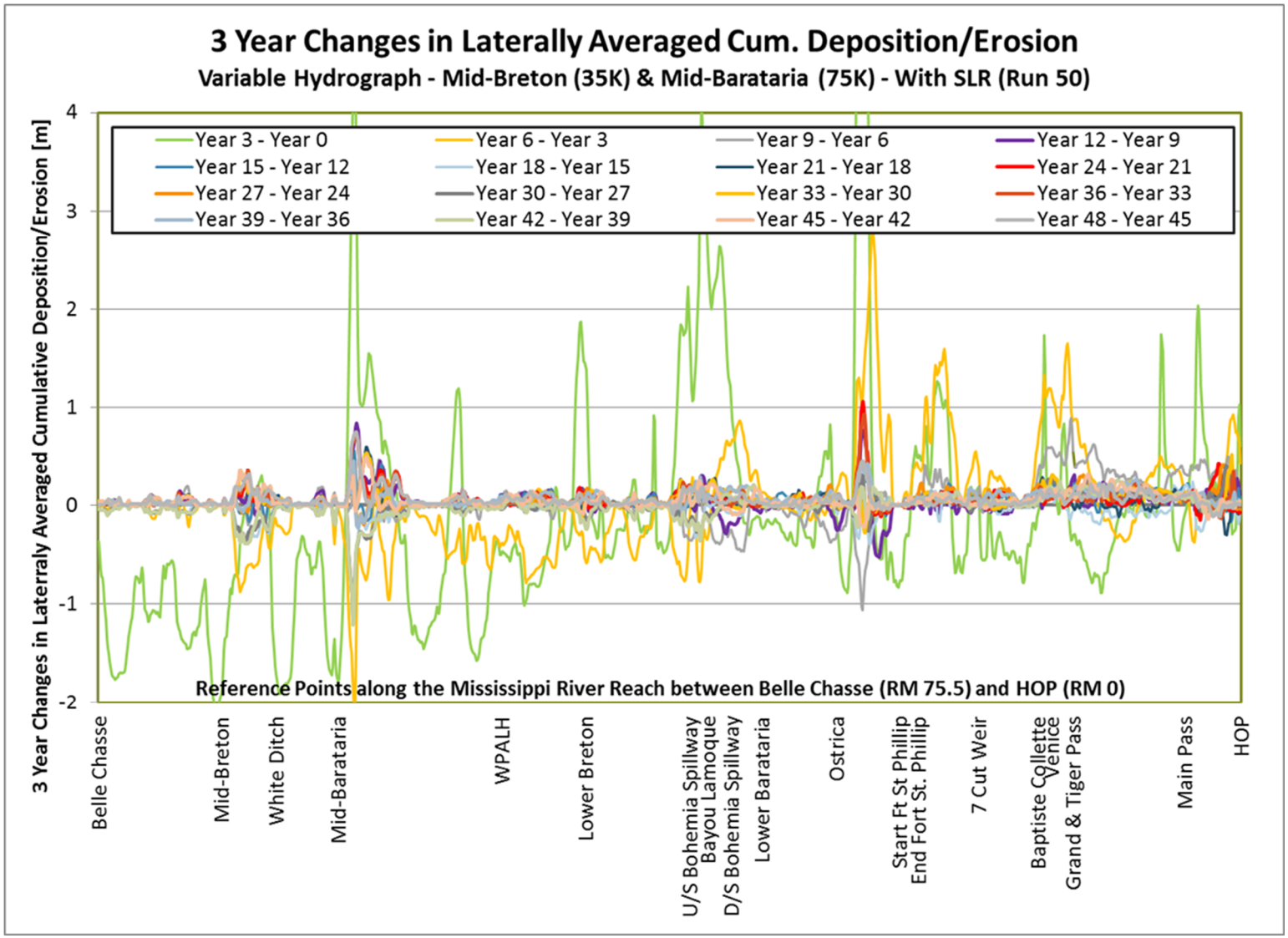

Figure R.3.2.10: 3- Year Changes in Laterally Average Cumulative Deposition/Erosion due to SLR – Variable Hydrograph, 2 Diversions (Mid-Breton & Mid-Barataria 75K) – With Sea Level Rise (Run 50)

APPENDIX R3.3.1

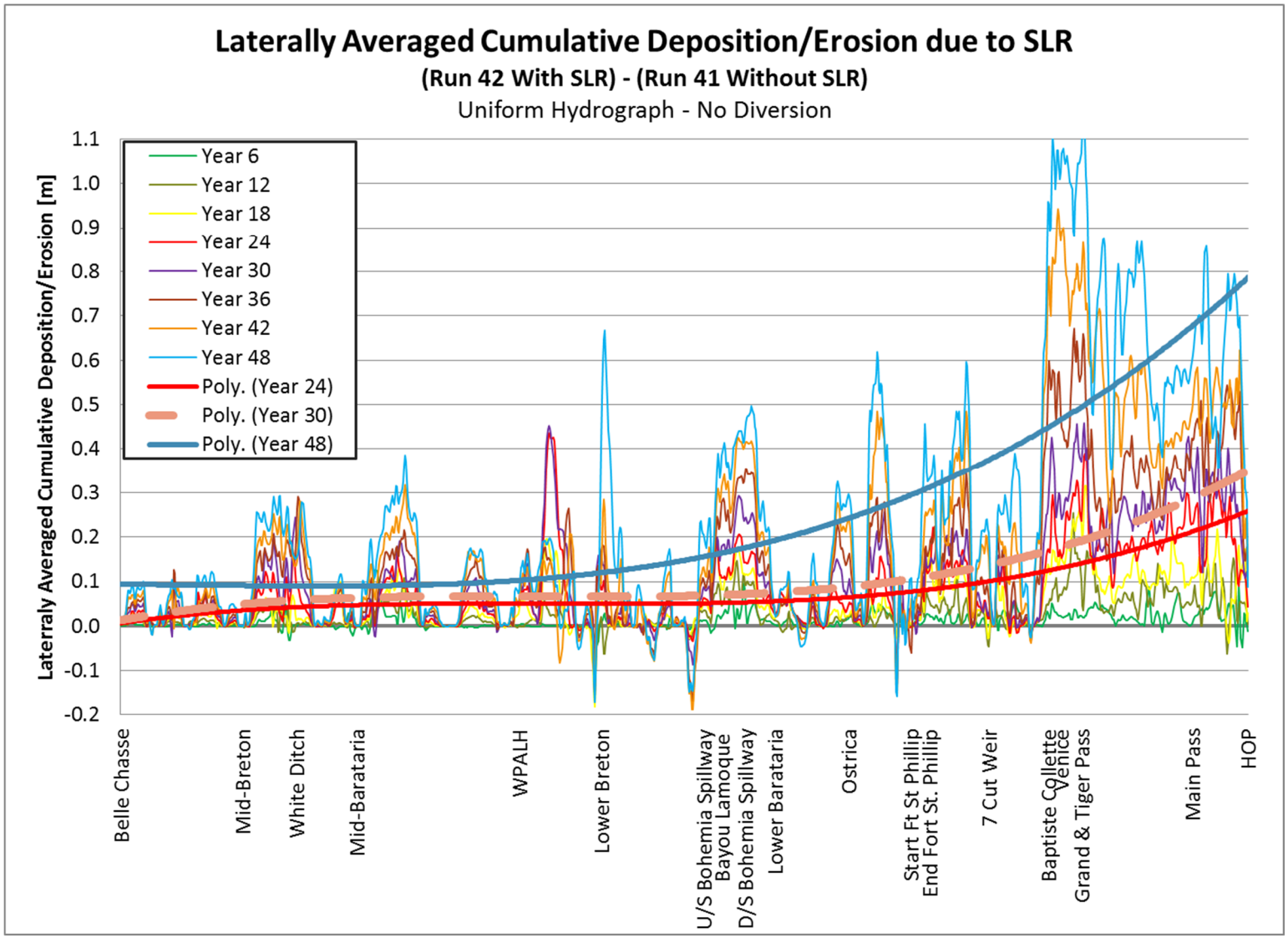

Figure 7.3.3.2.1: Laterally Average Cumulative Deposition/Erosion due to SLR – Uniform Hydrograph - No Diversion

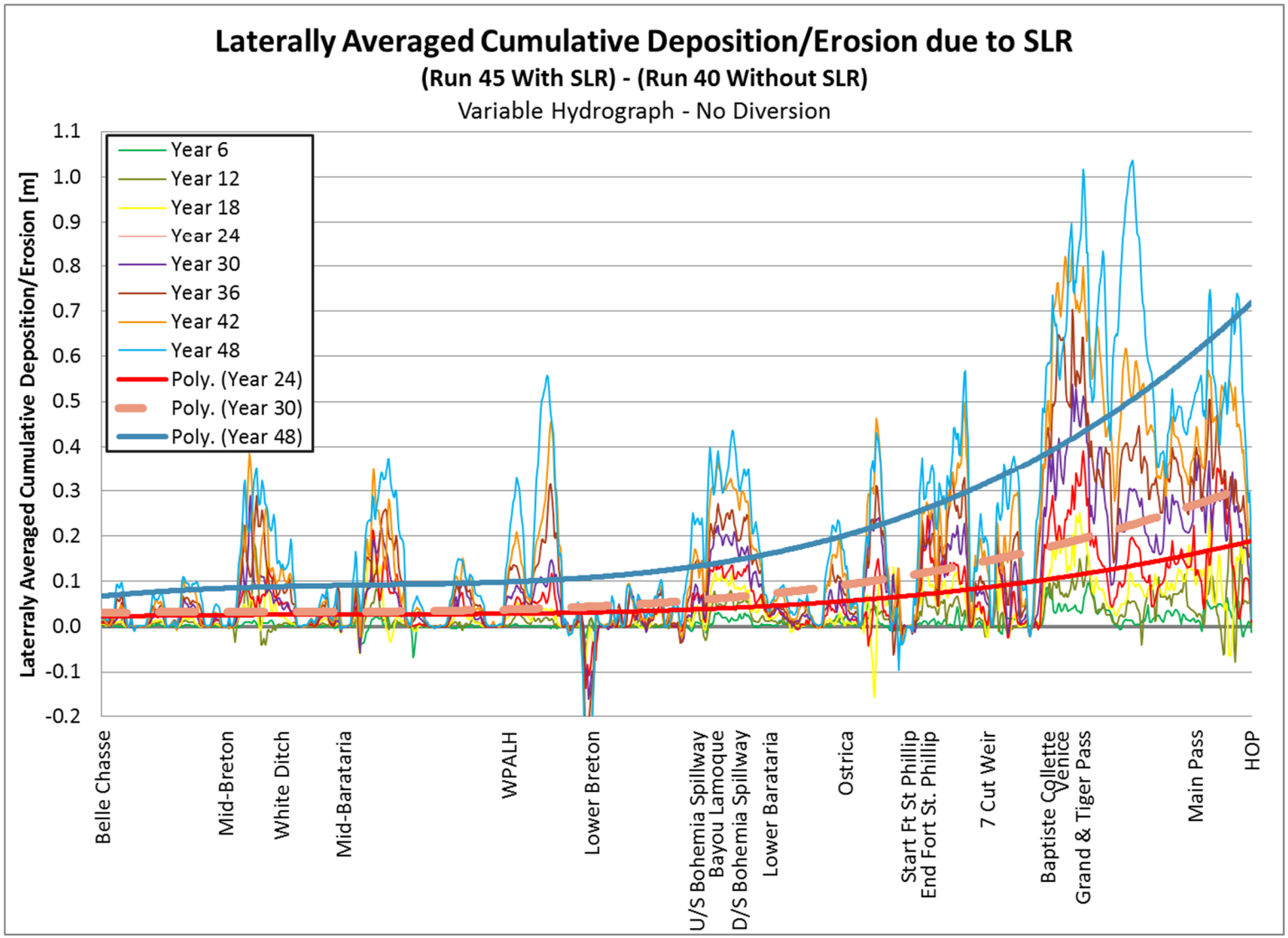

Figure 7.3.3.2.2: Laterally Average Cumulative Deposition/Erosion due to SLR – Variable Hydrograph - No Diversion

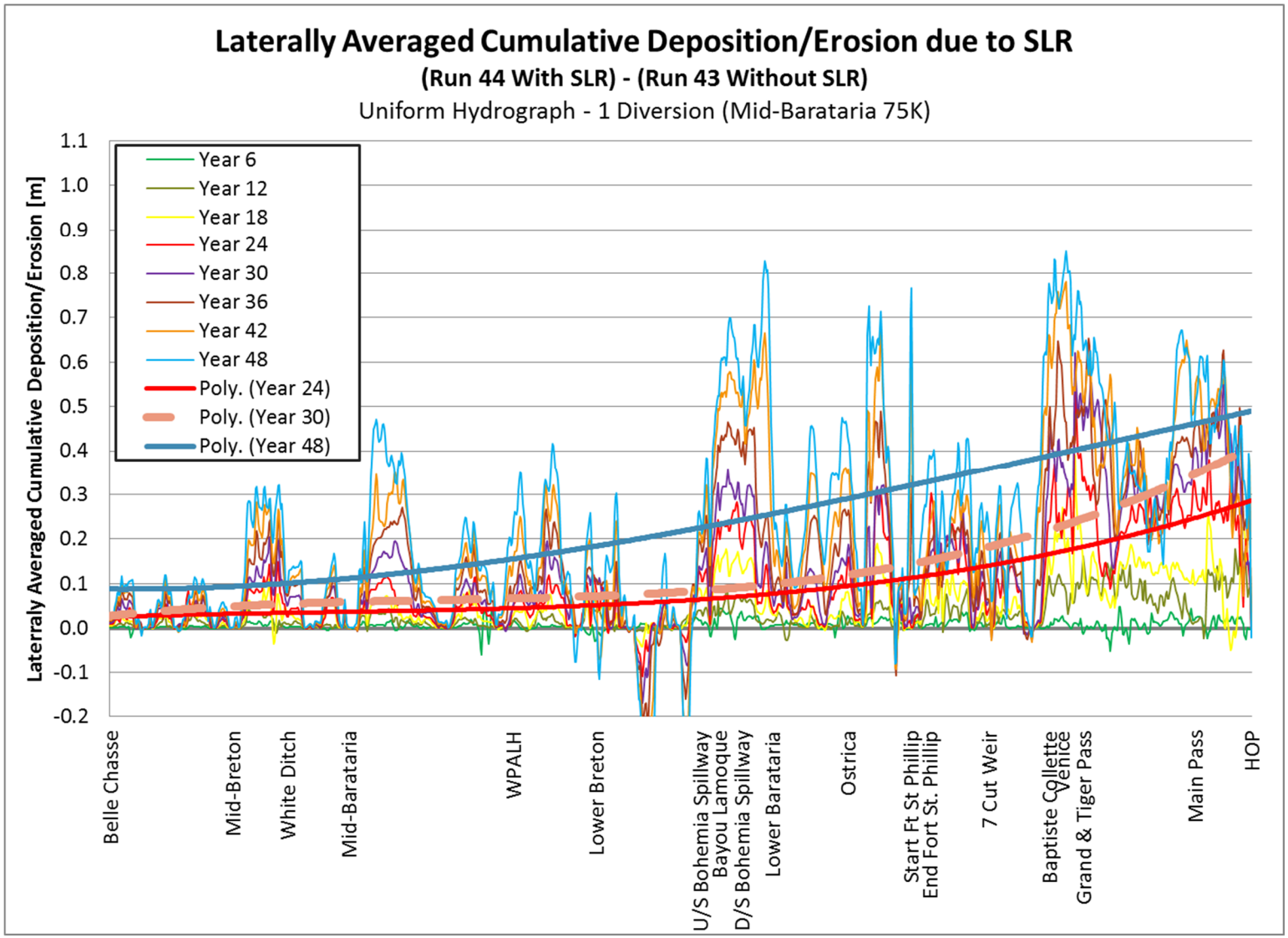

Figure 7.3.3.2.3: Laterally Average Cumulative Deposition/Erosion due to SLR – Uniform Hydrograph - 1 Diversion (Mid-Barataria 75K)

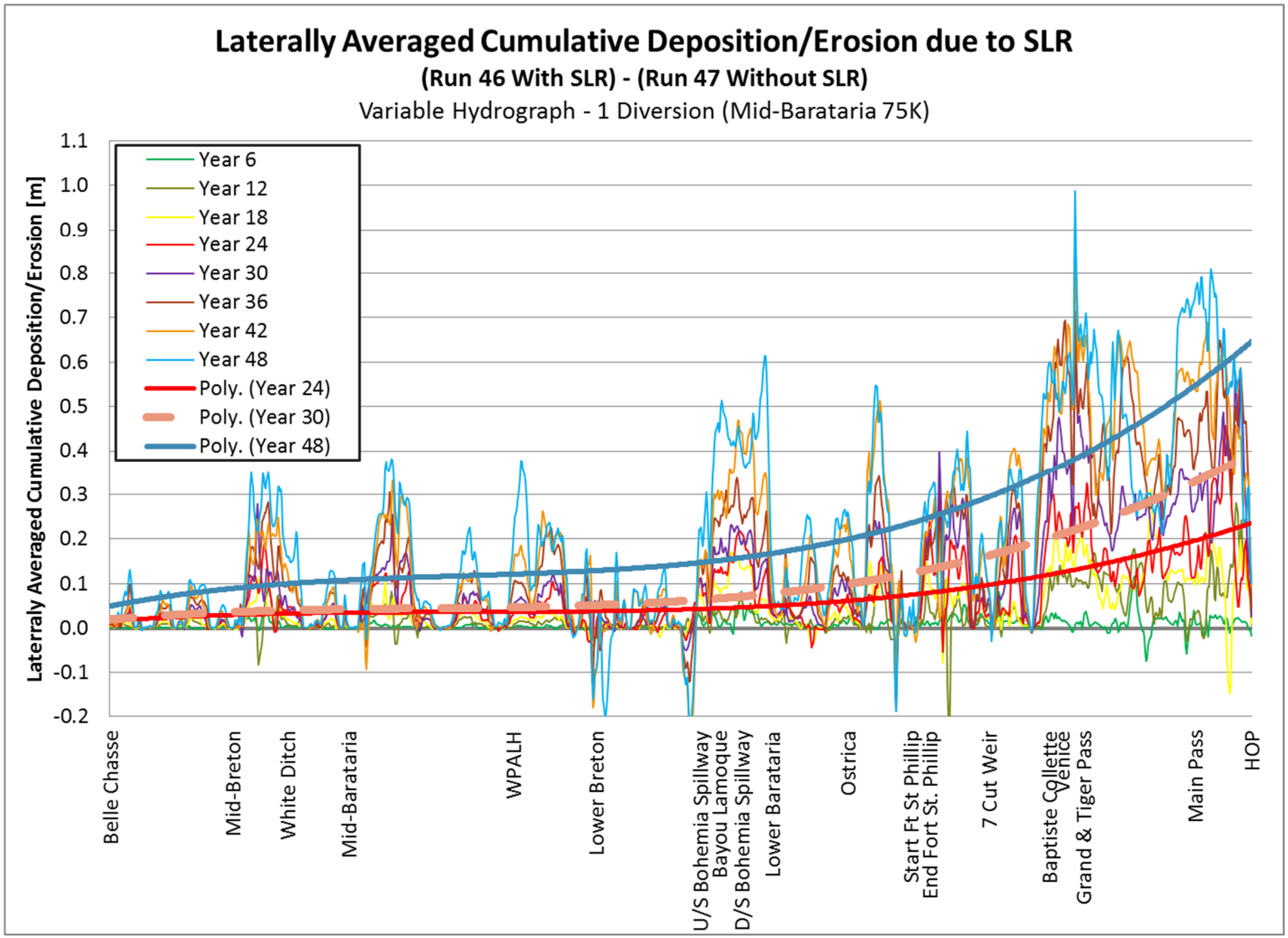

Figure 7.3.3.2.4: Laterally Average Cumulative Deposition/Erosion due to SLR – Variable Hydrograph - 1 Diversion (Mid-Barataria 75K)

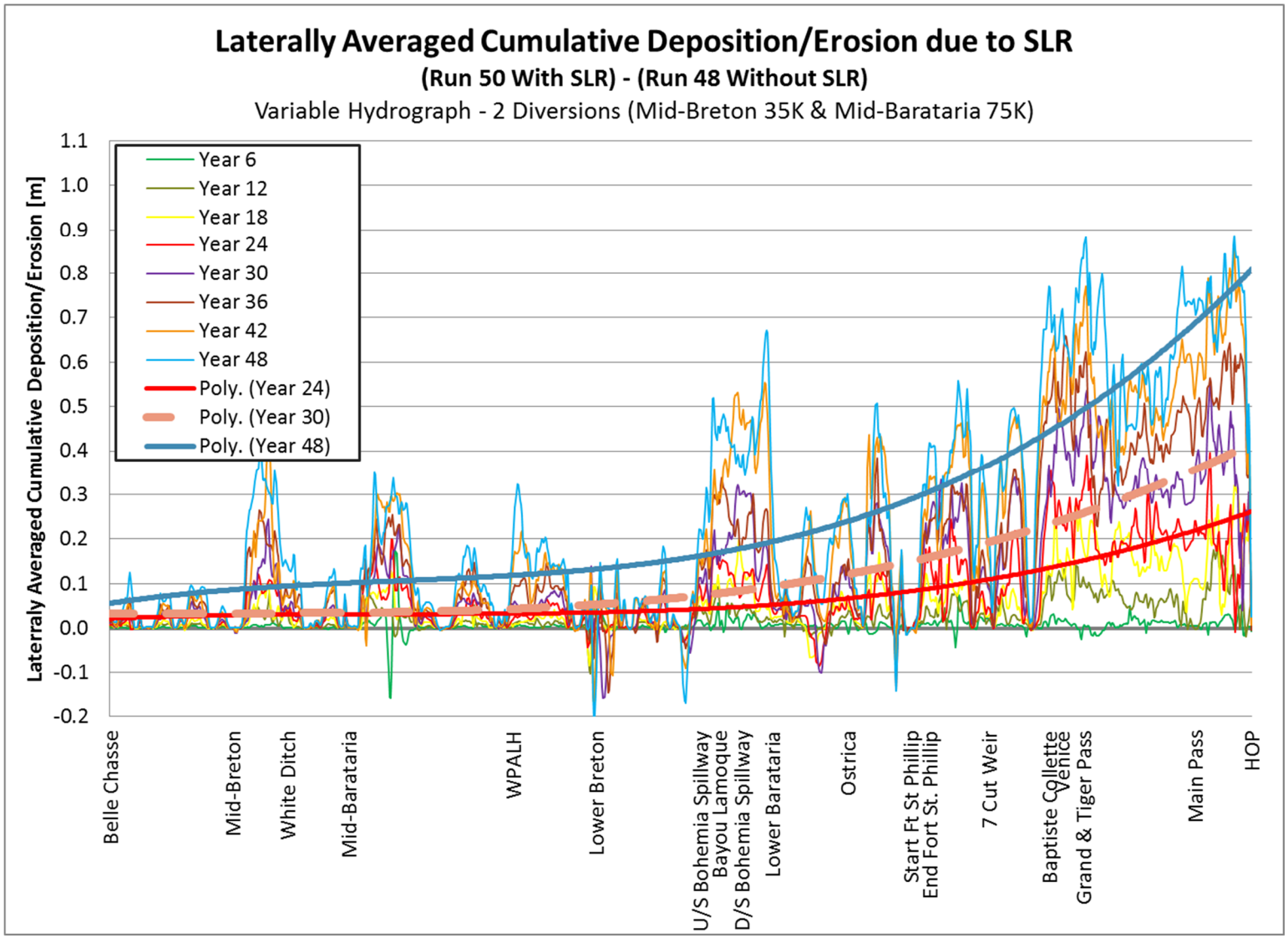

Figure 7.3.3.2.5: Laterally Average Cumulative Deposition/Erosion due to SLR – Variable Hydrograph - 2 Diversions (Mid-Breton 35K & Mid-Barataria 75K)

APPENDIX R3.3.2

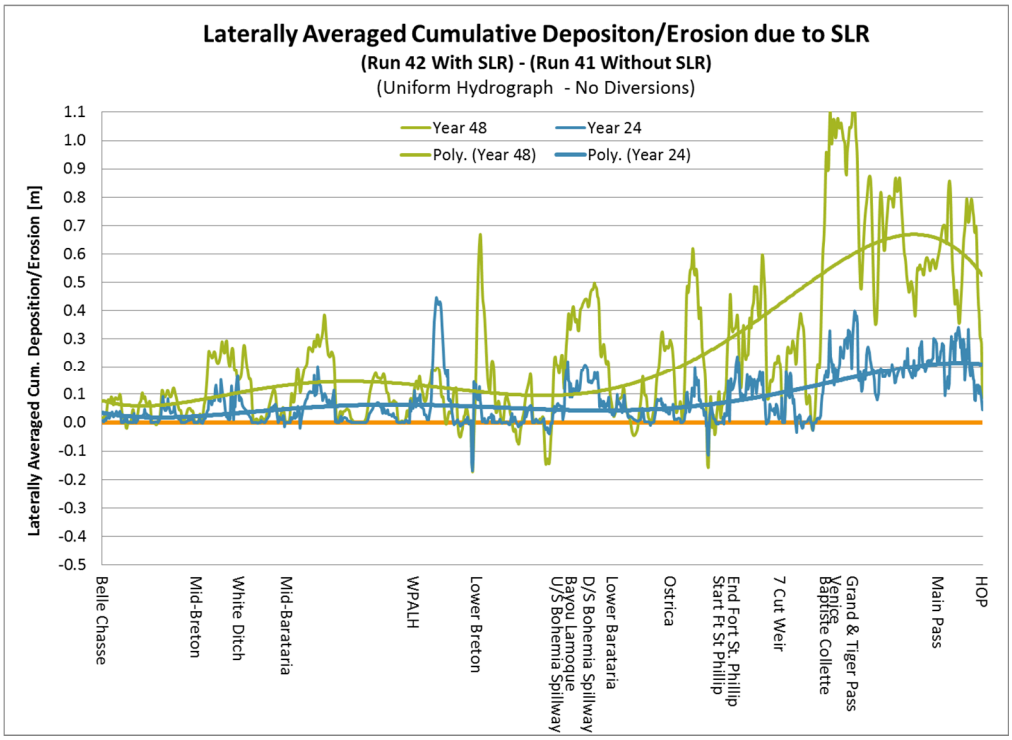

Figure 7.3.3.2.6: Laterally Averaged Cumulative Deposition/Erosion due to SLR (Uniform Hydrograph – No Diversions)

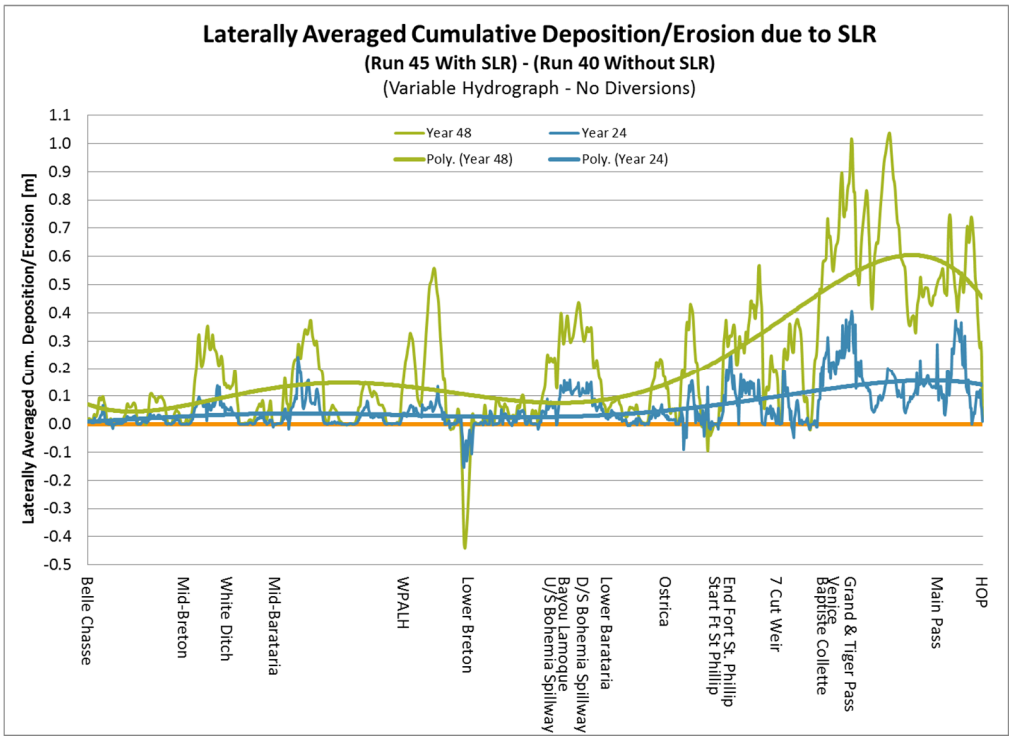

Figure 7.3.3.2.7: Laterally Averaged Cumulative Deposition/Erosion due to SLR (Variable Hydrograph – No Diversions)

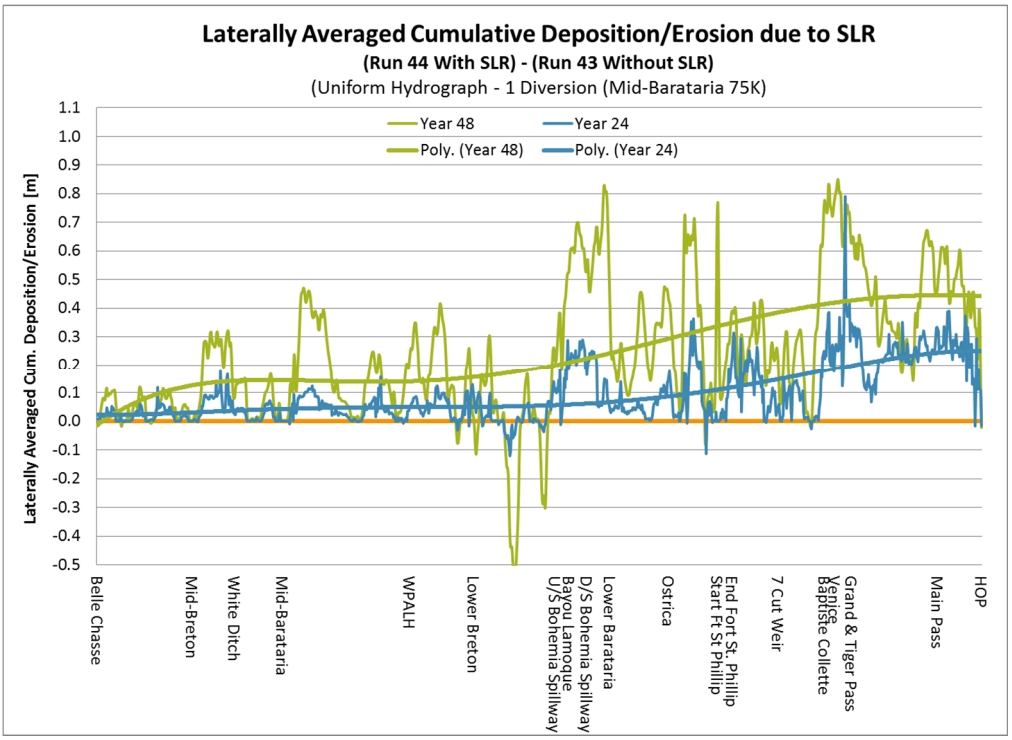

Figure 7.3.3.2.8: Laterally Averaged Cumulative Deposition/Erosion due to SLR (Uniform Hydrograph – 1 Diversion (Mid-Barataria 75K))

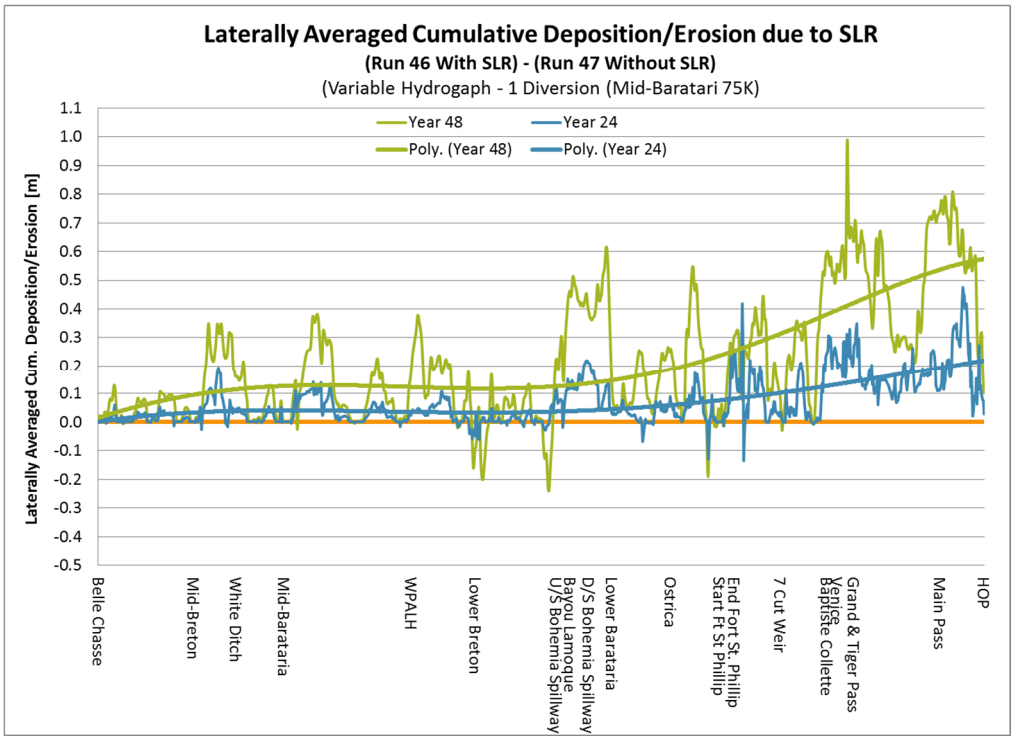

Figure 7.3.3.2.9: Laterally Averaged Cumulative Deposition/Erosion due to SLR (Variable Hydrograph – 1 Diversion (Mid-Barataria 75K))

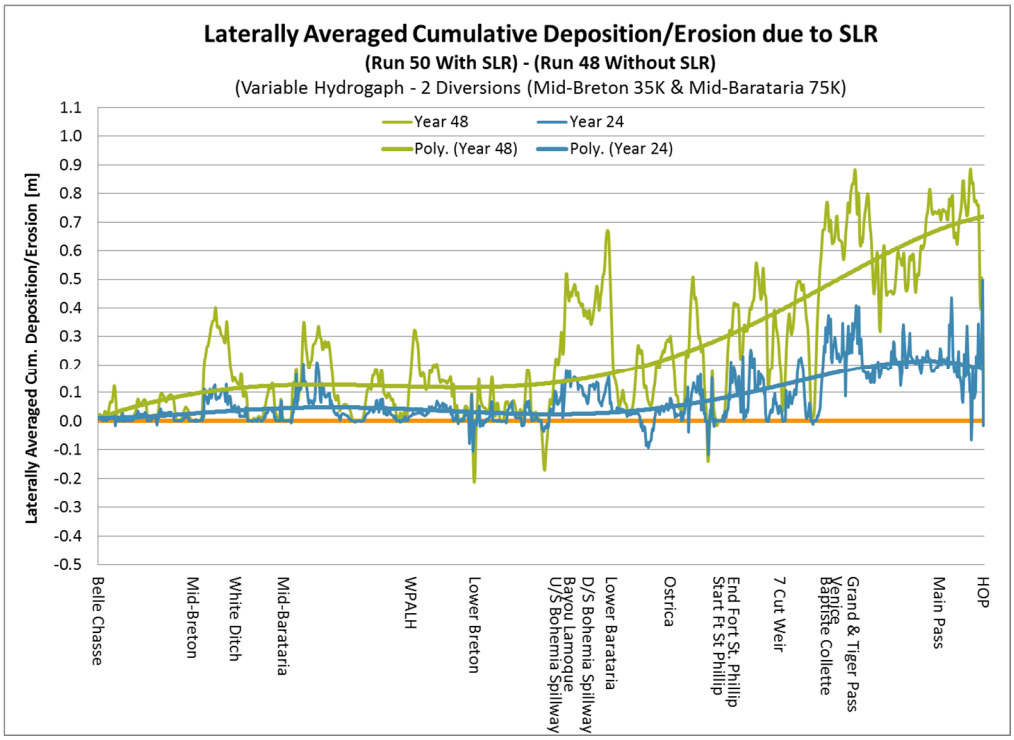

Figure 7.3.3.2.10: Laterally Averaged Cumulative Deposition/Erosion due to SLR (Variable Hydrograph – 2 Diversions (Mid-Breton 35K & Mid-Barataria 75K))

APPENDIX R4

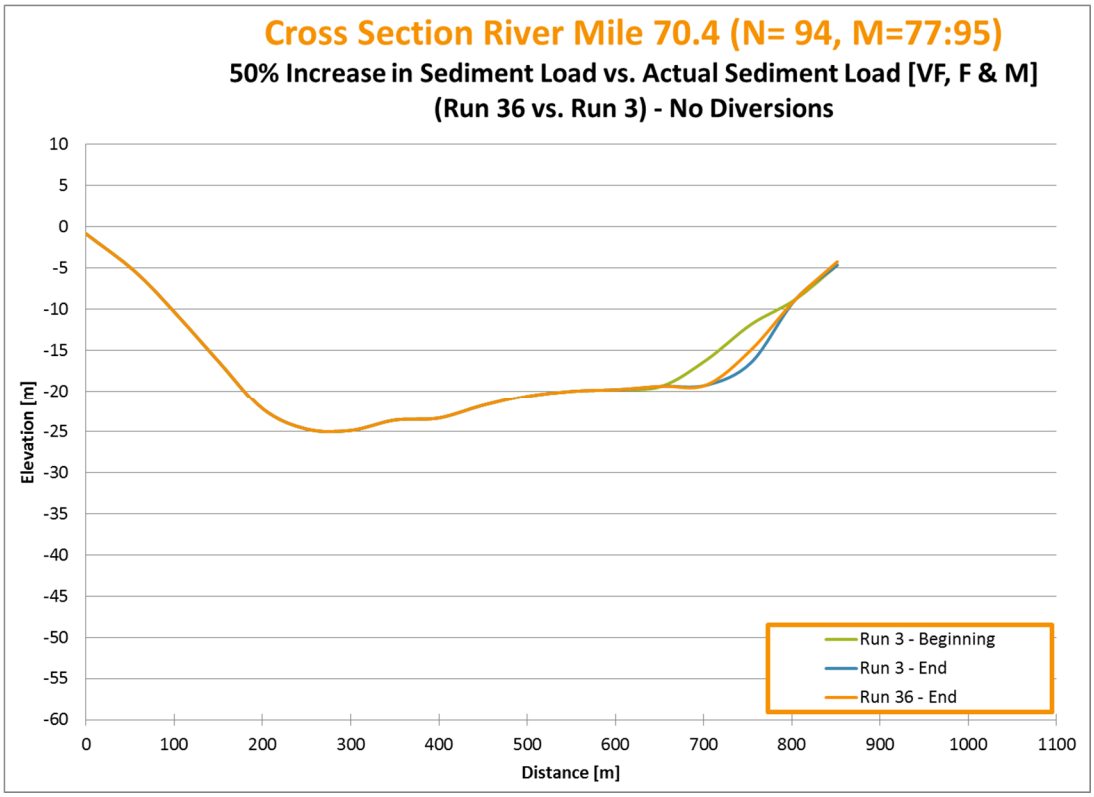

Figure R.4.1: Cross Section River Mile 70.4

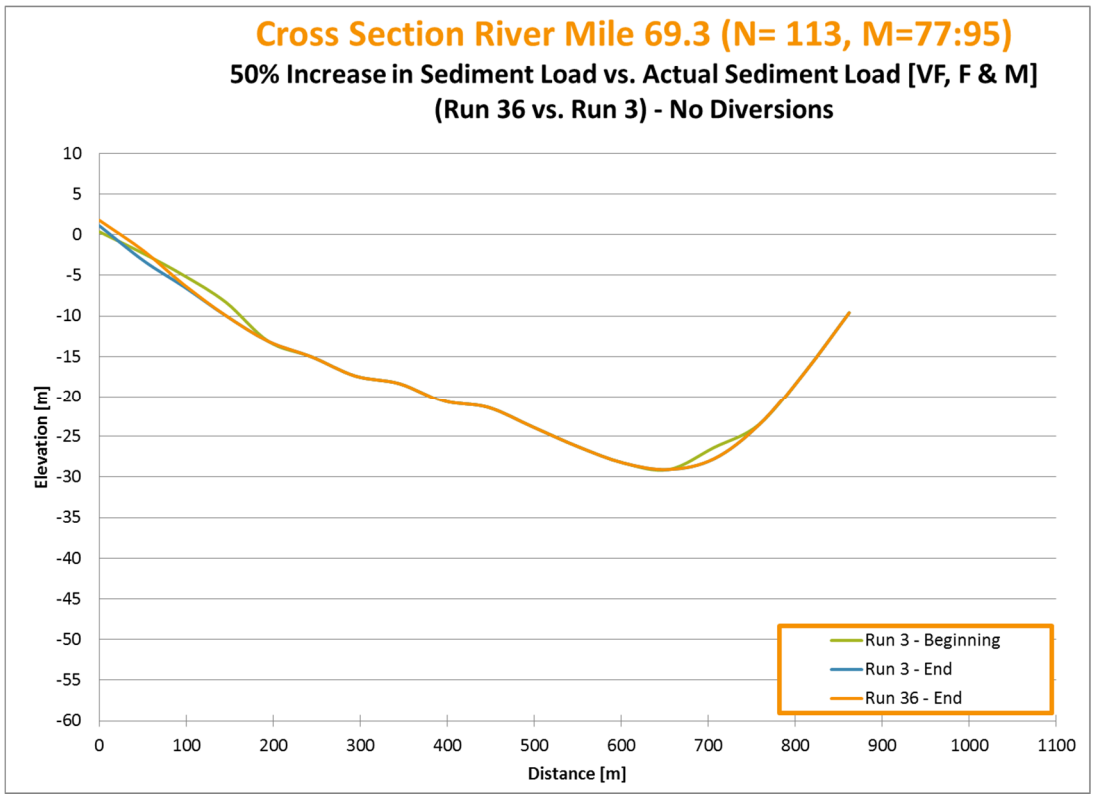

Figure R.4.2: Cross Section River Mile 69.3

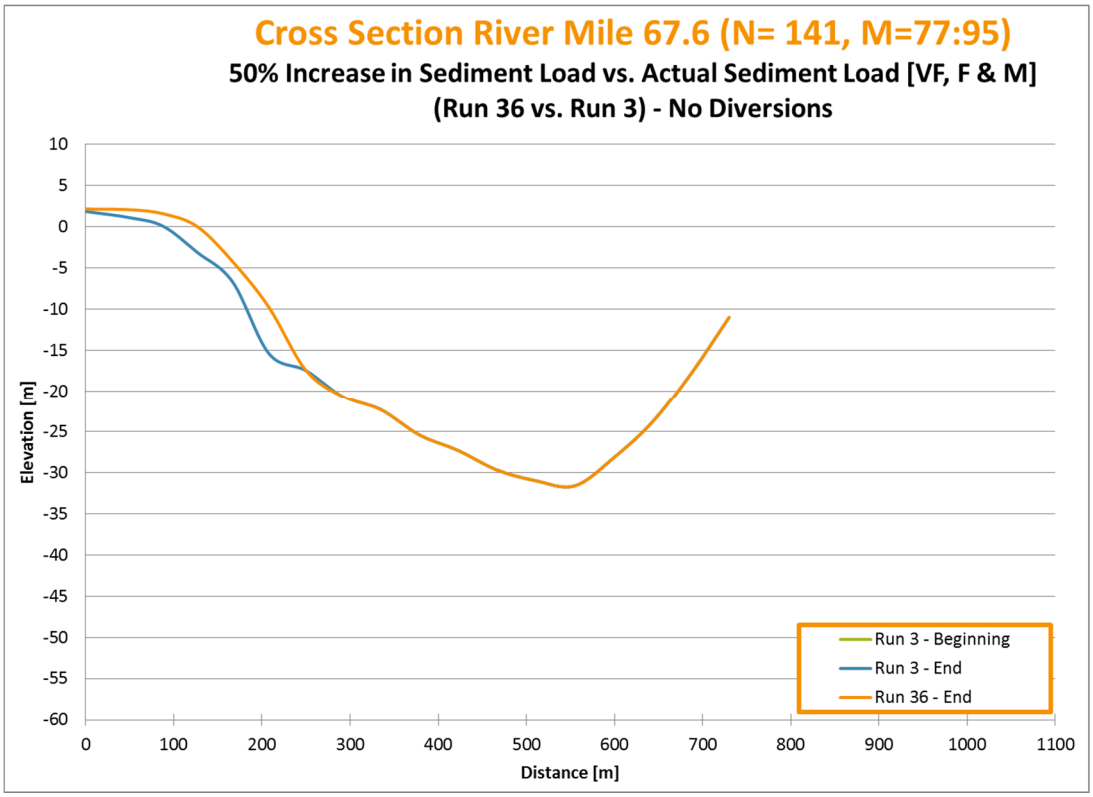

Figure R.4.3: Cross Section River Mile 67.6

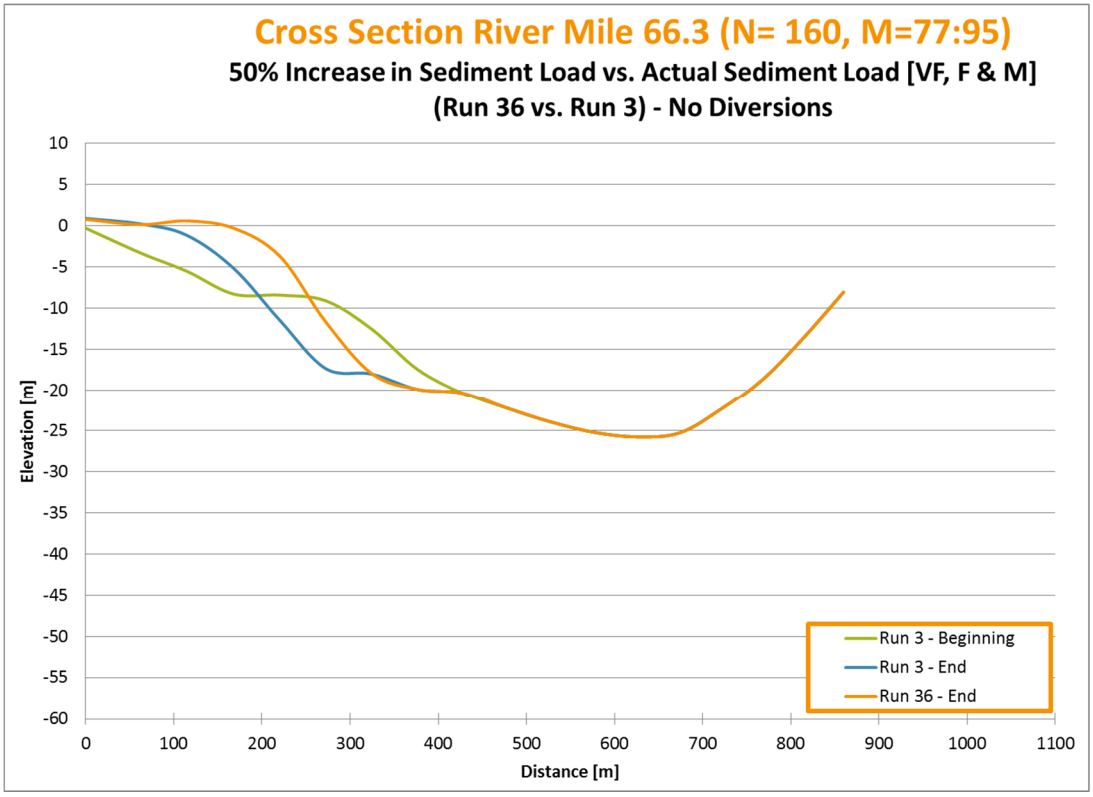

Figure R.4.4: Cross Section River Mile 66.3

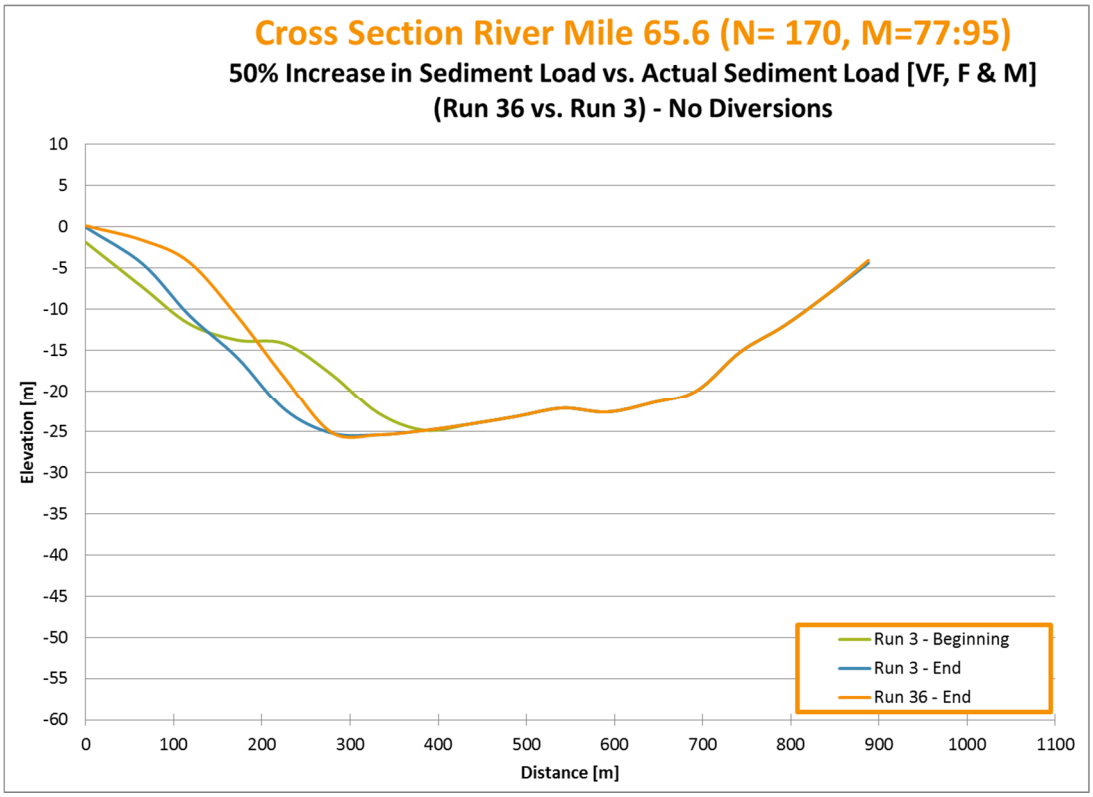

Figure R.4.5: Cross Section River Mile 65.6

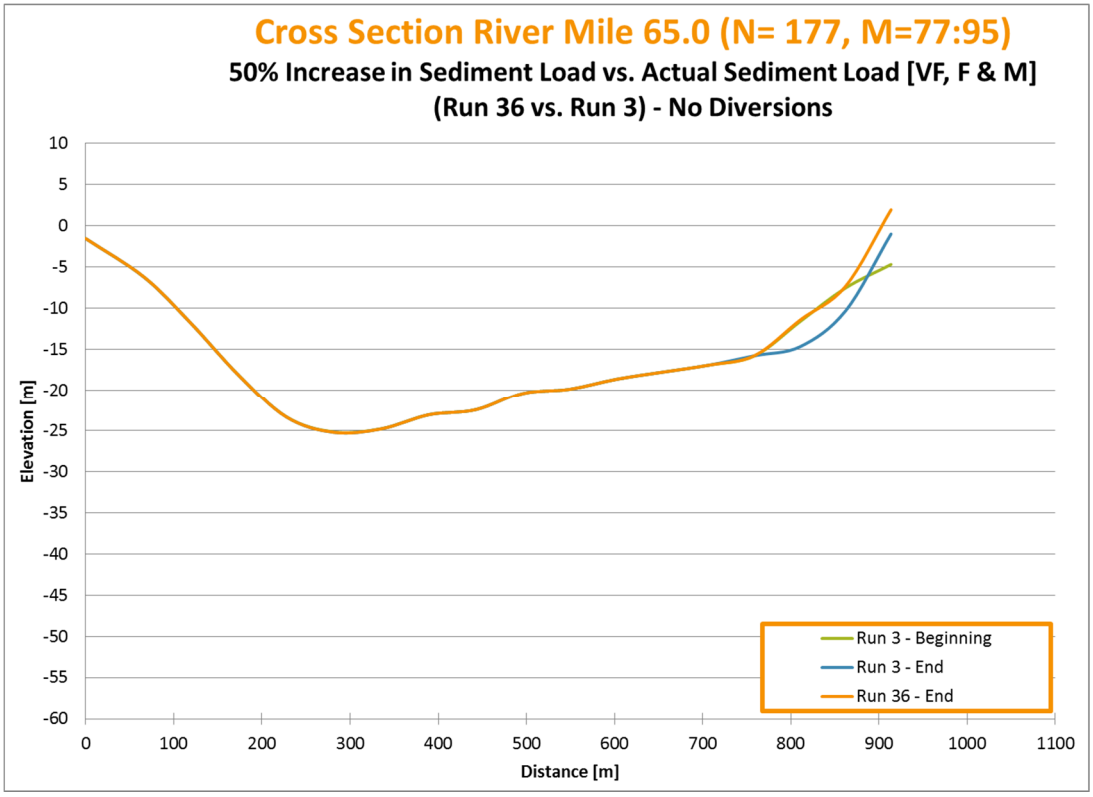

Figure R.4.6: Cross Section River Mile 65.0

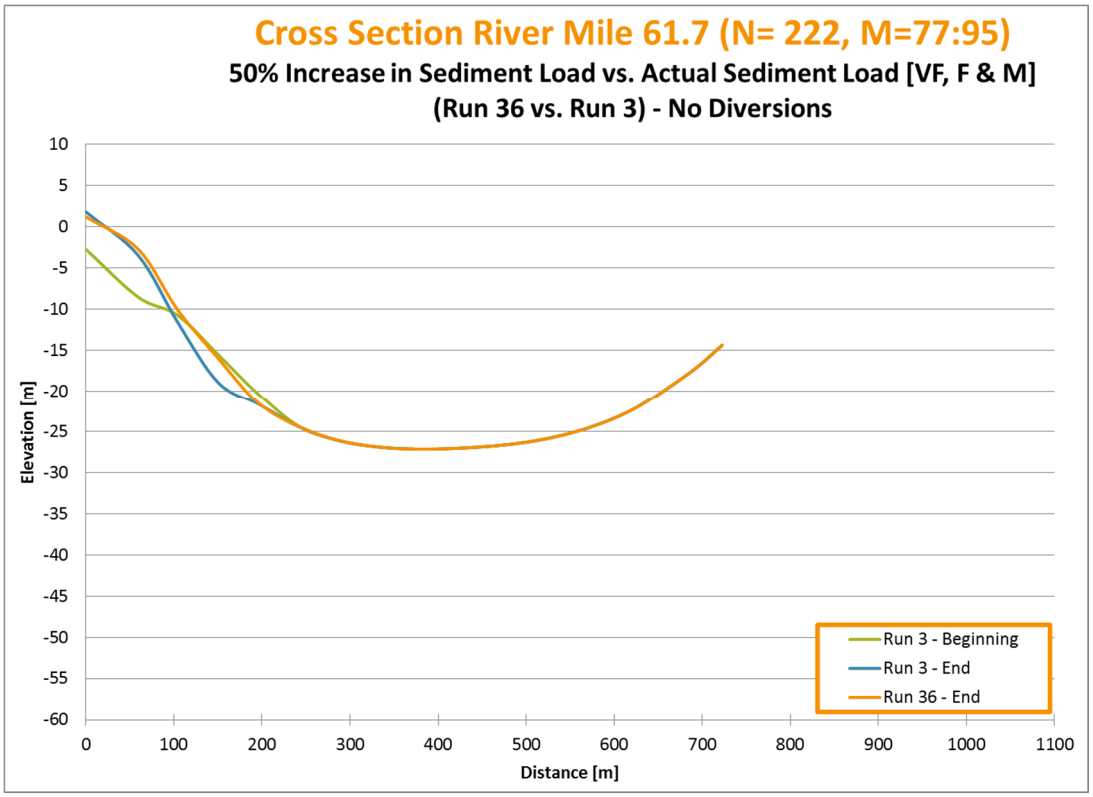

Figure R.4.7: Cross Section River Mile 61.7

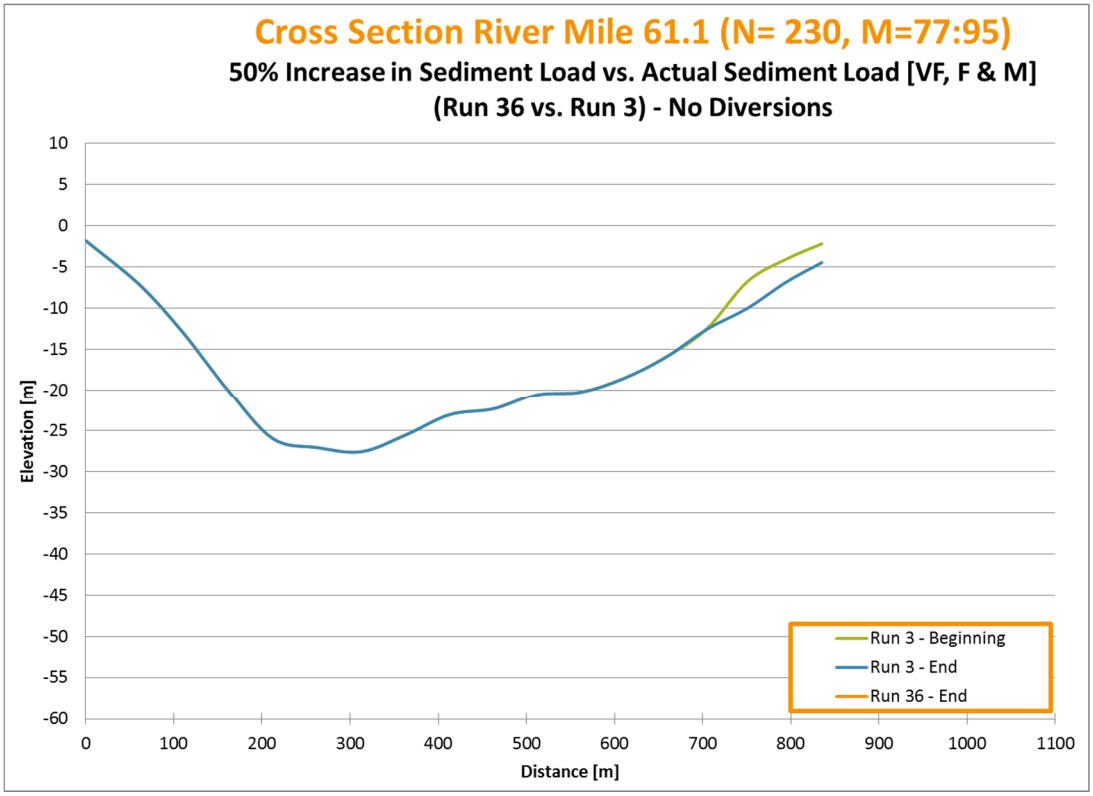

Figure R.4.8: Cross Section River Mile 61.1

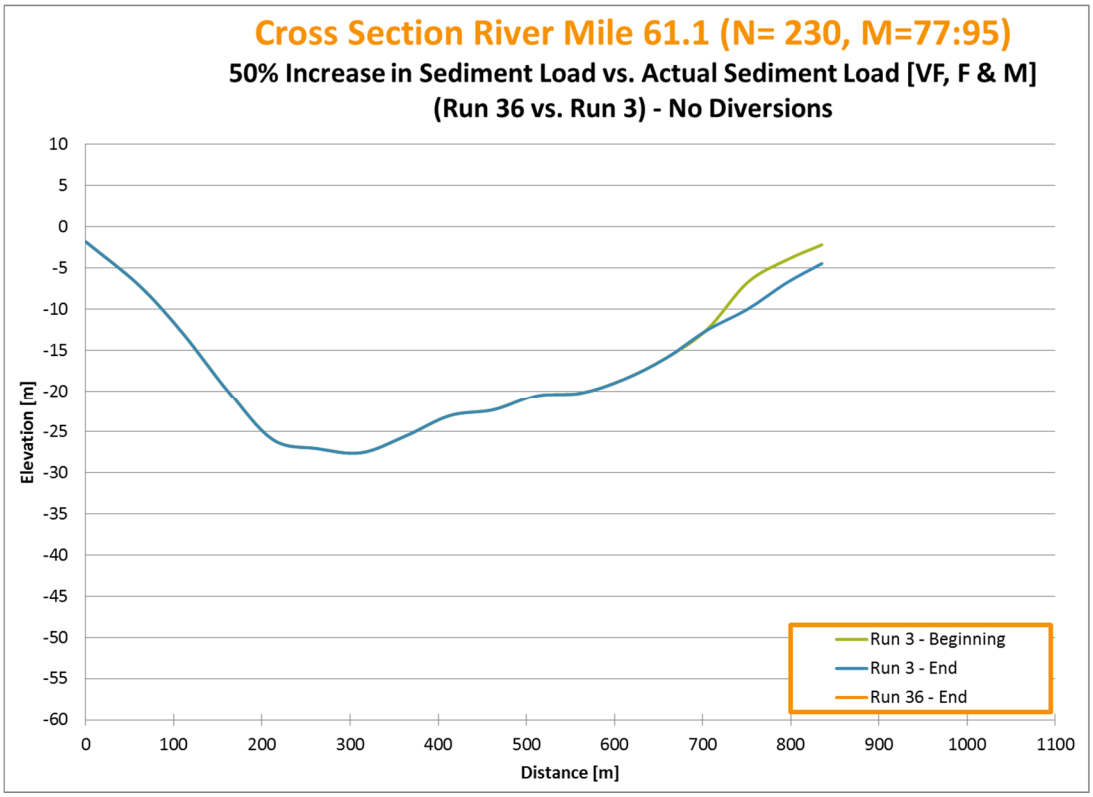

Figure R.4.9: Cross Section River Mile 61.1

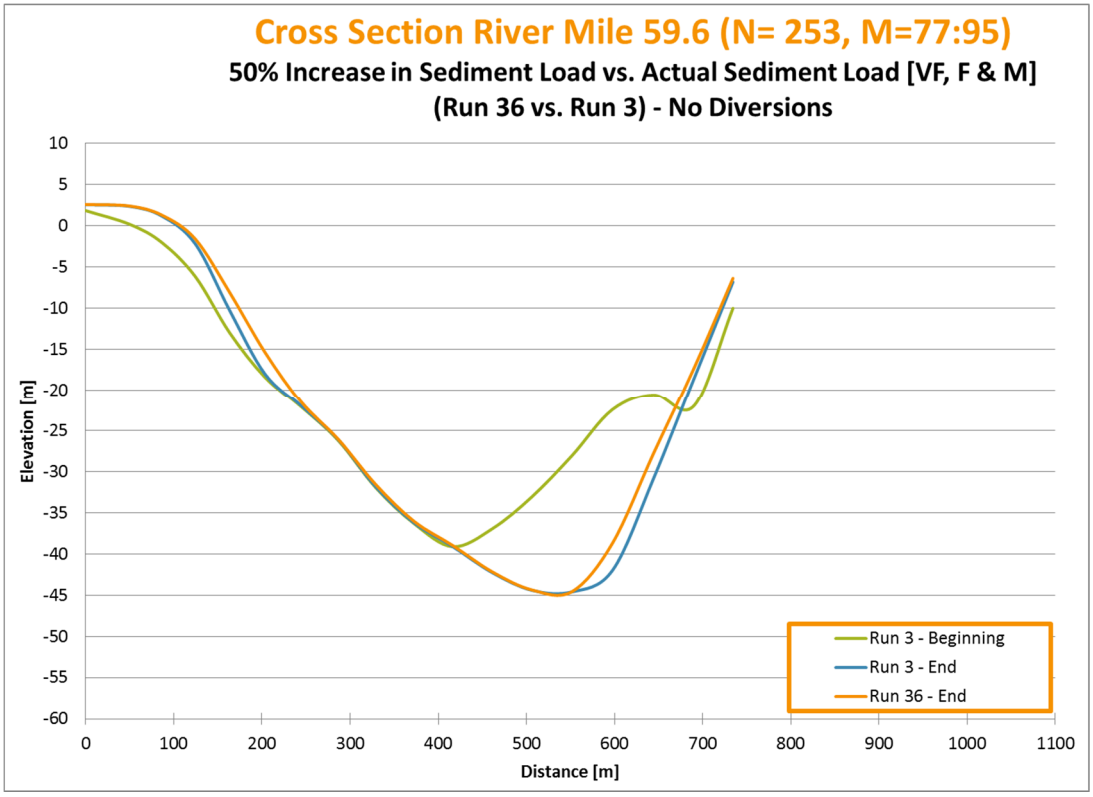

Figure R.4.10: Cross Section River Mile 59.6

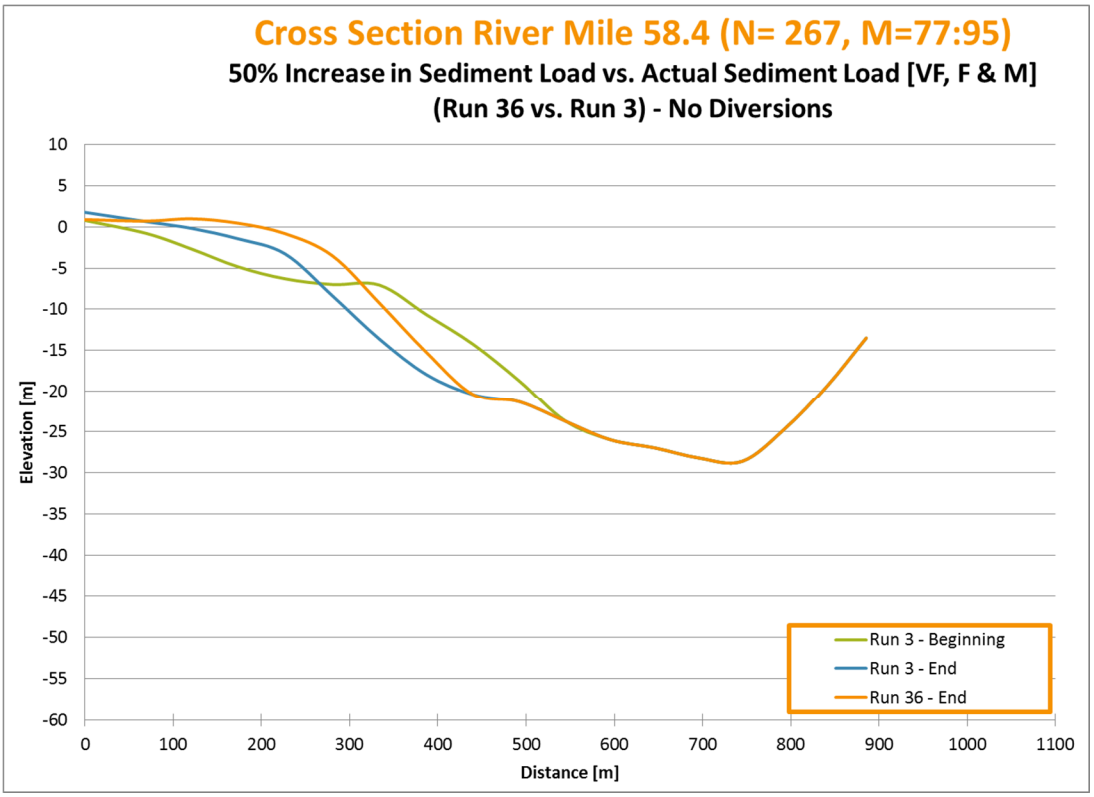

Figure R.4.11: Cross Section River Mile 58.4

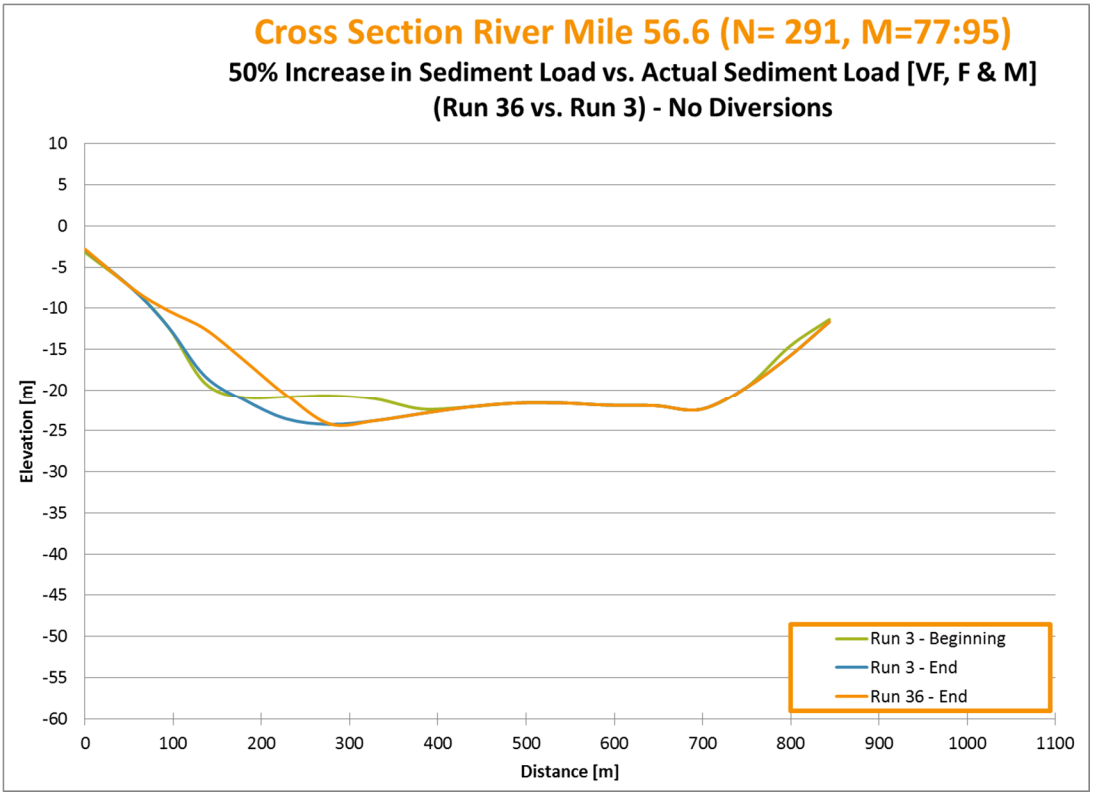

Figure R.4.12: Cross Section River Mile 56.6

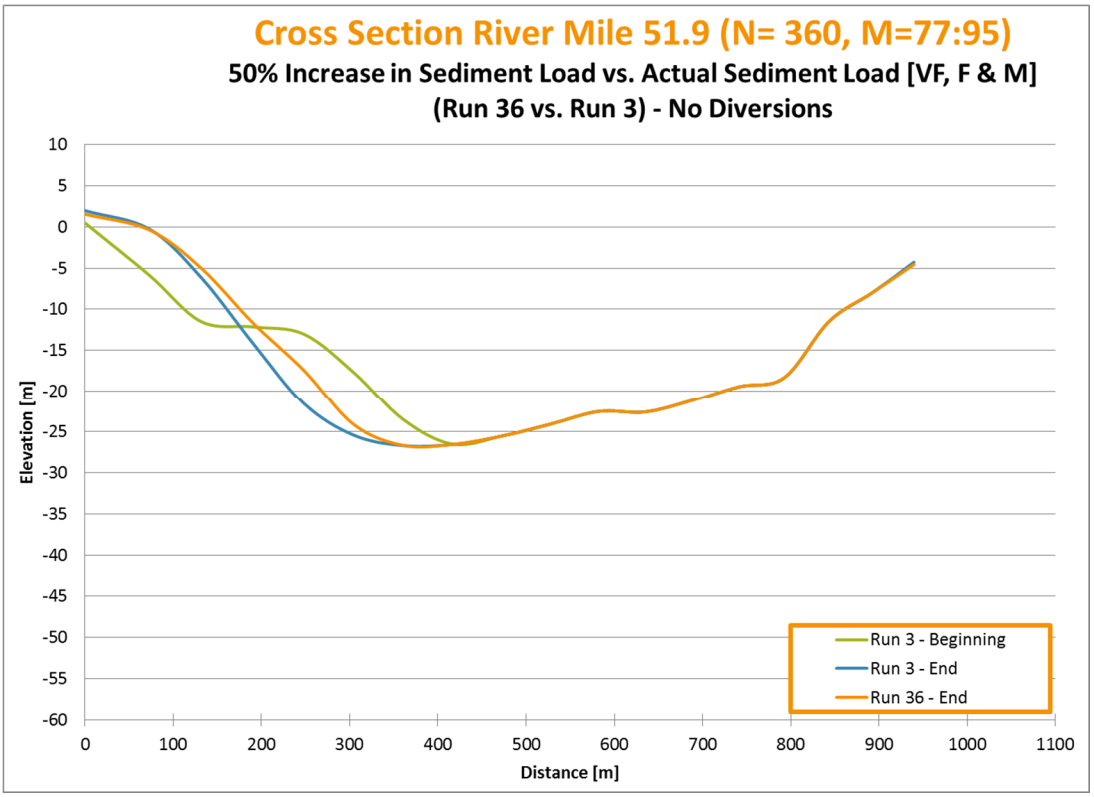

Figure R.4.13: Cross Section River Mile 51.9

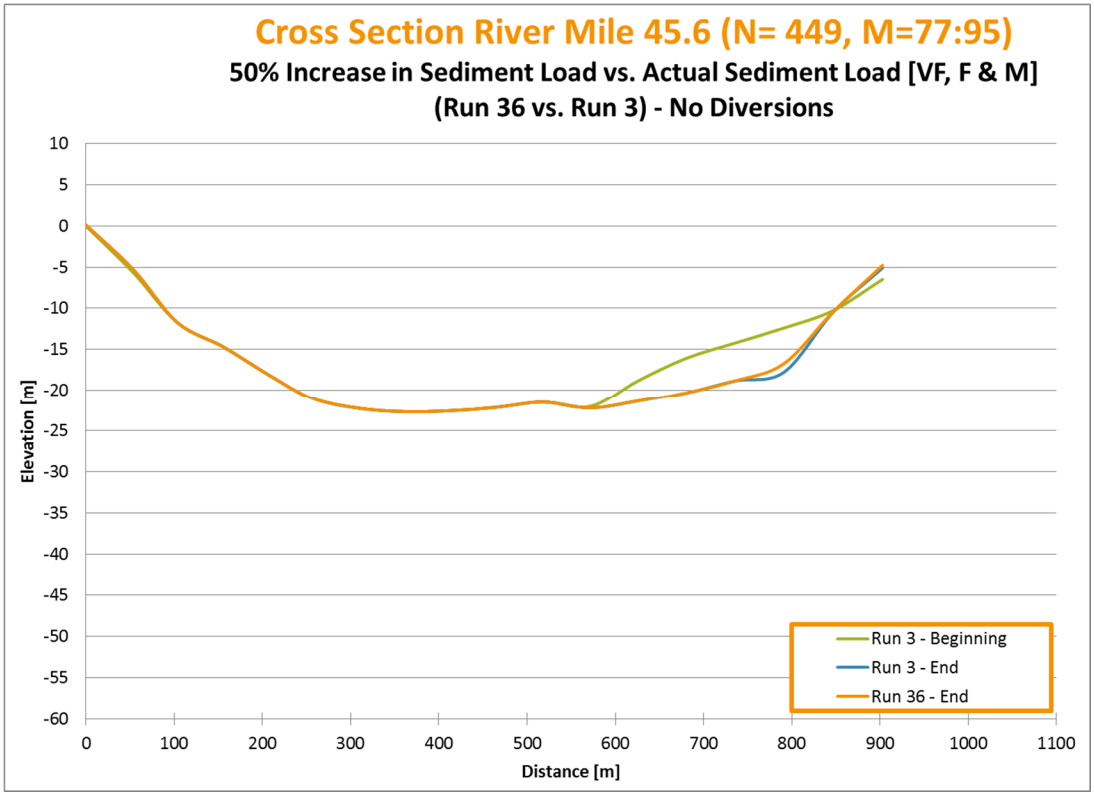

Figure R.4.14: Cross Section River Mile 45.6

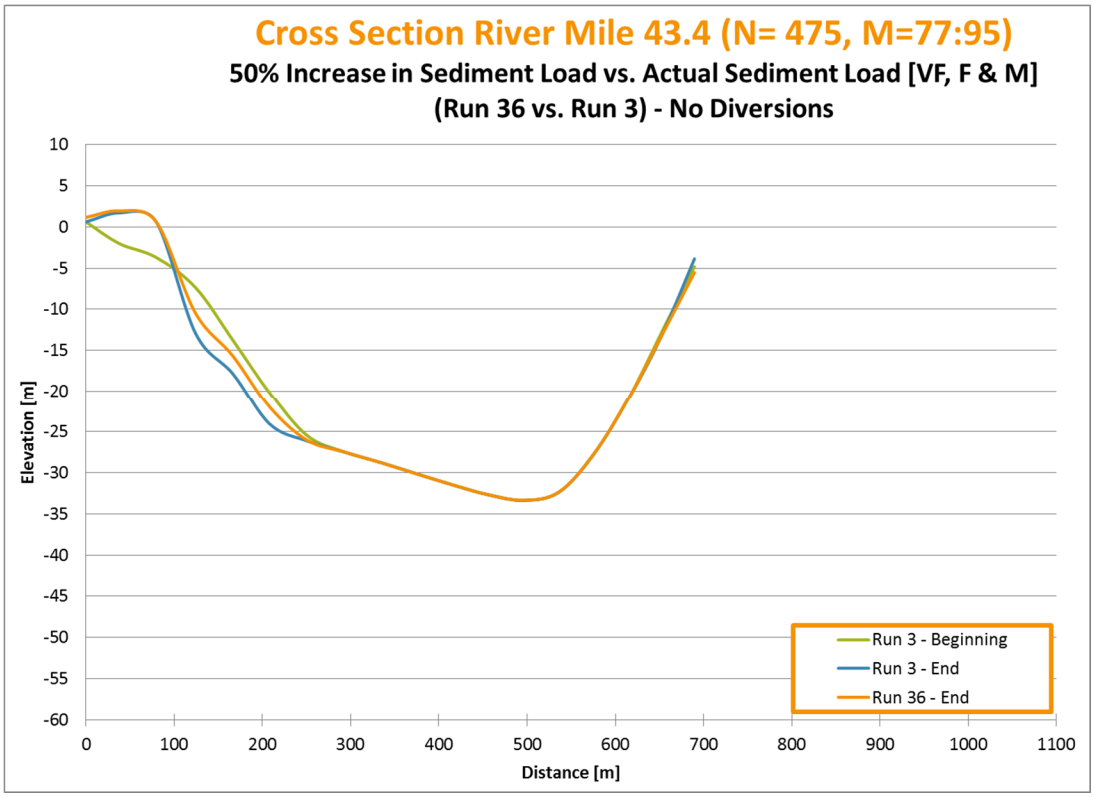

Figure R.4.15: Cross Section River Mile 43.4

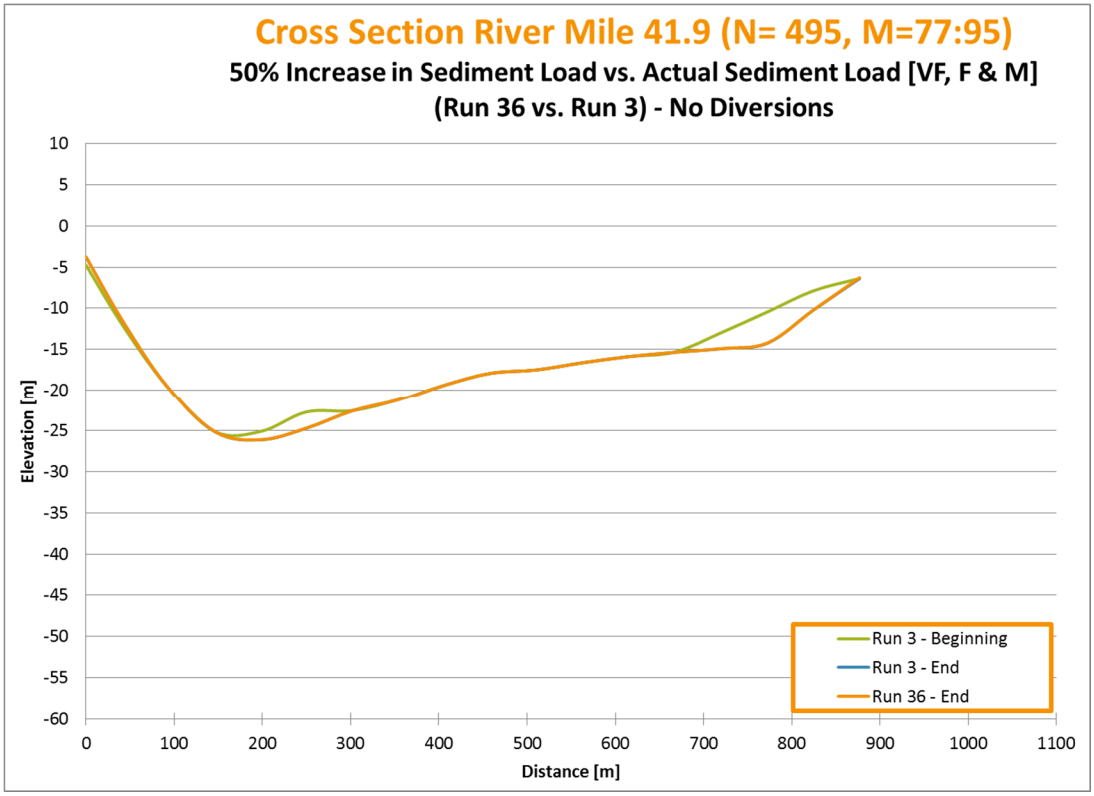

Figure R.4.16: Cross Section River Mile 41.9

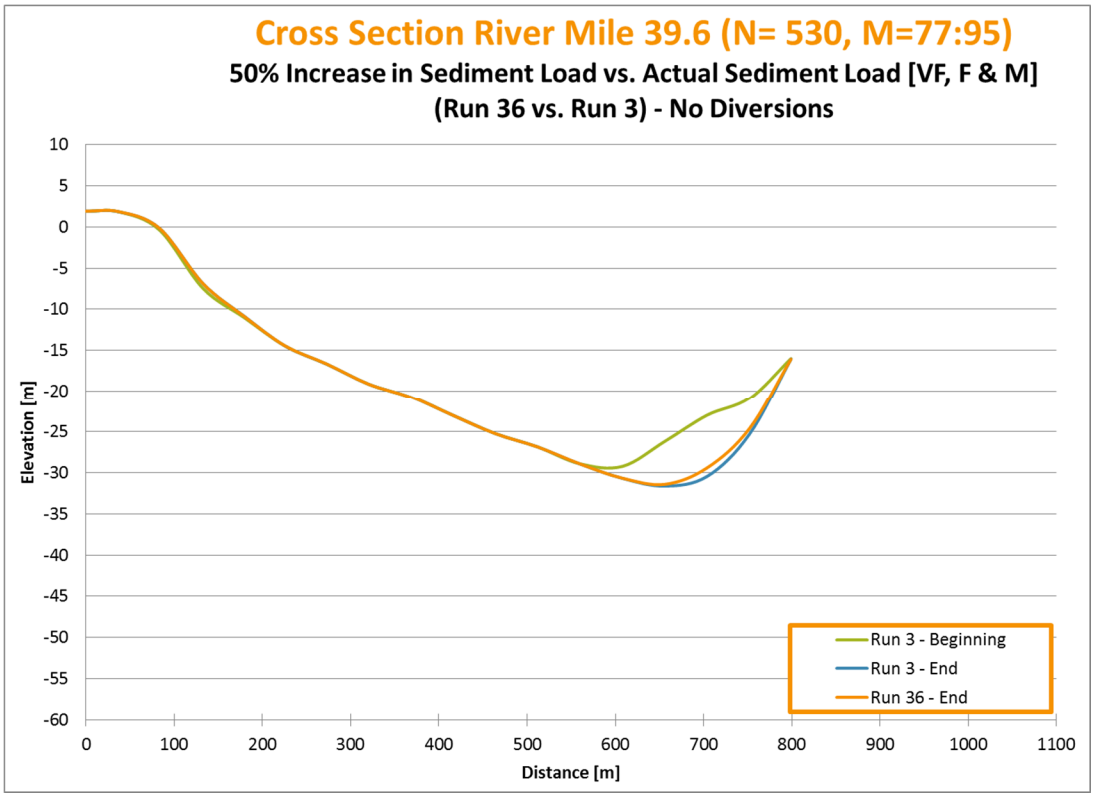

Figure R.4.17: Cross Section River Mile 39.6

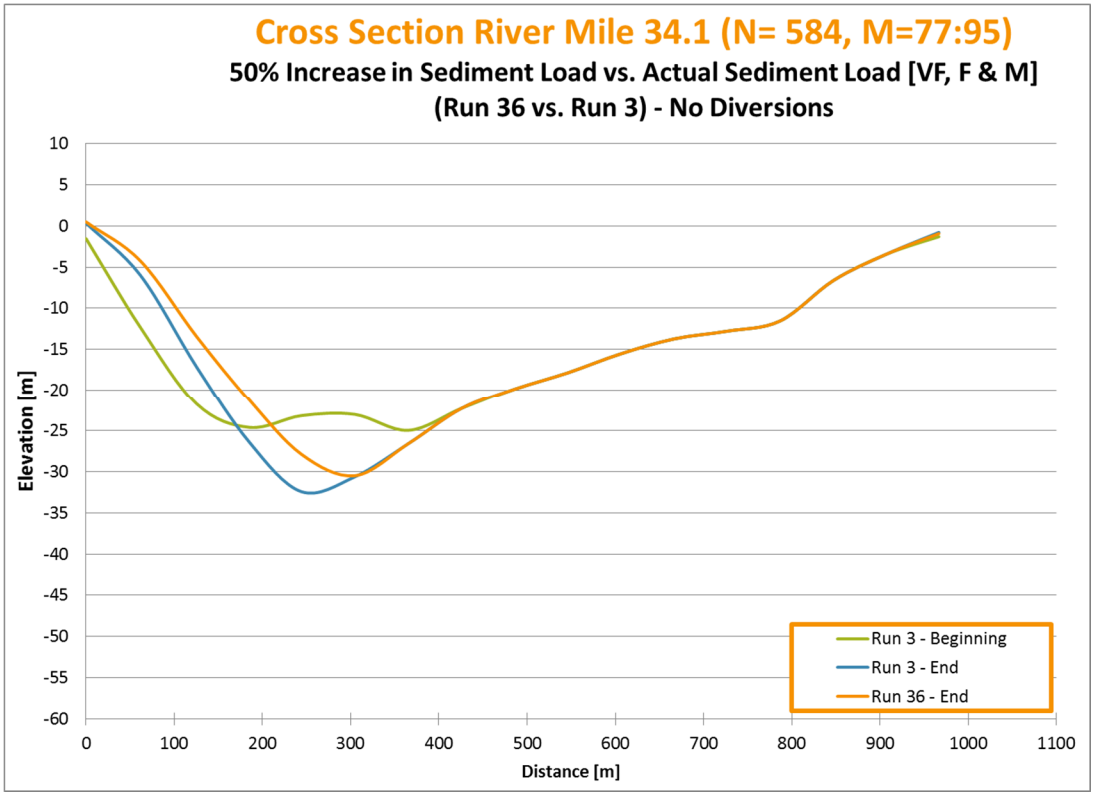

Figure R.4.18: Cross Section River Mile 34.1

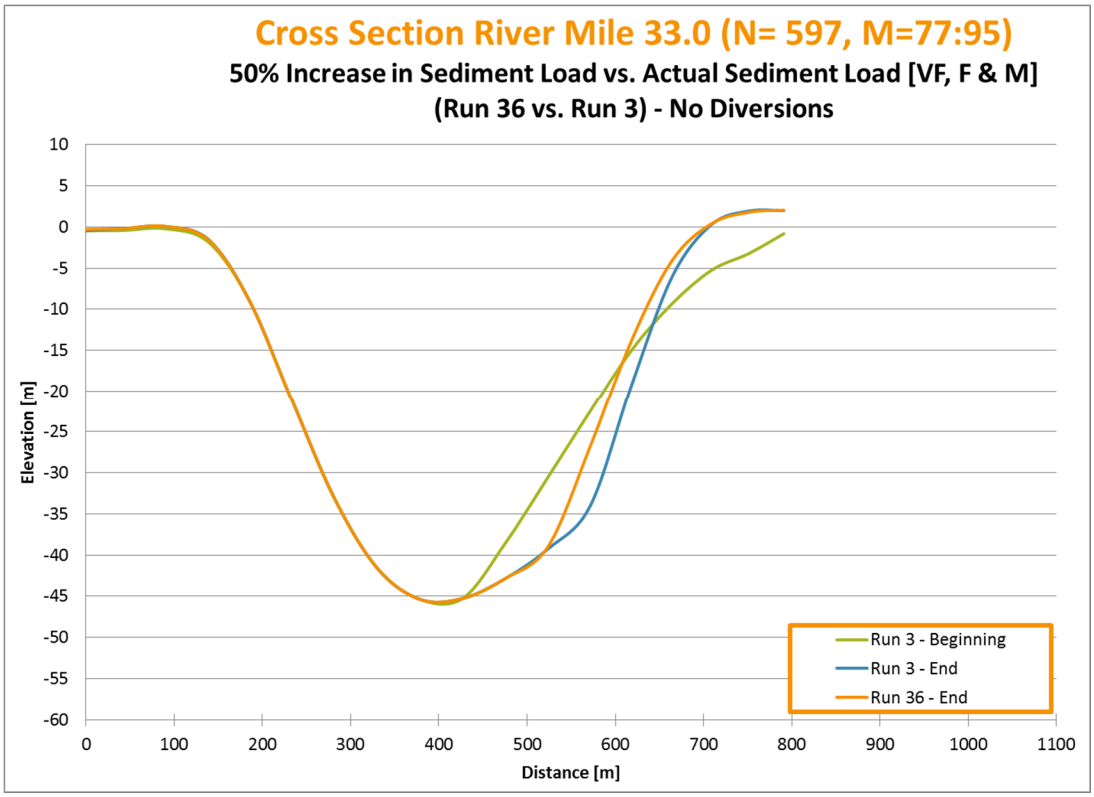

Figure R.4.19: Cross Section River Mile 33.0

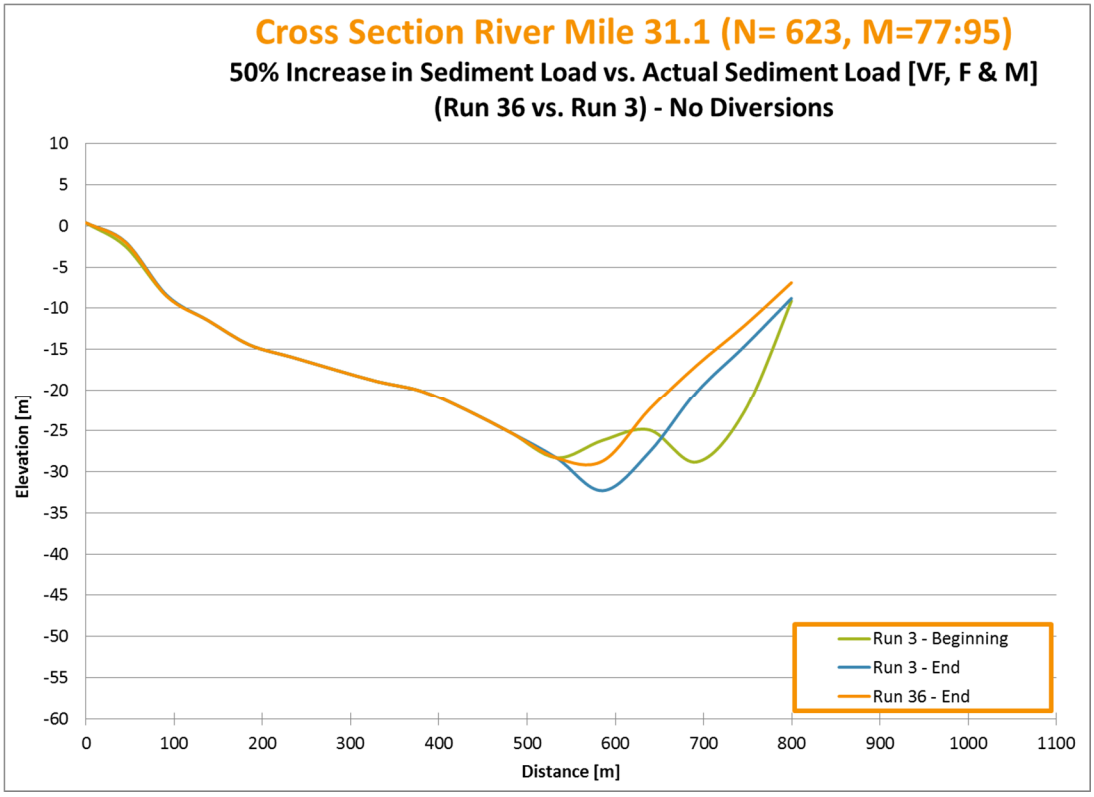

Figure R.4.20: Cross Section River Mile 31.1

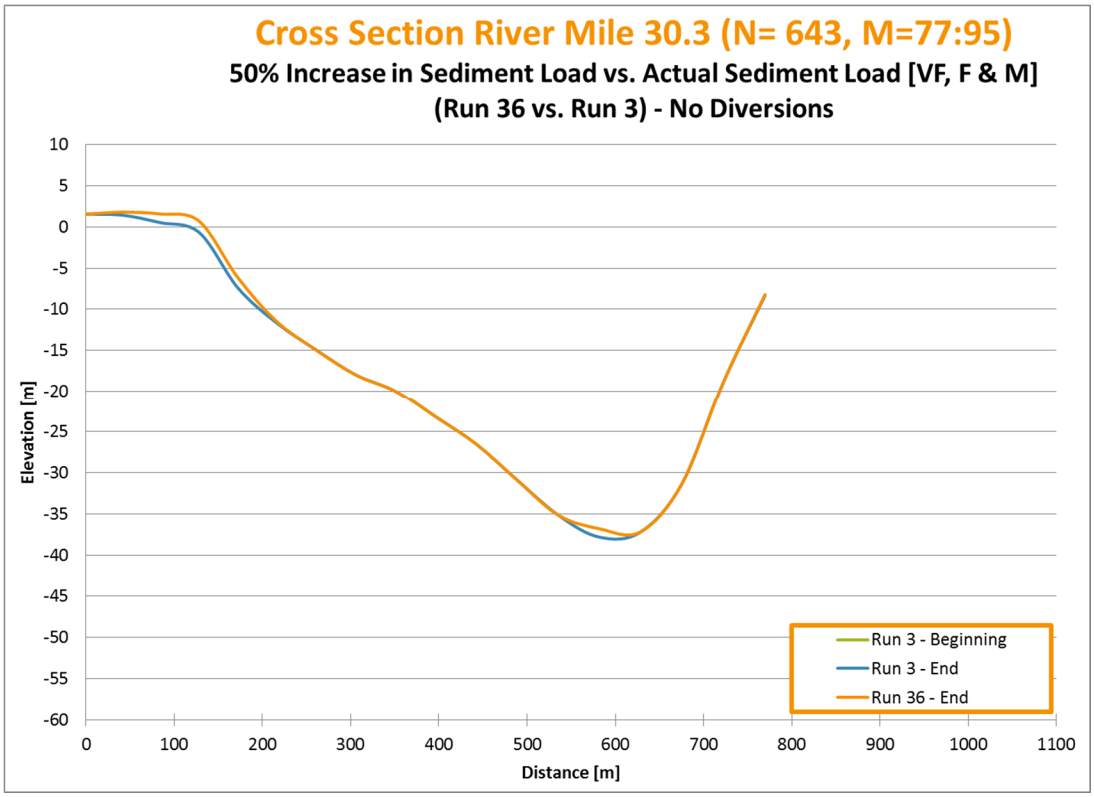

Figure R.4.21: Cross Section River Mile 30.3

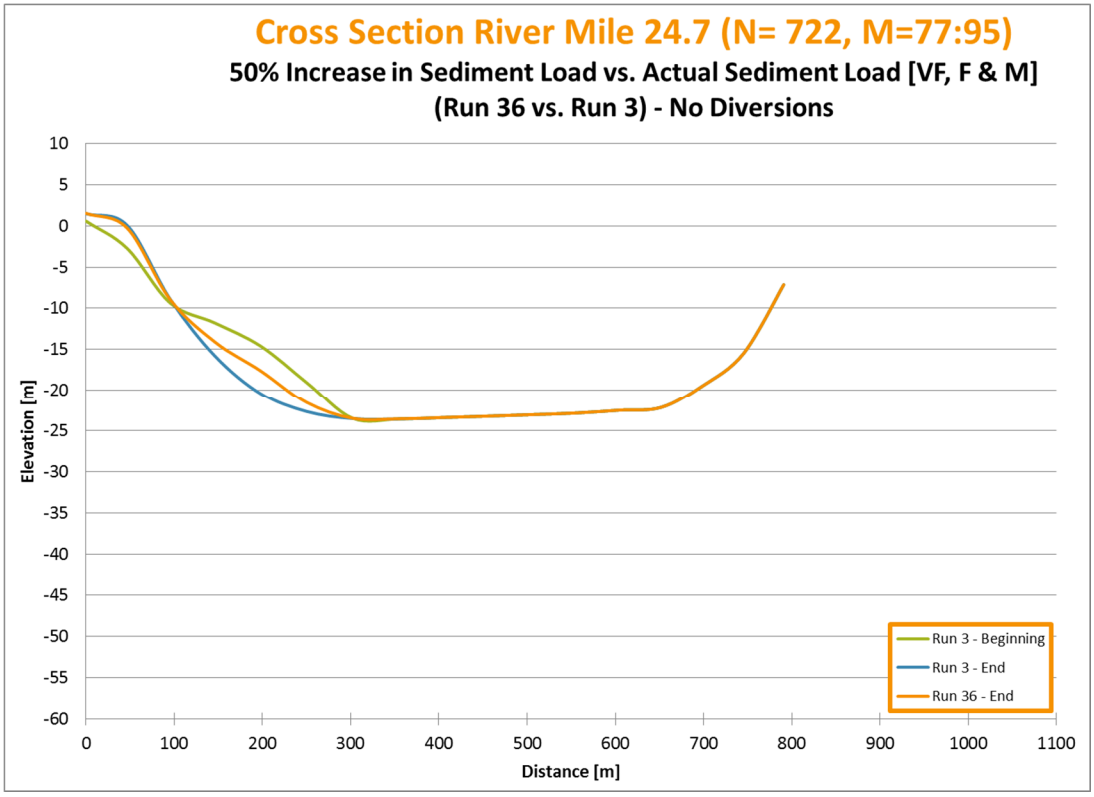

Figure R.4.22: Cross Section River Mile 24.7

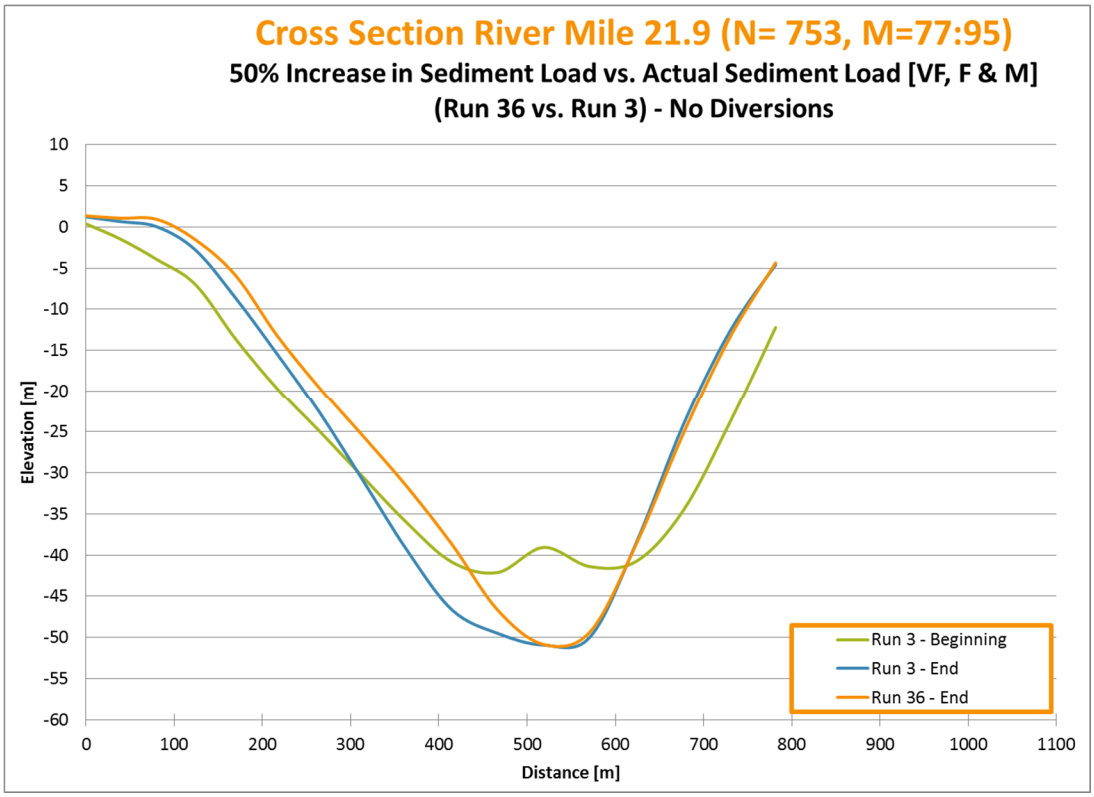

Figure R.4.23: Cross Section River Mile 21.9

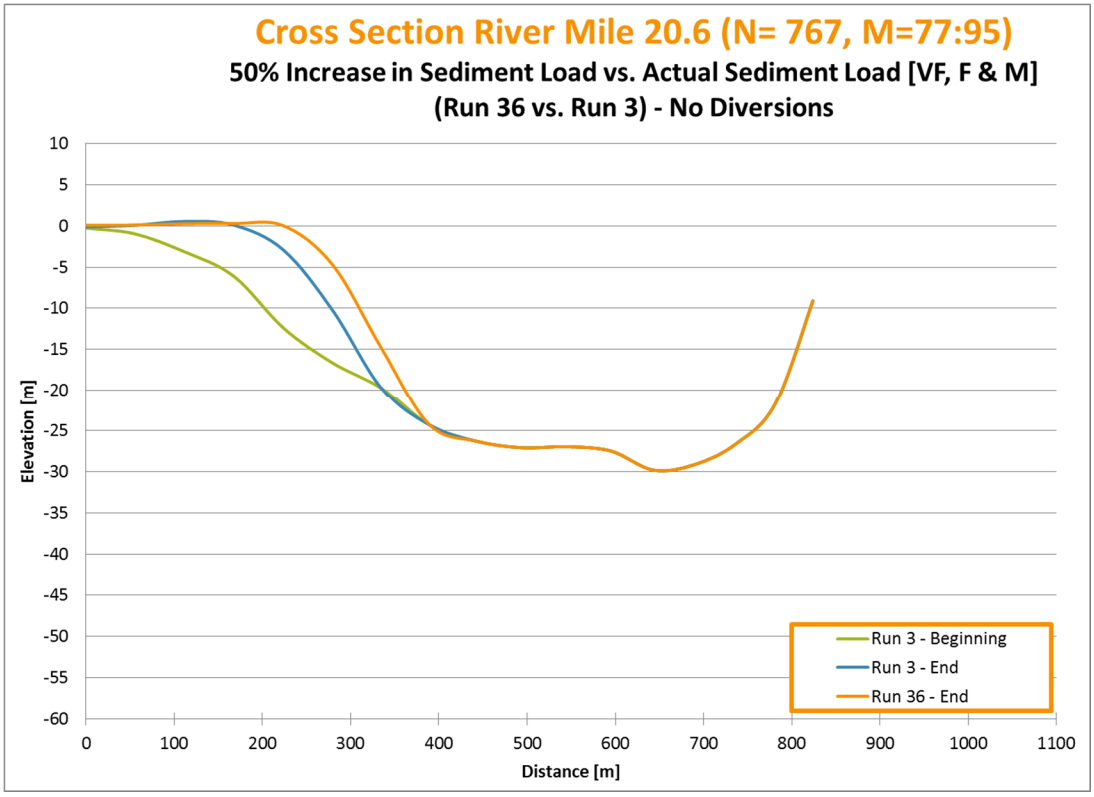

Figure R.4.24: Cross Section River Mile 20.6

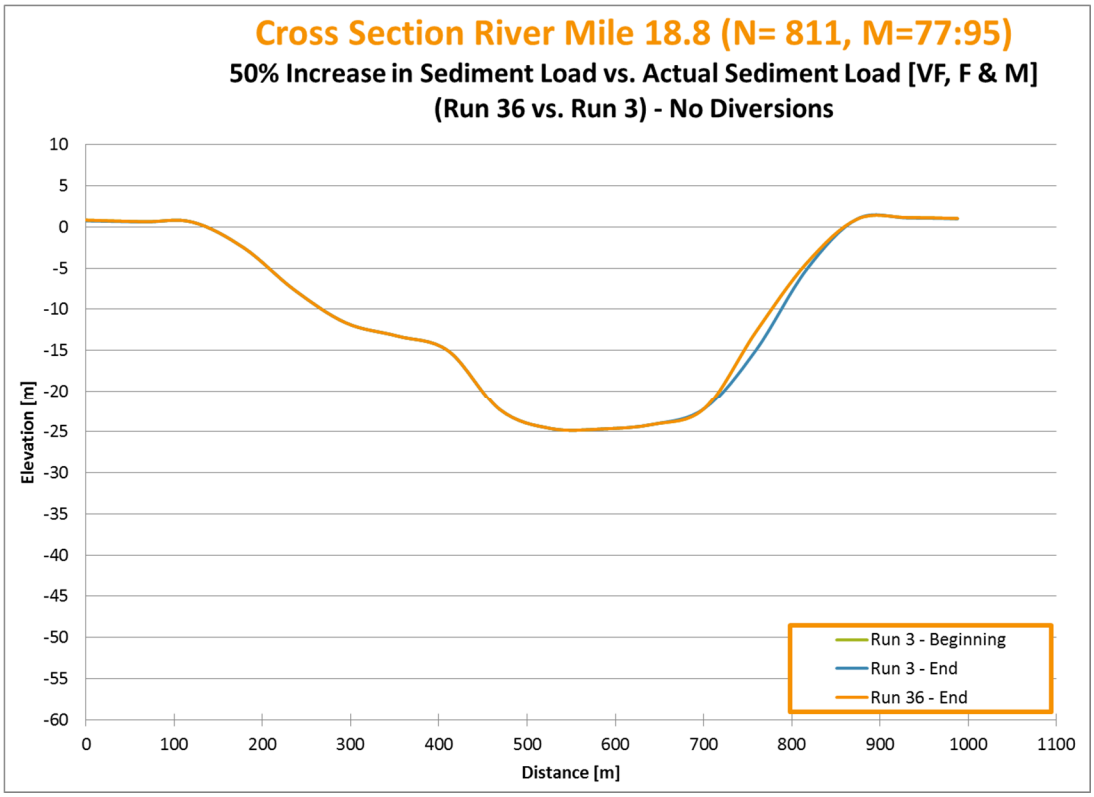

Figure R.4.25: Cross Section River Mile 18.8

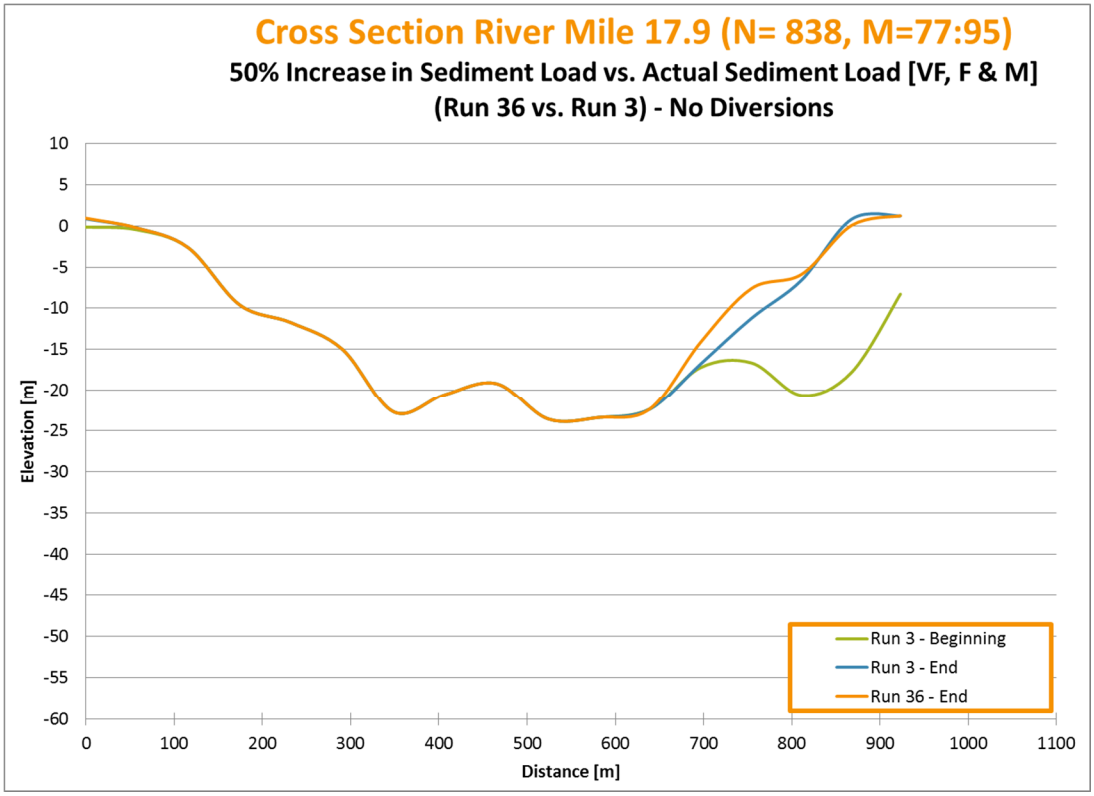

Figure R.4.26: Cross Section River Mile 17.9

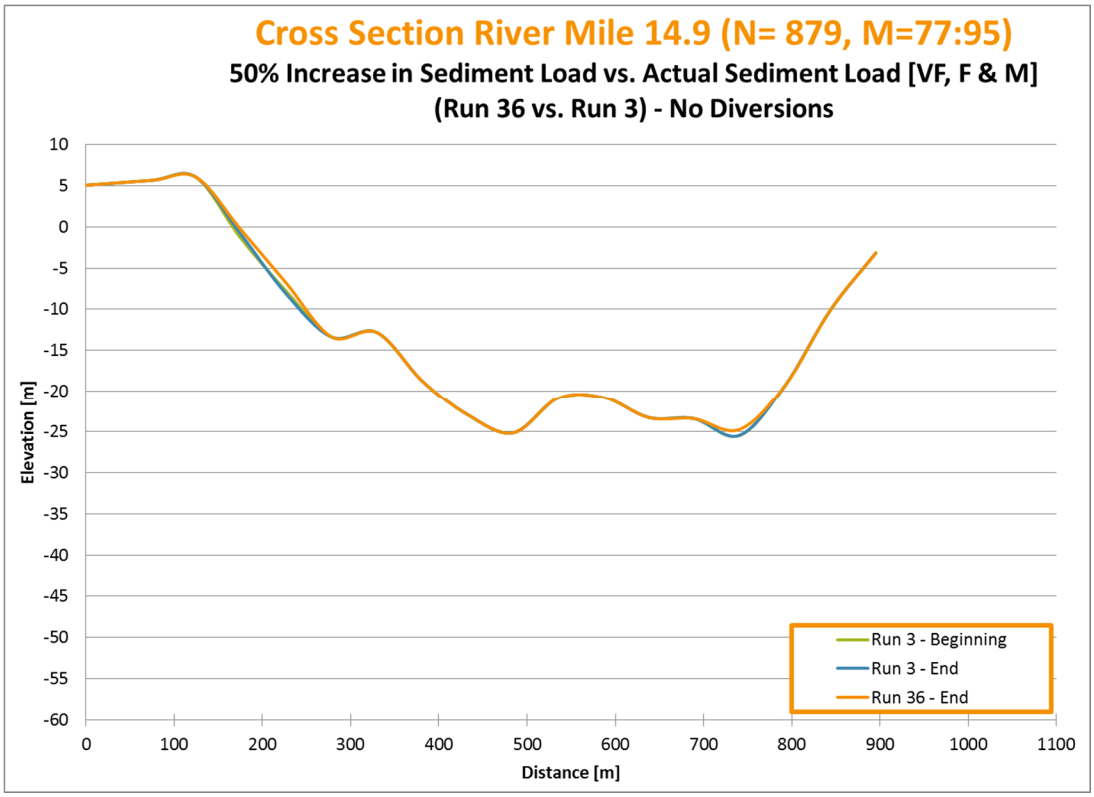

Figure R.4.27: Cross Section River Mile 14.9

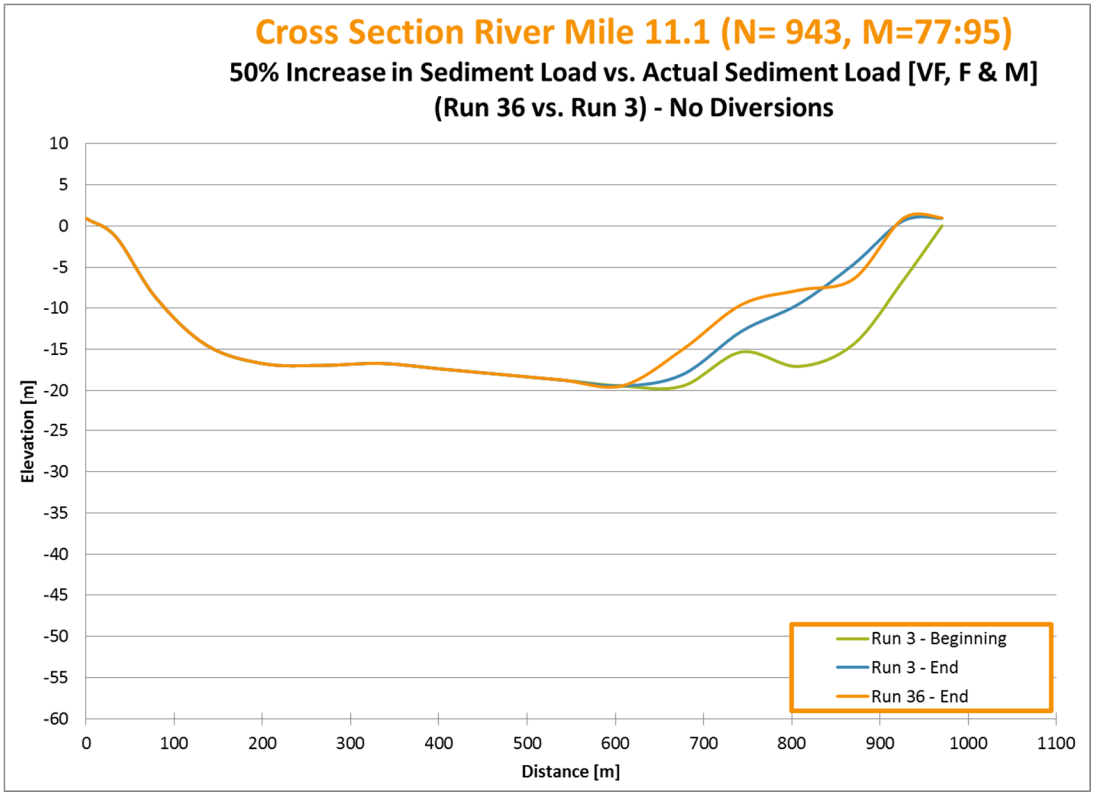

Figure R.4.28: Cross Section River Mile 11.1

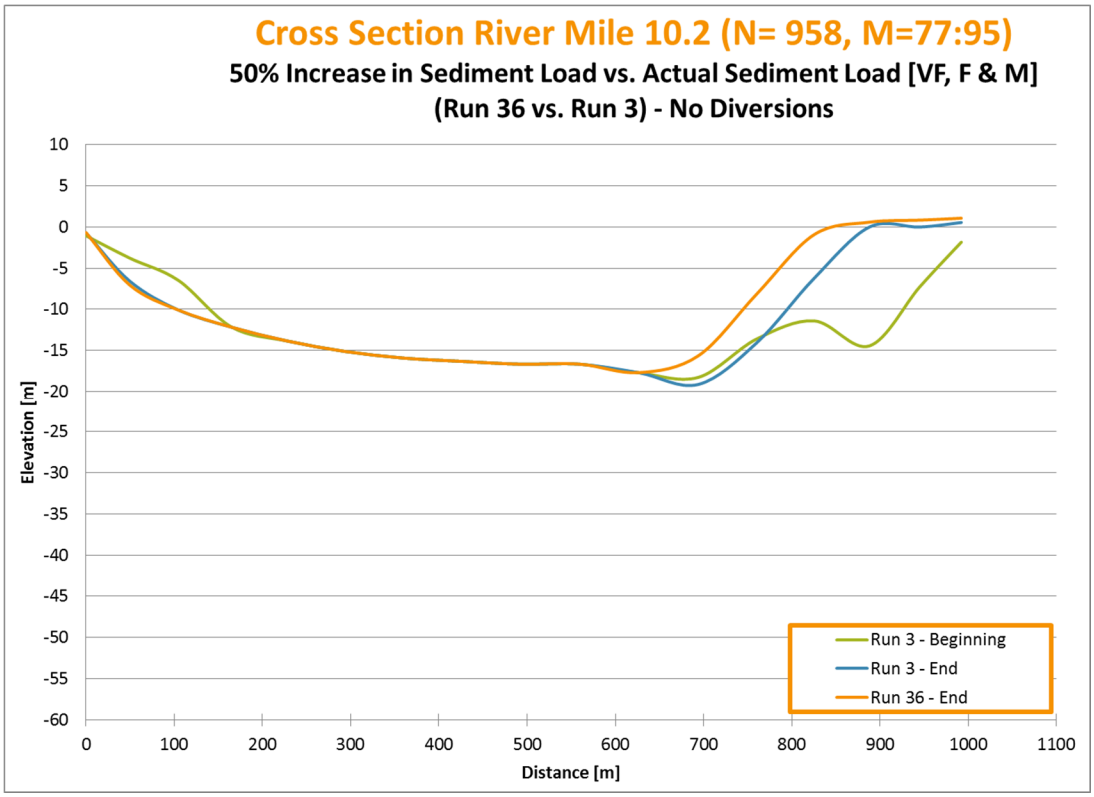

Figure R.4.29: Cross Section River Mile 10.2

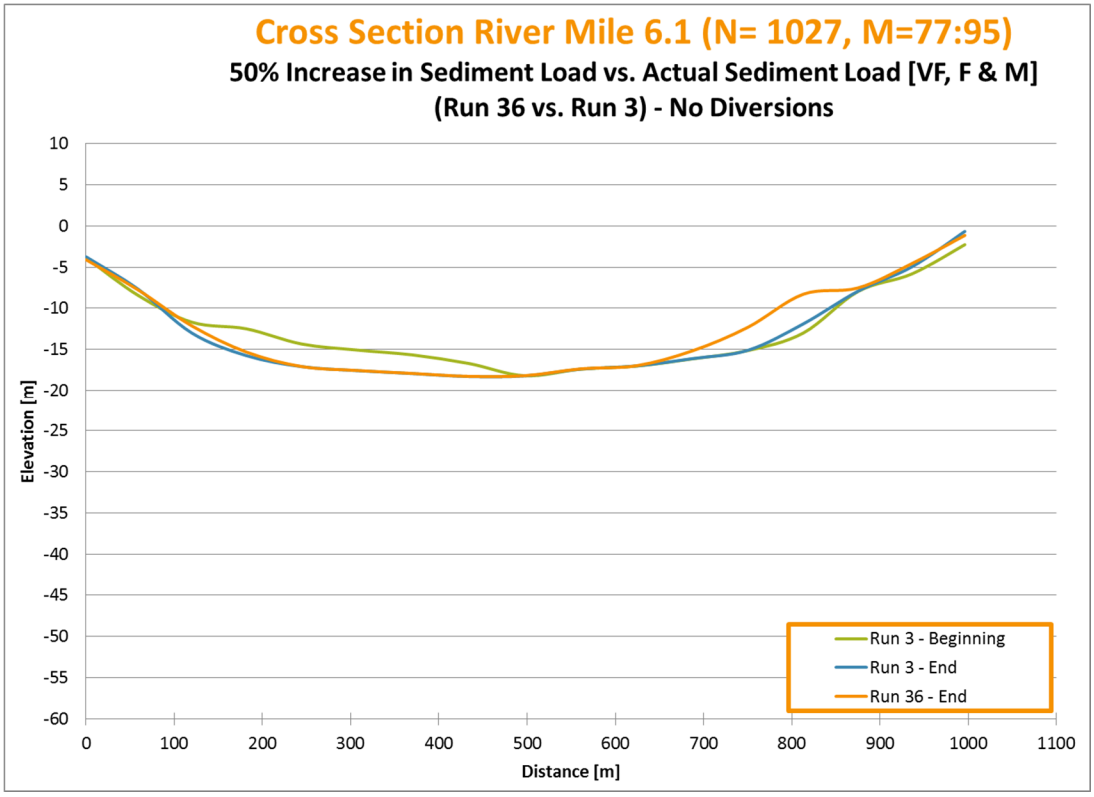

Figure R.4.30: Cross Section River Mile 6.1

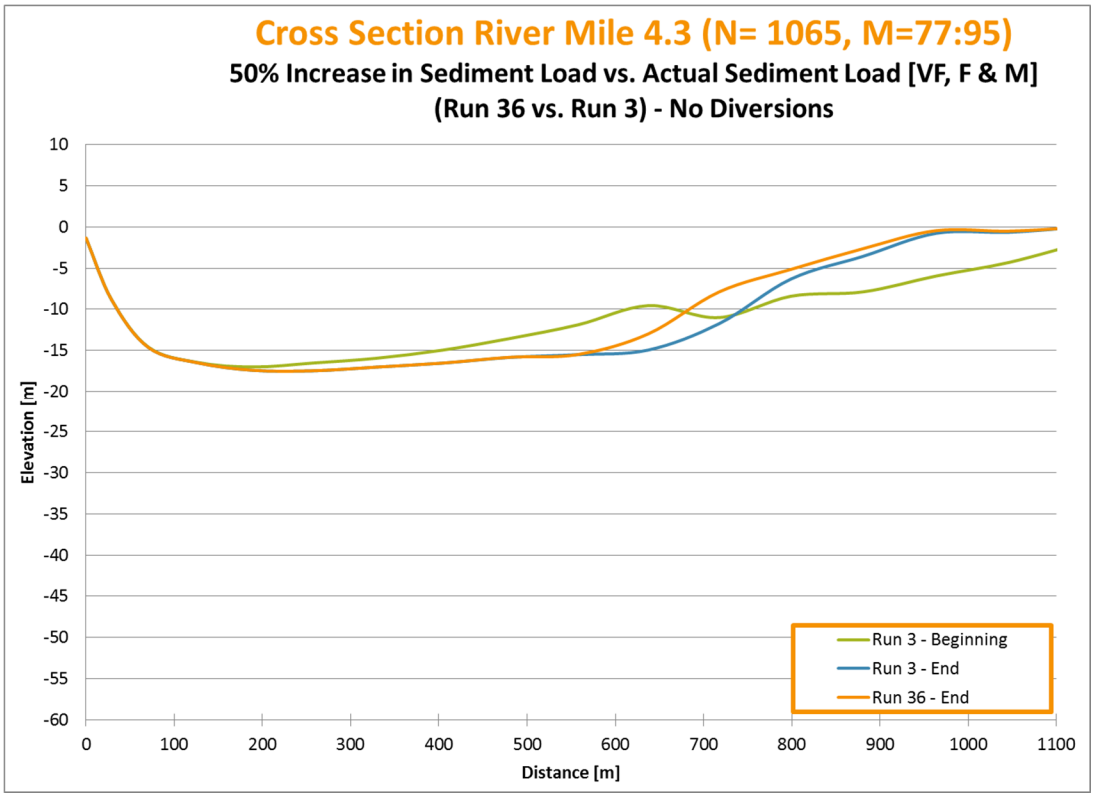

Figure R.4.31: Cross Section River Mile 4.3

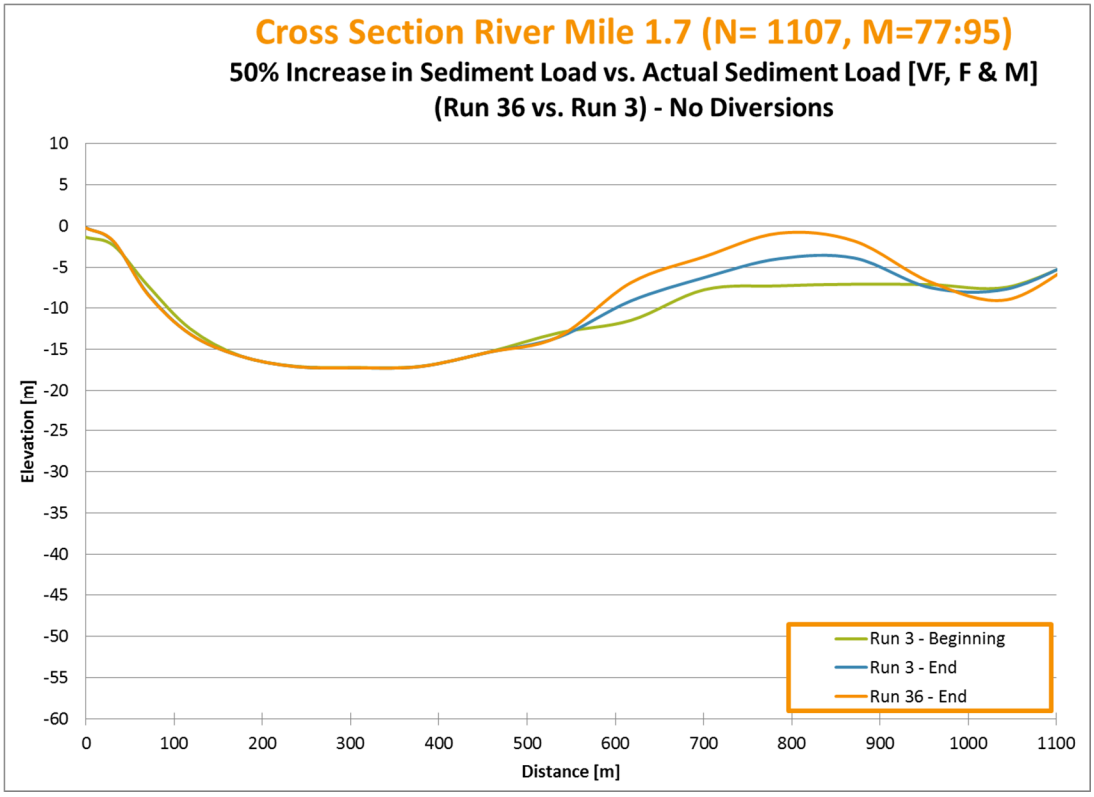

Figure R.4.32: Cross Section River Mile 1.7

VITA

Nina Janita Reins was born in Nordhorn, Germany on September 15, 1977. In 1997 she graduated from High School (Lise Meitner Gynasium) in Neuenhaus, Germany. In 2001 she graduated from the University of Applied Science (Fachhochschule Oldenburg/ Ostfriesland/ Wilhelmshaven) in Oldenburg, Germany with a Bachelor (Dipl.-Ing. [FH]) in Engineering (Bauingenieurwesen). She worked during her studies in construction management and conducted her thesis *"Implementation of New Safety Law for Engineering Sites applied to the Ems Dock and Levee Gate Project"* in collaboration with Claudia Staroste at the Harbor Government in Emden.

After graduation she left Germany for a six months internship in Houma, Louisiana and returned to Germany in 2002. Upon her return she worked in roadway design until she enrolled into Tulane University's Master's program in 2003. In 2005 she graduated with her Masters in Science in Engineering with a focus in coastal engineering and river morphology. Her thesis *"Sediment Investigations in the Vicinity of Old River Complex: Red River above Old River Outflow Channel"* and published in 2010.

In 2004 she co-founded the New Orleans Professional Chapter of Engineers Without Borders and has supported local post-Katrina projects as well as latrine construction in Nicaragua. Since graduation from Tulane University in 2005, she has resided in New Orleans, Louisiana where she currently works as a senior engineering professional in the coastal engineering and program management.

Since her enrollment at the University of New Orleans (UNO) in the Engineering and Applied Science Doctoral Program she has focused her studies on morphological river analysis on the Lower Mississippi River. This research represents the final outcome of the conducted research.

She holds an Environmental Professional Engineering (PE) License and is a certified Project Management Professional (PMP).